POWERLINE BUSHFIRE SAFETY PROGRAM

Vegetation Conduction Ignition Test Report - Final

16 July 2015

Report and analysis by Dr Tony Marxsen, Marxsen Consulting Pty Ltd

This report was commissioned and produced with the authorisation of the Powerline Bushfire Safety Program, Department of Economic Development, Jobs, Transport and Resources.

State Government Victoria

Centre of Excellence - Electricity Bushfire Safety

The Victorian Government is committed to leading ground-breaking research and accelerating the development of innovative technologies in the field of powerline bushfire safety.

The 10 year, $750 million Powerline Bushfire Safety Program (PBSP) was established in December 2011 for the purpose of implementing the recommendations from the Victorian Bushfires Royal Commission and subsequent Powerline Bushfire Safety Taskforce.

The PBSP's primary purpose is to reduce the harm to people and property from bushfires started by electricity assets. This includes a five year, $10 million Research and Development Fund that invests in R&D initiatives aimed at reducing the risk of fires starting from powerlines.

The Victorian Government is committed to ensuring that the fight against the threat of bushfires uses the best proven technologies available and draws upon the know-how of those at the forefront of innovation. The critical areas of funding priority include:

- bushfire mapping and modelling;
- powerline faults and fire ignition; and
- improved powerline conductor technology.

Working closely with industry, regulators and the research community the PBSP has undertaken projects which aim to improve the knowledge of bushfire behaviour, bushfire risk and advancing technological solutions that both contribute to enhanced safety on Victoria's electricity distribution network and leave a legacy that will continue well after the life of the program.

The world first research in this paper is one of these priority projects. The Vegetation Conduction Ignition Testing project seeks to improve fault signature detection technology by:

- identifying which plant species, that are found around or under powerlines in Victoria, are the most and least likely to start a fire through the conduction of electricity; and
- delivering a reference database of related fault signatures so as to drive the development of fault detection technology.

The Victorian Government is making available the findings from this research in order to foster commercial development of new or enhanced products to further technology that prevents bushfires from powerlines.

Disclaimer

This report outlines the results of tests carried out for the Powerline Bushfire Safety Program at a purpose-built facility in Springvale Victoria in the first half of 2015 in accordance with an Agreement between Marxsen Consulting Pty Ltd and the Victorian Department of Economic Development, Jobs, Technology and Resources. This report contains test results, observations, analysis, commentary and interpretation.

Subject to the Agreement, no warranty can be offered to third parties for:

- The application of anything in this report for any purpose other than those required by the specific objectives of the test program stated in the body of this report.
- The direct application of anything contained in this report to any situation other than those that were recorded in the tests.

A complete set of test records is available in the public domain or (in the case of very large video files) upon request from the Powerline Bushfire Safety Program. Readers are advised to rely on their own analysis of these records if they wish to use this report for any purpose other than the specific objectives of the test program stated in the body of this report.

Readers should in particular note the following qualifications:

- The information in this report relates to 22kV powerline vegetation faults only. Readers who wish to use these results to derive conclusions for other types of powerline faults should rely on their own investigations.
- Definitions of worst case fire risk conditions for ignition were derived from limited data and small numbers of tests. No warranty is offered that even worse fire risk condition will not occur in practice.
- All reasonable care has been taken to clearly outline the rationale and evidence for findings, but readers should make their own judgements of the merits such findings before relying on them.
- Where a level of statistical uncertainty is stated, this is a statistical measure which cannot be applied to individual cases or small numbers of cases, but can only be validly applied to cohorts of cases large enough to meet the normal criteria set out in statistical theory.
- Quantification of statistical certainty has not been possible for many findings due to test-to-test variation of factors that influence ignition outcomes. In such cases, readers should form their own judgement of the level of confidence they can place on the findings concerned.
- Many assumptions were used to generate insights, derive findings and interpret results. All reasonable care has been taken to explicitly document these assumptions and explain the rationale in each case, but no warranty can be offered that such documentation is complete or that any implicit or explicit assumptions used are valid.
- Where mathematical theory has been used to derive insights from test results, care has been taken to outline the theory and how it was applied. However, no warranty is offered that the theory employed is valid or correctly applied.

Contents

List of abbreviations

Acronym	Explanation
22kV	22,000 volts – the 'wire to wire' voltage on most of Victoria's electricity networks
50Hz	50 cycles per second – the frequency of electricity distributed in Victoria
ACR	Automatic Circuit Recloser – a pole-mounted HV switch with inbuilt protection relay
Amp, A	Amperes – the unit used to measure flow of electric current
DBRG	The Distribution Business Reference Group – network owner senior executives
DSDBI	The Victorian Department of State Development, Business and Innovation
ESV	Energy Safe Victoria – Victoria's energy safety regulator
HF	High-frequency
HRLT	HRL Technology Pty Ltd
LF	Low-frequency
Ohm	The unit of measurement of electrical resistance (ratio of voltage to current)
PBST, PBSP	Powerline Bushfire Safety Taskforce (2011) and Program (current)
SWER	Single-Wire-Earth-Return: a low cost, single wire rural powerline technology
TWG	The PBSP Technical Working Group
VESI	The Victorian Electricity Supply Industry

1 Summary of findings

The findings of the 2015 Vegetation Conduction Ignition test program are summarised in Table 1.

Table 1: 2015 Vegetation Conduction Ignition Tests - summary of findings

1. Ignition processes in powerline vegetation faults	
1a	The vegetation conduction ignition process follows a sequence of four phases: development of full conductor-vegetation contact; expulsion of moisture; progressive charring of bark extending from the thinner end of the vegetation sample; and flashover when flame bridges the high voltage conductors.
1b	During the third phase of development of ignition (progressive charring of bark extending from the thinner end of the vegetation sample), electric arcs spontaneously occur in the flame along the branch and this causes large fluctuations in the current flow since such arcs intermittently short-circuit portions of the path between the high-voltage conductors.
1c	The range of vegetation moisture content in tests was restricted by the mild, humid summer of 2014-15. Conditioning at 45°C for up to 24 hours prior to most tests was successful in reducing moisture content but it is not known if this is an accurate reflection of changes that occur in extreme summer weather.
1d	Below about 10-15% moisture content, branches do not conduct enough current to cause thermal runaway, i.e. heat generated by the current is balanced by heat loss into the air and sample temperature stabilises at a relatively low level so ignition never develops. Similarly, grasses act as electrical insulators at low moisture content levels, taking no current at all.
1e	The range of branch diameter that could be safely tested was limited. Larger sample sizes drew high levels of initial current and the current increased very quickly to reach the pre-set limit in a few seconds at most. On the basis of the test results, it was considered possible that vegetation faults involving larger branch sizes might be rapidly detected, allowing action to be taken before fire risk can arise. However, this could not be tested in this project.
1f	Laboratory analysis of pre-test samples supported visual observations that most current flow was in the layers immediately under the bark - the Phloem and Cambium layers. These layers had significantly higher conductivity than other parts of the sample.
1g	Tests to simulate reclose onto a vegetation fault, i.e. where high voltage is restored after a delay, indicated that the physical changes produced by current through the vegetation are irreversible, i.e. the fault current tends to 'take up where it left off' or it goes directly to flashover after a brief delay.
2. Ignition in 'branch touching wire' earth faults	
2a	The initial level of current flow in a 'branch touching wire' fault depends on many factors including vegetation moisture content and the level of ionic compounds in the sap, as well as the branch diameter.
2b	The initial current in 'branch touching wire' faults that produce fire risk is too low to be detected by powerline protection technologies currently in use in rural Victoria.
2c	'Wire touching branch' faults can only be reliably detected once the fault current has grown beyond its initial value. The time taken for this to happen gives opportunity for ember production and hence, fire risk.
2d	With traditional earth-fault detection sensitivity of 5-10 amps on rural powerlines in Victoria, 'branch touching wire' earth faults are certain to produce a fire in worst case conditions.

2e	If powerline earth-fault protection systems were to detect and respond to 0.5 Amp faults within two seconds, fire risk in 'branch touching wire' faults in worst case conditions would be reduced tenfold compared to current levels.
2f	It was not possible to reliably quantify the influence of sample moisture content on fire risk due to the large number of independent variables in the ignition tests and Melbourne's mild damp 2014/15 summer.
2g	Different species show widely varying fire risk in 'branch touching wire' faults. Of the species tested, the worst fire risk in 'branch touching wire' faults is Willow (Salix Sp.) and the best is Peppercorn (Schinus Molle). Other species tested fall between these extremes.
2h	Species with high fire risk tend to take longer for fault current to fully develop. Species with faster fault current development tend to have lower fire risk because the fault reaches the detection threshold before ember production fully develops.
2i	The type of bark on some species appears to have a significant effect on their fire risk in 'branch touching wire' faults.
	3. Ignition in 'wire into vegetation' earth faults
3a	Within the limits of certainty set by the smaller number of tests performed, 'wire into bush' faults are likely to have a higher fire risk than 'branch touching wire' faults. If powerline protection systems can detect and respond to a 0.5 amps earth fault, fire risk from 'wire into bush' faults might be cut by about 80%.
3b	Of the few middle storey species successfully tested, Burgan and Gorse were worse than Blackberry. Silver Banksia appeared to have a lower fire risk. There is considerable uncertainty in these results due to the relatively small number of tests available for analysis.
3c	'Wire into bush' test results tended to be binary: either the fault quickly produced a substantial fire; or it pruned back vegetation (without creating significant fire risk) until current ceased to flow. 'Pruning' and 'cooking' outcomes featured in 'wire into bush' tests.
3d	'Wire into grass' tests produced even more binary results: if the grass had enough moisture to conduct current, a flashover to ground occurred almost instantly; if not, nothing happened even when dry grass was pressing against the live wire for an extended period.
3e	The fire probability results for 'wire into grass' faults in worst case conditions should be drawn from the results of the 2014 REFCL Trial rather than the tests in this program. In all tests that produced fire risk, ignition was driven by the occurrence of flashovers, i.e. the 'wire into grass' fault either became a 'wire on ground' fault (where fire risk is due to flashover to ground) or was not a fault because no current flowed.
	4. Ignition in 'branch across wires' faults
4a	The rate of growth of fault current is four times faster in 'branch across wires' faults than in 'branch touching wire' faults.
4b	If fault currents could be limited to a specific low value by powerline protection systems, fire risk would be lower in 'branch across wires' faults than in 'branch touching wire' faults for the same current limit. However, no powerline protection technology is available today that offers this capability.
4c	Assuming all 'branch across wires' faults progress to flashover (whereupon the high voltage is removed by powerline over-current protection), the fire probability from 'branch across wires' faults on real networks is likely to be not less than 55%.

4d	Fault detection and response within about five seconds might achieve substantial reductions in 'branch across wires' fire risk. Fault detection times longer than about 20 seconds would be unlikely to significantly reduce fire risk in such faults.
	5. Vegetation fault signatures
5a	A large data base of fault signature records was successfully compiled during the test program, including recordings of faulted conductor voltage and fault current in phase-to-earth vegetation faults and phase-to-phase vegetation faults.
5b	Background network voltage noise recordings were successfully gathered over a six-week period, including phase-to-earth voltages and phase-to-phase voltages. The level of broad-band network voltage background noise was about 0.3-0.8 volts, dominated by local industrial load and AM radio stations.
5c	High-frequency voltage disturbances in tests were most commonly caused by very fast step discontinuities in the fault current or by bursts of high-frequency noise in the fault current. The physical processes behind these features are not known, though there was a tendency for discontinuities to occur near or following fault current zero-crossings and noise bursts to occur near or following peaks in the 50Hz fault current waveform.
5d	The high-frequency voltage noise produced in Phase 1 of a vegetation fault was generally much smaller than the total network background noise. However, it could still be seen in test spectrograms, indicating faults might be reliably detected by better signal processing.
5e	One specific proprietary partial-discharge detection system currently under development to detect pole-fires produced records that indicated it may be capable of detecting low-current vegetation faults.
5f	It was confirmed that a specific fault signature detection relay developed for the North American market did not detect any of the 1,038 vegetation faults in the test program.

2 Executive summary

Powerline faults can start fires in a variety of ways. The least known and most challenging ignition process to understand is ignition through conduction of high voltage electricity through vegetation.

The latest research in the Victorian Government's Powerline Bushfire Safety Program described here, has focused on this issue with two goals: first, identify the worst species for fire starts from powerline faults and understand their ignition processes; and second, compile a reference data base of vegetation fault signatures (electrical signals caused by vegetation faults) to support development of better fault detection technology.

2.1 Context

The Black Saturday bushfires in Victoria in February 2009 killed 173 people, injured more than 4,000 more and caused $4.4 billion of economic damage to the state. To address the powerline-related recommendations of the subsequent Royal Commission, the Victorian Government established the Powerline Bushfire Safety Taskforce which recommended among other actions, focussed research to improve the state of knowledge on how fires start from powerline faults and how they might be prevented.

This research program is now administered by the Powerline Bushfire Safety Program within the Victorian Department of Economic Development, Jobs, Transport and Resources. A key focus of the research is ignition processes from the electric energy released into the environment when powerline faults occur.

There are three well-known ignition mechanisms that operate in powerline faults: incandescent metal particles emitted when high voltage conductors clash; high voltage arcs that occur near vegetation; and high voltage current that passes through vegetation. Previous research projects have focused on the first two of these. The project reported here covers the third: vegetation conduction ignition.

In February and March 2015, an extensive test program at Springvale in south-eastern Melbourne generated new insights and quantified fire risk results for three vegetation fault configurations: 'branch touching wire'; 'branch across wires'; and 'wire into vegetation'. This report presents details of the project and its findings.

2.2 Findings: ignition processes in powerline vegetation faults

The vegetation conduction ignition process in branch/wire faults was found to follow a consistent sequence of phases, illustrated in Figure 1 below: development of full conductor-vegetation contact; expulsion of moisture; progressive charring of bark extending from the thinner end of the vegetation sample; and finally, flashover when flame bridges the high voltage conductors.

Fire risk arises mainly in the third phase when the outer layer of the branch progressively burns and chars from one end to the other, as shown in Figure 2. During the third phase, electric arcs sometimes spontaneously occur in the flame along the branch causing large fluctuations in the current flow (such as those visible in Figure 1) by intermittently short-circuiting portions of the path between the high-voltage conductors. A typical instance of such arcs is shown in Figure 3.

Figure 1: Tests 426 - typical variation of fault current in the four phases of vegetation fault development

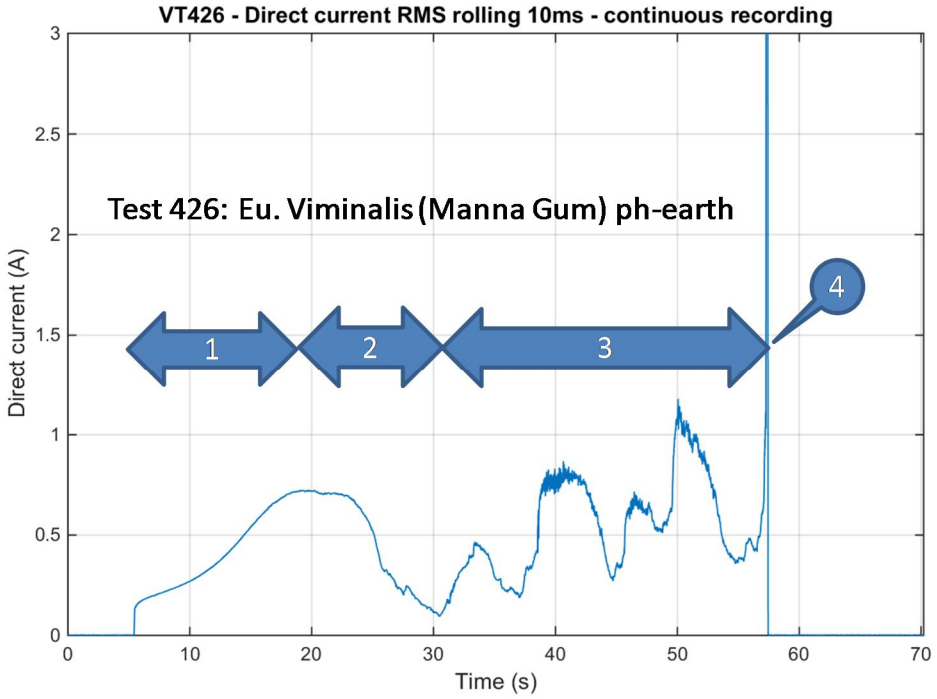

Figure 2: Test 447 - progressive spread of flame from one end of the branch to the other (flashover at 1m: 44s)

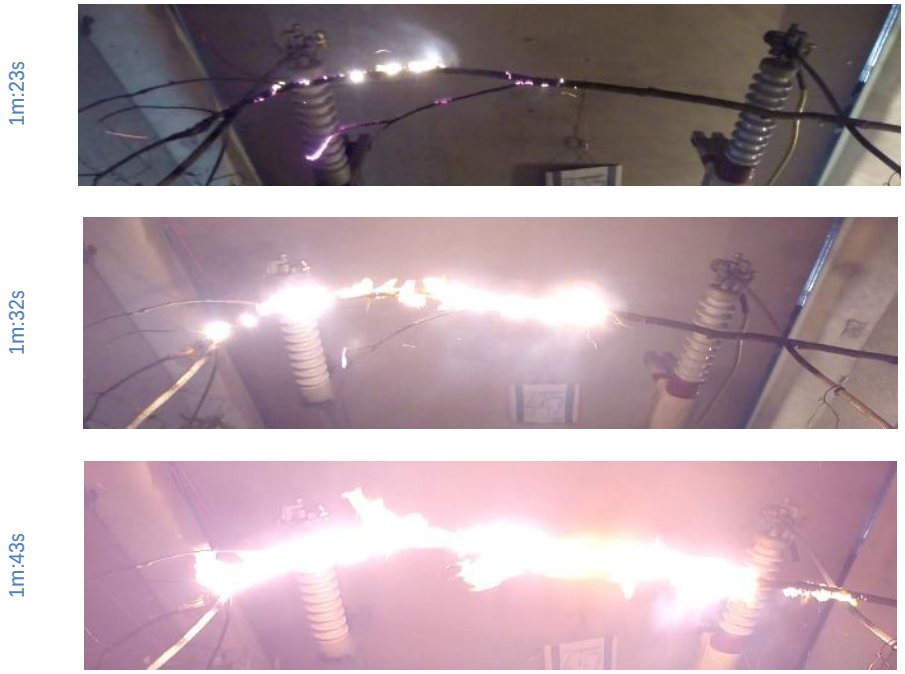

Figure 3: Test 26 - electric arcs jumping through flame to short-circuit part of current path through branch

Laboratory analysis of pre-test samples showed the layers immediately under the bark had significantly higher conductivity than the inner part of the sample. This was supported by post-test examination of samples that showed the core wood was generally only scorched and discoloured but not charred or burned, as shown in Figure 4.

Figure 4: example of intact core wood with destroyed outer layers after a high current ignition test

At moisture contents below about 10-15%, branches did not conduct enough current to ignite. Similarly at low moisture content levels, grass acted as an electrical insulator, taking no current.

Tests to simulate reclose onto a vegetation fault, i.e. where high voltage is restored after a delay, indicated that the physical changes produced by current through the vegetation are irreversible, i.e. when re-energised, the fault current tended to 'take up where it left off' or it went directly to flashover after a very brief delay.

2.3 Findings: fire risk from 'branch touching wire' powerline faults

A total of 389 tests qualified as potentially realistic representations of 'branch touching wire' powerline earth faults. The following findings were derived from these tests:

The initial level of fault current flow in a 'branch touching wire' fault depends on many factors including vegetation moisture content and the level of ionic compounds in the sap, as well as the diameter of the branch.

The levels of initial fault current in most tests were too low by a factor of five to be detected by the powerline protection technologies most currently used in rural Victoria. 'Wire touching branch' faults can therefore only be reliably detected once the fault current has increased and the time taken for this to happen provides opportunity for ember production and hence, fire risk.

The average fire risk in this fault class is shown in Figure 5 as a function of the fault detection sensitivity of the powerline protection system.

With traditional earth-fault detection sensitivity of 5-10 amps on rural powerlines in Victoria, 'branch touching wire' earth faults are certain to produce a fire in worst case conditions. If powerline earth-fault protection systems were to detect and respond to 0.5 Amp faults within two seconds, fire risk in 'branch touching wire' faults in worst case conditions would be reduced tenfold compared to current levels.

Figure 5: probability of a fire versus fault current limit – 'branch touching wire' earth faults

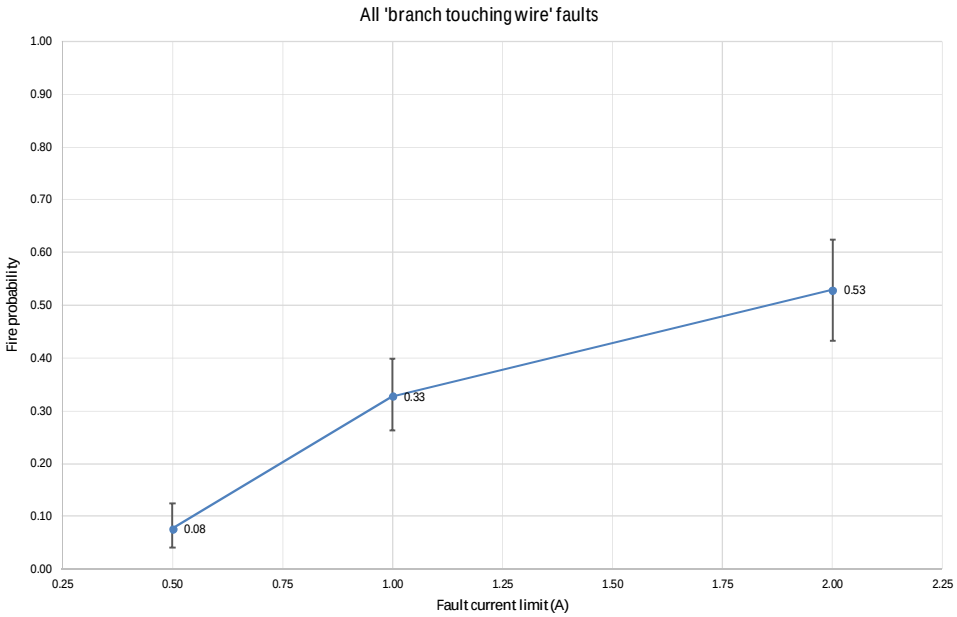

Different species show widely varying fire risk in 'branch touching wire' faults. Of the species tested, the worst fire risk was Willow (Salix Sp.) and the best was Peppercorn (Schinus Molle). Other species tested fell between these extremes. Results with one amp current limit provide the species ranking by fire risk in Table 3.

Table 2: species risk ranking – fire probability for tests with a one amp current limit

Species	Average fire probability
Salix species (Willow)	1.00
Fraxinus Angustifolia (Desert Ash)	0.58
Acacia Mearnsii (Black Wattle)	0.57
Pinus Radiata (Radiata Pine)	0.55
Eucalyptus Baxteri & Obliqua (Stringybark)	0.53
Eucalyptus Viminalis (Manna Gum)	0.50
Acacia Melanoxylon (Blackwood)	0.23
Cotoneaster Glaucophyllus (Cotoneaster)	0.21
Acacia Pycnantha (Golden Wattle)	0.10
Pittosporum Undulatum (Native Daphne)	0.07
Allocasuarina Verticillata (Drooping Sheoak)	0.05
Schinus Molle (Peppercorn)	0.00

Species with high fire risk tend to take longer for fault current to fully develop. Species with faster fault current development tend to have lower fire risk because the fault reaches the detection threshold of powerline protection systems before ember production fully develops. The type of bark on some species appears to have a significant effect on their fire risk in 'branch touching wire' faults.

It was not possible to reliably quantify the influence of sample moisture content on fire risk, mainly due to the large number of independent variables in the ignition tests and Melbourne's mild humid 2014/15 summer.

2.4 Findings: fire risk from 'wire into vegetation' powerline faults

A total of 71 valid tests (51 bush and 20 grass) designed to simulate 'wire into vegetation' powerline faults were successfully completed. Within the limits of certainty set by the smaller number of tests performed, 'wire into bush' faults are likely to have a higher fire risk than 'branch touching wire' faults. If powerline protection systems can detect and respond to an earth-fault drawing 0.5 amps, fire risk from 'wire into bush' faults might be cut by about 80%.

Of the few middle storey species successfully tested, Burgan and Gorse were worse than Blackberry. Silver Banksia appeared to have a lower fire risk. There is considerable uncertainty in these results due to the relatively small number of tests available for analysis.

'Wire into bush' test results tended to be binary: either the fault quickly produced a substantial fire; or it pruned back vegetation without creating significant fire risk, until current ceased to flow. 'Pruning' and 'cooking' outcomes[1] featured in 'wire into bush' tests.

'Wire into grass' tests produced even more binary results: if the grass had enough moisture to conduct current, a flashover to ground occurred almost instantly; if not, nothing happened even when dry grass was pressing against the live wire for an extended period. The fire probability results for 'wire into grass' faults in worst case conditions should be drawn from the results of the 2014 REFCL Trial rather than the tests in this program.

The assessment of fire results in these tests proved much more challenging than in 'branch/wire' faults and a conservative approach was taken wherever there was doubt. To achieve higher levels of accuracy and certainty in fire probability estimates, a revised experiment concept and improved access to a wider range of samples might be required.

2.5 Findings: fire risk from 'branch across wires' powerline faults

A total of 331 valid 'branch across wires' ignition tests was performed on ten upper story species. The rate of growth of fault current was four times faster in 'branch across wires' faults than in 'branch touching wire' faults. The initial current was also 70-80% higher.

If fault currents could be limited to a specific low value by powerline protection systems, fire risk would be lower in 'branch across wires' faults than in 'branch touching wire' faults for the same current limit. However, no protection technology is available today that offers this capability.

Assuming all 'branch across wires' faults progress to flashover whereupon the high voltage would be removed by powerline over-current protection, the fire probability in a 'branch across wires' fault on a real network is likely to exceed 55%. Figure 6 shows the proportion of these tests that resulted in a fire risk that also had durations less than a given number of seconds.

[1] Pruning: the arcs between the high-voltage conductor and the vegetation burned back leaves and twigs to create an air-gap whereupon current ceased to flow. Cooking: the high voltage current heated the bush to the point where it effectively cooked, i.e. lost its structural integrity and flopped away from the conductor, causing current to cease. These effects have been previously reported by A D Stokes in the 1990s.

Figure 6: proportion of fire results versus test duration – phase-to-phase tests without flashover

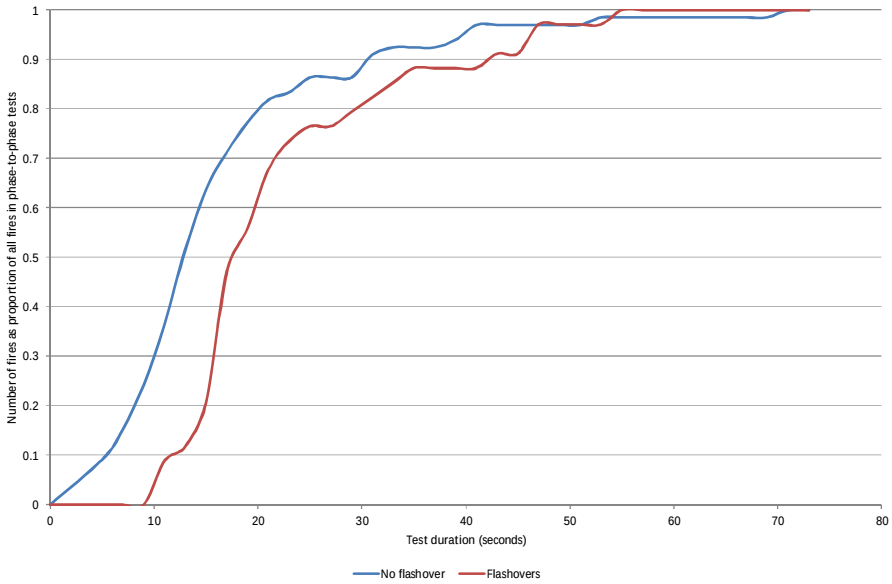

Figure 6 provides a potentially useful guide to the fault detection speed that would be needed to reduce fire risk in 'branch across wires' faults. It indicates that fault detection times longer than about 20 seconds would be unlikely to dramatically reduce fire risk in such faults. Detection and response within about five seconds might be required to achieve substantial reductions in fire risk.

These time scales are much shorter than those that have been demonstrated by high-impedance fault detection schemes developed to date.

2.6 A new data base: vegetation fault signatures

A large data base of fault signature records was successfully gathered during the test program, including low-noise wide-band recordings of network voltage and vegetation fault current. Background network voltage noise recordings were also successfully gathered over a six-week period. The level of broad-band network voltage background noise was about 0.3-0.8 volts, dominated by local industrial load and AM radio stations.

The fault signature data base produced in the test program comprises about 50,000 files totalling more than 300GB of data.

High-frequency voltage disturbances in tests were most commonly caused by very fast step discontinuities in the fault current or by bursts of high-frequency noise in the fault current. The physical processes behind these features are not known, though the discontinuities in current tended to occur more commonly near current zero crossings and high-frequency noise bursts tended to occur at higher values in the 50Hz current waveform.

The high-frequency voltage noise produced during Phase 1 of a vegetation fault was generally much smaller than the total network background noise. However, it could still be seen in test spectrograms, indicating faults might be reliably detected by better signal processing. An example is the 'wire into bush' test shown in Figure 7 below.

One specific proprietary partial-discharge detection system produced records that indicated it may be capable of detecting low-current vegetation faults. It was also confirmed that a specific fault signature detection relay developed for the North American market did not detect any of the 1,038 vegetation faults in the test program.

Figure 7: Test 335 'wire into vegetation' test of Silver Banksia bush

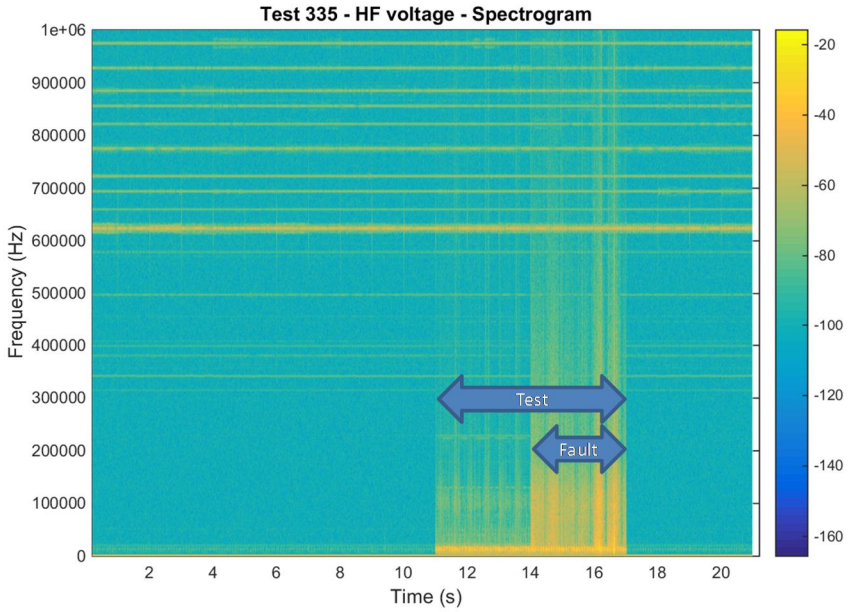

The fault signature data base will be made available in the public domain and provided to equipment suppliers and research teams to stimulate development of improved fault detection algorithms and products.

2.7 The experiment design

The goal of the project was to fully understand ignition that results from conduction of electricity through vegetation. The archetypal fault geometries chosen for the tests were:

- Branch touching wire – branch laid across two high voltage conductors, one earthed and one with full nominal phase voltage applied, i.e. with 12.7kV between them.
- Wire into vegetation – a high voltage conductor energised at 12.7kV dropped into or sitting in earthed vegetation, either grass or a bush.
- Branch across wires – branch laid across two high voltage conductors connected to two separate phases of the incoming high voltage supply, i.e. with 22kV between them.

The rig used to simulate these fault geometries is shown in Figure 8. It was located inside an insulated shipping container in simulated extreme fire weather conditions.

Figure 8: test rig in the ignition test area and arrangement for 'wire into bush' test

To assess comparative fire risk of different species, a high-performance powerline protection system was simulated: the high voltage was removed once a pre-set fault current limit was reached. The choice of current limits in tests was informed by the capabilities of various earth-fault protection technologies applicable to multi-wire powerlines in Victoria. The species with the highest fire probability at the lowest realistic current limit setting was considered 'worst case' for fire risk.

The conceptual model of a fire start was one in which ignition at height produced falling embers to ignite dry grass at ground level. The tests showed production of embers of all sizes, from tiny sparks to sizeable chunks of glowing burned bark or twig. Only embers of significant size that were already well-alight were seen to have the temperature and thermal capacity required to fall several metres through turbulent air and land with enough heat energy remaining to ignite dry grass.

An unambiguous definition of fire risk was developed based on the size and temperature of embers falling to the floor of the test rig. This was applied using infrared video from a FLIR T460 thermal camera. Typical images for an ignition and a non-ignition are shown in Figure 9. The cross-hairs locate the hottest point in the image and show its temperature in the top-left corner of the screen.

Figure 9: thermal images of ignition and non-ignition (false colour: dark patches are water expelled from sample)

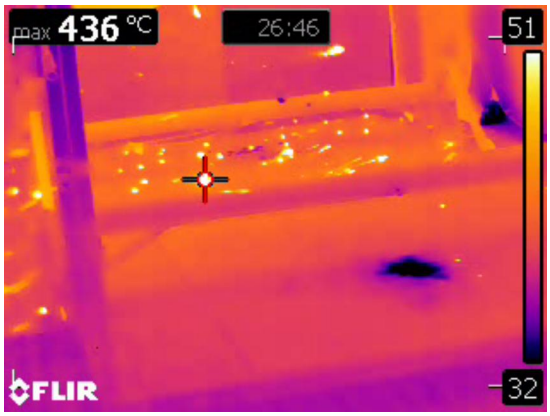

Test 100: clear fire start – embers hotter than 400°C.

Test 101: clear non-fire – embers never exceed 122°C.

The experiment design for collection of fault signatures was much more challenging. After consideration of options, it was decided to perform the tests on a rig connected to a real network via current-limiting resistors. Measurement systems for voltage and current were designed for low noise levels and wide bandwidth.

2.8 The test facility

A temporary test facility was built inside the security fence shared by substations SV (Springvale) and SVW (Springvale West). It comprised a high-voltage supply area, a test rig built into two shipping containers, two cold stores for sample storage and a control hut which was galvanically isolated from other areas of the site. The test facility concept and general layout are shown in Figure 10.

The test facility design embodied safety architecture to ensure not less than three layers of precaution applied for any identified risk. A formal risk due diligence was completed and work practices were agreed jointly with the host network owner United Energy Pty Ltd. All activity on the test site was controlled by an accredited and authorised high-voltage operator.

Vegetation samples were procured from vegetation management contractors on an opportunity basis. Some species proved unavailable and some remained in short supply throughout the test program. The initial concept was that vegetation samples would be harvested continuously throughout the fire season so the effect of hot summer curing of vegetation could be explored. However, the mild 2014/15 Melbourne summer failed to provide any natural 'Code Red' day

samples, though some slight evidence of seasonal conditioning was found in the moisture content analysis results. Only six of 33 test days reached 30°C and only one reached 35°C. To simulate more extreme conditions samples were conditioned at 45°C for 16-24 hours prior to tests.

Figure 10: field test facility concept for vegetation conduction ignition tests

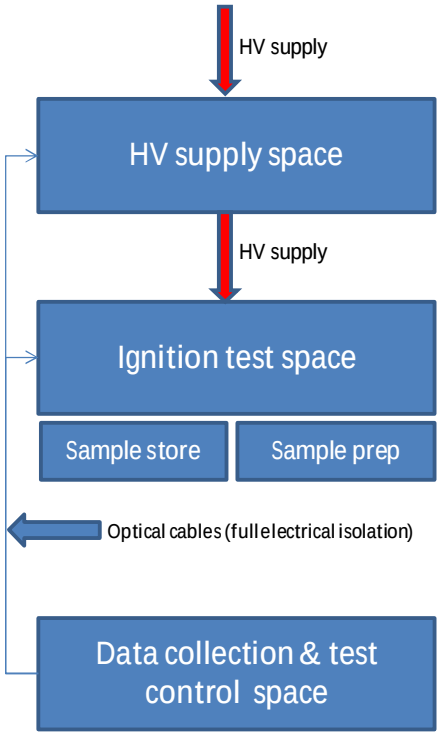

Includes:
- HV supply to site (2 phase)
- HV isolation and earthing (visible to site workers) controlled by optical cable
- Visible warning of HV presence on site
- Earthing to limit step and touch to safe levels on site
- HV current limiting resistor
- ACR with full protection suite controlled by optical cable
- Local protection graded with sub SV

Includes:
- Safety interlock on physical access
- Climate controlled ignition test space
- Controlled air speed
- Two parallel conductors to simulate overhead powerline
- Live wire drop mechanism for 'wire into bush' faults
- 3 phase wide-band voltage divider and digital transducers
- Wideband digital current transducer
- SD video camera
- Optical transmitters for cables to data collection space

Includes:
- PLC controller to automate test run sequence
- Optical cable controls on HV switches and ACR
- Optical receivers for cables from transducers
- Multi-channel high-speed digital data recording
- Video recording
- Test controller and data controller desks
- Team workspace

3 The project

The Vegetation Conduction Ignition Test Program was established by the Powerline Bushfire Safety Program (PBSP) as a limited duration research project.

3.1 Genesis and objectives

In September 2011, the Powerline Bushfire Safety Taskforce (PBST) recommended investment in research to improve knowledge and expertise in options to reduce ignition of bushfires by powerline faults. The Victorian Government accepted this recommendation and established the PBSP, charging it with (among other objectives[2]) identification of high-priority information gaps and administration of a program of research to address these.

In May 2013, the PBSP sponsored a workshop of government and industry stakeholders and research institutions to identify priority research areas. Research into vegetation conduction ignition was identified as a high priority. The PBSP subsequently established the vegetation conduction ignition test program to:

- Better understand bushfire ignition processes in powerline faults that involve vegetation – in particular, identify any 'worst case' species suitable for use in subsequent tests of powerline protection technologies; and
- Create a reference data base of fault signatures for vegetation conduction faults with the aim of supporting development of improved fault detection technologies.

The vegetation conduction ignition tests complement earlier test programs that studied arc-ignition, both in metal-to-metal earth faults near vegetation[3] and in 'wire on ground' earth faults[4].

In detail, the objectives of the vegetation conduction ignition test program were to:

1. Identify the species of trees, bushes and grasses that represent the highest fire risk from electrical conduction;
2. Identify the risk posed by smouldering material or flames due to volatile vapours produced during the conduction of electricity;
3. Identify how this risk varies over a summer period due to the vegetation drying;
4. Identify how this risk varies with wind speed;
5. Record the electrical signatures of many different vegetation contacts and fire starts for future electrical signature recognition research; and
6. Develop a list of worst case vegetation and the test conditions for use in further testing of powerline protection systems.

The vegetation conditions assumed for the testing were those that exist on days of high bushfire risk plus any variations that may be caused by other factors such as long periods of drought.

[2] See www.energyandresources.vic.gov.au/energy/safety-and-emergencies/powerline-bushfire-safety-program

[3] See www.esv.vic.gov.au/Portals/0/About%20ESV/Files/RoyalCommission/HRL%20final%20report.pdf

[4] See www.energyandresources.vic.gov.au/energy/safety-and-emergencies/powerline-bushfire-safety-program/refcl-trial-report

3.2 Governance

The PBSP team was given oversight of the test program with the support of Energy Safe Victoria (ESV) and each of the electricity distribution businesses in the Victorian Electricity Supply Industry (VESI). A Technical Working Group (TWG) comprising technical expert representatives from each of these organisations supported the test program.

Arrangements for project governance are illustrated in Figure 11. The identities of the key roles are set out in Section 3.4 below.

Figure 11: Governance arrangements

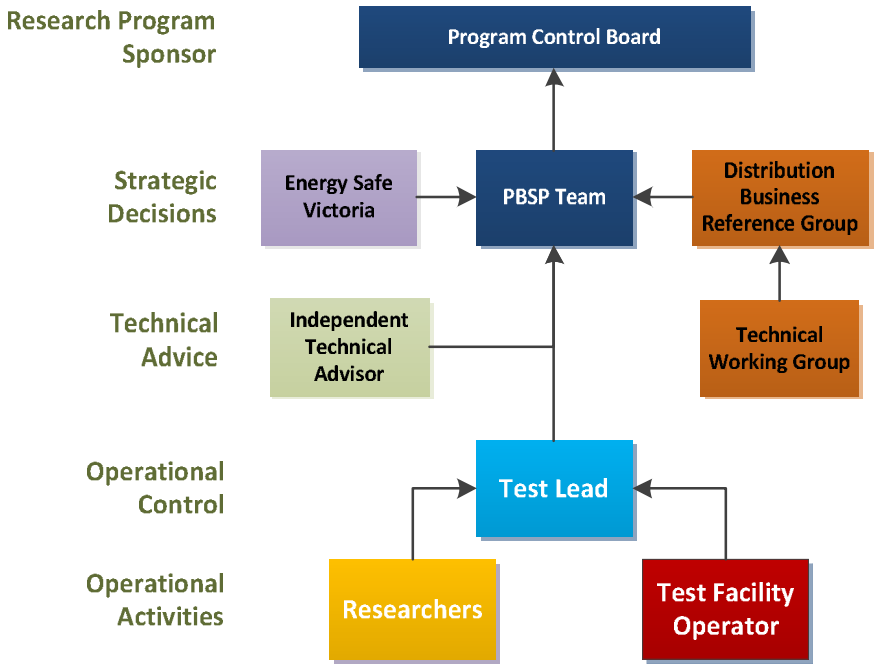

The Test Lead had operational control over the research program, including responsibility for managing consortium partners and direct engagement with the host distribution business for each stage of the testing, although all contracts were made directly with the PBSP team in DEDJTR. The host distribution business, United Energy, had operational decision-making power on all aspects of the work that had potential to affect the broader distribution network and its connected customers.

The PBSP Team, ESV and the Distribution Business Reference Group (DBRG) exercised oversight of activities and results as they emerged and authorised any strategic changes to the research program as required. The PBSP team in turn reported to a multi-agency Program Control Board, which sponsored the research program and was the ultimate decision-maker.

3.3 Project timeline

The test program ran for five months from issue of the Request for Quotation for the position of Test Lead in November 2014 to delivery of the program report in July 2015. The timeline of key project activities is shown in Figure 12.

Figure 12: Schedule of major activities

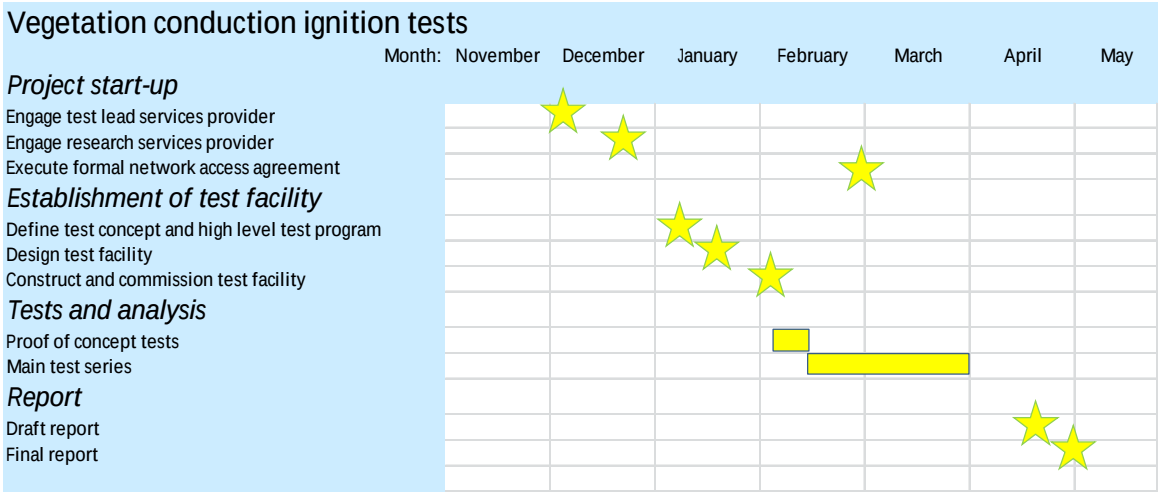

3.4 Project team

The key project team members were:

Role	Name	Affiliation
Program Director	Ashley Hunt	PBSP Director
Project Manager	Kay Charman	PBSP project manager
Independent Technical Advisor	Gary Towns	Facio Pty Ltd
Test Lead	Tony Marxsen	Marxsen Consulting
Test Manager	Blake Stewart	HRL Technology
Network Protection	David Wilkinson	United Energy
Test Controllers	Wayne Highmore, David Falkingham	United Energy (ZNX)
Data Managers	Marc Listmangof, Sam Creek	HRL Technology
Test Rig Operator	Adrian Graves	HRL Technology

The project specification itemised the proposed contents of this report as:

- Project objectives; research methodology; and vegetation selection and preparation;
- Test arrangements and parameters; electrical signatures for the tests;
- Observations of the physical changes in the vegetation and any observed charring, smouldering or flames during the tests; and
- Results and conclusions which will cover the:
    - Time to develop a fire hazard for different vegetation categories and species;
    - Effect that vegetation sample diameter and length of conduction path have on the fire risk;
    - Voltage, current and frequency characteristics; and
    - Effect that vegetation moisture content and wind have on these results.

4 Ignition of vegetation by conduction of high voltage electricity

The vegetation conduction ignition tests confirmed the general features of vegetation faults reported by others[5] at various times over the last few decades. The point of difference between these tests and previous ones was the focus on quantification (with quantified statistical confidence limits) of fire risk from a range of species. Given the improvements in monitoring and measurement technology that have occurred since previous research was undertaken, major additional insights were also gained into the ignition process itself. These insights are summarised here.

4.1 Summary of findings

This section sets out evidence for the more general findings from the vegetation conduction ignition tests, viz. those related to the conduction of fault current and the ignition process itself:

1. The vegetation conduction ignition process follows a consistent sequence of phases: development of full conductor-vegetation contact; expulsion of moisture; progressive charring of bark extending from the thinner end of the vegetation sample; and flashover when flame bridges the high voltage conductors.
2. During the third phase of development of ignition (progressive charring of bark extending from the thinner end of the vegetation sample), electric arcs spontaneously occur in the flame along the branch and this causes large fluctuations in the current flow since such arcs intermittently short-circuit portions of the path between the high-voltage conductors.
3. The range of vegetation moisture content in tests was restricted by the mild, humid summer of 2014-15. Samples were conditioned at 45°C for up to 24 hours prior to most tests in an attempt to produce moisture levels considered to be more realistic for extreme summer fire weather. Conditioning was successful in reducing moisture content but it is not known if this is an accurate reflection of changes that occur in extreme summer weather.
4. Below about 10-15% moisture content, branches do not conduct enough current to cause thermal runaway, i.e. heat generated by the current is balanced by heat loss into the air and sample temperature stabilises at a relatively low level so ignition never develops. Similarly, grasses act as electrical insulators at low moisture content levels, taking no current at all.
5. The range of branch diameter that could be safely tested was limited. Larger sample sizes drew high levels of initial current and the current increased very quickly to reach the pre-set limit in a few seconds at most. On the basis of the test results, it was considered possible that vegetation faults involving larger branch sizes might be rapidly detected, allowing action to be taken before fire risk can arise. However, this could not be tested in this project.
6. Laboratory analysis of pre-test samples supported visual observations that most current flow was in the layers immediately under the bark, known as the Phloem and Cambium layers. These layers had significantly higher conductivity than other parts of the sample.
7. Tests to simulate reclose onto a vegetation fault, i.e. where high voltage is restored after a delay, indicated that the physical changes produced by current through the vegetation are irreversible, i.e. the fault current tends to 'take up where it left off' or it goes directly to flashover after a brief delay.

[5] For example, A D Stokes at the University of Sydney, T R Blackburn at the University of New South Wales, and B Don Russell at Texas A&M University. For details, see Appendix E: Associated research.

4.2 The four phases of a powerline 'branch on wire' vegetation fault

The most frequently performed tests comprised a branch laid across two powerline conductors which were energised to apply a high voltage between the two branch-conductor contact points. When allowed to progress to completion, virtually every such test followed the same four stages of development, generally with some overlap of individual stages. The four stages were:

4.2.1 Phase 1: development of conductor-vegetation contact

As soon as high voltage was applied to the vegetation sample, sparks could be seen at the contact points between the conductor and the sample. Sometimes these sparks were visible for a short distance (typically not more than 100mm) as they were carried away in the wind.

Over a period which might extend for several tens of seconds or might only take a few seconds, each contact point was progressively wrapped in a ball of plasma or flame that extended almost right around the branch above the point where it rested on the conductor. The visual appearance of this process is illustrated in Figure 13.

Figure 13: Test 181 - development of conductor-branch contact in Phase 1

After 8 seconds - sparks

After 11 seconds – plasma/flame 'ball'

Since plasma and flame are conductors, this development provided a much larger contact area for the current to enter the branch. As the effective contact area increased, the fault current also increased to reach a 'first maximum' value. Examples of extended current entry into the thick end of the sample (evidenced by dendritic burn marks) are shown in Figure 14:

Figure 14: evidence of current entry over an extended area via plasma/flame

The increase in fault current during Phase 1 is shown in Figure 15. It usually took around 10-15 seconds for the current to build to its first peak, though in extreme cases, it could take more than a minute.

Figure 15: Tests 426 and 407 - typical variation of current in phases of vegetation fault development

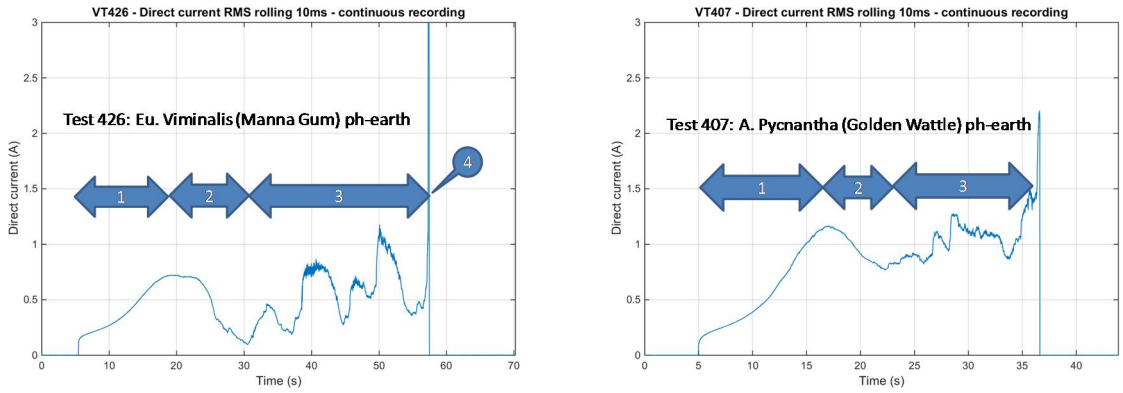

Tests in which current was interrupted during Phase 1 almost never produced fire risk.

4.2.2 *Phase 2: expulsion of moisture*

Following the first peak of current, the most noticeable feature of many tests was the expulsion of moisture from the sample in the form of steam and water, often accompanied by a very loud[6] continuous whistling or squealing noise. Jets of steam could sometimes be seen issuing from the branch. In some tests, a stream of water could also be seen falling from the sawn end of the sample as can be seen in Figure 16.

Figure 16: Water expulsion in Phase 2

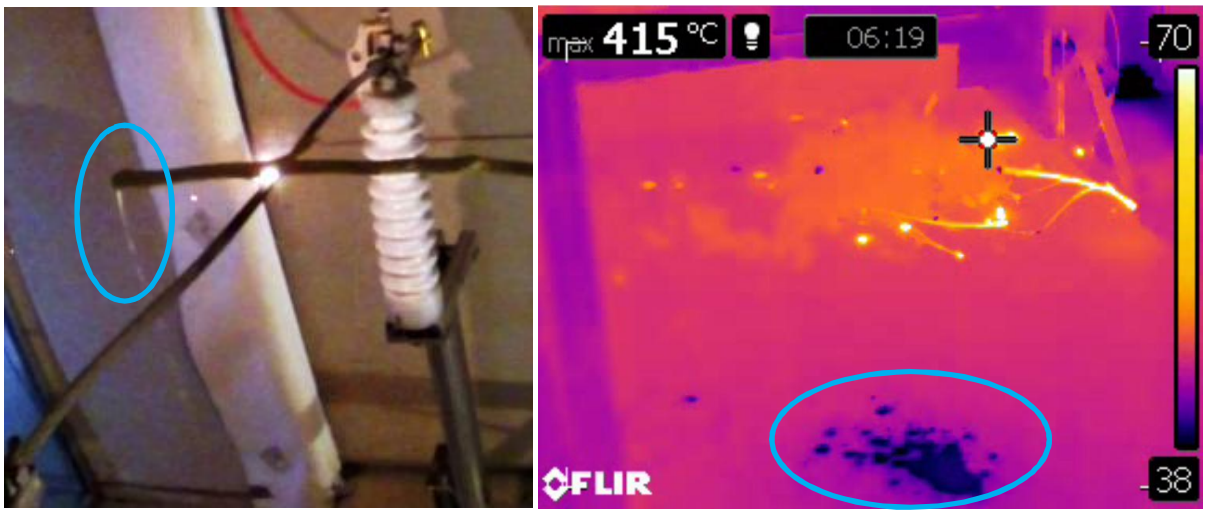

Test 33: stream of water falling from sample end Test 275: IR video shows water spatter fallen from sample end

Post-test examination of samples indicated the loud squealing noise may have resulted from expulsion of steam through small splits in the tough outermost layer of bark. In a few tests of Pinus Radiata (Radiata Pine) and Schinus Molle (Peppercorn) violent steam explosions occurred late in Phase 3 of the test, releasing hot water from the wooden core of the sample onto the test rig floor.

[6] This noise was usually audible across the test site despite the test being contained in a closed, fully insulated shipping container.

During the expulsion of moisture in Phase 2, the current plateaued and even showed a substantial decline from its first peak before Phase 3 commenced - as illustrated in Figure 15 above. Tests did not normally terminate in Phase 2 as the current had already peaked, i.e. if a test did not reach the pre-set current limit before the decline of current started in Phase 2, it usually continued into Phase 3.

4.2.3 Phase 3: progressive charring extending from the thinner end

After moisture expulsion started to fade, flame slowly spread along the branch from one or both ends. This process is illustrated in Figure 17 which shows the progression of Phase 3 in a phase-to-earth test of a Manna Gum (Eucalyptus Viminalis) sample.

Figure 17: Test 447 - progressive spread of flame from one end of the branch to the other (flashover at 1m: 44s)

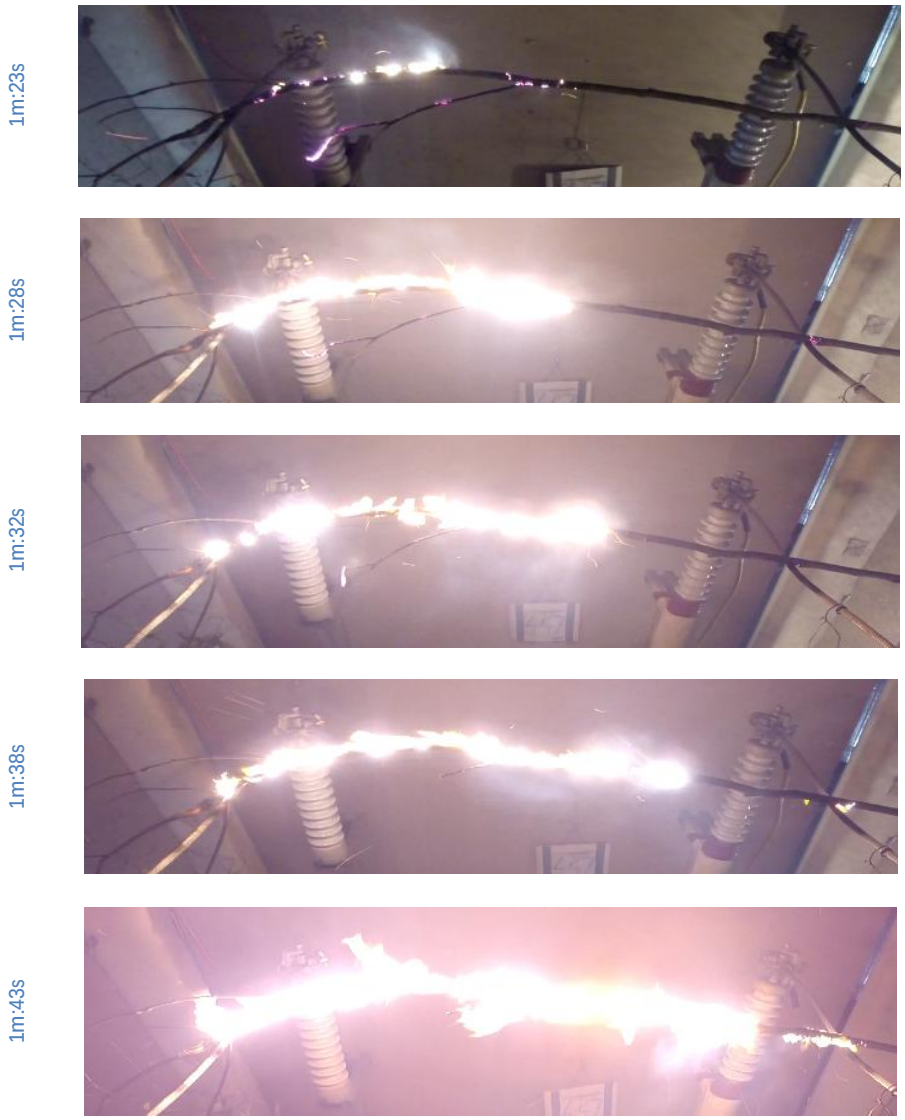

Generally, this occurred from the thinner end towards the thicker, presumably because of factors such as:

- Higher resistance of thinner sections generated more heat from the same current; and

- Lower mass of thinner sections meant a higher temperature increase for the same amount of heat.

Occasionally a test would show multiple break-outs of flame along the length of the sample rather than a steady progression from one end. Some of these tests gave a strong visual impression of a layer of arc or flame just below the external surface of the bark. This was consistent with moisture and conductivity test results (see Section 4.4.2 below) showing the outer layers of samples had slightly higher moisture content and significantly higher conductivity than the average taken across a full transverse section of the sample.

Post-test examination showed the spreading of Phase 3 flame was associated with progressive charring of the bark. In many tests, this charring did not seem to penetrate the core wood of the branch to any significant degree, though it often completely burned through smaller branchlets and twigs. As Phase 3 progressed, small pieces of burning bark and twigs could often be seen to break off and fall, creating potential fire risk. This propensity to shed burning embers varied by species.

As more and more of the branch became covered in flame, intermittent electric arcs would sometimes appear in the flame. These would short-circuit the burning section of branch as shown in Figure 18, causing large fluctuations in the current - as can be seen in Test 426 in Figure 15 above.

Figure 18: Test 26 - electric arcs jumping through flame to short-circuit part of current path through branch

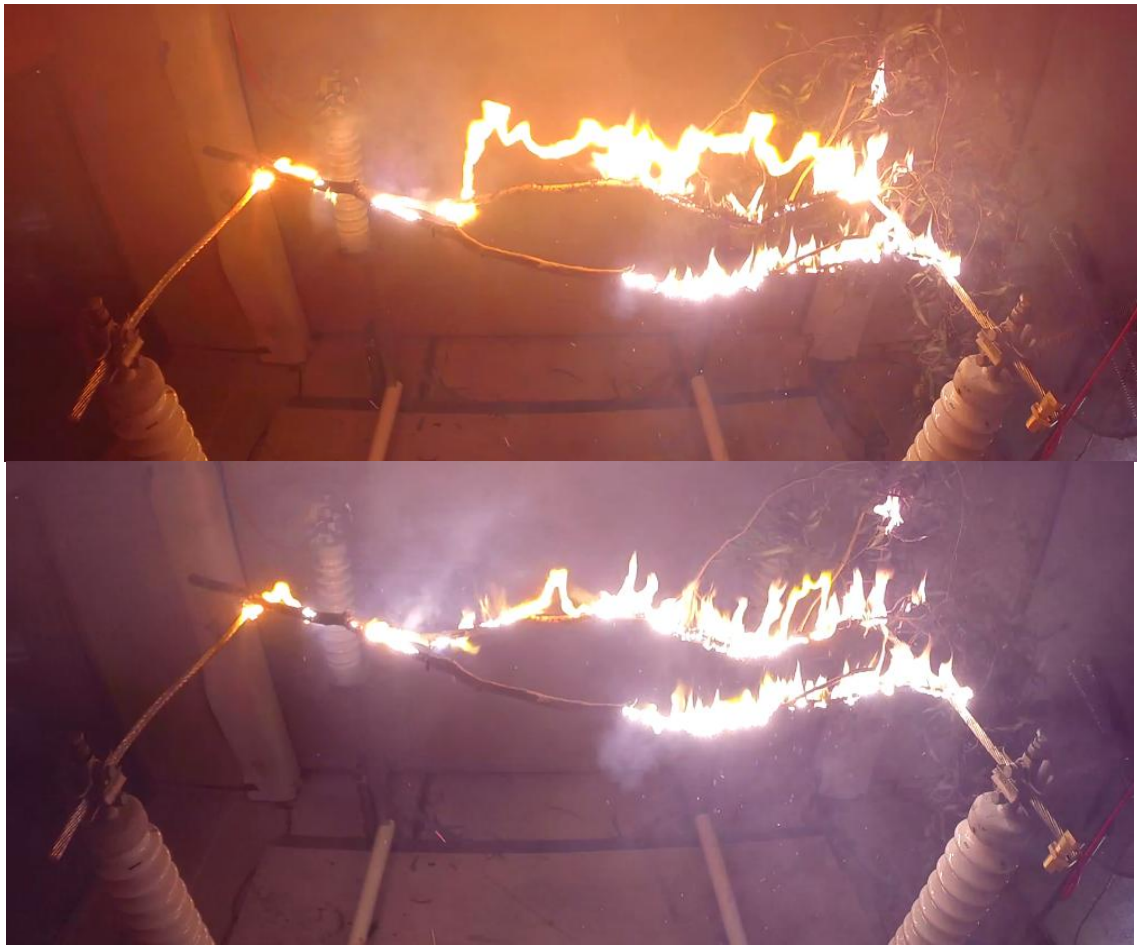

As the section of non-burning branch became smaller, the current increased at an increasing rate.

4.2.4 Phase 4: flashover

As soon as the flame extended from conductor to conductor in an unbroken path, flashover occurred and the current went to the maximum value allowed by the 200Ω high voltage resistors in each phase of the supply – 45 amps in phase-to-phase tests and 65 amps in phase-to-earth tests.

Figure 19: Test 7 phase-to-phase test current waveform – transition to flashover

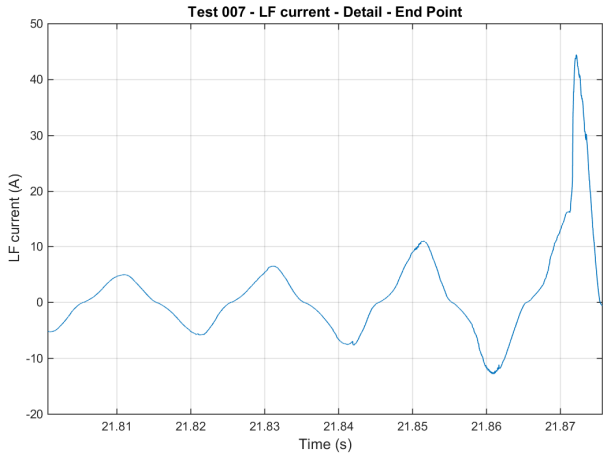

Figure 20: Test 7 - RMS value of flashover current

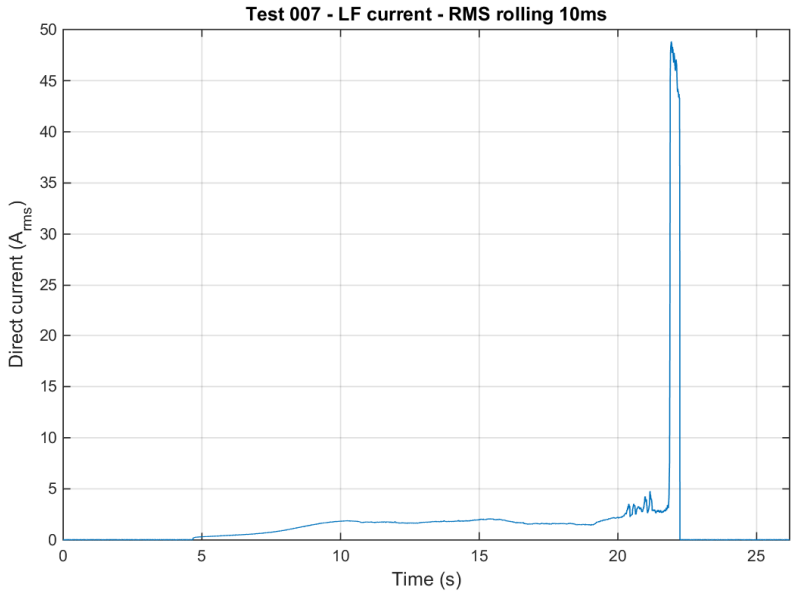

In the great majority of tests, a pre-set current limit was applied, i.e. the rig HV supply switch was automatically opened when current reached a pre-set value, usually 0.5, 1.0, 2.0 or 4.0 amps. Such tests often ended during Phases 1 or 3 (in Phase 2, current often declined before increasing again in Phase 3). Flashover was only routinely entertained in tests performed to study the complete fault development process.

4.3 Pruning and cooking faults

Observations by A D Stokes in past research projects at Sydney University were also seen in some tests:

- Pruning faults: some 'wire into vegetation' faults resulted in the leaves and twigs close to the high voltage wire being burned off whereupon the current ceased. In effect, the high voltage had pruned back the bush until there was sufficient clearance to stop current flow.
- Cooking faults: 'branch touching wire' and 'branch across wires' faults sometimes resulted in the branch being effectively cooked – the branch heated up, lost its structural integrity, went limp and fell off the test rig, ending the test. Similar branches of the same species were sometimes subsequently fastened to the high voltage conductors with copper wire to prevent them falling. This was based on the hypothesis that if the branch were longer it would stay in contact with the high voltage despite the cooking process.

4.4 Influencing factors

Three factors that influence the development of a vegetation fault were explored:

- Wind
- Moisture and conductivity
- Branch size.

Each of these is discussed briefly below.

4.4.1 Wind

The initial ignition event in powerline vegetation conduction faults usually occurs at height – either eight to ten metres above ground for a branch/wire interaction or 0.2- 1.5 metres above ground for a 'wire into vegetation' fault. Vegetation at both these heights experiences significant wind on days of extreme fire danger. The analysis of Black Saturday meteorological records in the 2011 PBST arc-ignition[7] research estimated 10kph as worst case (i.e. lowest) wind speed at 0.5m height. Page 43 of the report contains the additional estimate of worst case 20kph wind speed at ten metres height.

Wind has a number of countervailing effects on ignition, all of which have been demonstrated in previous research. It:

- Increases the supply of Oxygen and by doing so can fan small flames into larger ones;
- Disperses flammable gases produced by heat-induced pyrolysis which can prevent ignition;
- Reduces fuel temperature (towards 45°C in these tests), which can extinguish a fire.

In the context of powerline vegetation faults, wind also affects whether ignition at height will lead to fire risk at ground level. It influences ember production and shedding and if strong enough, it can blow a burning branch off a powerline causing it to fall into vegetation below.

The presence of wind was considered in the design of the experiment and rig. The test program was carried out with fan-induced 45°C airflow sufficient to cause visible disturbance to leaves and twigs similar to that often observed in high fire risk weather[8]. In the tests reported here, wind was

[7] Lowest wind speed is worst case. See HRL Technology Pty Ltd, *Probability of Bushfire Ignition from Electric Arc Faults*, December 2011 (www.esv.vic.gov.au/Portals/0/About%20ESV/Files/RoyalCommission/HRL%20final%20report.pdf)

[8] Consistent with 15-20kph according to standard indicators for assessment of wind strength against the Beaufort Scale.

simulated using a large pedestal fan directed at the ignition test space. Airflow in the test space was turbulent and circulatory as it was not possible to arrange laminar flow without excessive heat loss from the test rig container. The achievement of worst case temperature (45°C) in the ignition test space was given higher priority than achievement of a particular airflow pattern.

Spot checks revealed airflow in the test rig container reached about 10-15kph with considerable variation depending on the location of the sensor and the extent of foliage on the sample. Fan performance was not entirely consistent over the full series of tests and the effect of air speed variations on fire risk appeared somewhat random. Tests with completely still air sometimes produced more embers than tests with wind, whereas in other tests the reverse was observed. Systematic investigation to quantify the effect of wind speed would have required more tests than were possible in the test program and it was not attempted.

4.4.2 Moisture content and conductivity

The initial concept of the vegetation ignition test program was that vegetation samples would be continuously harvested throughout the fire season so the effect of hot summer curing of vegetation could be explored. This proved not possible – the summer of 2014/15 was mild and humid with frequent showery weather and very few really hot days as illustrated in Figure 21 and Figure 22 which show only six of 33 test days had ambient temperature above 30°C and only one reached 35°C.

Figure 21: ambient temperature over period of testing (test days only, data for 19 Feb pm missing)

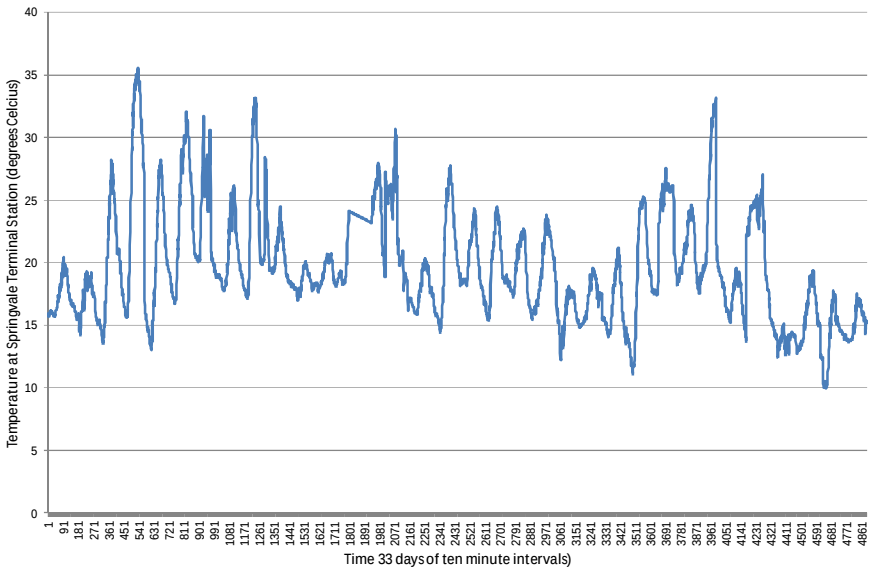

Figure 22: six test program days that reached 30 degrees

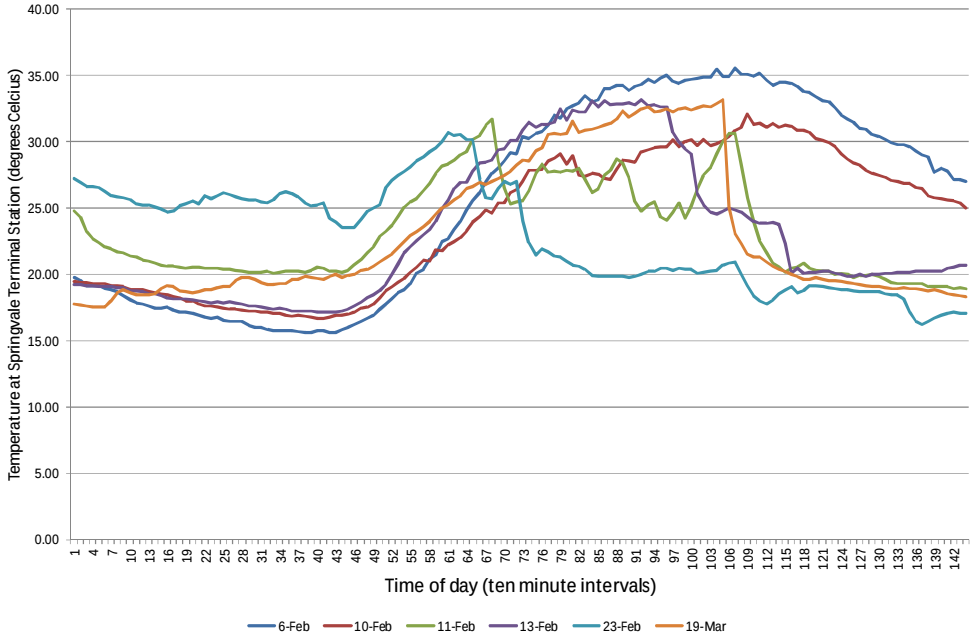

The summer failed to provide any natural 'Code Red' day samples, though some slight evidence of seasonal conditioning was found in the analysis of moisture content results as shown in Figure 97 on page 102.

To generate material variation in moisture content in the early proof-of-concept tests, samples were conditioned at 45°C for periods ranging from 15 minutes to 170 hours before an ignition test. In the main test series, overnight conditioning (16-24 hours) became the norm. Conditioning produced visible changes in some samples – outer green layers became thinner, leaves first became limp then brittle. Later in the test program, samples of deciduous species were starting to lose their leaves (even before conditioning) due to the onset of autumn.

Immediately before each test, a short length was cut from the end of the sample and sent in a sealed bag to the HRLT laboratory where a transverse section was cut from the sample for moisture analysis. Figure 96 on page 101 shows the distribution of moisture analysis results over the whole test program. It mostly varied between 30% and 50% and as shown in Figure 98 on page 102, the average moisture content for each species tested varied from 32% to 46% except for Schinus Molle (Peppercorn) which reached an average of 52%.

Review of test videos indicated the factors that most directly influenced ignition probability were likely to be primarily located in the outer layer of the sample– the Bark and immediately below it, the Phloem and Cambium layers.

Measurement of the moisture content of these outer layers proved a challenge as accurate moisture and conductivity analysis requires a certain minimum mass of material. However, enough measurements were successfully achieved (see Figure 23) to show a slight concentration of moisture in these layers and a much more significant concentration of ionic compounds, i.e. those which combined with water can carry electric current.

Figure 23: sample transverse profile – moisture and conductivity

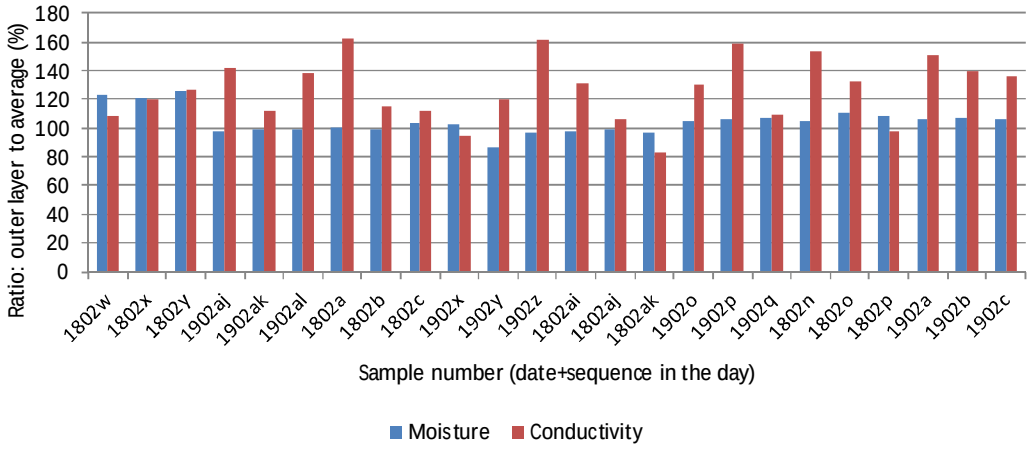

The transverse profile analysis covered four species and the average ratios are shown in Figure 24.

Figure 24: variation in transverse profiles of species tested

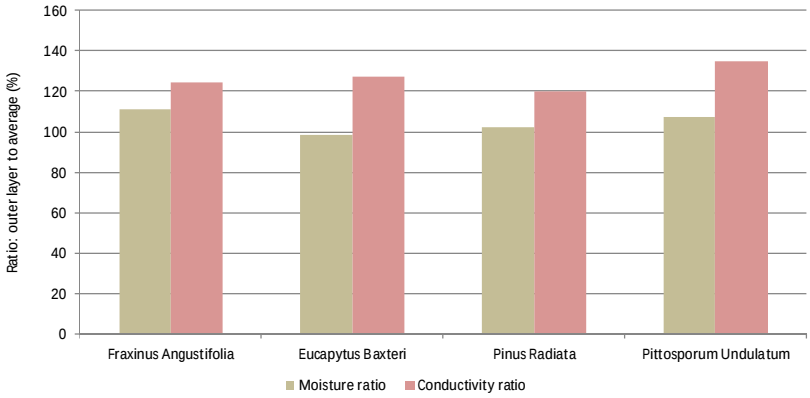

Visual examination of samples after particularly severe tests tended to confirm that the core wood was less involved in the ignition process than the outer layers. Even in severe tests, the revealed core wood was often seen to be intact, even if somewhat discoloured. Two examples are shown in Figure 25.

Figure 25: examples of intact core wood with destroyed outer layers after high current ignition tests

The concentration of current in the outer layers of the samples seemed more complete than the transverse conductivity profile alone could explain, though the measurement of this profile involved a degree of averaging of results which may have masked more dramatic differences of conductivity between layers. It is also possible the longitudinal water transport structure of the wood produces an anisotropic conductivity characteristic that limits the flow of current deeper into the branch. However, this hypothesis was not able to be tested in this project.

4.4.3 Branch diameter

Larger branches were discounted as fire risks based on a series of tests of larger diameter samples of different species in the early proof-of-concept tests. The samples are shown in Figure 26.

Figure 26: larger diameter samples tested in proof-of-concept tests

The large diameter samples drew too much current to be fully tested within the 20 amps capability of the test facility. Typical test results for larger diameter 'green' samples are shown in Figure 27.

Figure 27: typical test results for a large (80-90mm) diameter samples (Test 31 Manna Gum and Test 32 Blackwood)

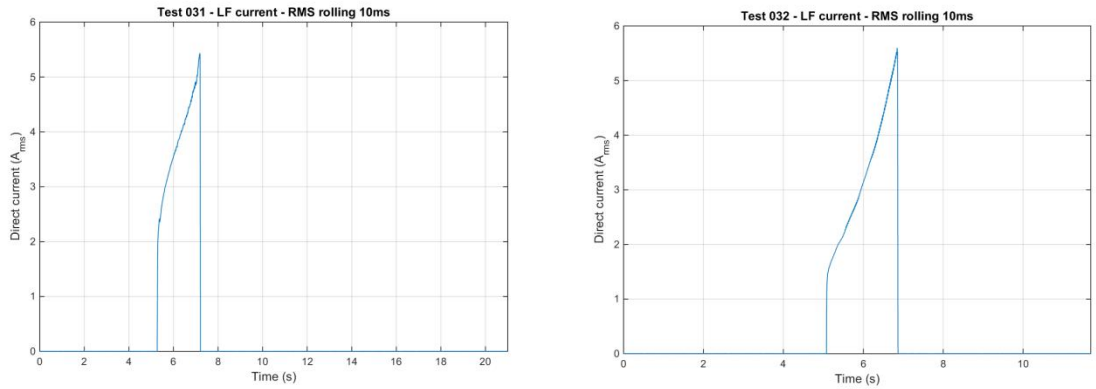

The tests illustrated in Figure 27 indicated that the current in tests of larger samples would very quickly exceed the safe rating (20 amps) of the test facility.

A second attempt to test a large diameter sample used a Manna Gum sample pre-conditioned for more than 128 hours in 45°C atmosphere. This lowered the moisture content from 46% in Test 31 shown above to 18% in Test 46 shown below. Whilst both the initial current and the rate of current growth in Test 46 were somewhat lower (see Figure 28), it was clear the test was still likely to exceed the 20 amp capability limit if allowed to fully develop. It was concluded the test current would be likely to exceed the 20 amp limit before the current peaked at the end of Phase 1, i.e. before any significant ignition process got underway.

Figure 28: Test 46 large diameter Manna Gum sample conditioned for 128 hours

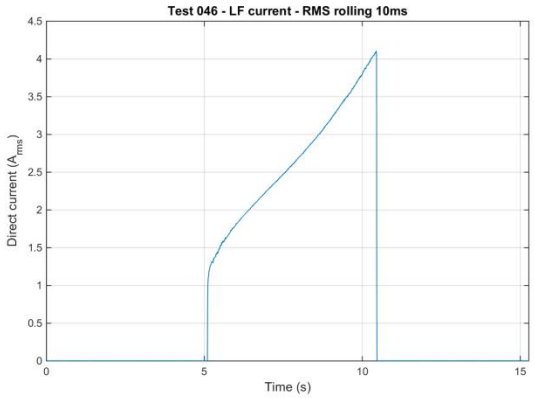

In a real network fault, the heating of a large diameter branch caused by such high current levels[9] might produce a series of steam explosions or a flashover with little fire risk. However, this hypothesis could not be tested in this project. Certainly, the fault may be likely to be quickly detected even by existing powerline protection systems, possibly before any major fire risk could arise.

After consideration of the results for large diameter samples, sample suppliers were asked to provide samples with a nominal diameter of 25-30mm. The distribution of sample diameters in the main test series is shown in Figure 101 on page 104.

[9] Assuming uniform heating, a current of 20 amps at 13kV delivers 260,000 watts which would raise the temperature of a 5kg branch of wood (including the 40% moisture content within it) from 45°C to 110°C in about two seconds.

4.5 Reclose onto a vegetation fault

Tests were performed to see whether the fault development phases described in Section 4.2 above were repeated if high voltage was re-applied after a delay. The tests showed that those sections of Phase 1 already experienced were not repeated, indicating that physical changes in the vegetation during Phase 1 may be permanent. This means that upon reclose, a fault would be detected much faster because the current starts at a higher level.

Consecutive tests at 1.0, 2.0 and 4.0 amp current limits were carried out on a single sample of Pittosporum Undulatum (Native Daphne) of 35mm diameter and 37% moisture content. Figure 29 implies the results can be stitched together to form an entire Phase 1 current development curve. The current in each test appeared to 'take up where it left off' in the previous test.

Figure 29: Tests 862 to 864 – consecutive tests on a single sample of Native Daphne

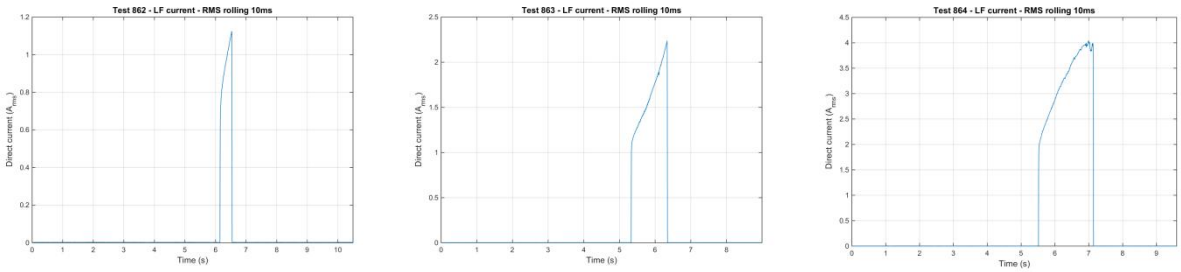

Current in tests 862, 863 and 864 'stitched' together on common vertical and horizontal scales:

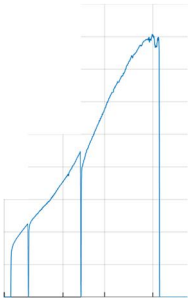

Tests 51 and 52 (Figure 30 below)were phase-to-phase tests performed on the same sample (one with 45mm diameter, much larger than normal), i.e. simulating a reclose with a very long delay setting (3-5 minutes). The tests demonstrated that the initial current level in the reclose event (Test 52: 3.4 amps) was closer to the final current (4.05 amps) in Test 51 than to the initial current (1.1 amps).

Figure 30: reclose test – 45mm Manna Gum, first and second 'shots'

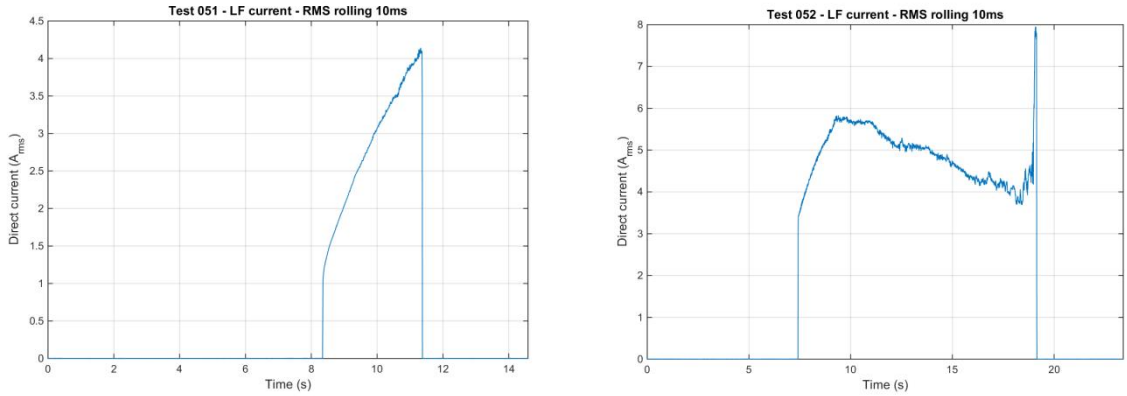

Similar observations were recorded in current-limited phase-to-phase tests on a large diameter (90mm) fully conditioned sample as shown in Figure 31. The effect was somewhat less (perhaps half) than that observed in tests on smaller samples, implying less physical change in the wood.

Figure 31: reclose tests on large diameter sample conditioned for 128 hours

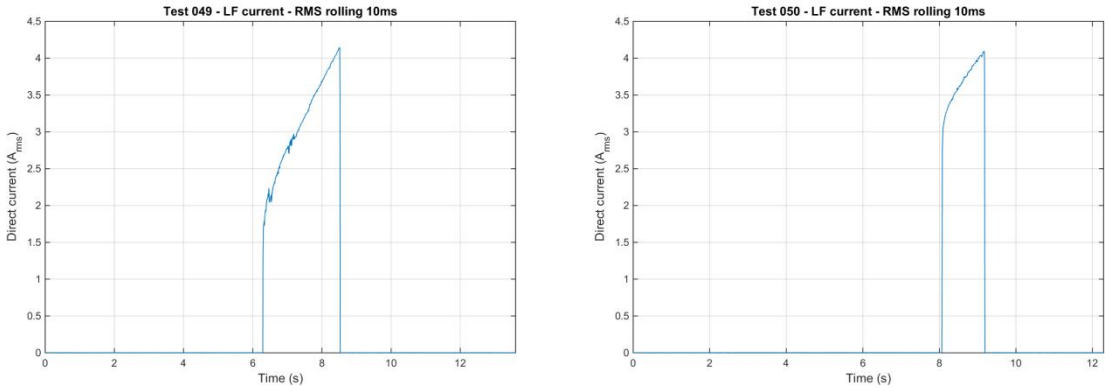

The results for other phases of fault development were not as clear as they were for Phase 1 – the current on reclose simply seemed to move very quickly from a steady value direct to flashover.

For example, in phase-to-phase Tests 44 and 45 (Figure 32 below), typical Manna Gum samples were subjected to the equivalent of reclose after 10 seconds and 20 seconds respectively. Although the original current development to flashover took 27 seconds in Test 44 and 72 seconds in Test 45, 'time to flashover' in the reclose events was only 1.2 and 0.8 seconds respectively. The initial current upon reclose was also higher than the initial current in the original fault.

Figure 32: reclose tests 44 and 45 – 30mm Manna Gum samples

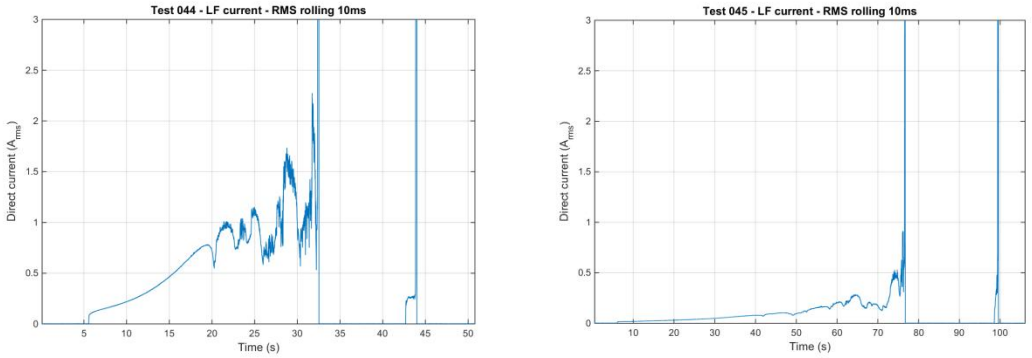

Tests 44 and 45 reclose events:

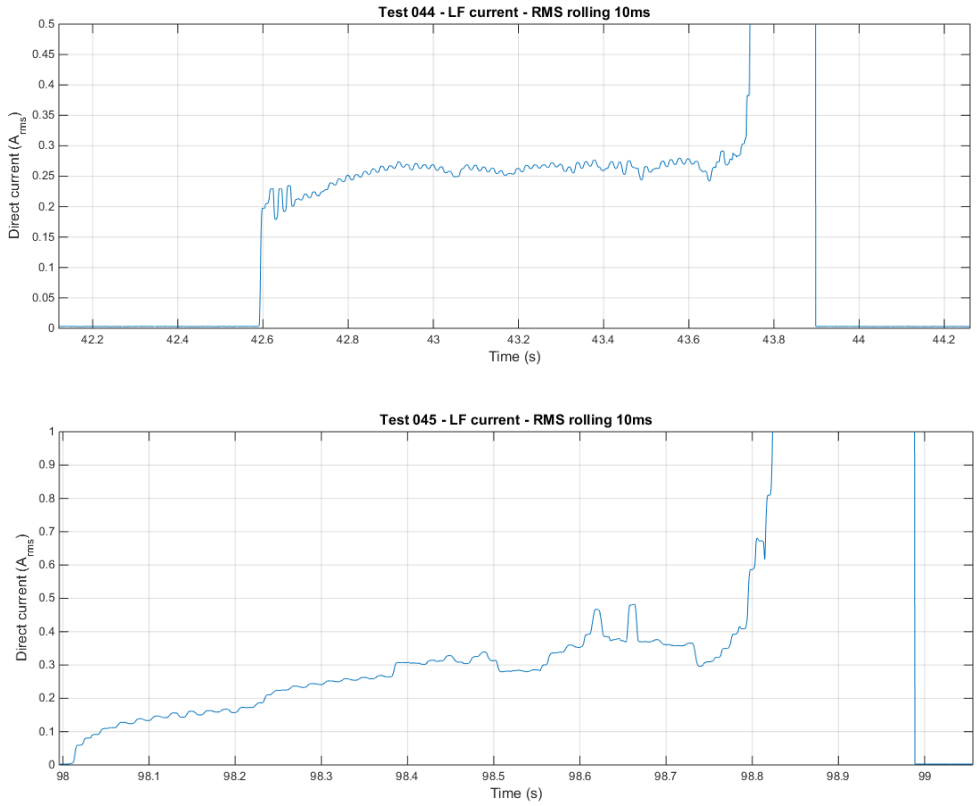

In summary, the test results indicate that a permanent fault may be detected much more quickly on a reclose than when it originally occurred.

5 Ignition of a bushfire by a powerline vegetation fault

All powerline fires start with a very small local ignition event. For a bushfire to occur, this initial ignition has to spread to sufficient fuel to support a sustained and growing fire.

5.1 Conceptual model of a bushfire start

In most bushfires started by powerline faults, the fuel for the fire start is thought to be the dry grass located at ground level below the powerline. Even though initial ignition may occur at the height of the conductors (typically eight metres above ground), reports of ignition of a bushfire at height are not common in powerline fire statistics. At eight metres height there is usually limited dry fuel (generally twigs and leaves have to be green to conduct electricity and ignite) so embers must travel to dry fuel located elsewhere for a fire to start. The most commonly recognised fire-start mechanism is for embers to fall into dry grass below the line.

This conceptual model of a fire start has guided the development of fire probability measurement in the vegetation conduction ignition test program described in this report. Some risk factors were not included in this investigation. These included the comparative tendency of particular species to shed limbs or fall over near powerlines in high fire risk weather conditions.

5.2 Achievement of rigour in fire risk test results

Review of test videos revealed how difficult it was to be completely certain of the ignition result in some tests, though the result in most tests was clear-cut.

5.2.1 Fire risk criteria for 'branch on wire' tests

The tests showed production of embers of all sizes, from tiny sparks to sizeable chunks of glowing burned bark or twig. The smallest embers were observed to burn to a cinder in a very short time, often travelling only a few centimetres before becoming a rapidly cooling black speck or burning up entirely. Only embers of significant size that were already well-alight were seen to have the temperature and thermal capacity required to fall several metres through turbulent air and land with enough heat energy remaining to ignite adjacent dry grass.

For ignition of dry grass and other ground-level vegetation, a falling ember must have enough thermal mass to heat the vegetation to a temperature above that vegetation's ignition temperature. The lowest ignition temperatures in published investigations[10] are for dry grass at around 250°C.

To provide an unambiguous definition of a fire risk in the vegetation conduction ignition tests, the following rule was applied:

A test was taken as having resulted in a fire if:

- Embers fell to the floor of the test rig and remained glowing for at least a second; and
- If the embers were small, e.g. small leaves, ember temperature exceeded 350°C; or
- If the embers were large, e.g. burned twig, ember temperature exceeded 250°C.

These rules were applied by reviewing infrared video produced by the FLIR T460 thermal camera in each test. This camera was focused on the floor of the test rig below the sample. Typical images for an ignition event and a 'near miss' (an event close to, but not quite ignition) are shown in Figure 33. The cross-hairs automatically locate the hottest point in the image and its temperature is shown in

[10] See Table 1 of www.esv.vic.gov.au/Portals/0/Consumers/Files/BushfireIgnitionReview.pdf

the top-left corner of the screen. For a temperature reading to be accepted as reliable, it was generally required to persist for two or more frames of the video.

Figure 33: thermal images of ignition event and 'near miss' (false colour: dark patches are water expelled from sample)

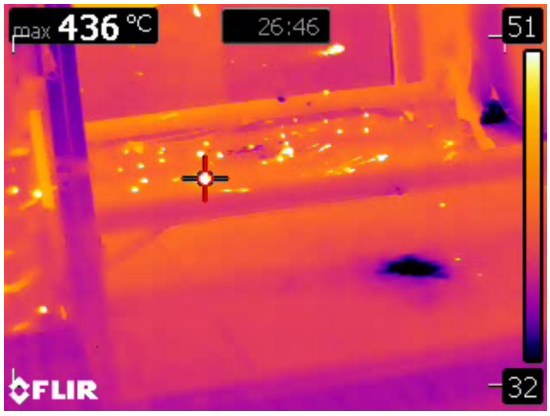

Test 100: clear fire start – embers hotter than 400°C.

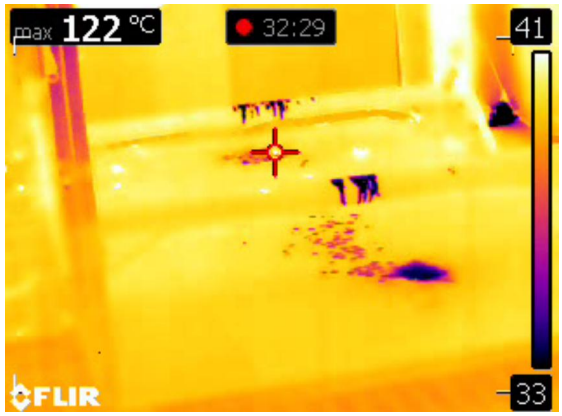

Test 101: clear non-fire – embers never exceed 122°C.

Test 222: 'close' fire start – embers hotter than 250°C.

Test 986: 'near miss' – embers below 250°C.

Clearly defined criteria and the use of the infrared camera simplified the challenge of reliable discrimination between ignition leading to real fire risk and ignition with no real fire risk.

5.2.1 Fire risk criteria for 'wire into vegetation' (bush and grass) tests

The goal of the project was to fully understand ignition that results from conduction of electricity through vegetation. In the case of simulated 'wire into vegetation' faults, i.e. 'bush' and 'grass' tests, this was a challenge as:

- The conceptual model of a bushfire start from a 'wire into vegetation' test was less clear; and
- A common test outcome was a flashover from the live conductor to earth with the consequential 65 amp arc immediately igniting all adjacent vegetation.

It was not possible to establish precise unambiguous rules to distinguish fire results from non-fire results for these tests. Complications included:

1. Bush tests: these often resulted in flashover to earth which potentially invalidated the test as a vegetation conduction ignition test. Some bush tests produced few embers while in others the whole bush seemed to rapidly increase in temperature to more than 250°C. Some understory species which were originally intended to be tested in bush tests were instead

tested in 'branch touching wire' tests as the samples provided were of sufficient length to allow this.

2. Grass tests: the results tended to be binary – either there was enough current to rapidly cause a flashover (sometimes in microseconds), in which case the ignition was caused by the arc[11], or there was no current at all despite vegetation being in solid contact with the live conductor with the result that nothing happened in the test.

Faced with this complex mix of factors, the research team derived fire results in bush and grass tests from close review of both visible light and infrared video of each test, informed by the test current profile which revealed the presence and timing of any flashover to earth that occurred. Ember production and sustained flaming were taken as evidence of a fire start.

5.3 What makes a species 'worst case' for powerline fire risk

The worst case species for fire risk is not simply the one that ignites most readily when exposed to high voltage. In real powerline faults, two factors must be considered to define worst case:

1. How likely is the fault to start a fire before the power is cut; and,
2. How hard is it to detect the fault so power can be cut before a fire can start?

The first factor is all about ignition from conduction of electricity through vegetation, but the second is about the conduction alone, i.e. the current the fault draws from the network. A fault that draws high current will be detected quickly, perhaps quickly enough to prevent a fire.

It is natural to ask 'how long does ignition take to occur?' as a first step in development of a powerline fire prevention approach. Indeed, this question was implied in the specification of contents for this report (page 20). However the vegetation conduction ignition tests revealed the really useful question in fire prevention is rather: 'regardless of how long it takes, will ignition occur before the powerline protection system can act to remove the voltage on the conductor?'

The reality is that 'time to ignite' is variable and hard to measure or characterise with any accuracy:

- If current flows through the vegetation and the conductors remain at high voltage, the fault will eventually go to flashover. The time this takes varies widely and flashover may not always involve fire risk[12].
- The production of falling embers can take place even after the high voltage is removed because the fire (at height) started by the current can continue to burn, i.e. time to (ground level) ignition is not always directly related to timing of the network response to the fault.
- If ignition is prevented by removal of the high voltage by the powerline protection system before the current rises to a level where significant embers can be produced, it doesn't matter how long this increase in current takes to occur, no fire will result.

To take 'time-to-ignite' out of the definition of worst case, the tests were run with high voltage removed as soon as the current reached a pre-set limit, regardless of how long this took. The probability of fire was then plotted against this current limit. This was seen as directly related to the type of powerline protection that might respond to vegetation faults earth faults. The 'worst case' species is then the species with highest fire probability at a particular (lowest detectable) fault current cut-off level. This view is reflected in the charts set out in Sections 6 and 7 below.

---

[11] Arc-ignition of grass in 'wire on ground' faults is fully covered in the report of the 2014 REFCL Trial.

[12] Over the whole test program, 44 tests progressed to flashover without creating a fire risk. However, flashover current was limited to 45 amps and interruption of this current was very fast (<100ms).

6 Ignition in 'branch touching wire' earth faults

When a tree branch touches a live high voltage conductor, current flows through the branch to the tree trunk and down to earth via the tree roots. The bulk of the tree acts as a series resistor of much lower value than the resistance of the branch, especially the thinner sections that might be touching the live conductor. In this test program, 'branch touching wire' faults were simulated by earthing one of the two conductors upon which the branch was laid and the tree trunk was represented by the 200Ω resistor in series with the high voltage supply[13]. The distance between conductors in all 'branch touching wire' phase-to-earth tests was 1.5 metres.

A total of 476 valid phase-to-earth tests were performed on twelve 'upper story' species as shown in Figure 34.

Figure 34: number of valid phase-to-earth tests by species

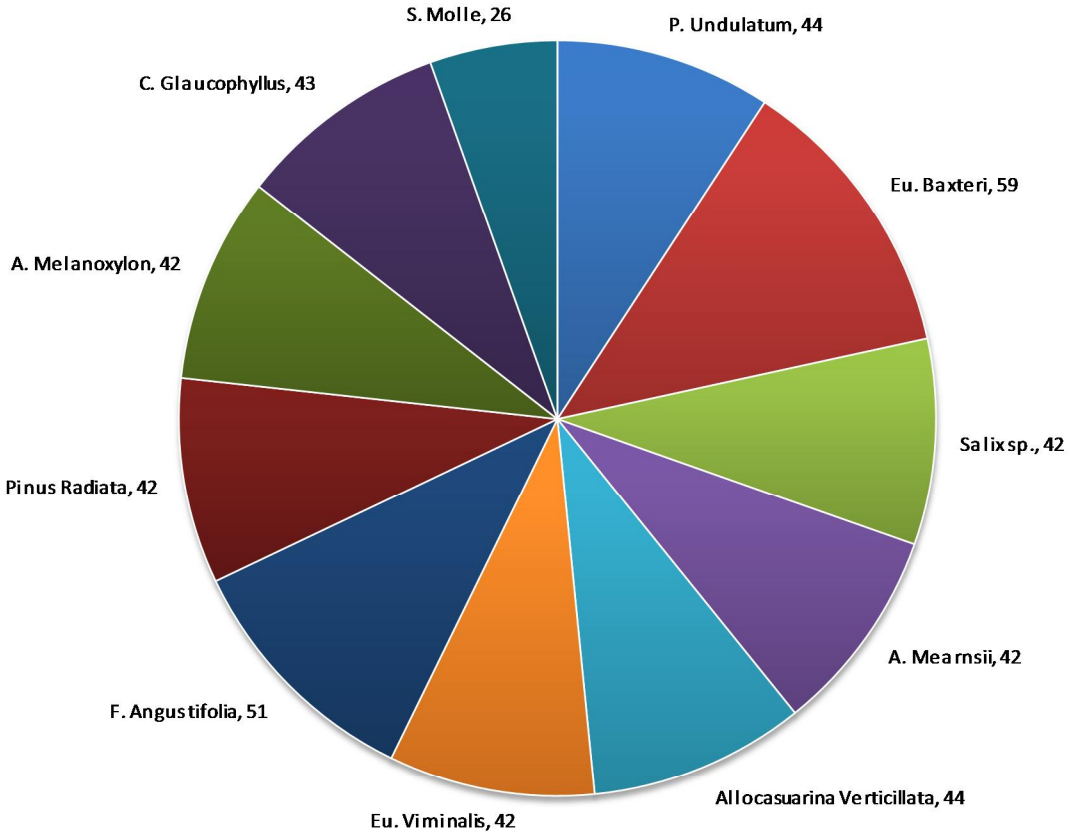

Of this total, 389 tests did not result in a flashover and so qualified as potentially realistic representations of 'branch touching wire' powerline earth faults. Phase-to-earth tests that resulted in a flashover were excluded as flashovers were considered unlikely in real 'branch touching wire' faults, i.e. their occurrence in earth fault tests was seen as due to the limited size of the test rig.

This section outlines the fire risk analysis of the 389 valid 'branch touching wire' test results. It sometimes draws on the wider population of tests to illustrate specific relevant issues.

[13] See *6.8 Relating the test configuration to real faults* on page 38.

6.1 Summary of findings

This section sets out evidence for the following findings from the 'branch touching wire' vegetation conduction ignition tests:

1. The initial level of current flow in a 'branch touching wire' fault depends on many factors including vegetation moisture content and the level of ionic compounds in the sap, as well as the diameter of the branch.
2. The initial current in 'branch touching wire' faults that produce fire risk is too low to be detected by powerline protection technologies currently in use in rural Victoria.
3. 'Wire touching branch' faults can only be reliably detected once the fault current has grown beyond its initial value and the time taken for this development provides opportunity for ember production and hence, fire risk.
4. With traditional earth-fault detection sensitivity of 5-10 amps on rural powerlines in Victoria, 'branch touching wire' earth faults are certain to produce a fire in worst case conditions.
5. If powerline earth-fault protection systems were to detect and respond to 0.5 Amp faults within two seconds, fire risk in 'branch touching wire' faults in worst case conditions would be reduced tenfold compared to current levels.
6. It was not possible to reliably quantify the influence of sample moisture content on fire risk due to the large number of independent variables in the ignition tests and Melbourne's mild damp 2014/15 summer.
7. Different species show widely varying fire risk in 'branch touching wire' faults. Of the species tested, the worst fire risk in 'branch touching wire' faults is Willow (Salix Sp.) and the best is Peppercorn (Schinus Molle). Other species tested fall between these extremes.
8. Species with high fire risk tend to take longer for fault current to fully develop. Species with faster fault current development tend to have lower fire risk because the fault reaches the detection threshold before ember production fully develops.
9. The type of bark on some species appears to have a significant effect on their fire risk in 'branch touching wire' faults.

6.2 Fire risk from 'branch touching wire' earth faults

The dependence of fire risk on current limit in 'branch touching wire' tests is shown in Figure 35[14].

[14] The fire probabilities shown in Figure 35 are reduced by the exclusion of results from phase-to-earth tests that resulted in flashover – which were considered unrealistic in 'branch touching wire' faults. Without this exclusion, the average fire probabilities with fault current limits of 0.5, 1.0 and 2.0 amps are slightly higher: 11%, 39% and 64%.

Figure 35: probability of a fire versus fault current limit – 'branch touching wire' earth faults

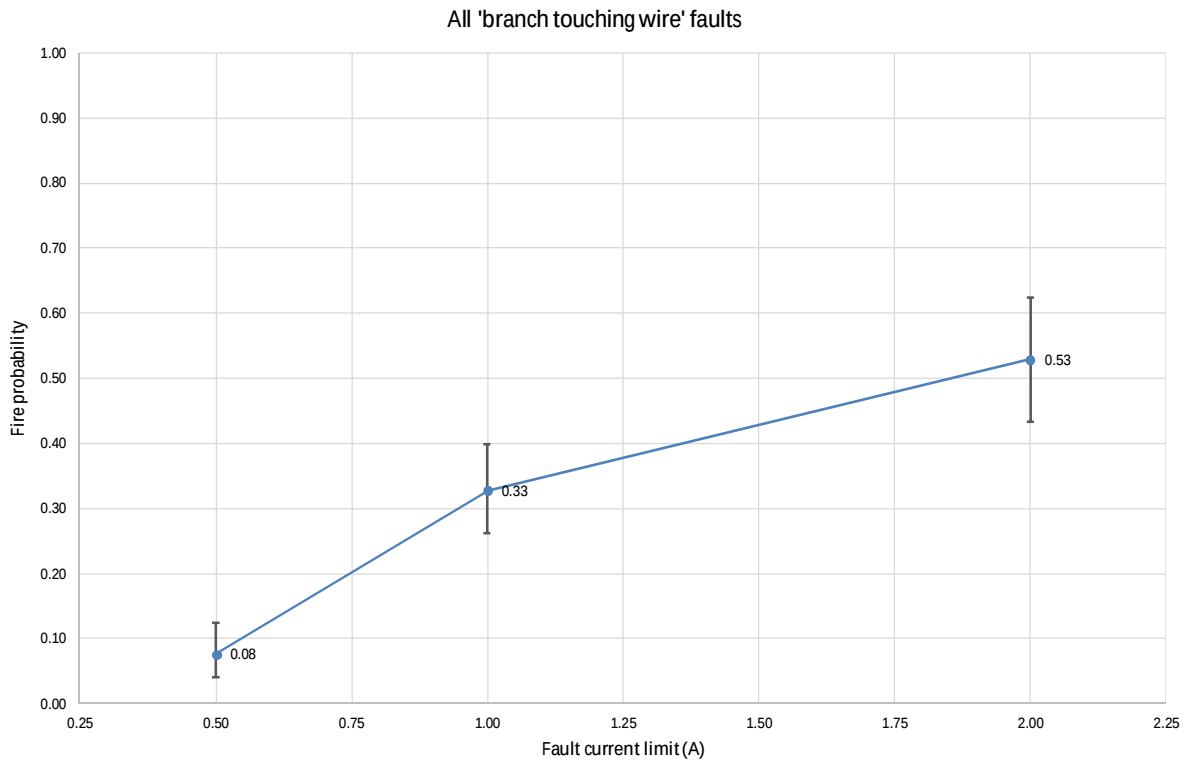

The choice of current limits used in tests was informed by the capabilities of various earth-fault protection technologies applicable to multi-wire powerlines in Victoria[15]. The values chosen (0.5, 1.0, 2.0 amps) were considered realistically achievable[16] with current technologies.

Extrapolating from Figure 35, it can reasonably be inferred that with most existing multi-wire powerline protection systems (namely Sensitive Earth Fault protection set to only detect fault currents of five to ten amps or more), a fire is close to 100% certain from a 'branch touching wire' fault in worst case conditions.

Figure 35 therefore invites the conclusion that if a multi-wire powerline protection system can detect earth faults of 0.5 amps and respond by quickly removing the voltage on the faulted conductor, the fire risk from this class of fault can be reduced about tenfold from existing levels.

6.3 Worst case species for fire risk in 'branch touching wire' faults

The tests showed significant fire risk variation by species as shown in Figure 36. It should be noted that the fire probability results shown here for each species are averages across a range of diameters, moisture contents and sap conductivities.

[15] Multi-wire powerlines total 50,000km route length in rural Victoria, i.e. 100,000 to 150,000 conductor-kilometres (depending on whether they are two-wire or three-wire). Single-wire (SWER) powerlines comprise 30,000 conductor-kilometres, i.e. 17-23% of the total overhead bare high voltage conductor.

[16] For example, the REFCL installed at Frankston South zone substation detects and responds to earth faults down to 2.0 amps. The 2014 REFCL Trial at Frankston demonstrated reliable fault detection at one amp fault currents and the REFCL Trial report recommended 0.5 amps fault detection sensitivity as appropriate and feasible for extreme fire risk days.

Figure 36: variation of fire probability by current limit for different species – 'branch touching wire'

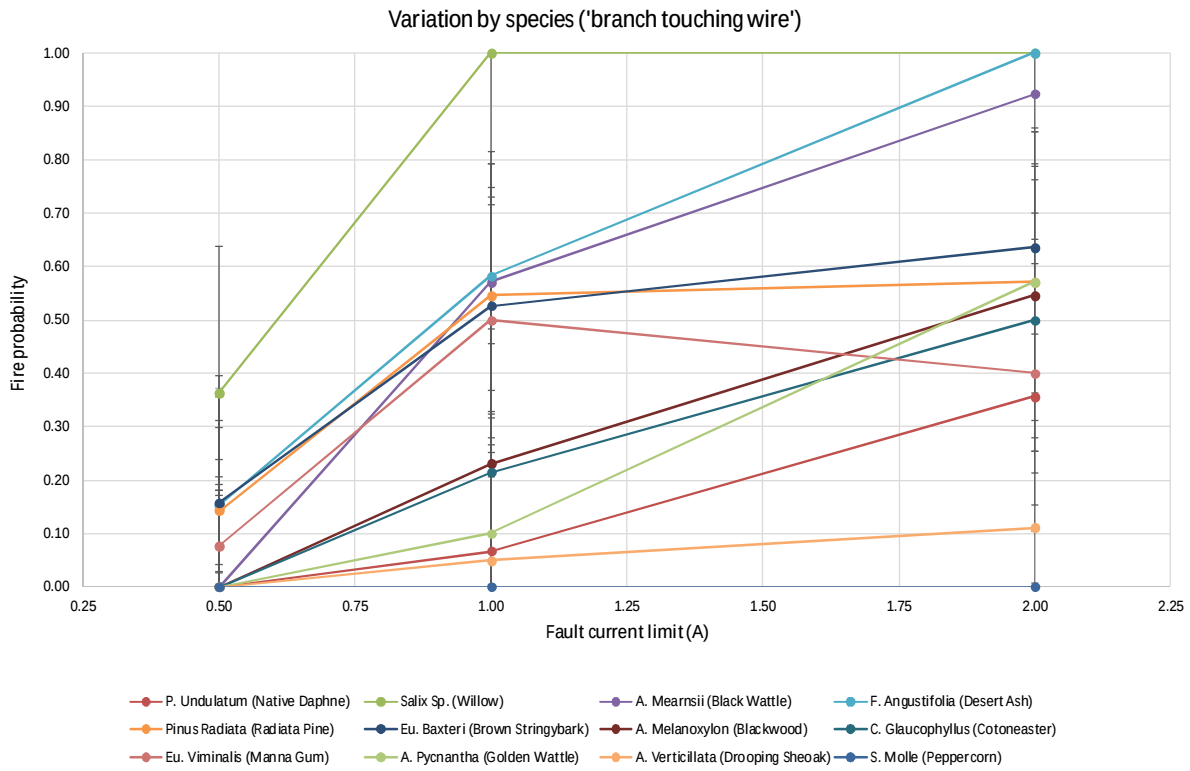

Of the species tested, Willow (Salix Species) was the worst case fire risk for 'branch touching wire' vegetation faults, followed by Desert Ash (Fraxinus Angustifolia). At the other end of the spectrum, Peppercorn (Schinus Molle)[17], Drooping Sheoak (Allocasuarina Verticillata) and Native Daphne (Pittosporum Undulatum) exhibited the lowest fire risk.

To provide reasonable statistical confidence, the plan was to test not less than 40 samples of each species, i.e. not less than 13 tests at each of three current limits (0.5, 1.0 and 2.0 amps). One species proved unavailable (Eucalyptus Goniocalyx – long leaf box) so no results were derived for it. Two (Schinus Molle – Peppercorn, Eucalyptus Obliqua – Stringybark) were available in limited quantities. In these cases, 1.0 amp tests were prioritised to give one comparative fire probability figure with adequate statistical certainty, leaving the results for other two current levels less certain. The limited number (11) of Eucalyptus Obliqua (Stringybark) samples was aggregated with the much larger cohort (48 samples) of seemingly identical Eucalyptus Baxteri (Brown Stringybark).

The limited number of tests meant a species' fire probability could only be estimated with a measure of uncertainty. The 95% confidence interval (CI) limits of the average fire probability were calculated to indicate the possible range of its true value, i.e. there is a less than one in twenty chance the true average fire probability falls outside this range. CI ranges for the highest (Willow), lowest (Peppercorn) and an intermediate (Manna Gum) fire risk species are shown to illustrate typical CI ranges in Figure 37.

[17] Peppercorn proved to have extremely low fire risk with no observed fire events in 22 'branch touching wire' tests, nor in any of the additional 20 phase-to-earth tests that resulted in flashovers. Even a phase-to-phase test of a Peppercorn branch with a 20 amps current limit (the limit of the test facility overcurrent protection system) only succeeded in producing a 'near miss' fire result.

Figure 37: fire probability 95% confidence interval ranges: Willow, Manna Gum, Peppercorn

Willow:

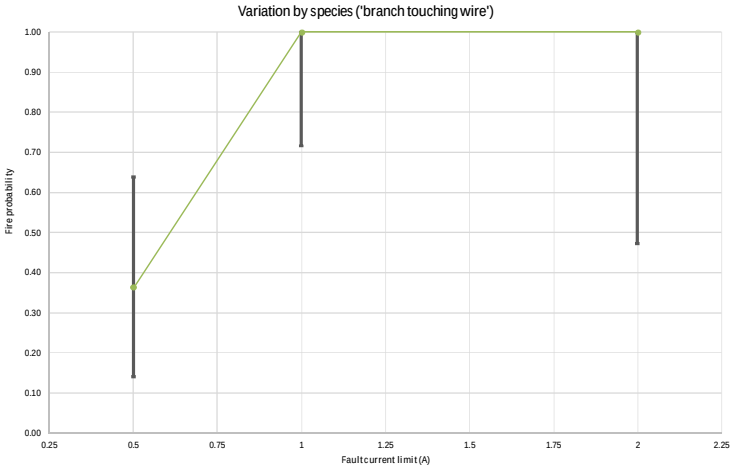

Manna Gum:

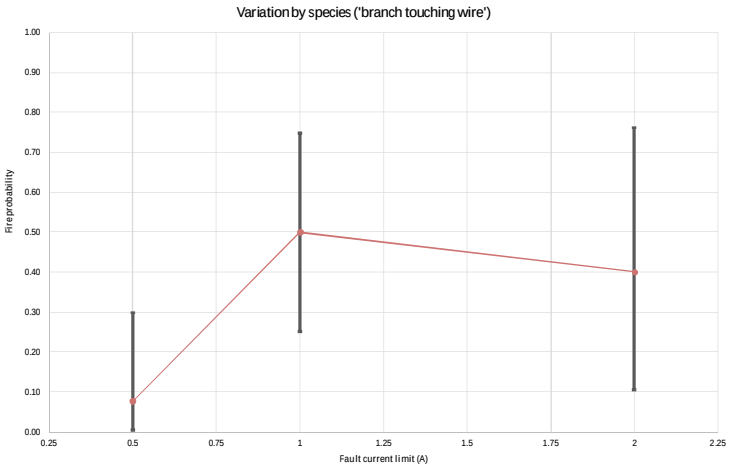

Peppercorn:

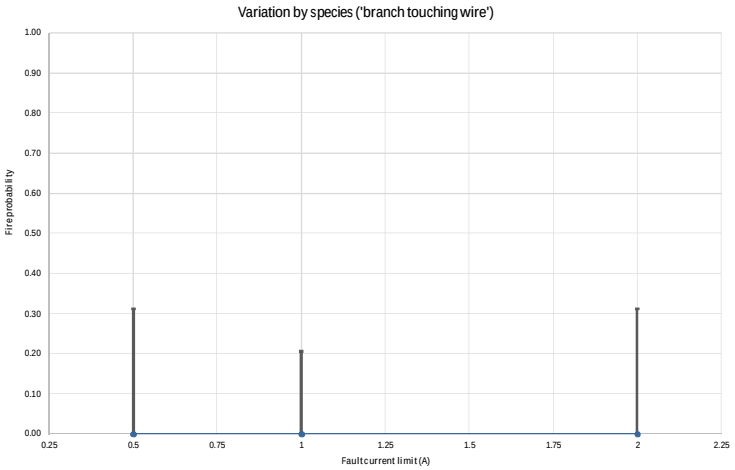

The results for tests with one amp current limit provide the species' ranking by fire risk in Table 3.

Table 3: species risk ranking – fire probability for tests with a one amp current limit

Species	Average fire probability	95% CI min/max	
Salix sp. (Willow)	1.00	0.72	1.00
F. Angustifolia (Desert Ash)	0.58	0.32	0.81
A. Mearnsii (Black Wattle)	0.57	0.33	0.79
Pinus Radiata (Radiata Pine)	0.55	0.28	0.79
Eu. Baxteri/Obliqua (Stringybark)	0.53	0.32	0.73
Eu. Viminalis (Manna Gum)	0.50	0.25	0.75
A. Melanoxylon (Blackwood)	0.23	0.07	0.48
C. Glaucophyllus (Cotoneaster)	0.21	0.06	0.46
A. Pycnantha (Golden Wattle)	0.10	0.01	0.37
P. Undulatum (Native Daphne)	0.07	0.00	0.27
Allocasuarina Verticillata (Drooping Sheoak)	0.05	0.00	0.21
S. Molle (Peppercorn)	0.00	0.00	0.21

6.4 What makes a species worst case?

Two factors appeared to influence the fire risk of a particular species:

- The rate of growth of current in the test; and
- The nature of the bark on the vegetation sample.

Figure 38 indicates that speed of fault current development may be a factor in a species' fire risk. Though there is not a strict one-to-one correspondence between Figure 38 and the ranking in Table 3, species that take a long time for the fault current to develop to reach the pre-set current limit tend to have worse fire risk performance than those where the current increases relatively quickly. This seems reasonable – a longer period of slow current growth allows time for the branch to ignite and shed glowing embers. Fire risk is lower if the high voltage is removed before ember production occurs.

Figure 38: average time taken for current to reach one amp in phase to earth tests

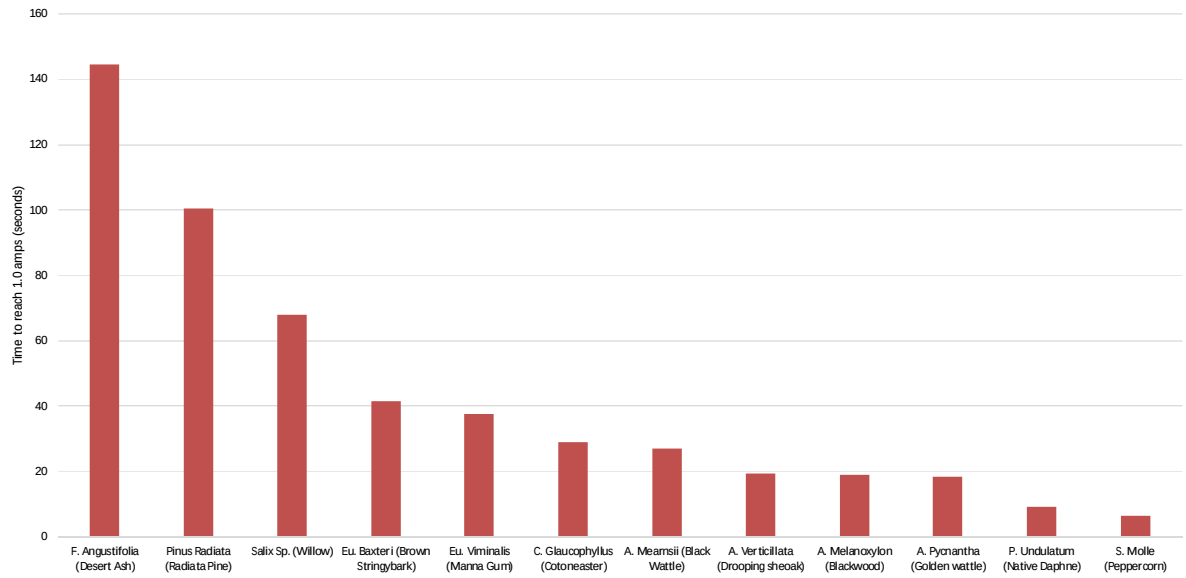

Review of video evidence and post-test examination of samples indicated the nature of the bark on some species may also affect fire risk. Stringybark and some other species with partially detached bark seemed to more easily create embers than species with 'tight' bark such as Native Daphne.

Two species had bark that appeared to behave differently to most. Both had low fire risk:

- Drooping Sheoak (Allocasuarina Verticillata) has a dry 'knobbly' fibrous moderately separable bark that does not appear to readily develop into hot glowing embers; and
- Peppercorn (Schinus Molle) has a relatively thick bark with a clear boundary between the bark and the core wood. The bark appears to smoulder or burn in situ and 'breakthrough' points have glowing edges that burn back but do not drop many hot glowing embers.

Figure 39: samples illustrating the variety of bark encountered in tests

Test 30: detaching bark still glowing on Blackwood sample after two amp phase-to-phase test with flashover.

Test 798: bark on Drooping Sheoak samples after one amp phase-to-phase tests, no flashovers.

Test 987: non-detaching bark glowing around a breakthrough on a Peppercorn sample after 20 amp phase-to-phase test.

The selection of species for this test program was done before there was an understanding of factors that would make a species worst case. It cannot be safely assumed that species not selected for tests will have lower fire risk than the worst identified in the tests, namely Salix Sp. (Willow).

6.5 Effect of moisture on fire risk

The effect of moisture content on fire risk was not able to be quantified with confidence.

Figure 40 illustrates the reason for this. To identify the effect of moisture, other factors must be eliminated from the comparison. First, the pre-set current limit has to be eliminated. Of 389 valid 'branch touching wire' tests, 116 were carried out with a one amp current limit. Next, individual test results have to be aggregated into 'bins' with a sufficient number of tests in each bin for a reliable average of the results. Of the 116 tests with one amp current limit, 110 had moisture content results that fell into bins with not less than ten similar tests.

The proportion of tests that resulted in a fire outcome in each of these bins is plotted in Figure 40, together with the number of valid tests in that bin. Only two bins contained more than 35 tests. The three others had low numbers of tests (10-15 in each) which meant higher levels of uncertainty in the estimated average fire probability.

Figure 40: effect of moisture on test fire outcomes – assessment of 110 'branch touching wire' tests

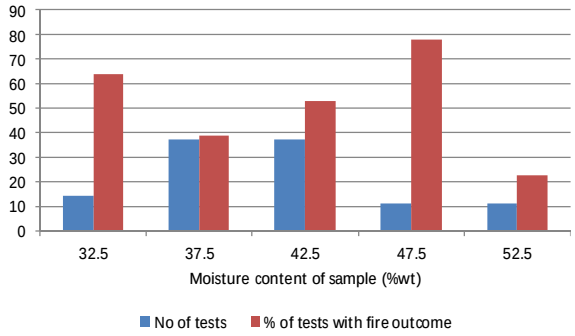

The pattern shown in Figure 40 does not provide any compelling insight into the effect of moisture content on fire probability.

6.6 The development of fault current in 'branch touching wire' earth faults

'Branch touching wire' tests followed the four phases described in Section 4.2 above. The high voltage supply was removed when the current reached the pre-set limit for the test. The development of current in each test was complex with wide test-to-test variation in the time taken for it to reach the pre-set limit as shown in Figure 41, Figure 42 and Figure 43.

The tests were of much shorter duration than those reported by previous researchers. Two factors may underlie this difference:

1. Much of the previous research into vegetation faults was done at lower voltage levels – 11kV and 6kV, rather than the 22kV and 13kV used in tests reported here. This test program showed speed of current development is very sensitive to voltage as outlined in Section 8.5.
2. It is not always clear from published reports of previous studies how vegetation samples were conditioned prior to tests, nor is data on moisture content often included. Conditioning (moisture content) may have an effect on the speed of fault development.

Figure 41: time for current to increase to a 0.5 Amp limit in phase-to-earth tests

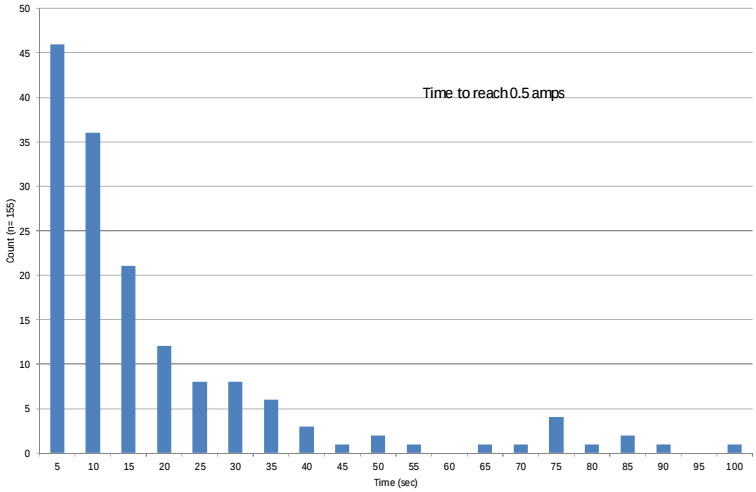

Figure 42: time for current to increase to a 1.0 Amp limit in phase-to-earth tests

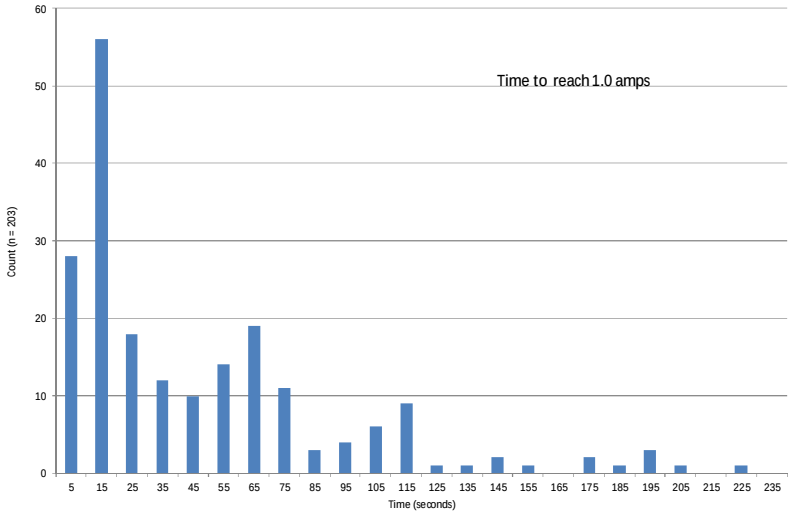

Figure 43: time for current to increase to a 2.0 Amp limit in phase-to-earth tests

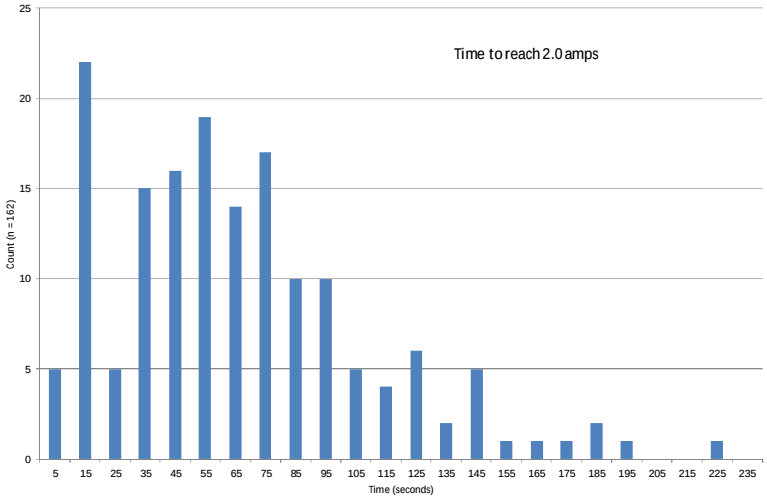

For the high voltage to be removed before ember production starts, it is of direct interest to know how fast the 0.5 amp current limit is reached in 'branch touching wire' faults. Figure 44 shows the data from Figure 41 with progressively expanded time scales.

Figure 44: time to reach 0.5 amps in phase-to-earth tests (expanded scales)

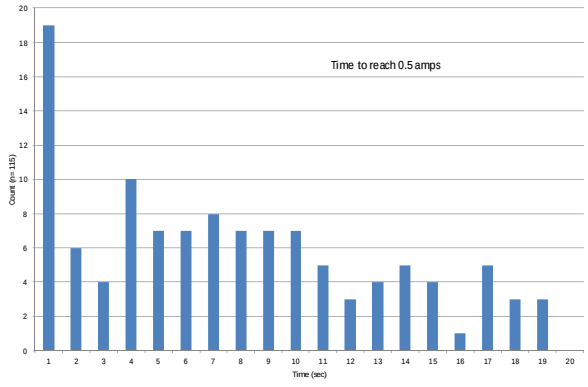

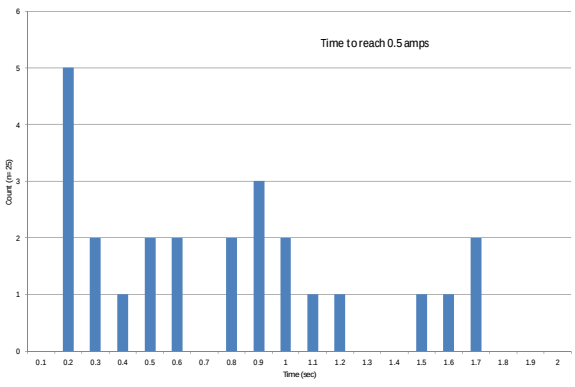

Of the 155 samples mapped in Figure 41, only about one sixth (25 tests) reached 0.5 amps in less than two seconds, mostly because they had high levels of initial current. Of this cohort of 25, 14 samples were low-risk species (Peppercorn, Native Daphne and Golden Wattle) and the remaining nine were mostly medium-risk species (Stringybark, Manna Gum, Blackwood, etc.). Only one test involved a high-risk species (Black Wattle). None of the 25 tests resulted in a fire.

This analysis of the time taken to reach the 0.5 amps current limit in phase-to-earth tests indicates that detection and response to a 'branch touching wire' earth fault within two seconds is very likely to realise the opportunity for tenfold reduction in fire risk indicated in Figure 35.

This conclusion is further reinforced by analysis of the eighteen 0.5 amp limit tests that produced fires: the shortest duration test (shortest time to reach 0.5 amps) to start a fire was a Willow sample that took 10.8 seconds to reach 0.5 amps. The next shortest were two at around 25 seconds (Radiata Pine and Blackwood). Again, fault detection and response within about two seconds would appear to be adequate to decimate fire risk in 'branch touching wire' faults.

6.7 Initial fault current in 'branch touching wire' earth faults

The initial value of current was measured and recorded for each test. This parameter is important in assessment of whether the fault can be detected by powerline protection systems or not.

The first cycle or two of fault current showed the branch usually (but not always) acted like a linear resistor with little waveform distortion. Some examples are shown in Figure 45.

Figure 45: examples of initial current waveforms in tests

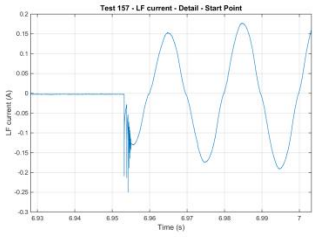

Test 157: 30mm Native Daphne phase-to-earth

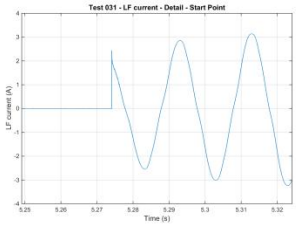

Test 31: 90mm Manna Gum phase-to-earth

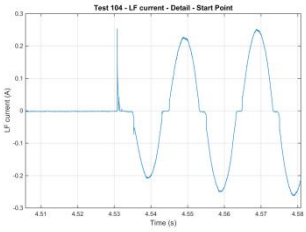

Test 104: 60mm Stringybark phase-to-earth

The measured initial current values for phase-to-earth tests are shown in Figure 46.

Figure 46: initial current in phase-to-earth tests

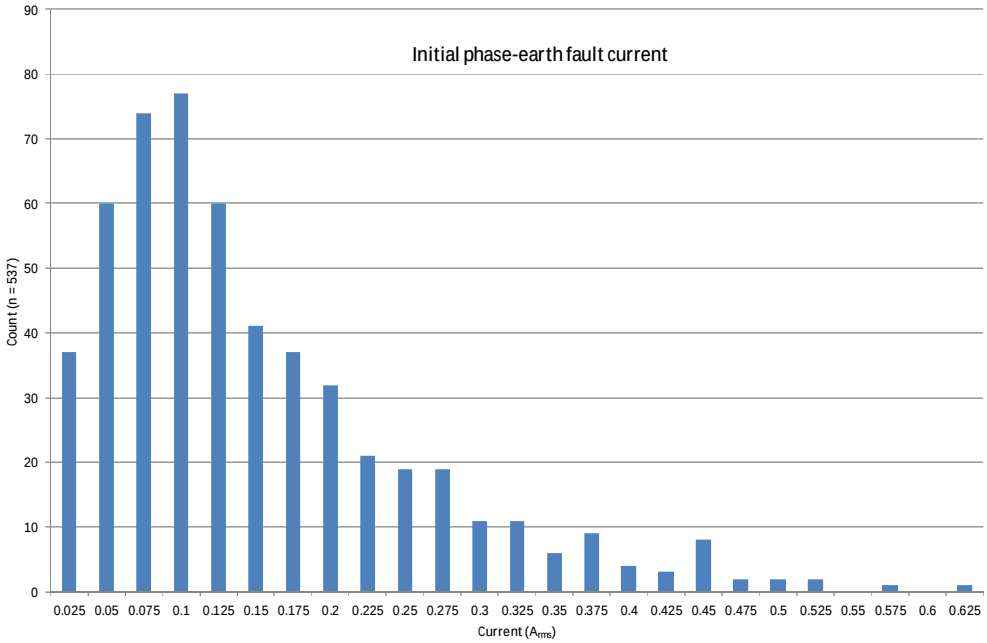

The initial current was considered likely to be influenced by a range of factors. Correlations were reviewed for:

- Moisture content (Figure 47) – higher moisture content increases initial current (moisture content below 15% can result in very low current – less than 5 milliamps);
- Diameter (Figure 48) – larger diameter increases initial current; and
- Conductivity (Figure 49) – higher conductivity increases initial current.

These correlations appear consistent with expectations based on the concept of the vegetation sample being a tapering rod of material, the conductivity of which is determined by both moisture and the level of ionic compounds contained within it.

Figure 47: correlation of initial phase-to-earth current with average sample moisture content

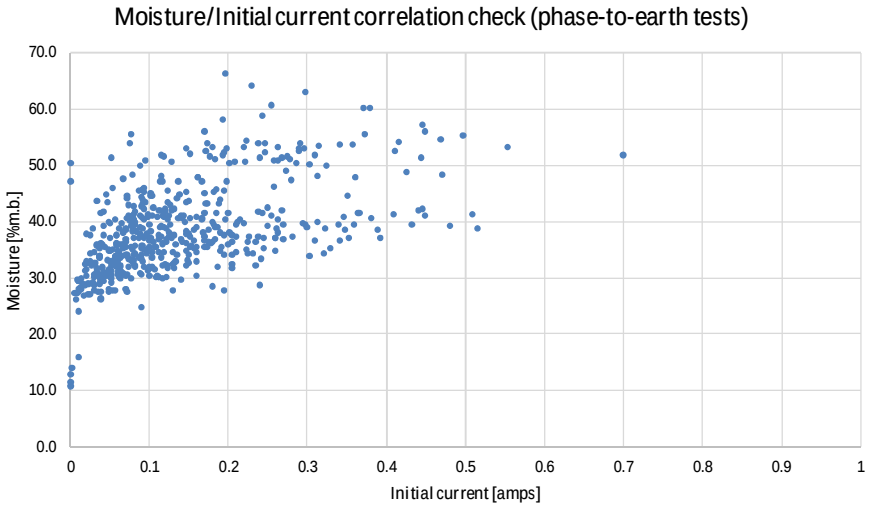

Figure 48: correlation of initial phase-to-earth current with sample diameter at thick end

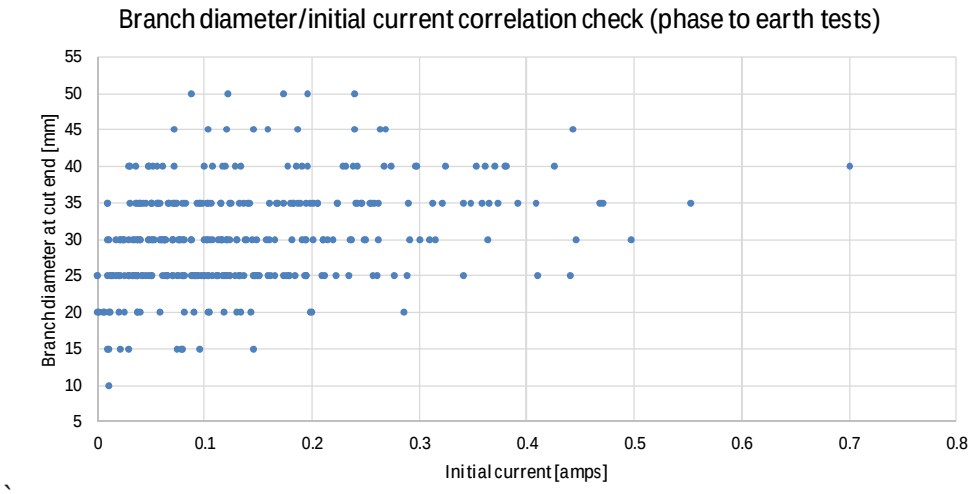

The few tests performed on larger diameter samples provided a more extensive indication of the effect of branch diameter on the value of initial current:

- In phase-to-phase Tests 4 and 10 (both Manna Gum 30mm diameter samples with 40% moisture content and conductivity of 215±30µS/cm) the samples drew almost identical initial current of 0.26±0.01 amps.
- In phase-to-phase Test 31, a 90mm diameter Manna Gum sample with 45% moisture content and conductivity of 139µS/cm drew an initial current of 2.0 amps, i.e. about eight times greater, which is close to the nine times increase in cross-sectional area compared to 30mm diameter samples.

The limited number of tests of larger diameter samples would support a 'constant conductivity' hypothesis that initial current varies as cross-sectional area for a fixed length, i.e. it is proportional to the square of the diameter.

Figure 49: correlation of initial phase-to-earth current with average sample conductivity

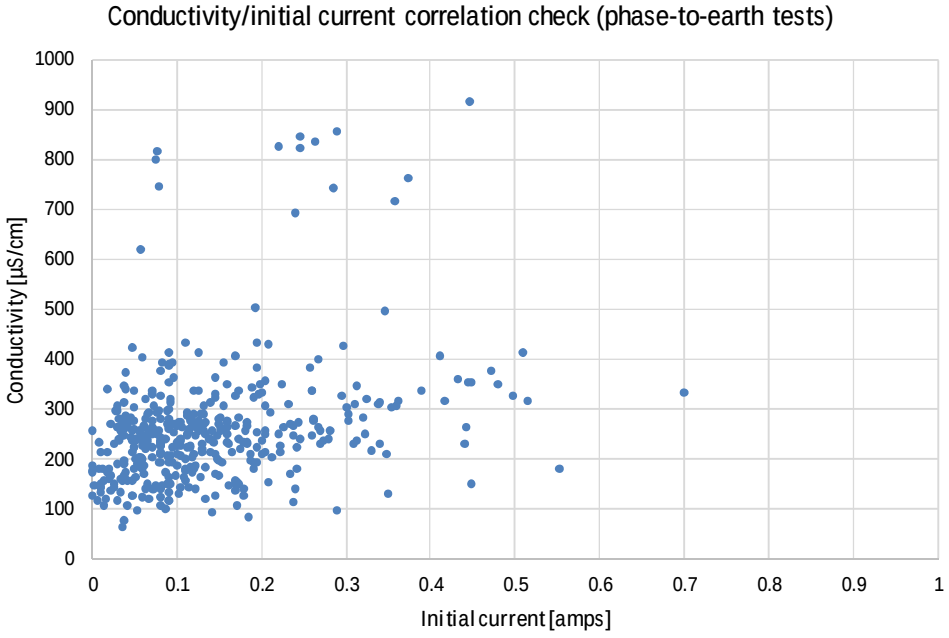

The check for correlation of initial current with conductivity analysis broadly confirms the expected result that higher conductivity levels result in higher initial current.

Regression analysis of 204 phase-to-earth tests (excluding conductivity outliers greater than 500µS/cm) shows the initial current might be predicted by the formula:

$$i_{amps} = -0.3 + 0.008\ Moisture_{\%} + 0.0004\ Conductivity_{\mu S/cm} + 17.8\ Area_{m^2}$$

The low p-values produced in the regression analysis indicate the coefficients are reasonably reliable – the full regression results are:

Regression Statistics	
Multiple R	0.715082694
R Square	0.511343259
Adjusted R Square	0.504013408
Standard Error	0.076203196
Observations	204

	Coefficients	*Standard Error*	*t Stat*	*P-value*	*Lower 95%*	*Upper 95%*
Intercept	-0.299981275	0.030116525	-9.960686836	3.09724E-19	-0.359367937	-0.240594613
Moisture	0.00786995	0.000732163	10.74890199	1.45582E-21	0.0064262	0.0093137
Conductivity	0.000396504	8.04144E-05	4.930757111	1.71747E-06	0.000237935	0.000555073
Area	17.80845362	3.978891079	4.475732878	1.27739E-05	9.962493327	25.65441391

This confirms the initial current increases with moisture content, conductivity and the cross-sectional area of the branch. However, the range of test-to-test variation (the standard error in the regression results above) is large. This might reasonably be expected given the non-ideal nature of the samples. For example, diameter often varied in very non-linear ways along the length of the sample. A single value (the diameter of the sample taken from the thicker end for moisture analysis) can only approximate the situation, especially if the branch divides.

It is also possible the correlations above were influenced by real species-to-species variations. Section 10.9 below outlines analysis results related to these.

6.8 Relating the test configuration to real faults

Some aspects of the test rig design are quite realistic, e.g. the conductor used was typical powerline conductor and the voltage applied was the usual phase-to-earth voltage of 12.7kV. Other aspects had to be more contrived to allow such an extensive test program to be carried out, e.g. applying voltage across just 1.5 metres of branch instead of between a branch at height and earth.

The measurement of initial fault current above allows the non-realistic aspects to be checked. From Figure 46, the median initial current in phase-to-earth tests with an average thick-end sample diameter of 25mm is 0.1 amps, i.e. the median value of sample resistance is about 130kΩ. Taking into account the 1.5 metre conductor spacing and assuming that on average the cross-sectional area of the branch decreases 50% along its length (radius decreasing linearly with distance), the average resistivity of the wood in the samples can be calculated to be about 125 Ω-m.

If we postulate more realistic geometry for a 'tree touching powerline' fault, the path resistance can be calculated using this value of wood resistivity (the same tapering – 50% reduction in area over the length – is assumed for each element). This gives:

Tree component	Length (m)	Diameter (m)	Resistance (Ω)	% of total
Trunk	3.0	0.75	295	0.2
Big branch	2.0	0.25	1772	1.3
Small branch	1.0	0.15	2461	1.8
Branch touching	1.5	0.025	132887	96.7
		Total	137415	100.0

It can be seen that 97% of the total resistance of current path through vegetation is in the last 1.5 metres, i.e. the portion studied in the tests, so it might reasonably be concluded that the test set-up is a fit-for-purpose representation of real 'tree touching powerline' faults.

7 Ignition in 'wire into vegetation' earth faults

Two different 'wire into vegetation' fault types were studied in the test program:

1. 'Wire into bush' where a live conductor falls into a bush but does not touch the ground; and
2. 'Wire into grass' where a live conductor falls into grass but does not touch the ground[18].

A total of 71 valid tests (51 bush and 20 grass) listed in Table 4 were successfully completed.

Table 4: valid 'wire into vegetation' tests

Class	Species		Tests	Fires
Bush	Rubus Fruticosus	Blackberry	21	9
	Ulex Europeaus	Gorse	12	6
	Kunzea Ericoides	Burgan	12	8
	Banksia Marginata	Silver Banksia	6	0
Grass	Lomandra Longifolia	Spiny-headed Mat-rush	11	3
	Poa Labillardieri	Common Tussock-grass	9	3

Figure 50: species tested in 'wire into vegetation' tests

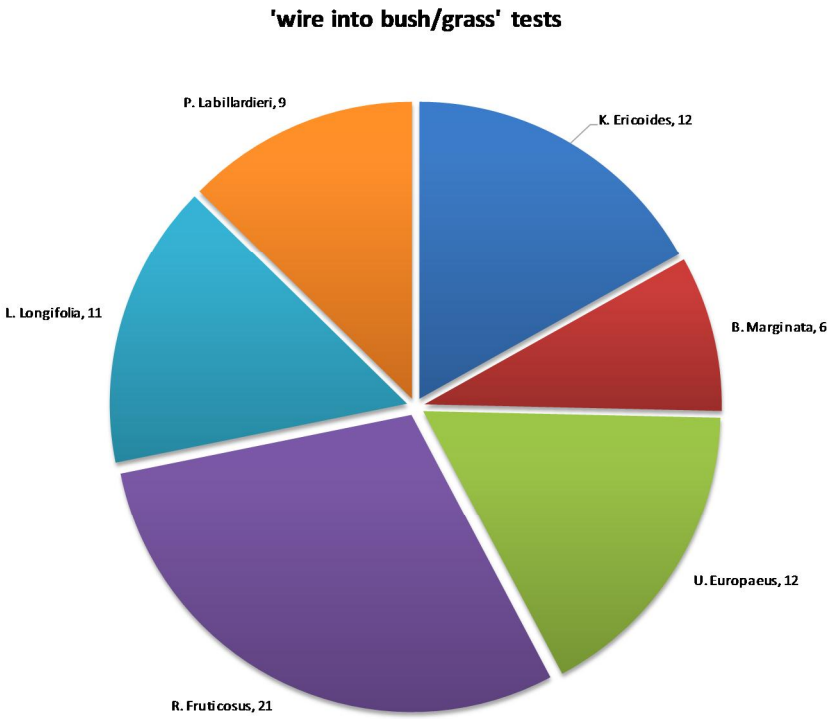

[18] Ignition of dry grass by a conductor arcing to ground was fully explored in the 2014 REFCL Trial.

7.1 Summary of findings

This section sets out evidence for the following findings from tests designed to simulate 'wire into vegetation' powerline faults:

1. Within the limits of certainty set by the smaller number of tests performed, 'wire into bush' faults are likely to have a higher fire risk than 'branch touching wire' faults. If powerline protection systems can detect and respond to an earth-fault drawing 0.5 amps, fire risk from 'wire into bush' faults might be cut by about 80%.
2. Of the few middle storey species successfully tested, Burgan and Gorse were worse than Blackberry. Silver Banksia appeared to have a lower fire risk. There is considerable uncertainty in these results due to the relatively small number of tests available for analysis.
3. 'Wire into bush' test results tended to be binary: either the fault quickly produced a substantial fire; or it pruned back vegetation without creating significant fire risk, until current ceased to flow. 'Pruning' and 'cooking' outcomes featured in 'wire into bush' tests.
4. 'Wire into grass' tests produced even more binary results: if the grass had enough moisture to conduct current, a flashover to ground occurred almost instantly; if not, nothing happened even when dry grass was pressing against the live wire for an extended period.
5. The fire probability results for 'wire into grass' faults in worst case conditions should be drawn from the results of the 2014 REFCL Trial rather than the tests in this program. In all tests that produced fire risk, ignition was driven by the occurrence of flashovers, i.e. the 'wire into grass' fault either became a 'wire on ground' fault (where fire risk is due to flashover to ground) or was not a fault because no current flowed.

The assessment of fire results was much more challenging than in 'branch/wire' faults and a conservative approach was taken wherever there was doubt. To achieve higher levels of accuracy and certainty in fire probability estimates, a revised experiment concept and improved access to a wider range of samples might be required.

7.2 Fire risk from 'wire into bush' earth faults

Average (across all tested species) probability of fire in 'wire into bush' tests is shown in Figure 51.

Figure 51: fire probability from 'wire into bush' tests

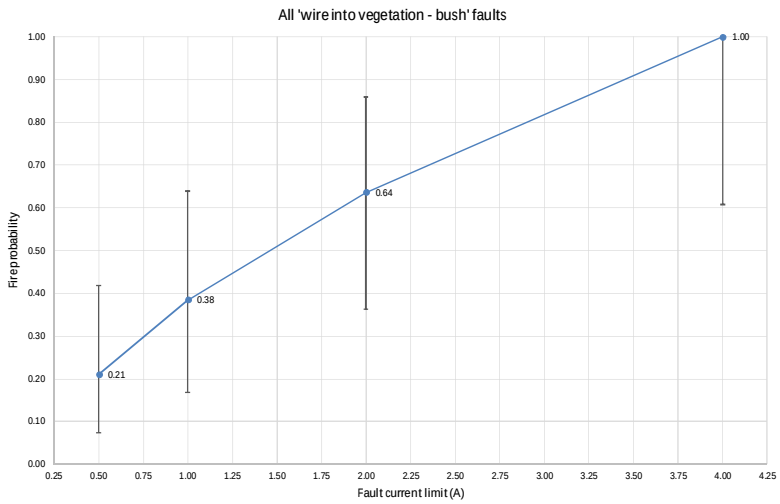

The results shown in Figure 51 imply that if a powerline protections system can detect and respond to earth faults that draw 0.5 amps, fire risk from 'wire into bush' faults might be reduced from 100% to 21%, i.e. five-fold.

The large 95% confidence intervals shown in Figure 51 reflect the comparatively smaller number of tests than was used to generate the same data for 'branch touching wire' faults shown in Figure 35. This was primarily due to unavailability of suitable bush samples.

The variation of fire risk across species is indicated in Figure 52.

Figure 52: variation by species in 'wire into bush' tests

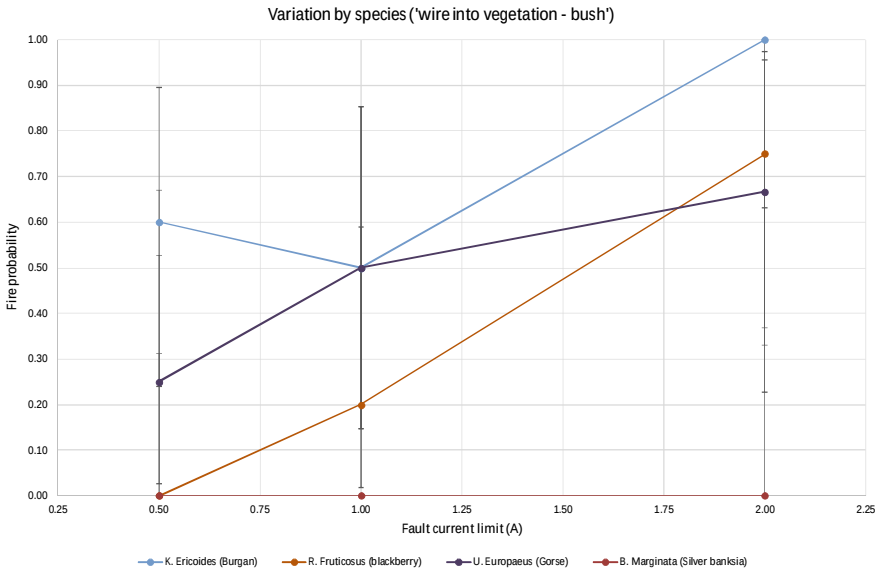

The 95% confidence interval limits for tests at 1.0 amps current limit are listed in Table 5.

Table 5: estimated fire probability of 'wire into bush' faults limited to one amp of fault current

Species	Average fire probability	95% CI min/max	
Kunzia Ericoides (Burgan)	0.50	0.15	0.85
Ulex Europeaus (Gorse)	0.50	0.15	0.85
Rubus Fruticosis (Blackberry)	0.33	0.08	0.68
Banksia Marginata (Silver Banksia)*	0.00	0.00	0.63

*No tests were carried out on Silver Banksia with a 1.0 amps limit; data shown is for two 2.0 amps tests.

The large 95%CI ranges shown in Table 5 reflect the small number of tests in each cohort once the total number of valid 'wire into bush' tests (51) is split by species and then split again by current limit value. All that can reliably be concluded from Table 5 is that Silver Banksia is probably a better (lower) fire risk than Burgan, Gorse and Blackberry.

7.3 Fire risk from 'wire into grass' earth faults

Twenty 'wire into grass' tests were carried out on just two species: Lomandra Longifolia (Spiny-headed Mat-rush) and Poa Labillardieri (Common Tussock Grass).

In each 'wire into grass' test, one of two outcomes were observed: a blaze/flashover (often occurring too rapidly to determine which happened first) or a nil result – no current flow despite good wire-to-grass contact. Though some pre-flashover current build-up was observed in tests on Spiny-headed Mat-rush, no clear instances of pure vegetation conduction ignition were observed – all ignitions were associated with flashovers and arcs.

In tests with Common Tussock Grass, all tests were performed with a 0.5 Amp current limit as higher current limits would have made no difference to the results – the sample either flashed over or

nothing happened for as long as the test lasted. In one test, the flashover occurred 12 seconds into the test, but there was no increase of current before it – the current went from less than 5mA to 65 amps in a few tens of microseconds. The other two flashovers occurred within microseconds of the test start.

Three flashovers occurred in tests with Spiny-headed Mat-rush, but in those tests there was some build-up of current in the one second period before flashover. An example is shown in Figure 53.

Figure 53: Test 524 – build-up to flashover in test with Spiny-headed Mat-rush

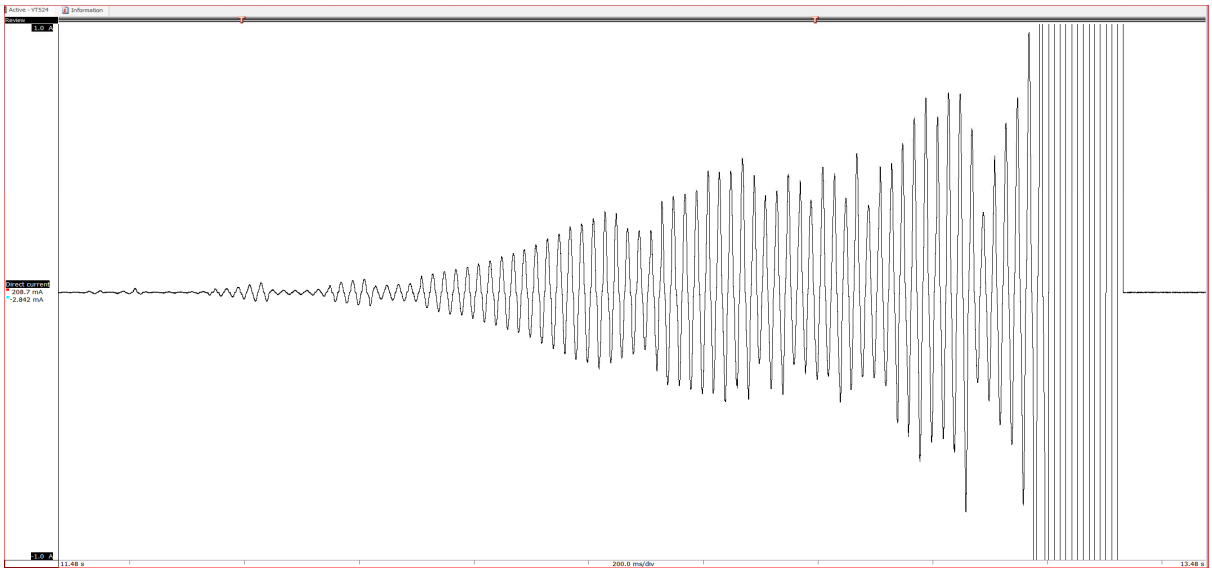

In Test 524, flaming started prior to flashover and continued after the high voltage was removed. However, it self-extinguished after the upper section of the sample was consumed. The condition of the sample after the test is shown in Figure 54:

Figure 54: Test 524 – Spiny-headed Mat-rush sample after ignition test

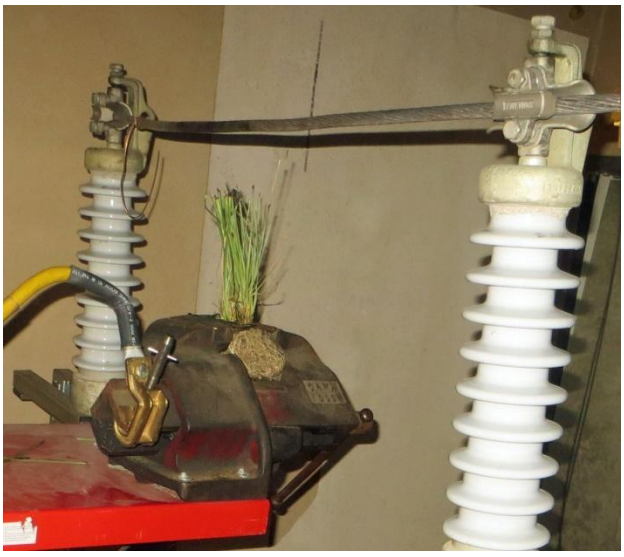

Test 524 was conservatively assessed as a fire, based on embers and flaming sustained for some seconds. It could be argued either way given the sample self-extinguished after 30 seconds.

In other tests on Spiny-headed Mat-rush, short bursts of current effectively pruned the grass strands that were in contact with the live conductor whereupon current ceased to flow, as shown in Figure 55 for Test 529 – which was rated as not having created a fire risk.

Figure 55: Test 529 – bursts of current in 'wire into grass' tests that do not results in flashovers

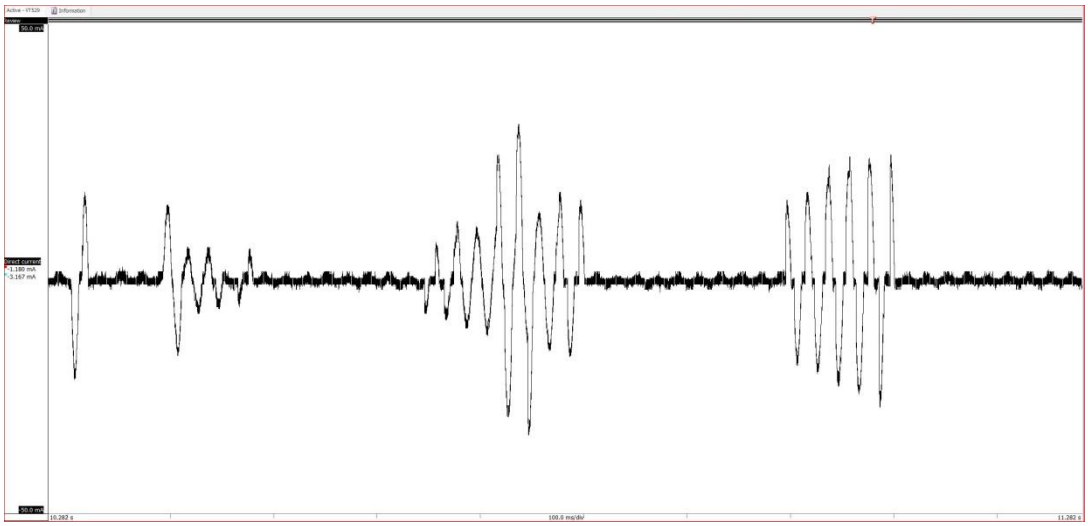

The established arrangements for procuring test samples from vegetation management contractors did not suit acquisition of grass samples so they were purchased from a wholesale plant nursery. Nursery products are well-nourished and well-watered at the time of sale, so the samples had to be conditioned for periods that ranged from four hours to one week in an attempt to replicate the condition of grass late in a hot dry summer.

The fire probability based on all 20 grass tests and using the same analysis methodology as used in other classes of tests is shown in Figure 56. The wide 95%CI ranges reflect the relatively small numbers of tests available to the analysis.

Figure 56: probability of fire in 'wire into grass' tests

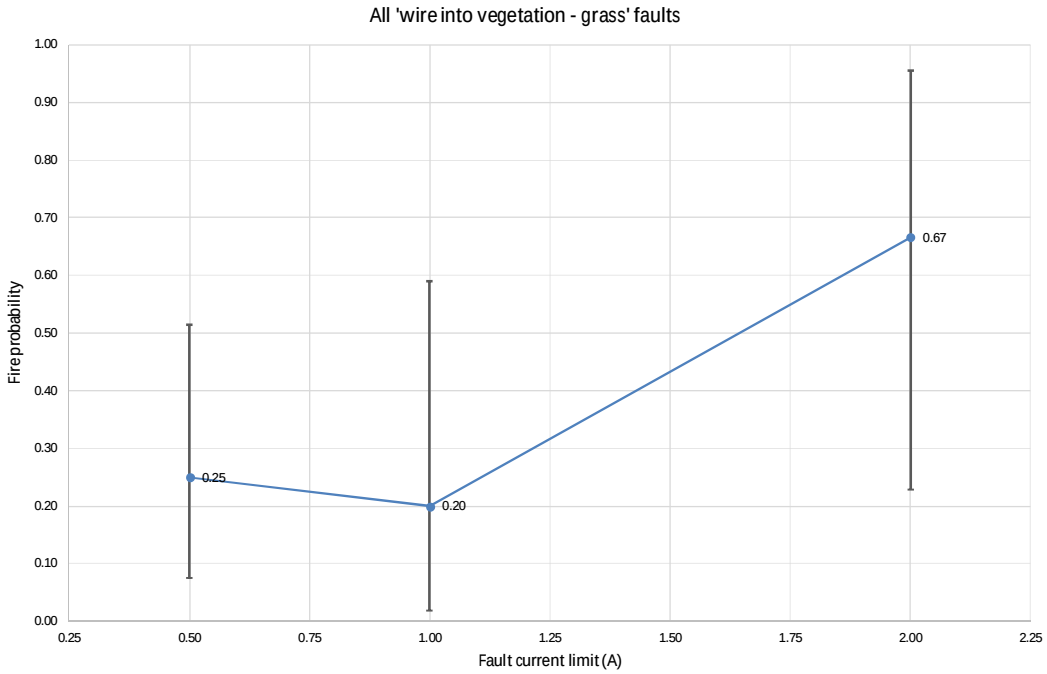

However, the results shown in Figure 56 are potentially misleading as 'wire into grass' tests had a binary fire outcome driven purely by the occurrence of flashovers. The results presented in the 2014 REFCL Trial report would be a much better guide to fire risk from 'wire into grass' tests.

8 Ignition in 'branch across wires' faults

When a branch becomes completely detached from a tree and falls onto a powerline to lie across two live conductors, it constitutes a phase-to-phase fault termed a 'branch across wires' fault. Such faults differ from 'branch touching wire' faults in two main respects:

1. The voltage applied across the length of the branch is 22,000 volts, i.e. more than 70% higher than that applied to tree branches in 'branch touching wire' faults; and,
2. There is no current to earth – current through the branch follows the same path as customer load current. This makes such faults very difficult to detect – a fault current of a few amps through the branch is easily masked by load current of tens or hundreds of amps flowing between the same two wires through customer supply substations.

331 valid phase-to-phase vegetation conduction ignition tests were performed on ten upper story species as shown in Figure 57. A total of 103 fire results and 228 non-fire results were recorded.

Figure 57: upper story species tested in 'branch across wires' fault tests

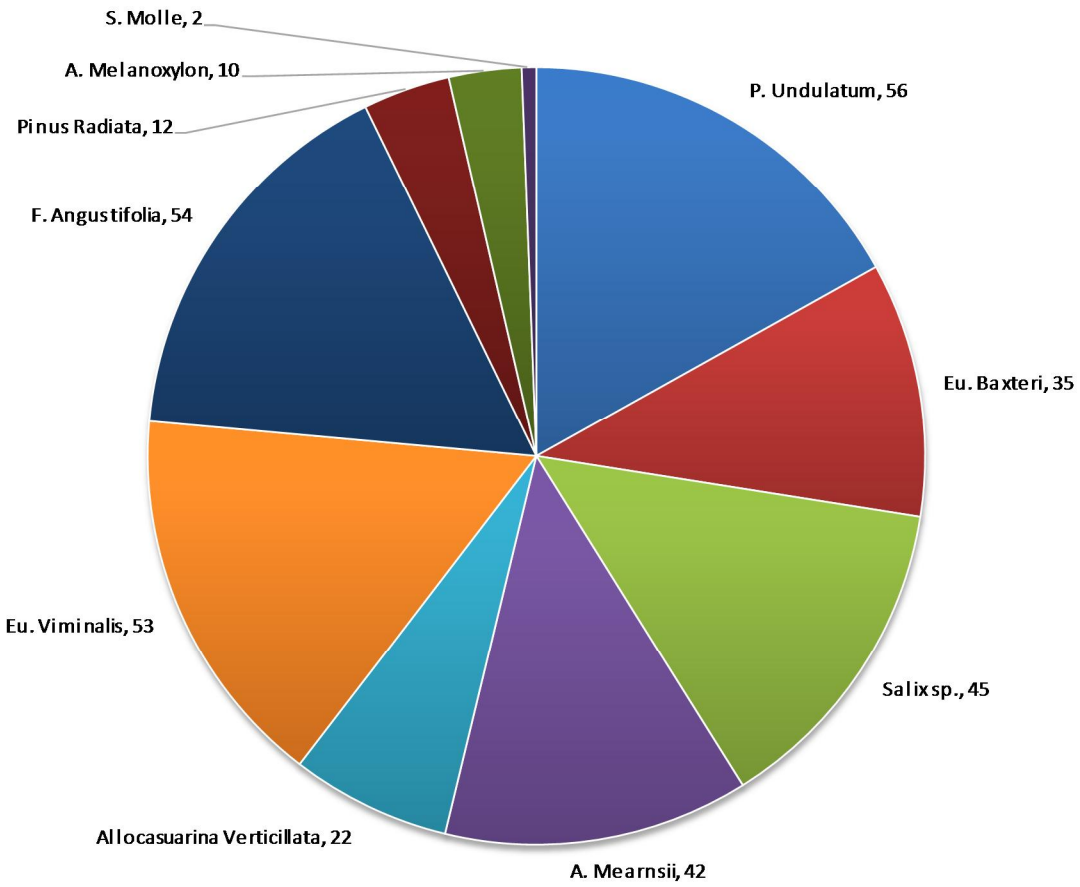

The plan was to test at least 40 samples of each 'upper story' species and this target was met for five species. When samples of a particular species proved scarce, phase-to-earth tests were given priority over phase-to-phase tests.

8.1 Summary of findings

This section sets out evidence for the following findings from the 'branch across wires' vegetation conduction ignition tests:

1. The rate of growth of fault current is four times faster in 'branch across wires' faults than in 'branch touching wire' faults.
2. If fault currents could be limited to a specific low value by powerline protection systems, fire risk would be lower in 'branch across wires' faults than in 'branch touching wire' faults for the same current limit. However, no protection technology is available today that offers this capability.
3. Assuming all 'branch across wires' faults progress to flashover (whereupon the high voltage is immediately removed by powerline over-current protection), the fire probability from 'branch across wires' faults on real networks is likely to be not less than 55%.
4. Fault detection and response within about five seconds might achieve substantial reductions in 'branch across wires' fire risk. Fault detection times longer than about 20 seconds would be unlikely to significantly reduce fire risk in such faults.

8.2 Fire risk in current-limited 'branch across wires' faults

There is no powerline protection system yet available that can reliably limit the current in 'branch across wires' faults, i.e. all such faults can be expected to progress to flashover. Alternatively, the branch may fall or be blown off the wires. The data base of fault signatures collected in this test program is intended to assist in development of improved fault detection technologies to address the challenge of faster detection of this class of faults.

The 'all tested species' average fire risk in 'branch across wires' faults is shown in Figure 58.

Figure 58: probability of a fire versus the maximum allowed fault current – 'branch across wires' faults

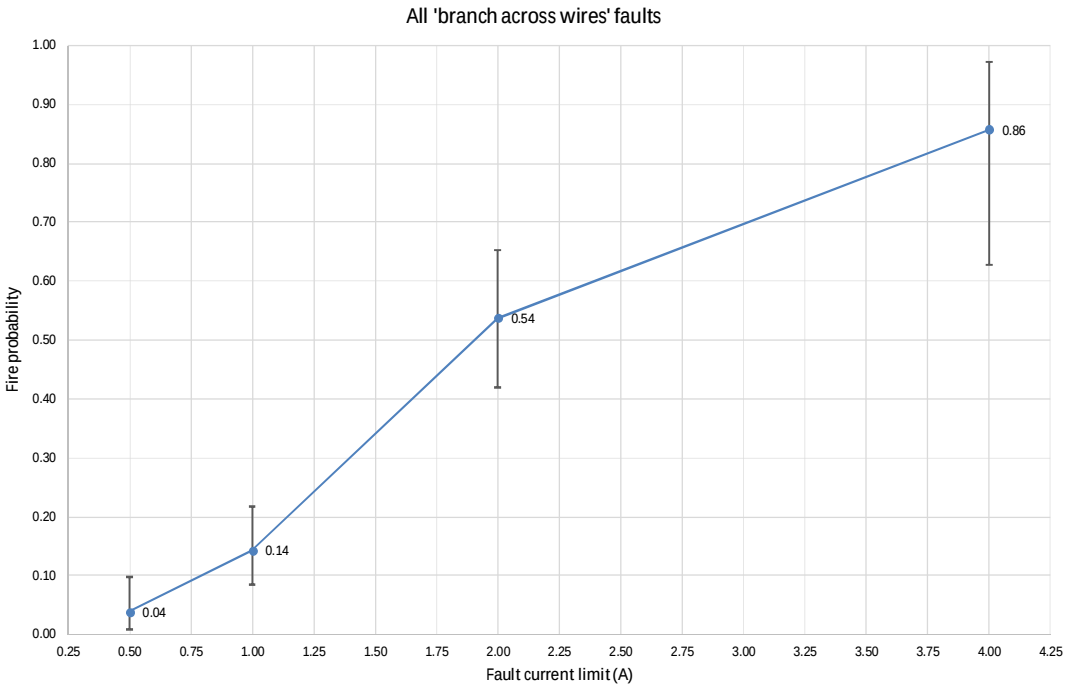

In this test program, the same methodology was used for 'branch across wires' faults as was used for 'branch touching wires' faults, except that tests that resulted in flashovers were taken to be valid since flashovers are a realistic outcome in such faults. The faster speed of development of current meant fire probability was lower for a given pre-set current limit than in a 'branch touching wire' fault with the same current limit (compare Figure 58 with Figure 35 on page 41). This is because the fault current increased more quickly to reach the limit and end the test, which provides less time for ember production to begin.

Given there is no known powerline protection system that can yet reliably detect phase-to-phase faults at these current levels, low current limits are not yet realistic and the fire probabilities shown in Figure 58 are almost certainly optimistic. The true probability will be that which applies in faults that progress to flashover.

8.3 Fire risk in 'branch across wires' faults that progress to flashover

In the absence of a powerline protection system that can detect a 'branch across wires' fault in time to interrupt current at a low level, such faults will inevitably progress to flashover. The flashover constitutes a phase-to-phase short circuit that will cause immediate disconnection of the powerline by protection systems. The fire probability in phase-to-phase tests that ended with a flashover might be a better indicator of the fire risk seen on real networks.

Of the 63 phase-to-phase tests that went to flashover, 35 produced a fire risk and 28 did not. This means the probability of a fire from a 'branch across wires' fault based on these tests was 55%.

This estimate may be somewhat optimistic. Phase-to-phase flashover current in tests was limited to 45 amps. On a real high voltage network it can be hundreds or thousands of amps. Once a flashover occurs, disconnection may be very fast, typically in 0.1 to 0.2 seconds if low-set instantaneous protection is enabled. The intense radiant heat and violence of the arc may be sufficient to make a fire more probable than the 55% result would indicate. Reviews of video records indicate that dislodgement of embers by the flashover 'explosion' is more likely to increase fire risk than any heating effect of the brief arc[19].

All that can be concluded from the test results is that the fire risk from 'branch across wires' faults on real networks with existing powerline protection systems is likely to be not less than 55%.

8.4 Variations of fire risk by species in 'branch across wires' faults

Significant variation of fire risk by species was observed as illustrated in Figure 59 which covers the five species for which more than 35 phase-to-phase tests were performed.

The ranking of species by fire risk in 'branch across wires' faults is less clear than in 'branch touching wires' tests. Willow is worst at low current limits, but is not as bad at higher current limits. Desert Ash remains a poor fire risk, Native Daphne is still better, but the ranking varies by current limit. It should be noted that at a current limit of 0.5 amps only three 'branch across wires tests produced fire risk, so it is perhaps not surprising that the ranking at low levels of current limit is uncertain.

[19] This is consistent with the 2011 arc-ignition research which showed radiant heat was not the dominant factor in ignition of dry grass close to an arc.

Figure 59: Fire probability by species for phase-to-phase faults

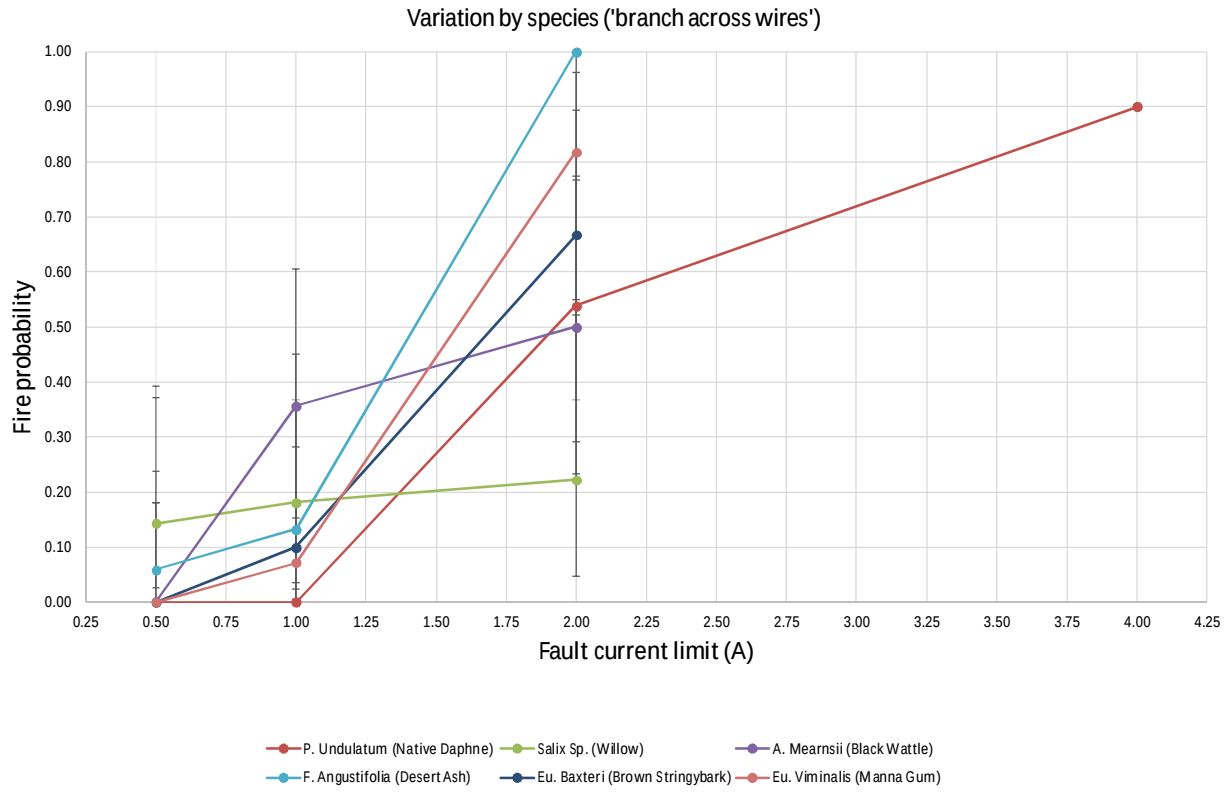

Enough tests (14) were performed on samples of Native Daphne to provide a reliable result at a 4 amp current limit. Another 22 four-amp tests were performed on a variety of other species, mainly Manna Gum and Stringybark.

8.5 Development of fault current in 'branch across wires' tests

Phase to phase faults showed the same four phases of development as the phase-to-earth tests with two changes:

8.5.1 Higher initial current

The initial current was higher than in the phase-to-earth tests. The median value of initial current was around 0.175 amps (see Figure 60)compared with around 0.10 amps for the phase-to-earth tests (see Figure 46) – this is precisely consistent with the 1.73:1 ratio of the voltages applied across the branch in the two tests (22kV and 12.7kV), which reinforces the finding that initially, a branch acts as a linear resistor.

Figure 60: initial current in 'branch across wires' tests

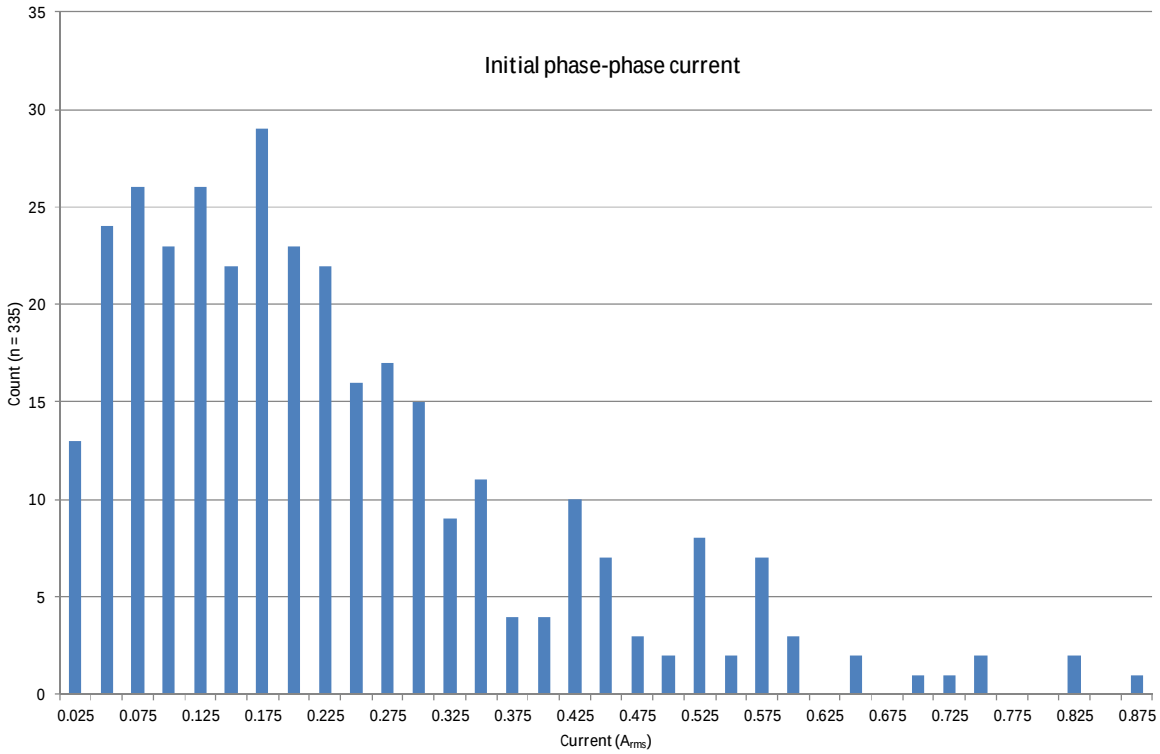

8.5.2 *Faster fault development*

Phase-to-phase faults developed about four times faster than similar phase-to-earth faults. This can be seen by comparing the time to reach two amps in phase-to phase tests (Figure 63 which shows a median of 15 seconds) with the same time in phase to earth tests (Figure 43 on page 47 which shows a median of 60-65 seconds).

The time for the current to reach each of the three set limits is shown in Figure 61, Figure 62 and Figure 63.

Figure 61: time to reach 0.5 Amps in 'branch across wires' tests

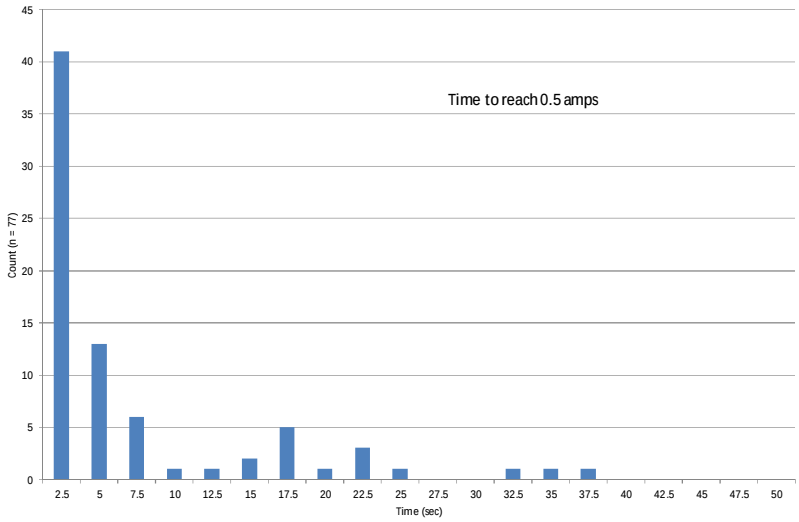

Figure 62: time to reach 1.0 Amp in 'branch across wires' tests

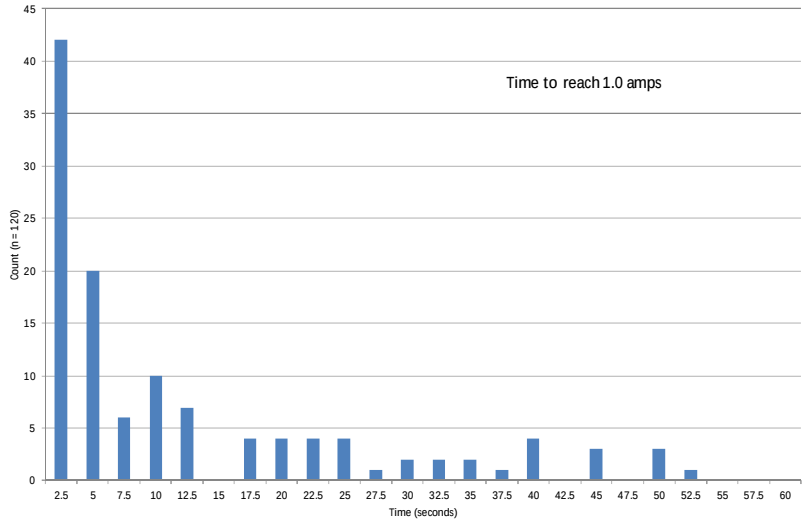

Figure 63: time to reach 2.0 Amps in 'branch across wires' tests

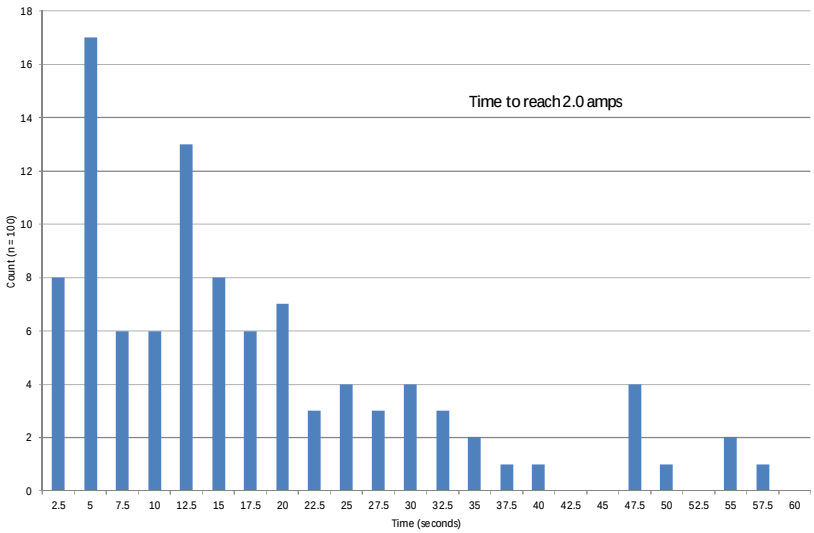

8.6 Development of fire risk in 'branch across wires' faults

As outlined in Section 5.3 above, the rate of growth of current may not reflect the rate of development of fire risk during a vegetation fault. However, test results indicate that fault response would have to be quick to cut fire risk.

There were a total of 66 fire results in the tests that did not result in flashovers and 34 fire results in tests with flashovers. Figure 64 shows the proportion of these totals that had test durations less than a given number of seconds.

Figure 64: proportion of fire results versus test duration – phase-to-phase tests without flashover

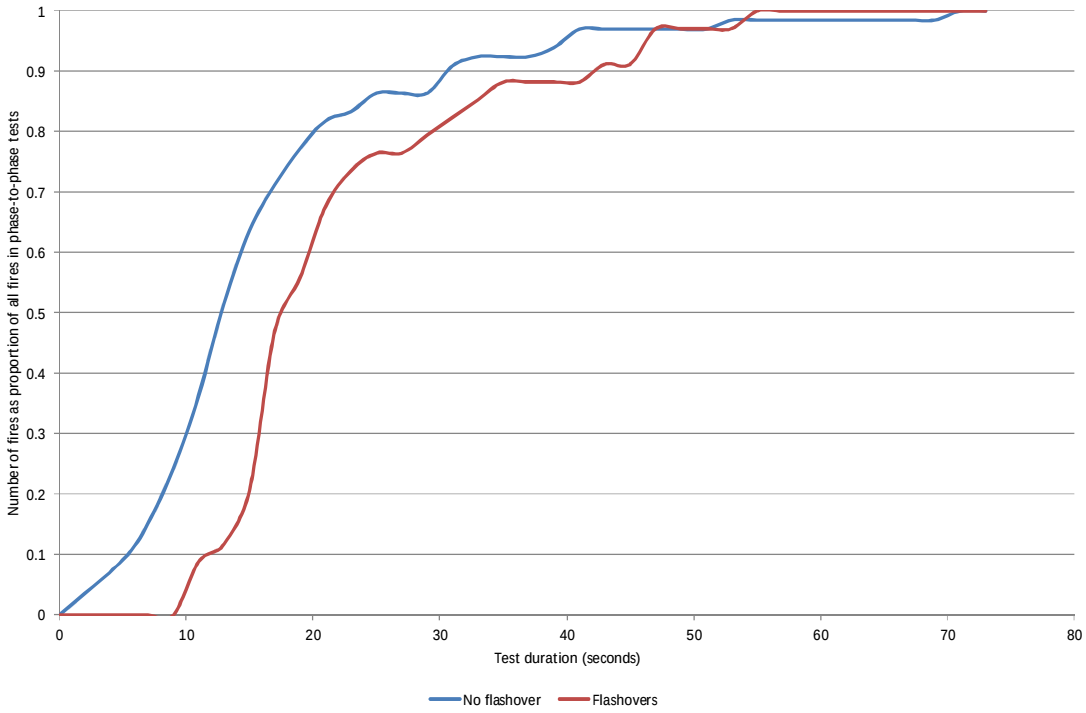

This analysis provides a potentially useful guide to the fault detection speed that would be needed to reduce fire risk in 'branch across wires' faults. From Figure 64, detection times for 'branch across wires' faults longer than about 20 seconds would be unlikely to dramatically reduce fire risk in such faults. Detection and response within about five seconds might be required to achieve substantial reductions in fire risk.

These time scales are much shorter than those that have been demonstrated by high-impedance fault detection schemes developed to date.

9 Vegetation fault signatures

The vegetation conduction ignition test program delivered a large data base of vegetation fault signatures – the electrical disturbances produced on a powerline network by a fault.

9.1 Summary of findings

This section sets out evidence for the following findings related to fault signatures:

1. A large data base of fault signature records was successfully compiled during the test program, including recordings of faulted conductor voltage and fault current in phase-to-earth vegetation faults and phase-to-phase vegetation faults.
2. Background network voltage[20] noise recordings were successfully gathered over a six-week period, including phase-to-earth voltages and phase-to-phase voltages. The level of broad-band network voltage background noise was about 0.3-0.8 volts, dominated by local industrial load and AM radio stations.
3. High-frequency voltage disturbances in tests were most commonly caused by very fast step discontinuities in the fault current or by bursts of high-frequency noise in the fault current. The physical processes behind these features are not known, though there was a tendency for discontinuities to occur near or following fault current zero-crossings and noise bursts to occur near or following peaks in the 50Hz fault current waveform.
4. The high-frequency voltage noise produced in Phase 1 of a vegetation fault was generally much smaller than the total network background noise. However, it could still be seen in test spectrograms, indicating faults might be reliably detected by better signal processing.
5. One specific proprietary partial-discharge detection system currently under development to detect pole-fires produced records that indicated it may be capable of detecting low-current vegetation faults.
6. It was confirmed that a specific fault signature detection relay developed for the North American market[21] did not detect any of the 1,038 vegetation faults in the test program.

The fault signature data base produced in the test program comprises about 50,000 files totalling more than 300GB of data. This data base will be made available in the public domain and supplied to equipment designers and research teams to stimulate development of improved fault detection algorithms and products.

9.2 The potential value of fault signature detection

The hypothesis driving fault signature research is that many high-impedance[21] faults, including vegetation faults, generate high-frequency electrical noise on the powerline network and that this noise can be used to detect such faults before the fault current increases to damaging levels.

---

[20] Background network current noise was not recorded in the test facility as the tests were carried out on a feeder that did not supply customers. The only current available for fault signature measurement was the fault current. Some low-bandwidth feeder current records were collected on another feeder by tapping into substation SV metering current transformer circuits.

[21] Confusion can arise from the use of the term 'high impedance' in this context unless the fault current level is specified. Some US research into high-impedance fault detection using fault signatures is focused on the problem of earth faults on four-wire HV networks. In such networks, the term 'high impedance' is often used to describe a fault that draws tens or hundreds of amps (instead of the usual thousands). One product developed from this research is the GE Multilin F60 Hi-Z relay which was included in the test program. This model is used successfully on four-wire networks in the US. This research and associated commercial products may be of limited relevance to Victoria's three-wire HV networks where the challenge is to detect faults that draw one amp or less.

A vegetation fault draws 50Hz fault current like any other type of powerline fault. The greatest potential value of fault signature research is in detection of those faults where the fault current cannot be distinguished from customer load currents, i.e. where there is no other way to detect the fault. Two such fault classes are of particular interest to Victoria's powerline bushfire safety efforts:

- 'Branch across wires' faults on multi-wire powerlines; and
- 'Branch touching wire' faults on SWER powerlines.

If fast sensitive fault signature recognition systems can be developed for these circumstances, the outcome may be a significant further reduction in powerline fire risk for Victoria.

9.3 Measurement of fault signatures

Detection of faults by fault signature recognition is generally approached as detection of a deviation from the 'normal' level of background electrical noise on the network. The fault signature data base contains records of fault test voltages as well as records of network background noise. Voltage and current records gathered into the signature data base are listed in Table 6.

Table 6: fault signature records available for vegetation tests

Record	Bandwidth	Comment
LF voltage	<5Hz to 50kHz	Phase to earth voltage in the test rig – all tests
HF voltage	10kHz to 1MHz	Phase to earth voltage in the test rig – all tests except Tests 822 to 1038 which recorded phase-to-phase voltage in the test rig
LF current	DC to 50kHz	Current in the vegetation sample – all tests
HF current	10kHz to 1MHz	Current in the vegetation sample – all tests
PD detector	1MHz to 250MHz	Two separate phases to earth, located 30 metres from test rig
SV current	<10Hz to 6.25kHz	Substation SV feeder metering current transformer (ratio 26.7:1)
SV voltages	<10Hz to 12.5kHz	Substation SV three-phase voltage transformer (ratio 22000:110)

Different research teams have focused on different parts of the high frequency spectrum in efforts to find patterns of high-frequency electrical noise that can reliably signal the presence of a fault some distance away along a powerline. The fault signatures in this test program were recorded over a wide range of frequency bands to support the widest possible variety of potential approaches.

Fault signatures and background noise signals were recorded using the wideband low-noise measurement systems described in *Appendix A: Voltage and current measurement*. Fault signatures were successfully recorded for the great majority of tests. Background noise levels were recorded on 18 days, usually at three different times during the day, over the last four weeks of tests. The records are listed in *Appendix D: Test records*. The set of records collected in each test was adjusted as new insights emerged.

9.4 Network voltage background noise levels

During the test program, regular records were taken of network background noise levels. Typically, a one-minute record was taken at the start and end of the day with another usually around the middle

of the day. These tests were performed with the two conductors in the test rig energised but with no vegetation sample between them[22].

The 12.7kV phase-to-earth voltage at the test rig was recorded in most background noise tests. Background network voltage noise proved higher than expected. The following examples illustrate its character.

9.4.1 Low-frequency network voltage background noise

Noise record No 94 taken at 3:32pm on 20th March 2015 provides a useful illustrative example. The raw low-frequency mid-record waveform and the full LF spectrogram are shown in Figure 65.

Figure 65: Noise test No 94 low-frequency phase-to-earth voltage waveform and spectrogram

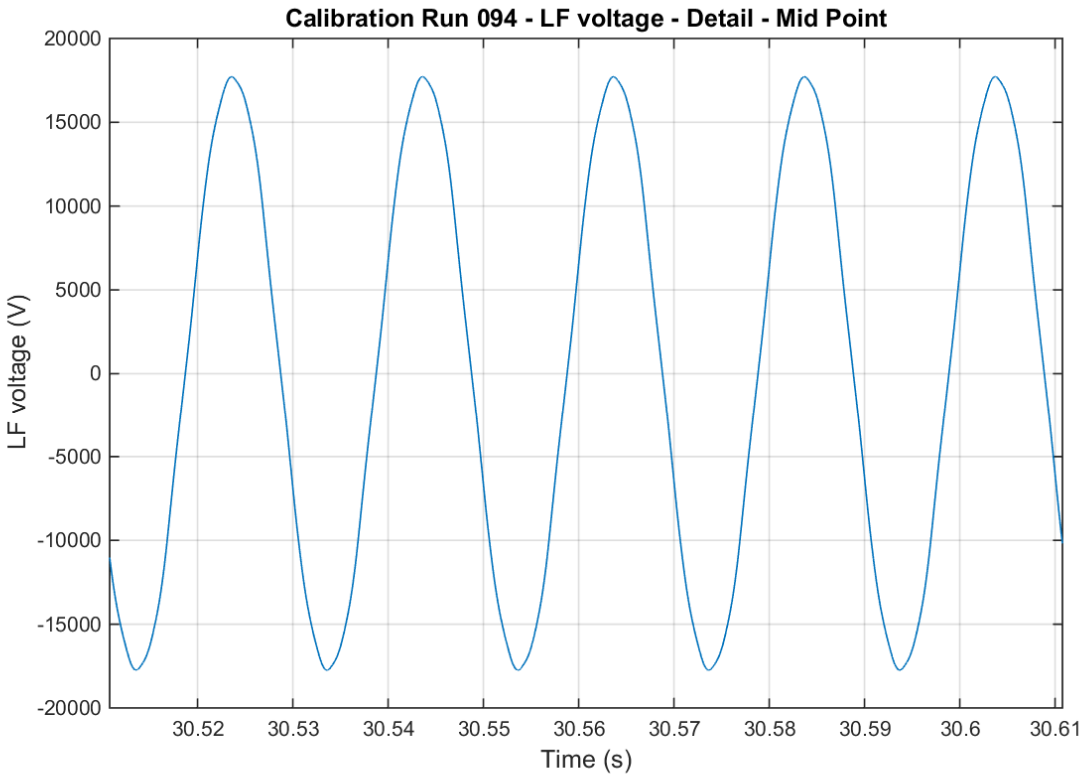

[22] In network background noise tests there was no current in the test rig, so the signals in the current channels comprised measurement system noise only (see *Appendix A: Voltage and current measurement*).

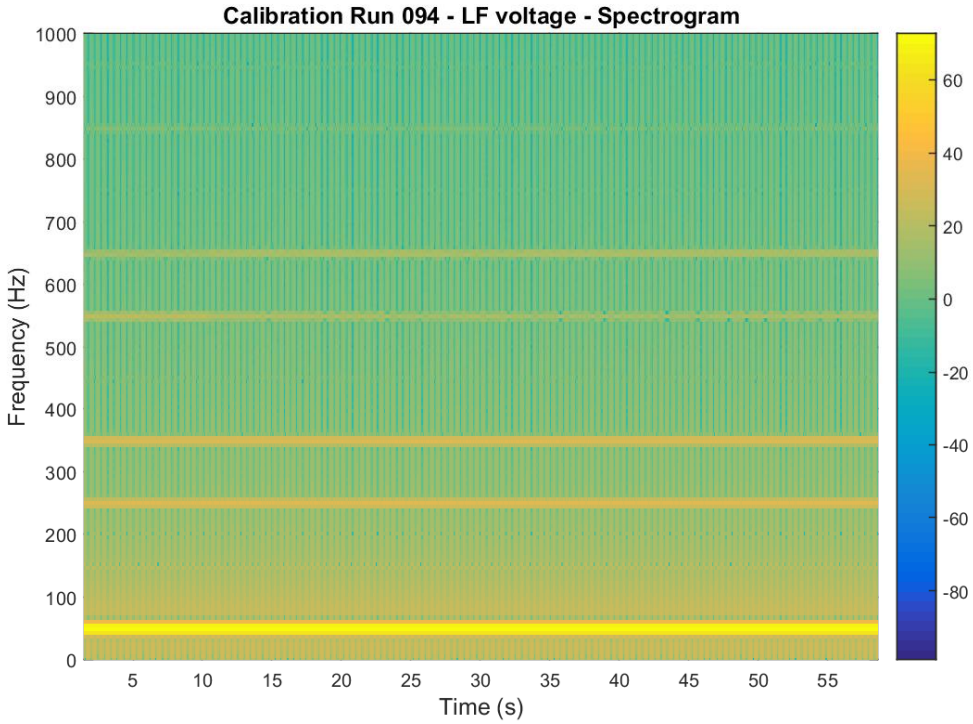

The full LF spectrum covering three frequency ranges up to 50 kHz is shown in Figure 66.

Figure 66: Noise test No 94 phase-to-earth LF voltage spectrum

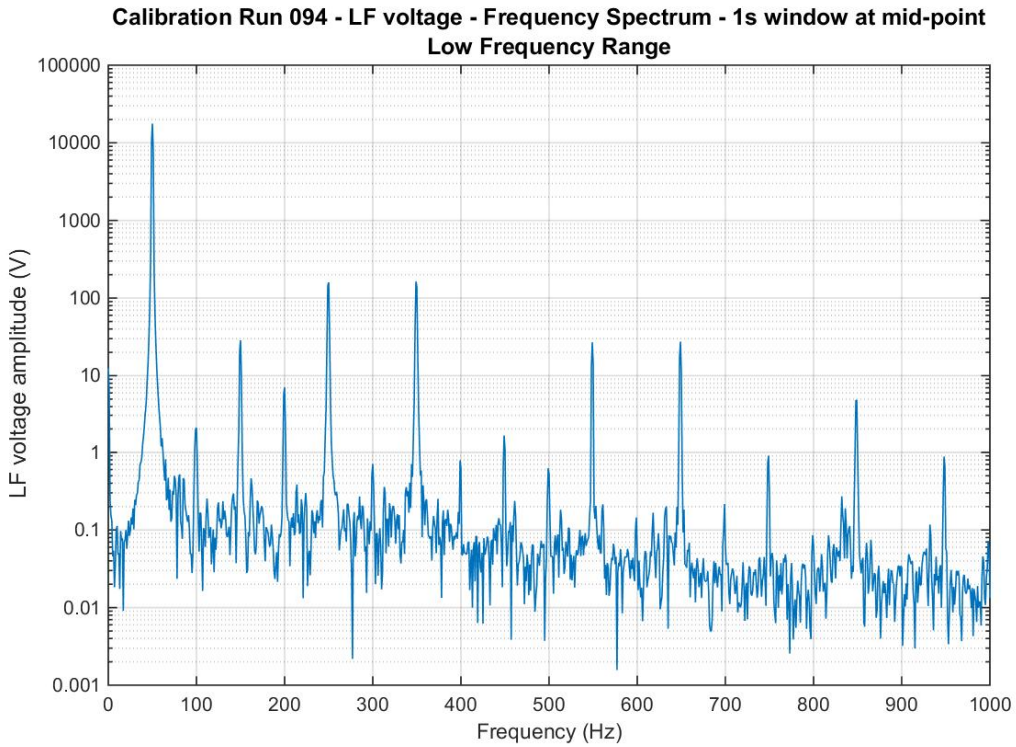

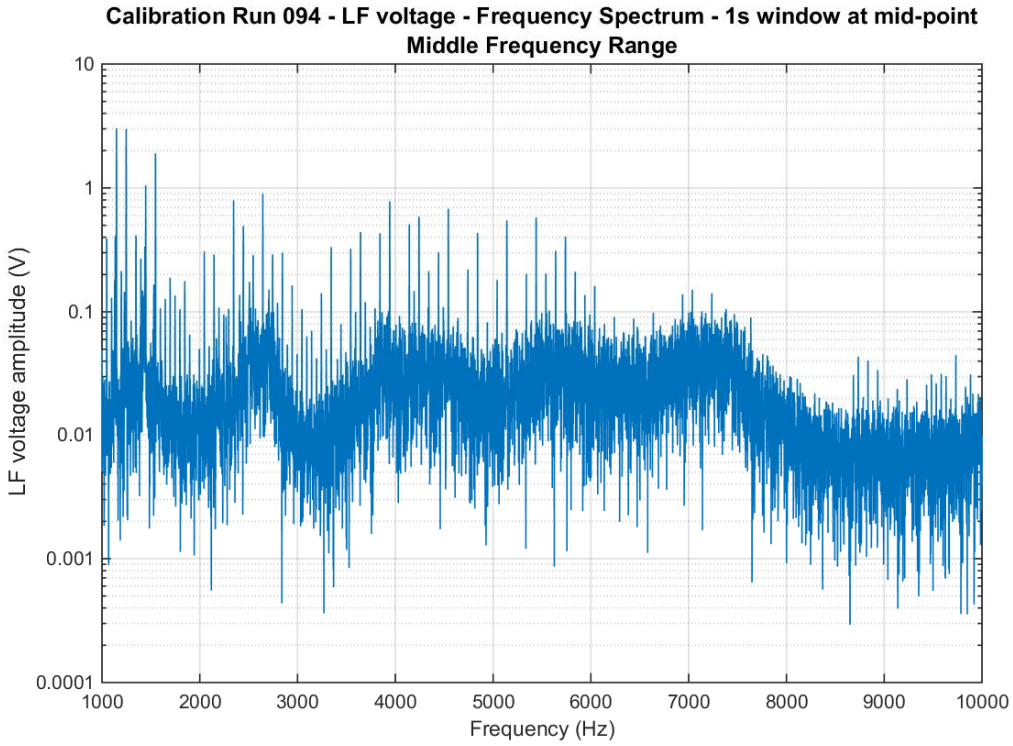

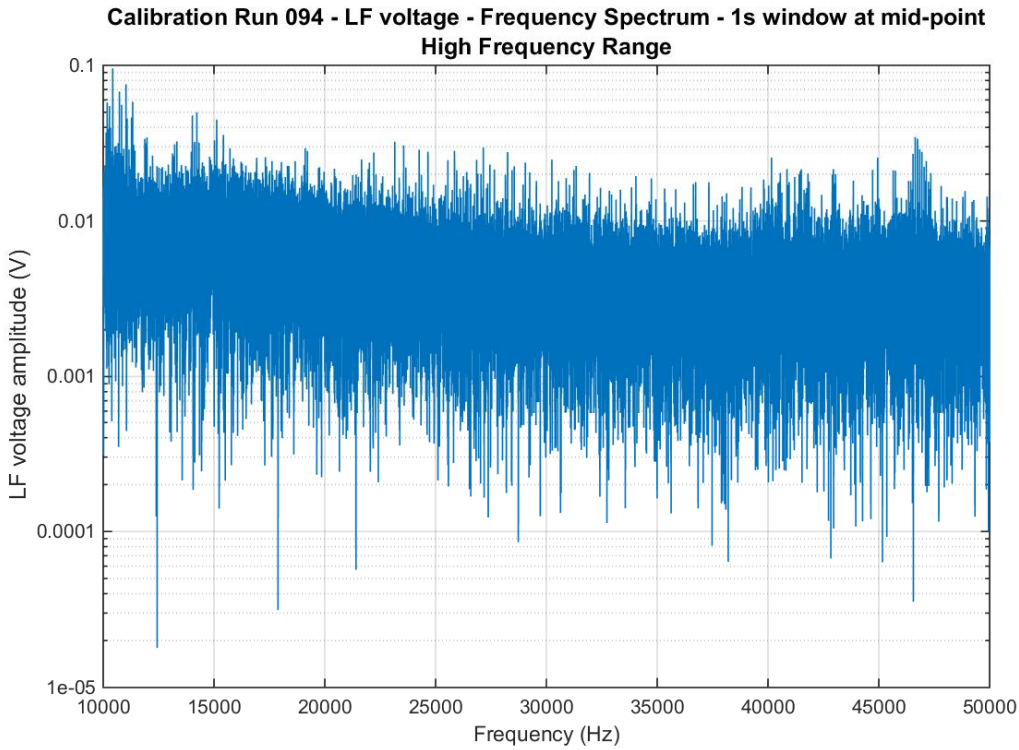

Harmonic distortion is dominated by the 5th, 7th, 11th, and 13th harmonics, with harmonic pairs visible in the spectrum well beyond 1,000 Hz. THD in noise test No 94 was calculated to be 1.2%.

9.4.2 High-frequency network voltage background noise

High-frequency network voltage background noise proved to be complex and it varied over time.

Typically, the high-frequency voltage noise was 0.3-0.8 volts. The largest components of this noise were found to be:

1. Disturbances due to industrial loads
2. Signals from AM radio stations.

Noise test No 94 demonstrates variability in high-frequency noise caused by one particular industrial load. The high-frequency voltage signal and waveform details at start, middle and end of the test are shown in Figure 67.

Figure 67: noise test 94 – phase-to-earth voltage waveforms

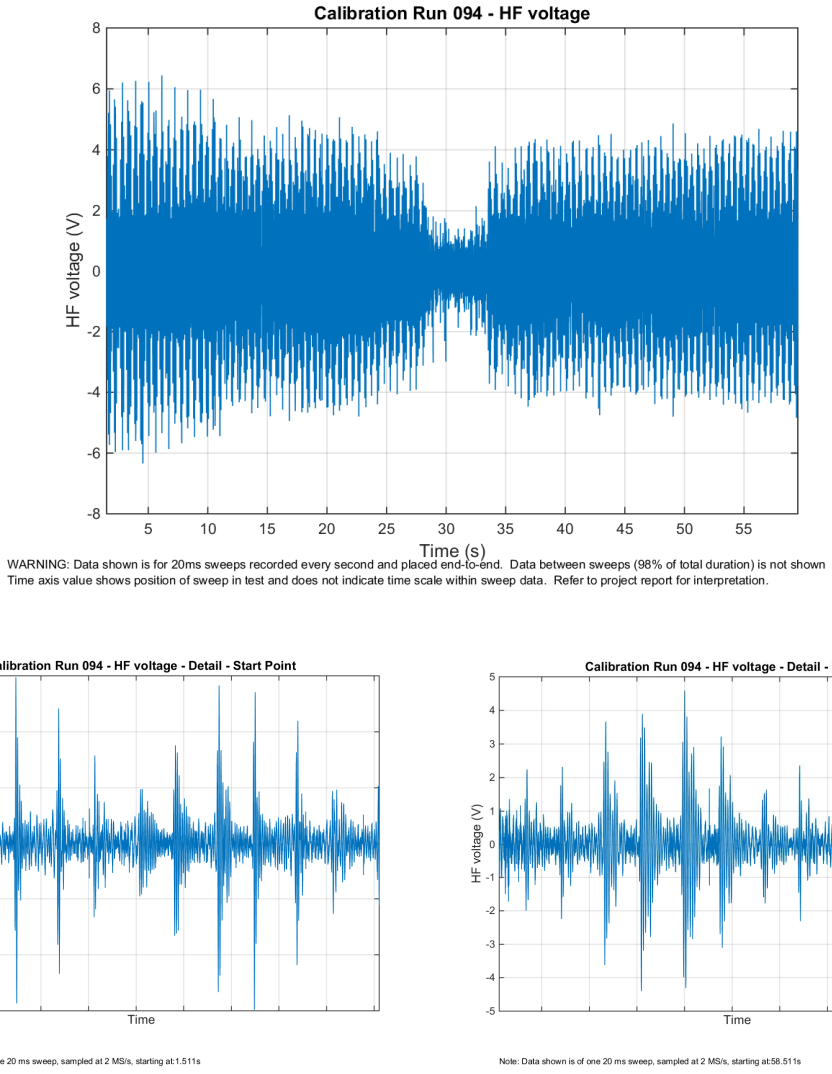

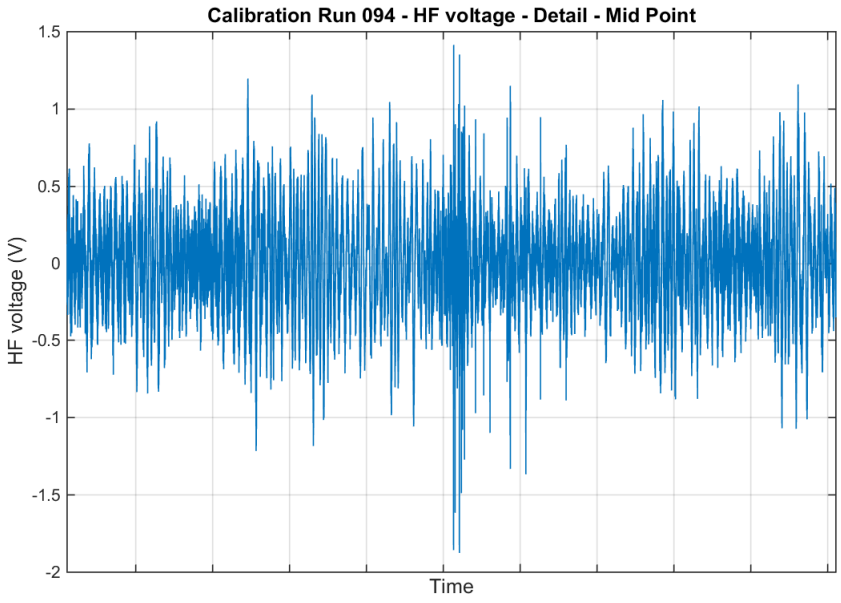

Note: Data shown is of one 20 ms sweep, sampled at 2 MS/s, starting at:30.511s

It can be seen that for about five seconds in the middle of noise test No 94, the magnitude of the high-frequency voltage noise on the network suddenly dropped to a much lower level due to the absence of a signal comprising a 600 Hz train of oscillatory pulses. The hypothesis adopted by the test team was that the noise source was a large three phase full wave thyristor motor/furnace controller which shut down for a few seconds in the middle of noise test No 94.

The high-frequency spectrum of network voltage background noise without this 600Hz noise source, i.e. during the mid-test 'gap', is shown in Figure 68 on the next page for frequencies up to 1MHz.

It can be seen that the high-frequency voltage noise has broad amplitude peaks around 7kHz, 10kHz, 15kHz and 100kHz before decreasing to less than 0.5mV beyond 500 kHz - except for a number of AM radio stations that have amplitudes up to 30mV. The only anomaly in the high frequency range was a strong (120mV amplitude) unidentified narrow-band source at 623 kHz. Attempts to locate or identify this source failed, other than to confirm it was not in the measurement system.

The high-frequency network voltage noise spectrum with the 600Hz pulse train present, i.e. with the large industrial load operating, can be seen in noise test No 93, taken at 9:29am the same day, six hours earlier. The high-frequency spectrum is shown in Figure 69.

The 600Hz source increases the overall voltage noise amplitude near 10 kHz to 800mV, i.e. an eightfold increase, as well as possibly increasing levels across the 9 kHz to 20 kHz band. It includes harmonics to 200 kHz but these are too small to increase total noise significantly. The spectrum above 200 kHz is largely unaffected by this source.

Apart from one or two brief shut-downs like that visible mid-way through noise test No 94, this particular noise source was continuously present throughout the 33 days of the test program. It dominated the amplitude of total high-frequency voltage noise in virtually all test measurements. Its amplitude varied randomly over a wide range. Generally it was relatively steady for a period of a few seconds or tens of seconds before suddenly changing to a new level and remaining steady again. The pattern of variation suggested a large grinding mill, furnace or similar machine fed with batches of material to process. This load was not identified during the test program.

Figure 68: Noise test No 94 phase-to-earth HF voltage spectrum

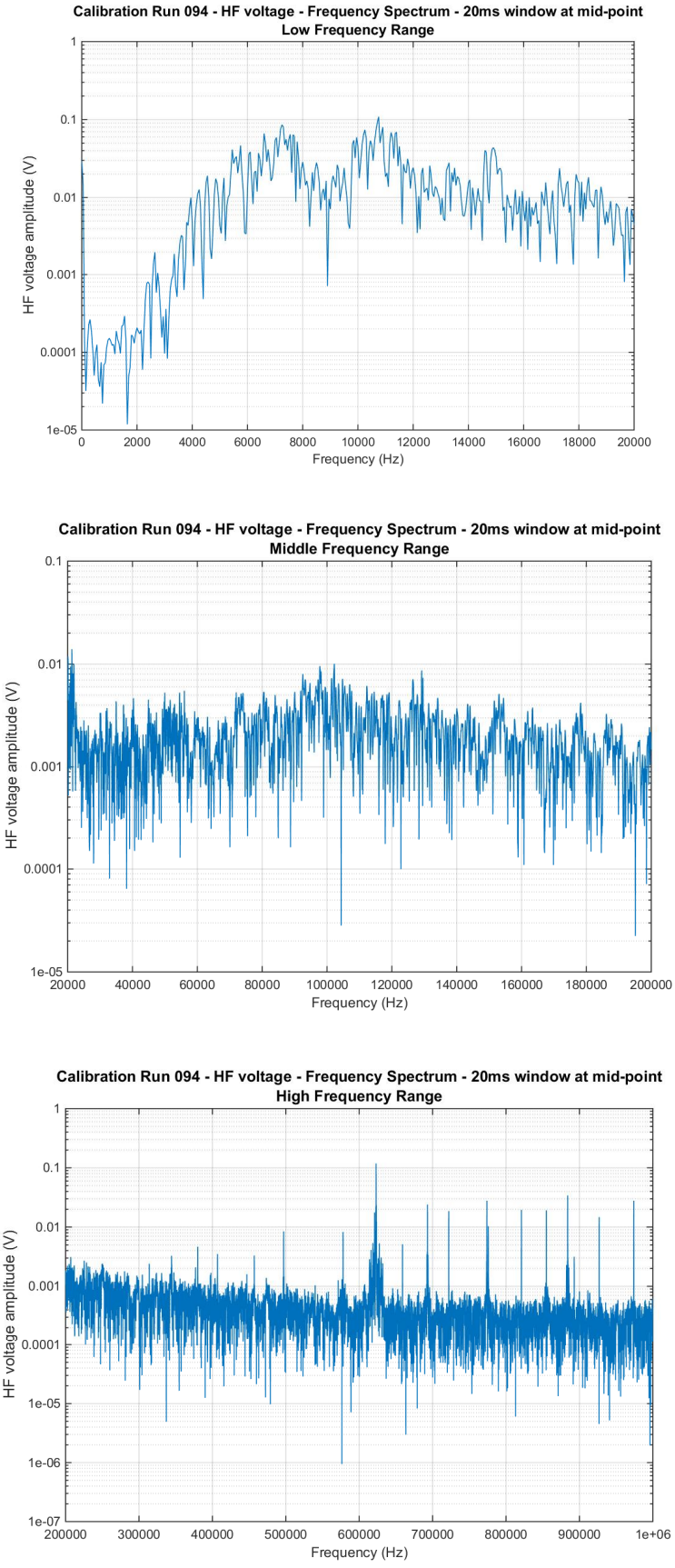

Figure 69: Noise test No 93 spectrum of HF phase-to-earth voltage noise with large industrial load operating

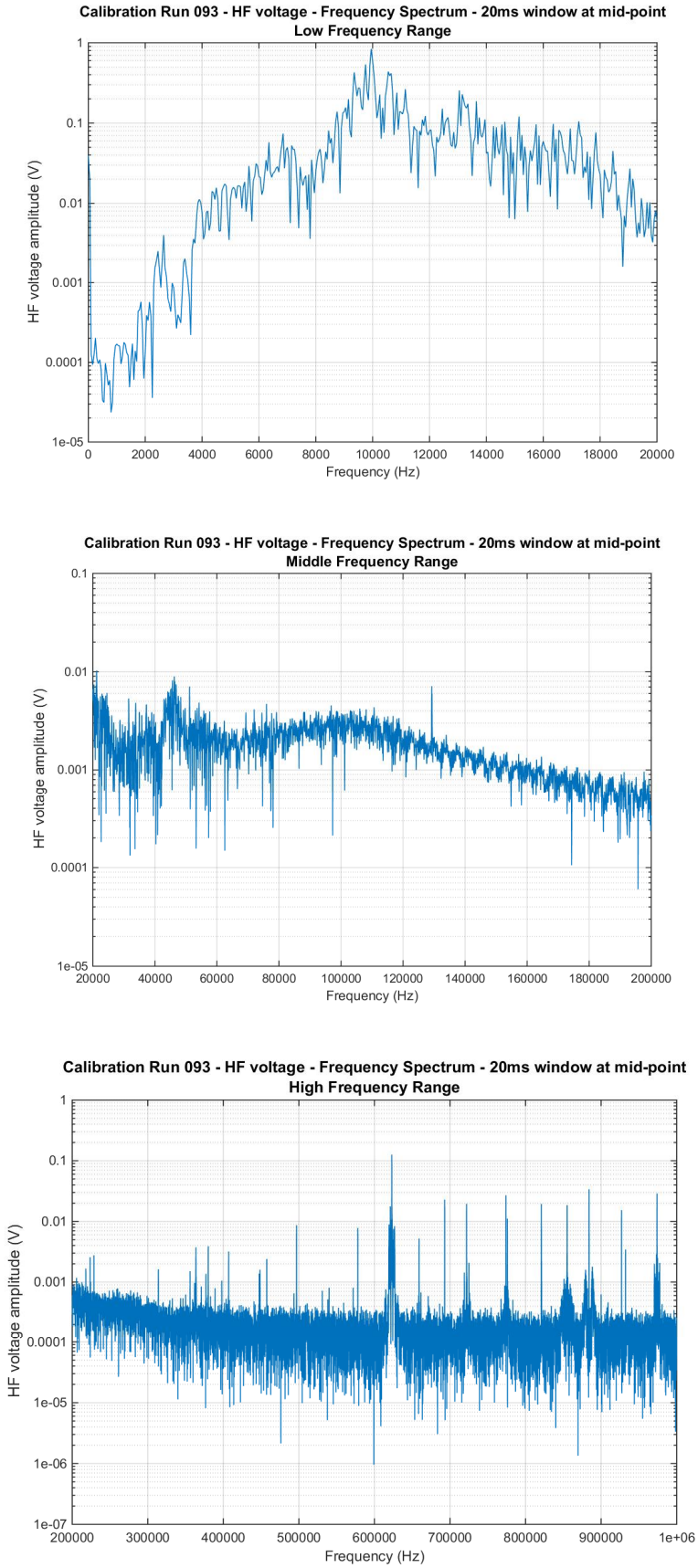

In the last week of tests (23rd to 27th March 2015 starting from Test 822), the high-frequency voltage measurement system was changed to measure phase-to-phase voltage. Low-frequency voltage measurement remained phase-to-earth. Noise test No 108 performed at 4:13pm on 26th March illustrates typical phase-to-phase voltage high-frequency background noise:

Figure 70: Noise test No 108 phase-phase HF voltage noise

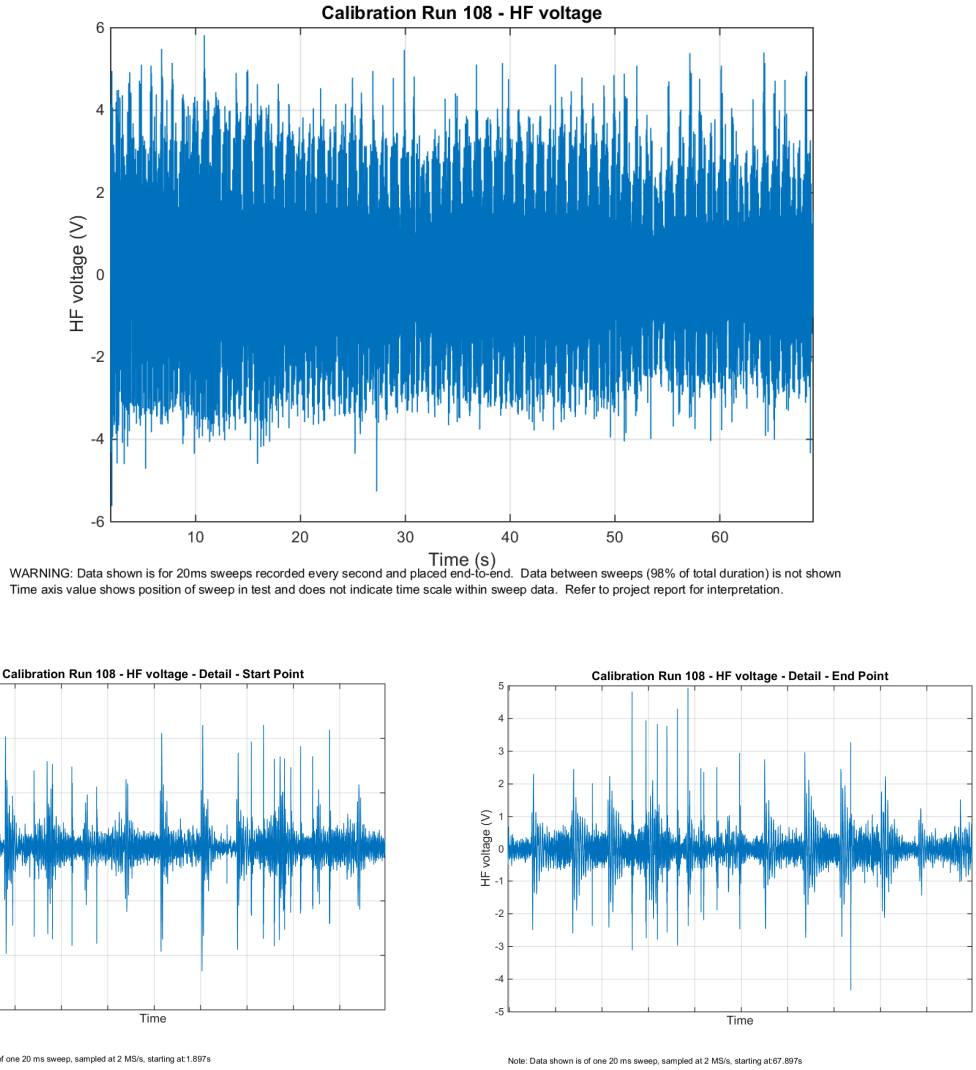

The high-frequency voltage waveform detail shows additional spikes compared to the phase-to-earth waveforms shown in Figure 67 and the amplitude of the 600Hz noise is somewhat reduced. The high-frequency spectrum of the phase-to-phase voltage is shown in Figure 71.

Figure 71: Noise test No 108 high-frequency spectrum of phase-to-phase voltage

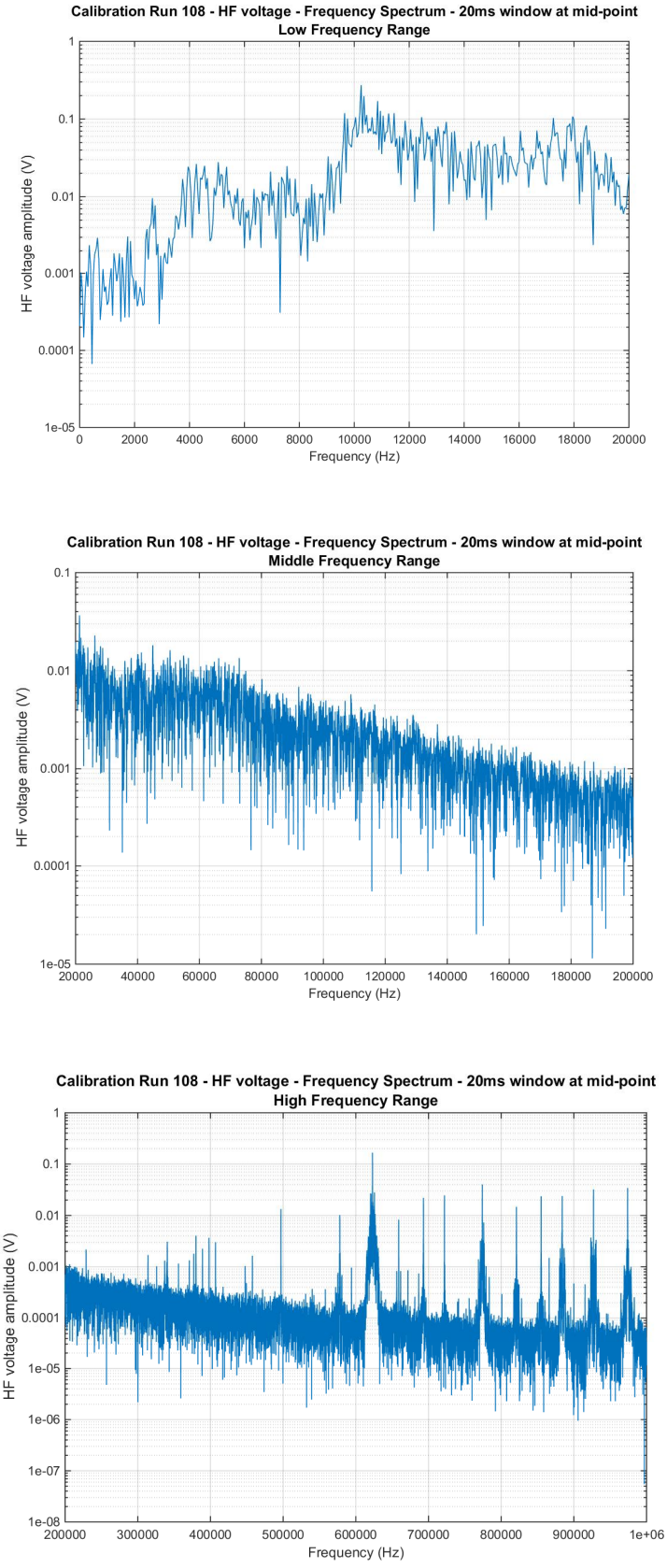

Comparisons of noise test No 108 (Figure 71) with noise test No 93 (Figure 69) show[23] the phase-to-phase high-frequency voltage noise differed from the phase-earth noise in a number of respects:

1. The amplitude of the 600Hz noise source was reduced by a factor of about three
2. Noise in the 6-9kHz band was reduced by a factor of about five
3. Other industrial noise sources increased the noise amplitude in the 15-20 kHz band
4. AM radio station noise increased somewhat and the baseline level of background noise in the 0.5-1.0MHz range reduced by a factor of about three.

The original objective of moving to phase-phase measurement of high-frequency voltage noise was to reduce the AM radio station noise in the record to better reveal the fault signature. This idea was based on the hypothesis that radio noise might be common-mode, i.e. the same AM radio signal would be picked up on each phase of the network. Tests 822 onwards showed this hypothesis offered little value, though the amplitude of high-frequency noise other than AM radio stations was reduced. It was decided to retain the phase-to-phase voltage measurement arrangement for the last week of tests (Test 822 and beyond) to collect sufficient records for the performance of this alternative high-frequency voltage measurement approach to be better understood.

9.5 The nature of high-frequency voltage noise caused by vegetation faults

The high-frequency voltage noise that constitutes the fault signature is generated by very fast disturbances in the fault current caused by changes in the fault impedance. At high frequencies, powerline networks are essentially 'quiet' in that they contain no internal high-frequency energy sources and high-frequency voltage disturbances are generally reflections of very fast variations in current path impedances (either faults or customer loads) or induced by EM radiation from external sources.

The following examples illustrate some of the variety of high-frequency phenomena visible in the fault signature test records, the most common of which were fast step discontinuities in fault current and short bursts of high-frequency noise in fault current. There may be other high-frequency phenomena contained in the 1,038 sets of test records that are not covered in this sample. However, this illustrative sample includes the most commonly observed forms of high-frequency voltage disturbance.

As faults develop, high frequency components generally increase in magnitude. By the time a fault had reached Phase 3, there was usually a substantial amount of high-frequency current and voltage noise generated. However, this late-stage abundance of high-frequency disturbance is of limited value in fault signature recognition as faults must be detected during Phase 1 if powerline fires are to be prevented.

9.5.1 Fast step discontinuities in the fault current

Test 700 was a 45 seconds long 2.0 Amp limit phase-to-earth test of Drooping Sheoak (Allocasuarina Verticillata) performed at 1:45pm on 17th March 2015. The profile of the fault current during Test 700 is shown in Figure 72.

[23] This is an illustrative comparison of two specific noise tests (No 93 and No 108). A more systematic comparison of all phase-earth noise test records with all phase-phase noise records was not attempted.

Figure 72: Test 700 fault current profile (phase-to-earth 2.0 Amp limited test of Drooping Sheoak)

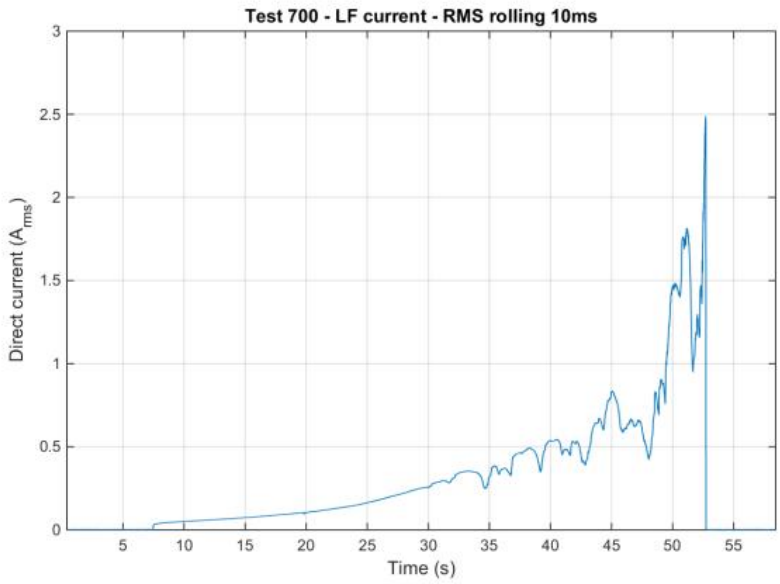

This test exhibited a relatively long (30 seconds) Phase 1, during which there was a significant level of high-frequency fault signature generation as shown in Figure 73.

Figure 73: Test 700 high-frequency voltage and current

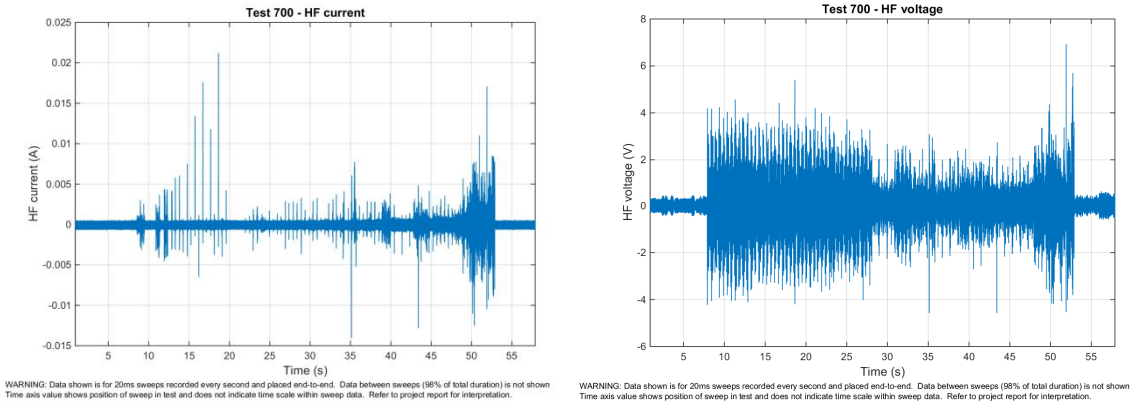

The HF voltage shown in Figure 73 is mainly caused by industrial load, not the fault. It appears when the test rig is connected to the network at the start of the fault and disappears when the network connection is broken to remove the fault, i.e. though it is not visible in the test record when the fault is not present, it is still present on the network. However, the disturbance caused by the fault can be seen in the raw data record by zooming in to examine the detail.

Sweep[24] 18 in the Test 700 record shows two spikes[25] that reflect sudden discontinuities in the fault current that in turn create voltage disturbances superimposed on noise caused by industrial loads.

[24] The recorded data included a 20ms sweep sampled at 2MS/s taken at intervals of one second throughout the test duration.

[25] The high-frequency measurement channels included high-pass filters to eliminate the 50Hz quantities. These show sudden step changes as fast spikes.

Figure 74: Test 700 Sweep 18 high-frequency fault current and voltage (20ms sample 18 seconds into the test)

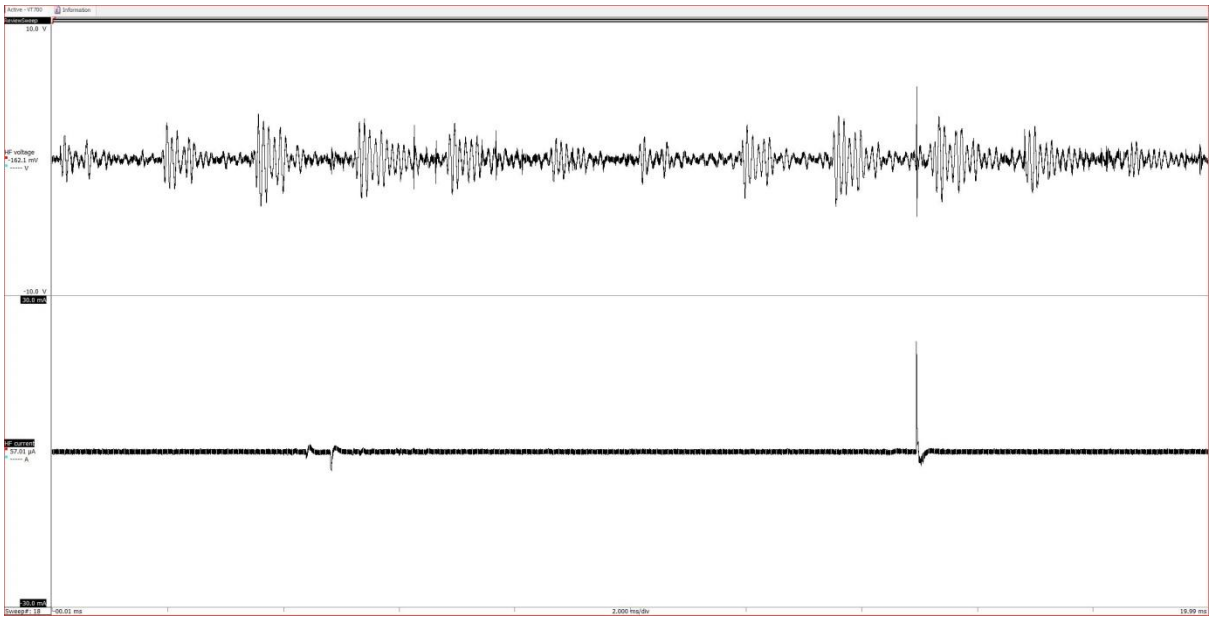

Zooming in further, Figure 75 shows the detail of a single fast fault current discontinuity that causes a disturbance in the voltage record. The magnitude of the current step change is around 20mA and the voltage disturbance is of the order of 10 volts peak-to-peak.

Figure 75: Test 700 Sweep 18 - zoomed view of single fast fault current discontinuity

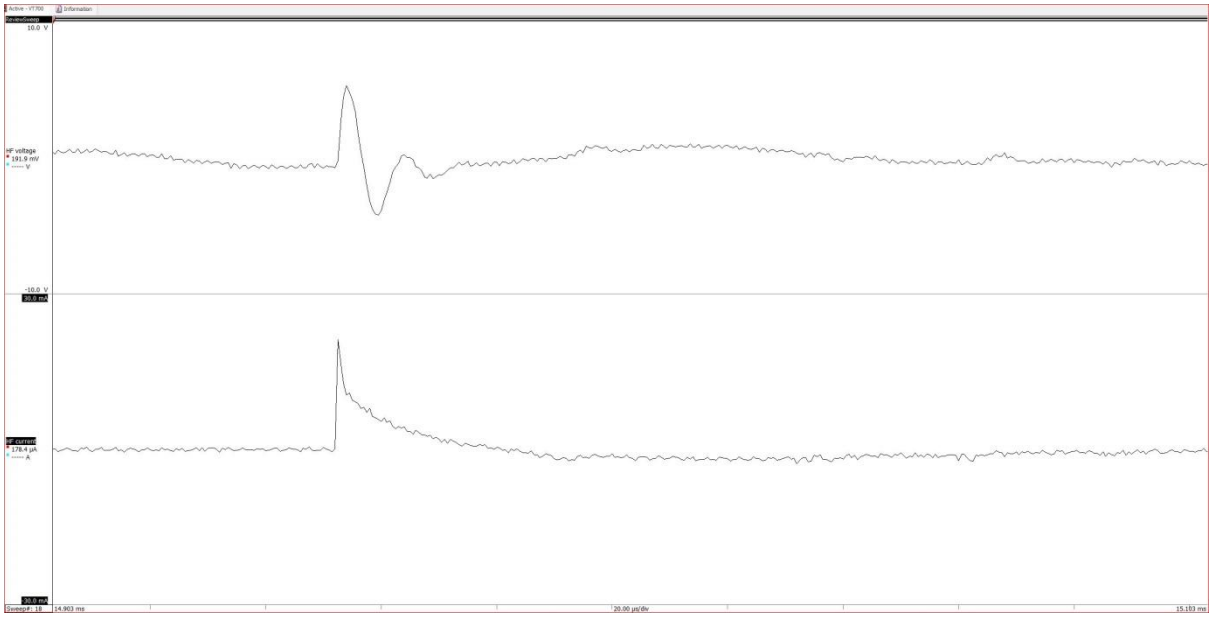

Figure 75 shows that in Phase 1 of Test 700, the high-frequency fault signature was caused by very fast discontinuities in the fault current. The rise-time of each current step is less than one sample period, i.e. less than half a microsecond. The fast step causes a strongly damped oscillatory response in the network voltage with a frequency around 100kHz. This response is most likely set by local network parameters, i.e. it reflects the local network's impulse response.

The physical process behind fast step discontinuities in the fault current is not known. During Phase 1 they seem to be generally associated with restrike of an arc after the zero-crossings of the fault current as shown in Figure 76.

Figure 76: Test 700 Sweep 16 - fault current discontinuity at zero-crossing and resultant HF current 'spike'

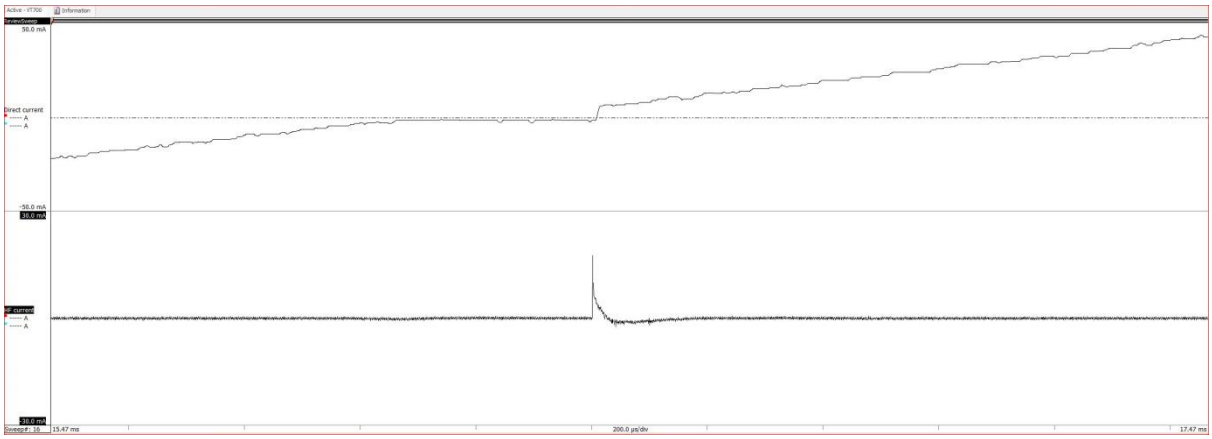

Fast discontinuity in fault current was the most commonly observed cause of high-frequency voltage disturbance in the tests.

9.5.2 Brief bursts of high-frequency fault current

Test 825 was a 22 second long phase-to-phase test of Willow (Salix Sp.) performed at 9:40am on 23rd March 2015. The profile of the fault current during the test is shown in Figure 77.

Figure 77: Test 825 fault current profile

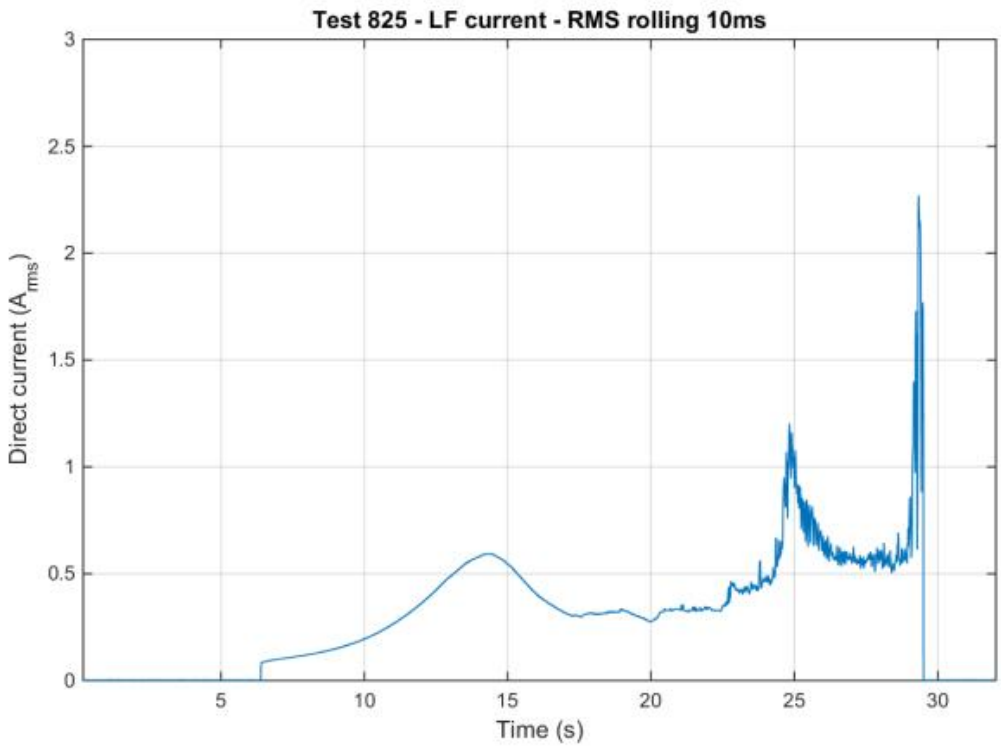

The high-frequency voltage and current records of Test 825 are shown in Figure 78.

Figure 78: Test 825 HF voltage (measured phase-to-phase) and fault current records

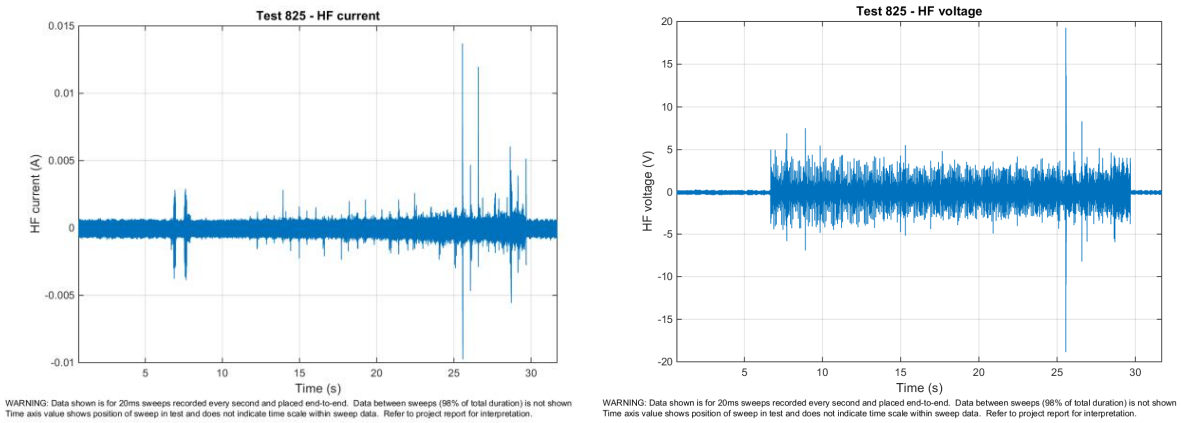

Test 825 produced very small high-frequency voltage signals in Phase 1 apart from two short bursts of noise close to the start of the test. These are shown in Figure 79.

Figure 79: Test 825 Sweep 7 - high-frequency bursts of fault current

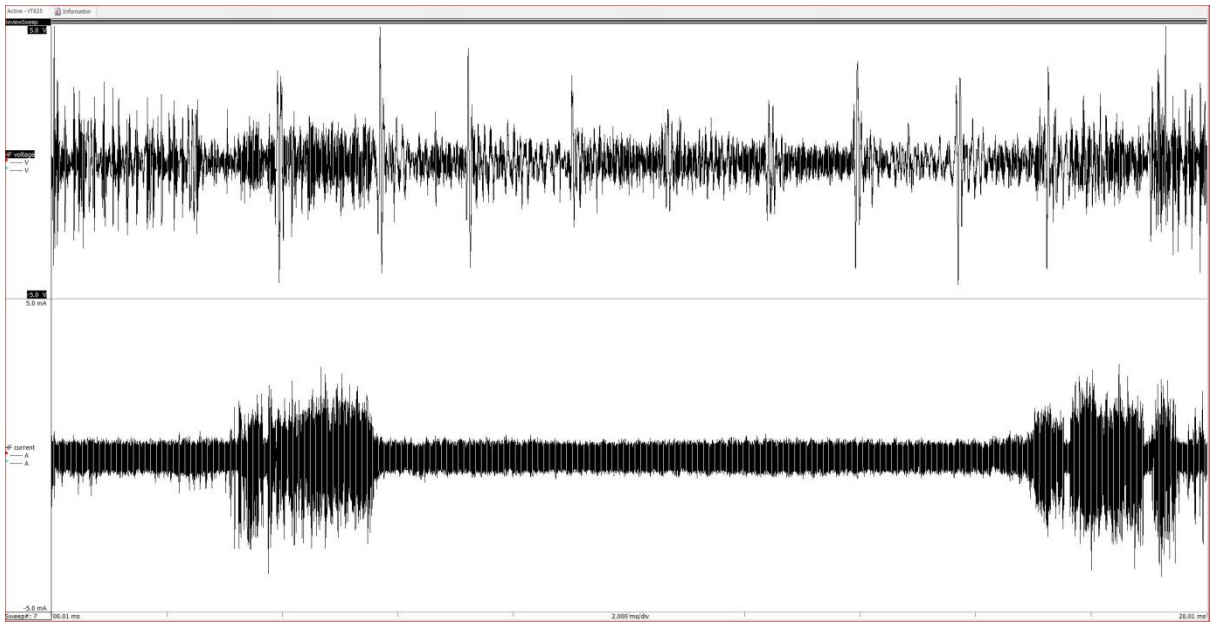

The magnitude of the current bursts is quite small (about 3-5mA peak-to-peak) and each one lasted only a few milliseconds. One can be seen in more detail in Figure 80. The frequency of the fault current variation in each burst is of the order of 800 kHz and the network response voltage (the small 800 kHz ripple superimposed on the underlying background noise) is of the order of 100mV rms.

The physical mechanism that creates these high-frequency bursts of fault current is not known. More often than not, they seem to occur in the second half of each half cycle of fault current, i.e. when the fault current 50Hz waveform is near or has just passed its peak value. However, this is not always so, e.g. it was not the case with the two bursts shown in Figure 79 above.

Figure 80: Test 825 zoomed view of high-frequency current burst

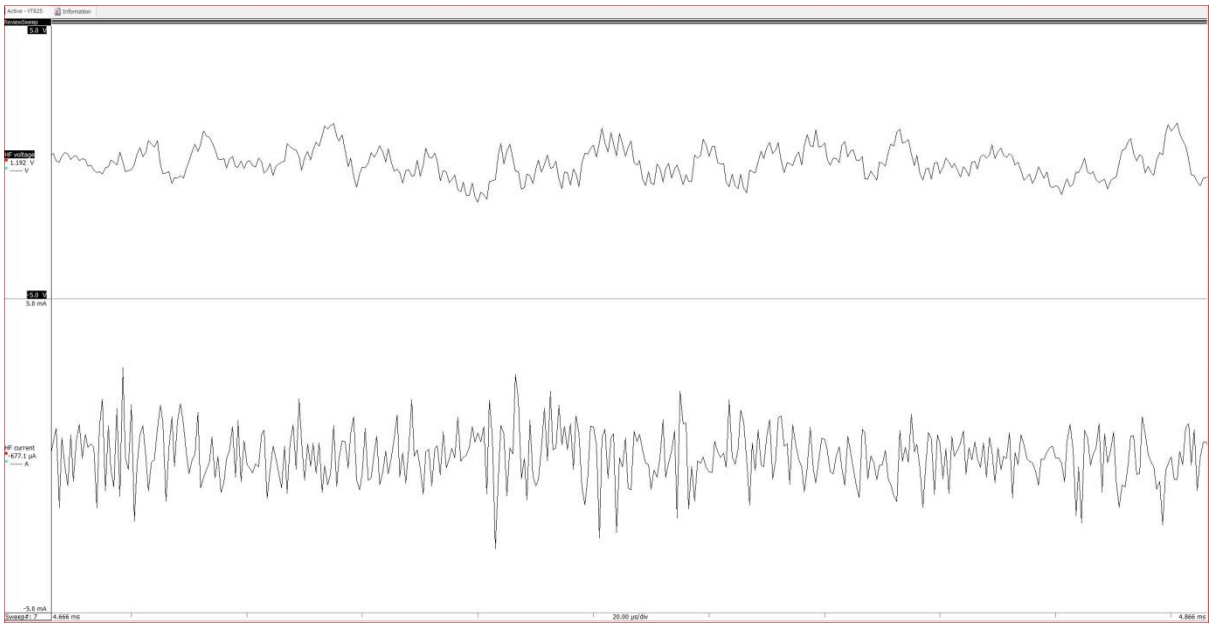

Short bursts of high-frequency current noise were almost as common a cause of high-frequency voltage disturbance as were sudden step discontinuities in fault current.

9.5.3 'chopped' fault current waveform

Test 67 was a 76 second long phase-to-earth test of Brown Stringybark (Eucalyptus Baxteri) performed at 10:17am on 11th February 2015. It continued until flashover. The fault current profile and high frequency records are shown in Figure 81.

Late in Phase 3 of Test 67, the fault current was 'chopped' as shown in Figure 82, generating large high-frequency current and voltage disturbances every 10 milliseconds, sometimes single discontinuities and at other times, bursts of multiple discontinuities.

This type of current 'chopping' was relatively uncommon and only seen very occasionally in test records. It is an extreme form of the fast step current discontinuities described in 9.5.1 above. Again, the physical process that causes this phenomenon is not known, though it does appear to relate to re-establishment of an arc after the current has gone through a zero-crossing.

Figure 81: Test 67 fault current profile

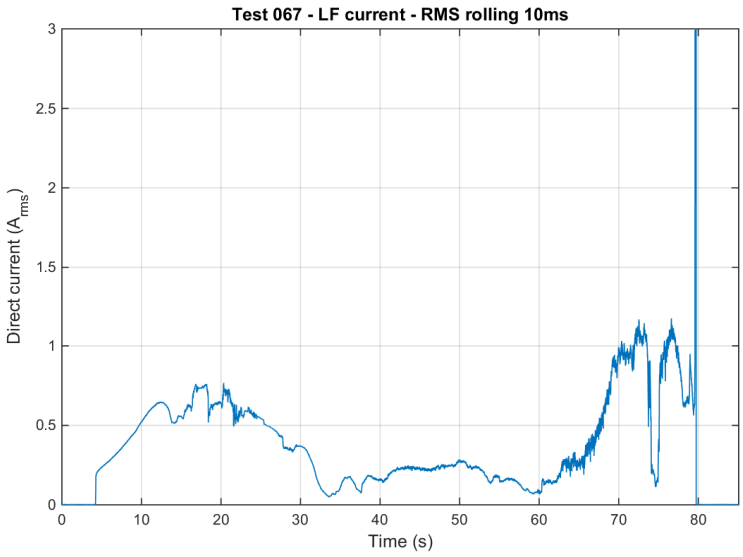

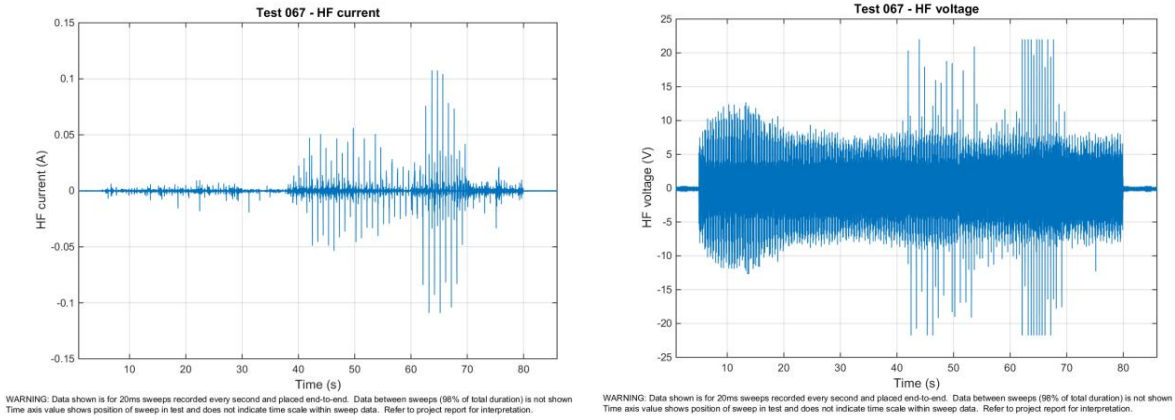

Figure 82: Test 67 Sweep 61 'chopped' fault current with resulting HF current spikes

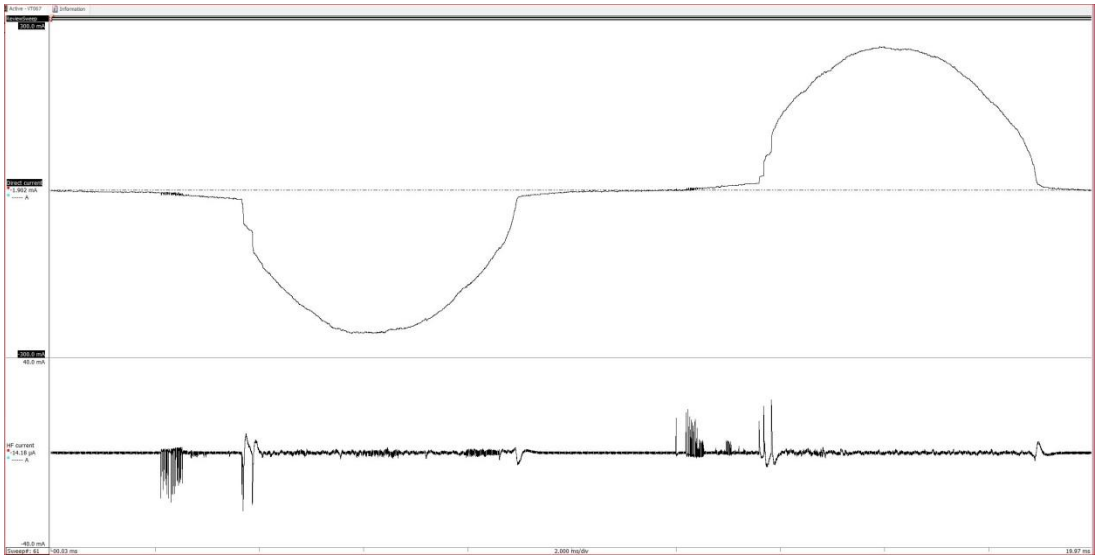

9.5.4 Fast discontinuities in fault current away from current zero-crossings

Occasionally, discontinuities in the 50Hz fault current waveform occurred near current peaks. These events generated particularly large high-frequency current disturbances. An example is shown in Figure 83 which shows a step discontinuity at the peak of the fault current waveform.

Figure 83: Test 479 Sweep 28 phase-to-phase test of Acacia Mearnsii

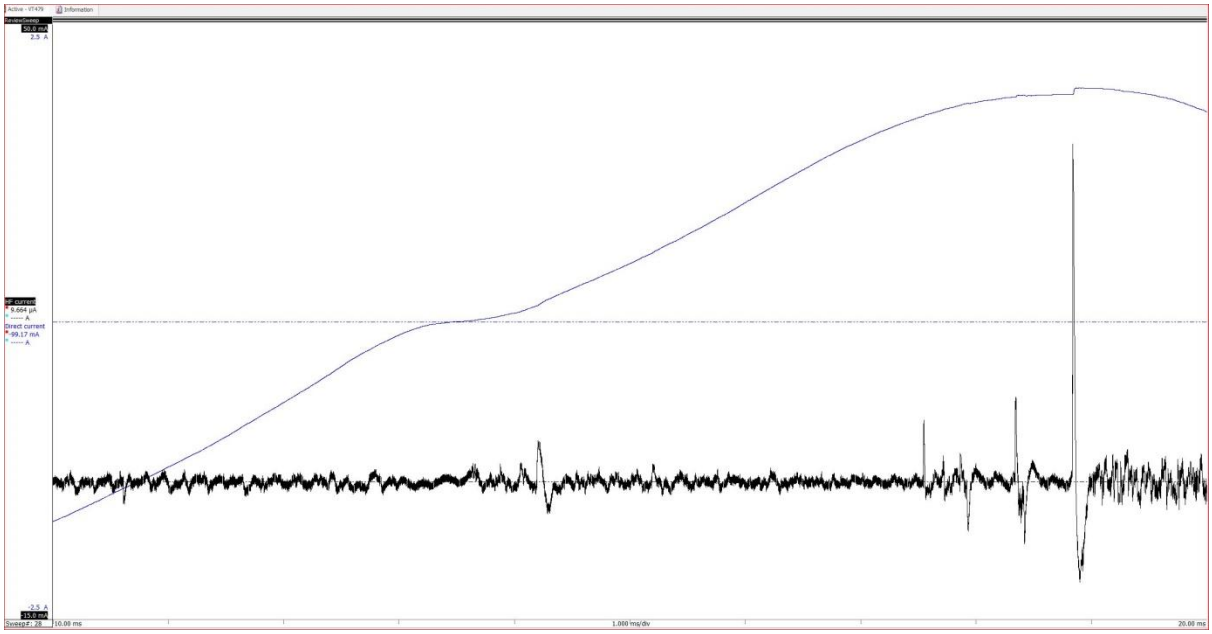

This example again illustrates how sudden discontinuities in fault current show as fast spikes in the high-frequency current record due to the high-pass frequency response of the HF recording channels used in the tests - sudden changes pass through while slower variations do not.

Powerline networks exhibit a tuned frequency response. So in a similar way to the high-frequency recording channels, a sudden step change in current is likely to be transformed into a damped high-frequency oscillation in the network voltage as illustrated in Figure 75 on page 77.

9.6 The data base of fault signatures

The data base contains data files for 1038 fault tests and 112 calibration/noise tests. The records fall into three categories:

9.6.1 Test facility fault signature records

The majority of graphics in this report are drawn from this category of test records. For each test, the records include:

1. The Gen3i DAQ system data files; and
2. A selection of charts produced after completion of the test program.

The charts are a useful guide to which detailed Gen3i data files deserve attention. The Gen3i files can be viewed and exported to other formats using the HBM Perception Viewer freeware.

This assembly of data is summarised and organised in two documents: the daily test logs which are scanned copies of the hand-written log sheet completed at the time of the test; and, the master analysis spreadsheet (filename: *PBSP_Runsheet and analysis_10-4-15_final*) which allows the 1038 tests to be sorted and charted as well as offering easy identification of all tests of a particular type.

This spreadsheet also contains all laboratory analysis results for moisture content and conductivity tests. It has been used to generate the summary table set out in *Appendix D: Test records* and many charts in this report.

The data base also contains video (visible-light and infrared) records of each test so the recorded electrical quantities can be correlated with the progress of the fault through the different phases of ignition.

The test facility records are calibrated, wide-band, low-noise records of the voltage and current at the fault location. They were collected using custom designed and constructed systems documented in *Appendix A: Voltage and current measurement*. These systems are not typical of equipment normally available in powerline networks or substations. These records should be viewed as a reference - an accurate measurement of network quantities, rather than as signals that could readily be provided at low cost to a protection relay or fault detector.

9.6.2 Zone substation SV records

The data base contains data collected by United Energy using an Elspec digital power quality meter located in the zone substation SV control room. This was connected to the station's existing metering current transformers and electromagnetic voltage transformers. These records reflect what could be readily made available to feed a fault-detection relay in existing substations at relatively low cost. Details of the Elspec PQM settings and connections are set out in *Appendix A: Voltage and current measurement*. An example of charts derived from an Elspec PQM test record is shown in Figure 84.

Figure 84: Test 110 Elspec PQM record of current with comparison to Gen3i data

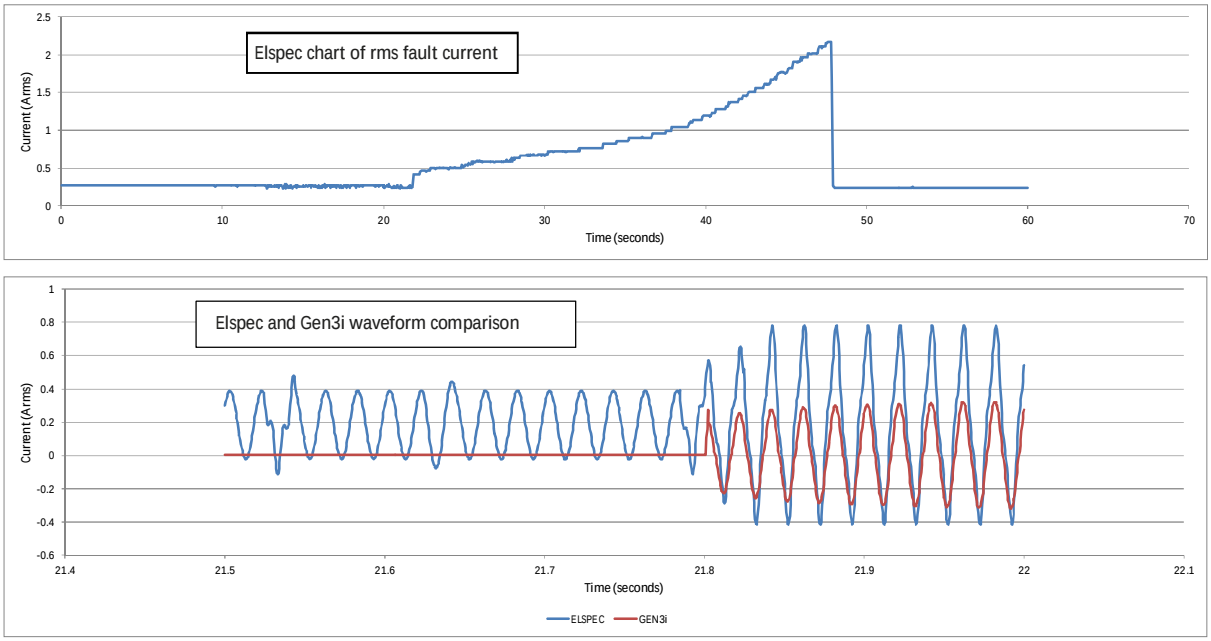

The lower bandwidth of the Elspec record is evident at the start of the fault current where the sudden step change in current is smoothed over a short period.

The Elspec data comprises about 250GB of files. No analysis of this data has yet been attempted.

9.6.3 IND Technology records

Data records collected by the IND Technology sensors mounted on the overhead powerline span feeding the test rig container are also stored in the fault signature data base. This is un-calibrated data collected at a sampling rate of 500MS/s using capacitive sensors (i.e. non-contact) to detect high-frequency disturbances in powerline voltages. The records were collected by a digital oscilloscope directly attached to the sensors. It is an example of a non-traditional but relatively low cost voltage waveform recording approach.

An example of the IND data is shown in Figure 85. It shows a typical network voltage disturbance with one thousand samples gathered over a 2µs period. The disturbance comprises a lightly damped 5 MHz sinusoid.

Figure 85: sample of IND Technology data for Test 1007

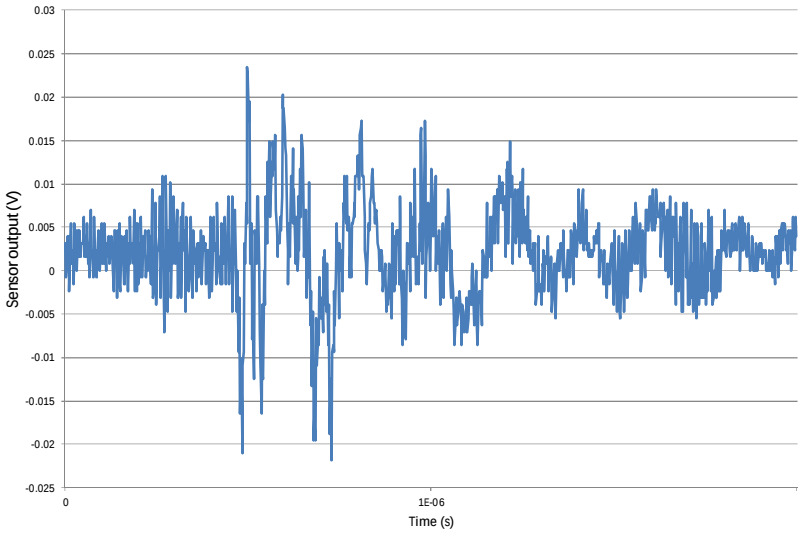

The IND Technology data in the fault signatures data base comprises 2,100 TDMS files in 670 folders totalling 12.4GB of data. No analysis of this data has yet been attempted.

9.7 Feasibility of fault detection by signature recognition

At completion of the test program, the key question about fault signatures is: 'do the recorded signatures appear potentially useful for detection of vegetation faults?' Two indications of the promise of fault detection were observed which would support an affirmative response to this question. These indications were:

9.7.1 Visibility of faults in high-frequency voltage records

Test 335 was a 'wire into vegetation' test on a Silver Banksia (Banksia Marginata) bush in which an energised high voltage conductor was dropped into the sample bush. The spectrogram of high-frequency voltage recorded in the test is shown in Figure 86. The high-frequency voltage disturbance caused by the fault current is clearly visible. The disturbance prior to the start of the fault current flow is the normal network background noise.

Figure 86: Test 335 'wire into vegetation' test of Silver Banksia bush

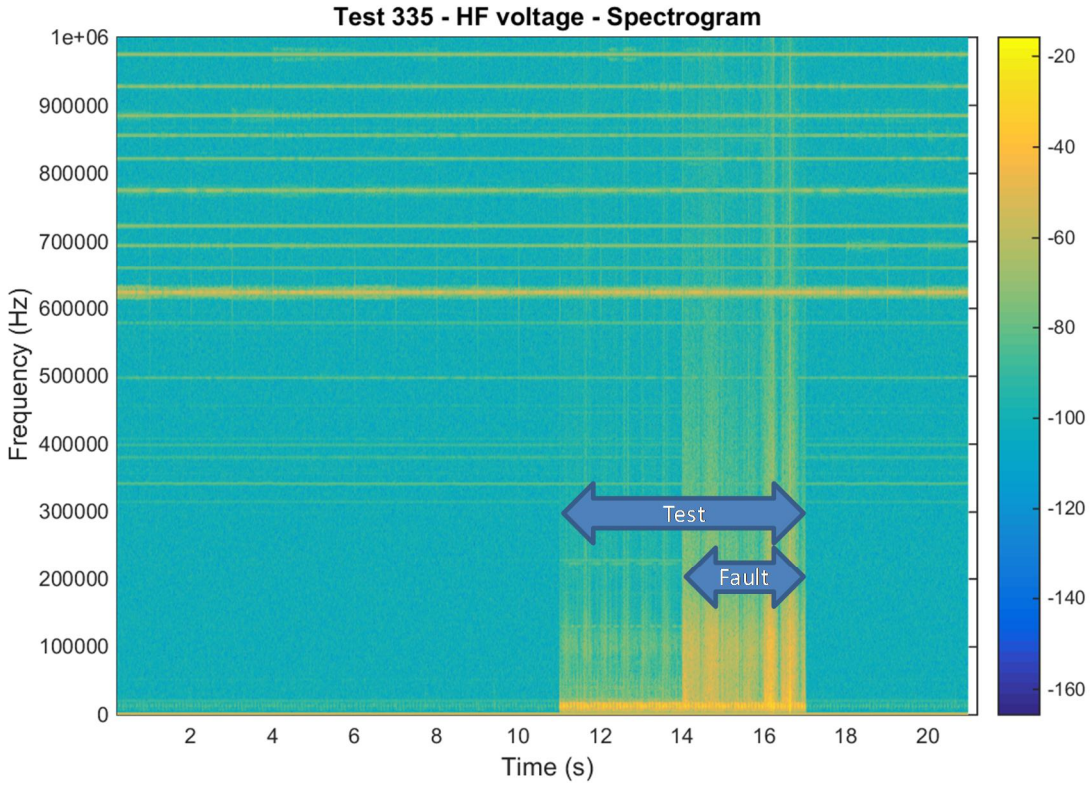

WARNING: Data shown is for 20ms sweeps recorded every second and placed end-to-end. Data between sweeps (98% of total duration) is not shown
Time axis value shows position of sweep in test and does not indicate time scale within sweep data. Refer to project report for interpretation.

In all but a few 'branch touching wire' tests, the fault was applied by connecting the test rig to the network to energise the conductors at high voltage. This had the effect of eliminating pre-fault and post-fault recording of the network voltage, so any change in network high-frequency voltage noise caused by the commencement of fault current flow was not clear in the fault records.

Test 1036 was performed differently to overcome this limitation to see if the fault could be identified in the test record. In this phase-to-phase test, one end of the sample of Desert Ash (Fraxinus Angustifolia) was suspended from the roof of the test rig container by an insulating cord and the high-voltage conductor was dropped onto it in the same way as in the 'wire into vegetation' tests. The other end of the Desert Ash sample was laid across the other high-voltage conductor in the normal way.

The high-frequency phase-to-phase voltage spectrogram for Test 1036 is shown in Figure 87 and the presence of the fault can be seen (albeit faintly) against the background network voltage noise. This type of test was performed with phase-to-phase voltage measurement and it is not known if the phase-to-earth voltage spectrogram would show the fault more clearly.

Figure 87: spectrogram of Test 1036

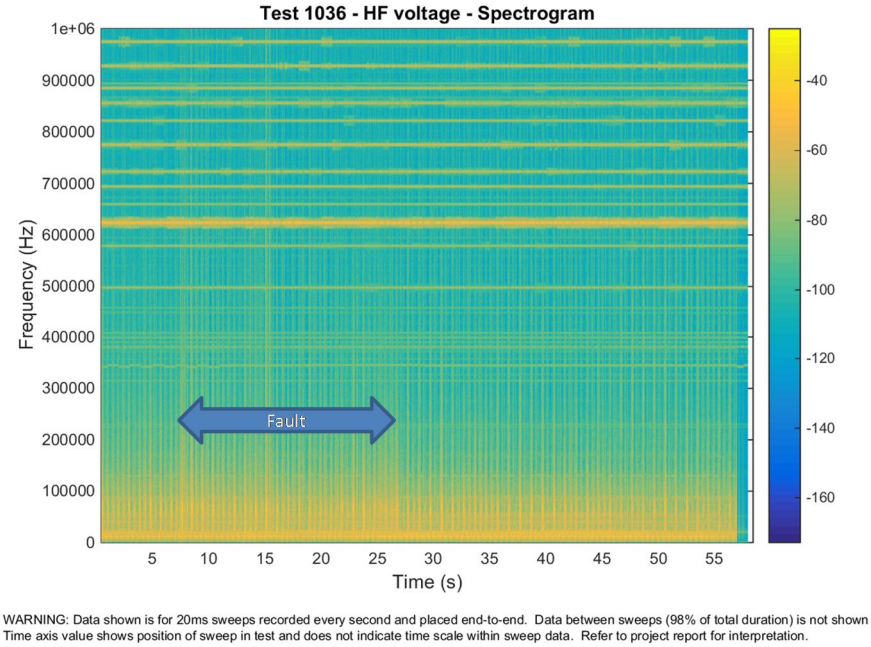

The signal processing used in the test program was relatively basic and designed solely to provide day-to-day guidance to manage the test program to meet its objectives. More sophisticated digital signal processing would almost certainly lead to clearer visibility of the presence of the vegetation faults.

9.7.2 Detection of fault using partial discharge detection approach

The IND Technology equipment was used to record high-frequency network voltage disturbances during the tests. For Test 1036 and some others the recording oscilloscope was replaced by the normal partial discharge detection equipment. It was found this system produced a clear signal for the presence of the vegetation faults as shown in Figure 88.

Figure 88: Test 1036 output of IND Technology partial discharge detection system

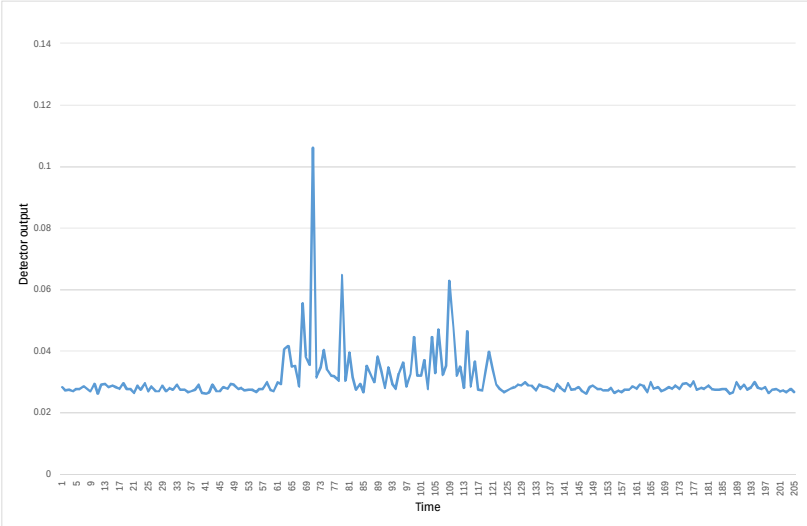

This preliminary indication provides support to the hypothesis that further development of signal processing algorithms may lead to fast reliable detection of vegetation faults.

9.8 The way forward: development challenges

The challenges facing developers of fault signature recognition algorithms and systems revolve around just a few key questions:

1. How can the disturbance created by a vegetation fault be best detected? There are many options that could be explored - ranging from frequency domain techniques to non-linear time domain techniques, hybrid approaches or multiple approaches plus voting algorithms.
2. How long does it take to achieve fast reliable detection of vegetation faults with no false positives? Detection during Phase 1 of the fault is required if fire risk is to be avoided.
3. How do different levels of network background noise affect fault detection? The network used for these tests was relatively noisy so the test records may approach worst case for fault detection, though this could only be verified by wider testing of network background noise levels. Other networks may be much 'quieter' with better prospects for clear detection of fault signatures. SWER networks are of particular interest and there is little or no published information on noise levels on such networks.
4. How far across the network can reliable detection of a vegetation fault be achieved? There are multiple studies of the potential to use powerline networks as a communication channel, e.g. for smart meters, load control, etc. However, it is not clear how these studies can be applied to transmission of fault signatures.

The fault signature data base should provide a rich source of data to test options to address Questions 1 and 2.

If the answers to Questions 1 and 2 are promising, Questions 3 and 4 may warrant further research. Possible topics would include measurement of background noise levels on rural and SWER networks; network propagation studies using wide-band high-frequency voltage signal injection; etc.

9.9 The vision: a low fire risk powerline network

To fire-proof a powerline network, a toolkit of diverse technologies would appear to be required:

- Zone substation REFCLs and distributed pole-mounted high-impedance fault passage indicators to reduce fire risk from earth faults on multi-wire powerlines
- Fault signature recognition to reduce fire risk from phase-to-phase faults on multi-wire powerlines
- Fast sensitive overcurrent protection plus fault signature recognition to reduce fire risk on SWER powerlines.

Based on research to date by Victoria's PBSP, such a toolkit could dramatically reduce fire risk from vegetation faults on Victoria's rural powerline networks.

10 Vegetation conduction ignition test program design

The detailed design choices that underpinned the test program are set out in the appendices to this report. The following is a summary of the main aspects.

10.1 Field test facility

A field test facility was constructed on about 1500 square metres of vacant land inside the security fence shared by Substations Springvale (SV) and Springvale West (SVW).

10.1.1 Concept

The concept of the field test facility was modelled on that developed for the 2014 REFCL Trial at Frankston. It is illustrated in Figure 89.

Figure 89: field test facility concept for vegetation conduction ignition tests

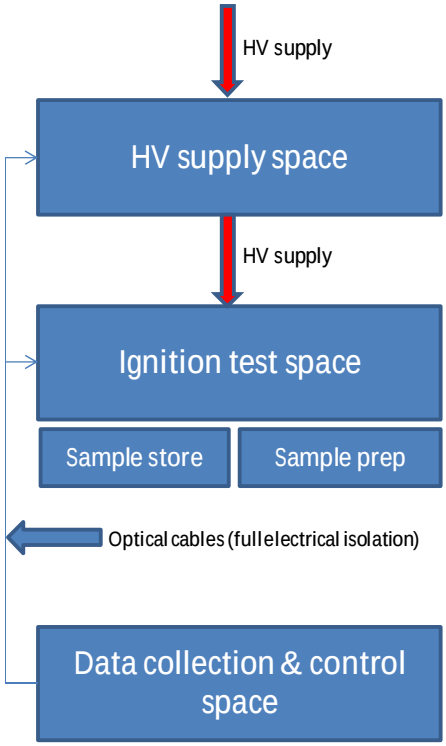

Includes:
- HV supply to site (2 phase)
- HV isolation and earthing (visible to site workers) controlled by optical cable
- Visible warning of HV presence on site
- Earthing to limit step and touch to safe levels on site
- HV current limiting resistor
- ACR with full protection suite controlled by optical cable
- Local protection graded with sub SV y

Includes:
- Safety interlock on physical access
- Climate controlled ignition test space
- Controlled air speed and temperature
- Two parallel conductors to simulate overhead powerline
- Live wire drop mechanism for 'wire into bush' faults
- Fire extinguisher
- 3 phase wide-band voltage divider and digital transducers
- Wideband digital current transducer
- SD video camera
- Optical transmitters for cables to data collection space

Includes:
- Independent LV power supply
- PLC controller to automate test run sequence
- Optical cable controls on HV switches and ACR
- Optical receivers for cables from ignition test space
- Multi-channel digital data recording
- Video record collection
- Test controller and data controller desks
- Team workspaces

The facility was constructed on approximately 1500m^2 of vacant land within the inner security fence of zone substations SV and SVW at Springvale in South-east Melbourne. The substation earth grid was extended to cover the test facility site and a crushed rock surface laid in accordance with substation construction standards designed to protect against step and touch potentials in the event of an earth fault somewhere on the network supplied by the zone substation.

Low voltage supply to the test facility was from substation SVW station service supply. High voltage supply was via the substation SV transfer bus plus a few spans of overhead line from a circuit breaker normally used to supply the station service transformers, i.e. no customers were on the feeder used to supply the test facility.

10.1.2 Safety architecture and procedures

The non-standard nature of high voltage test operations always involves the potential for safety risks that are unique to the test setup. Strong safety architecture was used to manage these risks on a sound strategic basis. The safety architecture used in the vegetation conduction ignition tests was built on that used in the 2014 REFCL Trial and included the following elements:

- Multiple (generally not less than three) layers of precaution against safety threats
- Control of access to the test facility – fence with gate locked whenever tests were underway, only one key-holder.
- Everyone in the Control Hut during tests – headcount before opening the rig earth switch.
- Galvanic isolation of Control Hut from test rig – high-pressure gas lines and optic fibres only.
- Comprehensive interlock logic on all remotely controlled functions – facility ACR switch, rig earth switch, rig HV supply switch, rig container door locks, rig access beacon.
- Strict compliance with standard safety approaches – clear documented roles, daily Job Safety Assessment and team discussion, formal Electrical Access Permit procedures, fully documented test procedures.
- Constant learning and daily team review of safety performance.

Formal procedures were developed and applied to a number of common test site activities:

- Start of day, end of day
- Test run
- Access to HV supply space in test rig container (Electrical Access Permit required)
- Access to high voltage resistors (Electrical Access Permit required)
- Access to sample handing container and test rig container (no permit required)

The two-month test program was successfully completed without any injury or safety incidents. An end-of-tests team review identified potential improvements for consideration in planning any future similar tests. These included:

- Retain the practice of changing samples without sliding the rig into the sample loading container – this is lower risk than the heavy physical work required moving the rig.
- Install a solenoid operated valve to prevent the HV supply probes being withdrawn from the rig busbars before the earth switch opens – ensures rig is discharged before disconnection.
- Provide a lighter sliding hatch to reduce physical effort required to access ignition test area.
- Install handles on the container doors or other mechanical aids to reduce the physical effort of opening the containers.

Include breaks in the test program plan to allow the team to refresh between bouts of intense activity, e.g. a pattern of two weeks on site, one week at the office.

10.1.3 Construction

The construction of the test facility is illustrated in Figure 90.

Figure 90: construction of test facility

Site prior to construction

Earth grid and crushed rock laid and poles erected

ACR (visible over roof of HV resistor cabinet), HV supply switch, rig earth switch and HV resistors in place (one visible)

Test rig container and sample loading container in place

Test facility complete with Control Hut and two portable cold stores, all inside safety fence.

Single line diagram of HV supply to test rig

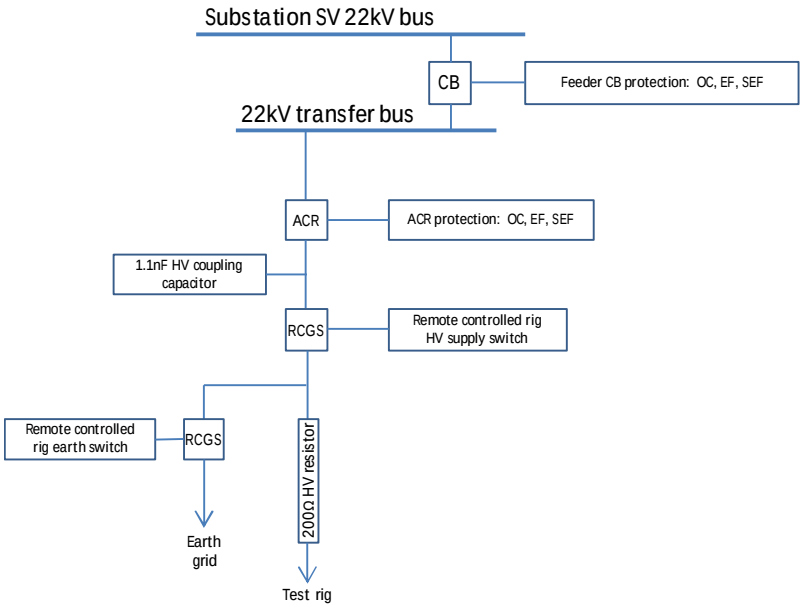

10.2 Selection of species

The species to be tested were selected in a study of about 4000 species carried out by Energy Safe Victoria (see *Appendix F: Selection of candidate species*). Species were selected for testing based on likelihood of location near powerlines in any of the high fire risk areas of the state identified by the PBSP as well as vegetation characteristics such as growth rate, moisture, volatiles, sap content, and bark type. The selected species are listed in Table 7.

European research into the comparative flammability of forest fuel beds (see Section 11.5.1 in Appendix E) highlighted the necessity of a clear distinction between 'ignitability' (how easily it ignites) and 'flammability' (how well it burns). However, as there was little data available on the former, the latter was used as a surrogate in the species selection.

Whilst the selection process was systematic, there is no guarantee that other species not selected would not constitute a worse fire risk than those that were tested in the program.

The test program was focused on quantification of the fire risk of the selected species. However, occasionally vegetation management contractors would supply small quantities of species not on the list. These off-list species included:

- Maple
- Paperbark
- Tea Tree
- Date Palm.

The records of tests on these species are contained in the test data base.

Table 7: species selected for tests

Botanical Name	Common Name	Growth Habit	Flammability	Volatile Vapour	Sap Composition	Bark Type	Canopy Density
Acacia Mearnsii	Black Wattle	Upper storey	High	Likely	Low moisture, High resin	Smooth	Dense
Acacia Melanoxylon	Blackwood	Upper storey	High	Likely	Low moisture, High resin	Rough	Dense
Allocasuarina Verticillata	Drooping Sheoak	Upper storey	Moderate	Unlikely	Low moisture; Low resin	Intermediate	Intermediate
Cotoneaster Glaucophyllus	Cotoneaster	Upper storey	Low	Unlikely	High moisture, Low resin	Smooth	Dense
Eucalyptus Baxteri	Brown Stringybark	Upper storey	High	Likely	Low moisture, High resin	Rough	Dense
Eucalyptus Goniocalyx	Long-leaf Box	Upper storey	High	Likely	Low moisture, High resin	Intermediate	Dense
Eucalyptus Viminalis	Manna Gum	Upper storey	High	Likely	Low moisture, High resin	Smooth	Sparse
Fraxinus Angustifolia	Desert Ash	Upper storey	Low	Unlikely	High moisture, Low resin	Smooth	Dense
Pinus Radiata	Radiata Pine	Upper storey	High	Likely	High moisture, High resin	Rough	Dense
Pittosporum Undulatum	Native Daphne	Upper storey	Low	Likely	High moisture, High resin	Smooth	Dense
Salix sp.	Willow	Upper storey	Low	Unlikely	High moisture, Low resin	Smooth	Dense
Schinus Molle	Peppercorn	Upper storey	Moderate	Not classified	Not classified	Intermediate	Dense
Acacia Pycnantha	Golden Wattle	Middle storey	High	Likely	Low moisture, High resin	Smooth	Dense

Botanical Name	Common Name	Growth Habit	Flammability	Volatile Vapour	Sap Composition	Bark Type	Canopy Density
Banksia Marginata	Silver Banksia	Middle storey	High	Unlikely	Low moisture; Low resin	Intermediate	Dense
Bursaria Spinosa	Sweet Bursaria	Middle storey	High	Unlikely	Low moisture; Low resin	Intermediate	Dense
Cytisus Scoparius	English Broom	Middle storey	High	Likely	Low moisture, High resin	Intermediate	Dense
Kunzea Ericoides	Burgan	Middle storey	High	Likely	Low moisture; Low resin	Intermediate	Dense
Lycium Ferocissimum	African Boxthorn	Middle storey	Moderate	Not classified	Not classified	Smooth	Sparse
Lomandra longifolia	Spiny-headed Mat-rush	Ground storey	Low	Unlikely	High moisture, Low resin	Not applicable	Not applicable
Nassella Neesiana	Chilean Needlegrass	Ground storey	High	Unlikely	Low moisture; Low resin	Not applicable	Not applicable
Poa Labillardieri	Common Tussock-grass	Ground storey	High	Unlikely	Low moisture; Low resin	Not applicable	Not applicable
Rubus Fruticosus	Blackberry	Ground storey	Low	Not classified	Not classified	Not applicable	Not applicable
Themeda Triandra	Kangaroo Grass	Ground storey	Moderate	Unlikely	Low moisture; Low resin	Not applicable	Not applicable
Ulex Europaeus	Gorse	Ground storey	High	Not classified	Not classified	Not applicable	Not applicable

NB: Samples were gathered on an opportunity basis with availability dependent on the current vegetation clearing activities of contractors. Not all selected species were available, e.g. no samples of Eucalyptus Goniocalyx (Long Leaf Box) were obtained. In some cases of unavailability, plants were purchased from nurseries. In others, they were harvested by members of the research team. Based on the samples obtained, Golden Wattle was tested as Upper Storey rather than as a bush even though it is rated 'middle storey'. Whilst Burgan samples were large enough to be tested as branches, they were bushy in character and are included in the 'wire into vegetation' results consistent with their 'middle storey' rating.

10.3 Experiment design

Details of issues considered in experiment design are set out in *Appendix C: Vegetation fault signatures: experiment* design.

The conduction ignition experiment design was relatively straightforward: different fault geometries generated electric current through vegetation and ignition results were observed and recorded, together with fault signatures. The archetypal fault geometries chosen for the tests were:

- Branch touching wire – branch laid across two high voltage conductors, one earthed and one with full nominal phase voltage applied.
- Branch across wires – branch laid across two high voltage conductors connected to two separate phases of the incoming high voltage supply, i.e. with 22kV between them.
- Wire into vegetation – a high voltage conductor dropped into or sitting in earthed vegetation, either grass or a bush.

To assess comparative fire risk of different species the high voltage was removed once a pre-set current limit was reached. The species with the highest fire probability at the lowest current limit setting was considered 'worst case' for fire risk.

The experiment design for collection of fault signatures was much more challenging. A review of technical literature revealed that 22kV distribution networks were likely to have very complex electrical characteristics at high frequencies. It was also clear that the high frequency current and voltage disturbances created by the fault would be influenced as much by the network as by the fault itself.

An important consideration was that the arrangement for connection of the test facility to the supply network must ensure any internal flashovers in the test rig did not generate dangerous levels of fault current nor present a risk to connected customers on the wider zone substation network. After consideration of options, it was decided to perform the tests on a rig connected to a real network via current-limiting resistors.

10.4 Rig design

The vegetation samples were tested in a specially designed test rig (Figure 91) constructed by HRL Technology. A schematic of the two containers housing the rig is shown in Figure 92.

Figure 91: Test rig container, sample handing container and sample cold stores

The test rig and sample conditioning space were built into two insulated shipping containers to allow easy temperature control, construction and earthing, as well as ease of transport and to allow the test space to be securely locked during testing. All internal metal surfaces in the two containers were earthed. The floor and selected wall and ceiling surfaces were lined with cement sheet – selected for its high electrical resistivity and flame resistance.

Both containers were fitted with a remote control interlock which locked the doors during testing. The test rig container could be accessed via the front door. However it was most frequently accessed from the sample conditioning container via an interlocked sliding hatch between the adjacent containers. As shown in Figure 92, the test rig container was divided into three areas; the camera area, the ignition test area and the high voltage apparatus area. The three areas were separated by polycarbonate panels which could be latched shut.

10.4.1 High voltage apparatus area

The high voltage apparatus area housed the primary transducers for measurement of test voltage and current. Two pass-through bushings penetrated the roof of the container to connect the high voltage supply from the network. Inside the container, the roof bushings were connected by flexible leads to ceiling-mounted copper bus bars mounted on stand-off insulators which then connected to the pneumatically actuated high voltage probes via flexible leads.

The high voltage apparatus area was sealed using polycarbonate panels and the high voltage probes were blocked from entering the ignition test area by a pneumatically actuated earthed metal shutter. Once the shutter was opened, the high voltage probes could be extended by pneumatic actuators to connect the ignition test area bus bars to the supply busbars in the high voltage apparatus area.

The sliding hatch between the test rig container and the sample conditioning container was locked shut by a pin attached to the shutter so the hatch could only be opened once the shutter was closed, i.e. the high voltage supply was withdrawn from the ignition test space behind and earthed metal screen.

10.4.2 Ignition test area

The ignition test area contained the test rig which supported the test sample on two parallel sections of typical Aluminium powerline conductor (19/3.25AAC). The conductors could be connected to the ceiling-mounted high voltage bus bars by flexible dropper cables or they could be earthed depending on the desired operating configuration for the test. By earthing one conductor, the test rig operated in the phase-to-earth configuration to simulate ‘branch touching wire’ faults. With both conductors connected to the high voltage busbars, the test rig operated in the phase-to-phase configuration to simulate ‘branch across wires’ faults. An earthed trolley was used to support vegetation samples for grass and bush tests to simulate ‘wire into vegetation’ faults. The arrangement is shown in Figure 93.

To record the test outcome, a remotely activated GoPro high definition digital video camera was mounted on the wall overlooking the vegetation sample on the test rig. A high definition security camera was mounted on the front wall of the ignition test area to provide a live video feed of the test progress. The test rig was mounted on tracks to allow the rig to be slid out of the ignition test area and into the sample conditioning container to allow for more access to the rig if needed.

Figure 92: Schematic of test rig and sample handling containers

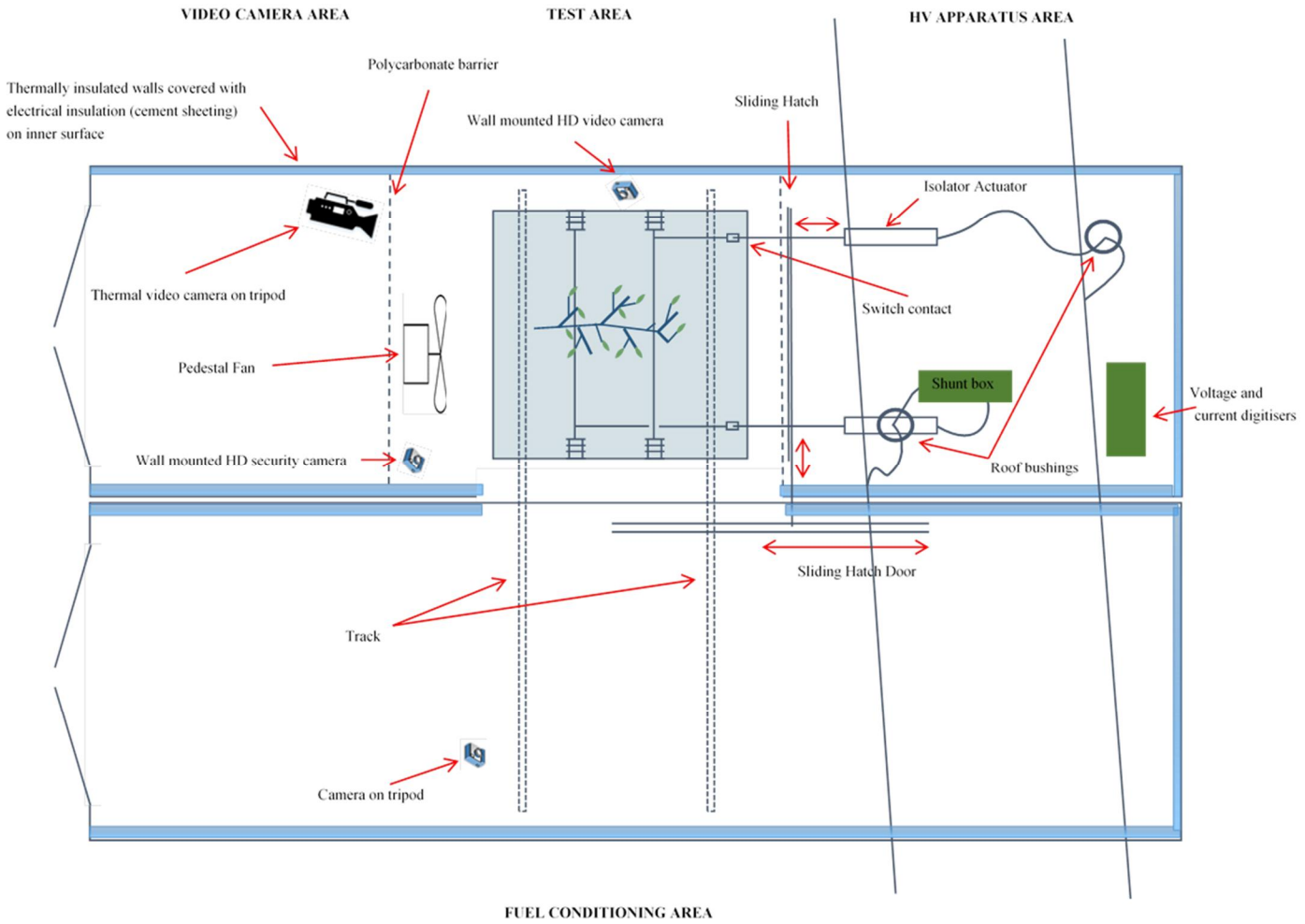

Figure 93: test rig in the ignition test area and arrangement for 'wire into bush' test

10.4.3 Camera area

The camera area contained a FLIR T460 infrared video camera which recorded any particles which fell from the vegetation sample during testing. The camera was used to determine if the embers were hot enough to be a fire risk in extreme fire weather conditions.

Several LCD lights were fitted around the interior of the containers and four internal security cameras were installed to allow the interior of both containers to be viewed remotely from the Control Hut at all times.

10.5 Current measurement

To enable wide-band, low-noise recording of test current, a HiLo Test 0.2Ω coaxial shunt was used. The voltage developed across the shunt was fed to digitisers via two separate channels:

- Low-frequency channel: the shunt output signal was sampled at 100kS/s with suitable anti-alias filters. This provided a DC-50kHz record of currents up to $7A_{rms}$ with 14-bit (2.4mA) resolution and wide-band noise levels below about 3mA. Narrow-band baseline noise in computed spectra was about 1µA.
- High-frequency channel: the shunt output signal was fed through a three stage RC high-pass filter with a 10 kHz corner frequency. It was then sampled at 2MS/s with suitable anti-alias filters. This provided wide-band (10kHz-1MHz) records of high frequency current components up to $180mA_{rms}$ with 14-bit (30µA) resolution and wide-band noise levels below about 300 µA. The narrow-band baseline noise levels in computed high-frequency voltage spectra were observed to be around 200nA.

Full details of the current measurement system are set out in *Appendix A: Voltage and current measurement*

10.6 Voltage measurement

To capture wide-band, low noise records of test voltage, two Omicron 24kV 1.1nF coupling capacitors were combined with bottom-end capacitors to form a dual channel capacitive voltage divider (CVD). Two layers of over-voltage protection were included in each channel – a 125V

bidirectional voltage limiting diode embedded in the coupling capacitor itself and a 350V spark gap contained in the bottom-end termination box. The two channels of the CVD were recorded differently:

- Low-frequency channel: a 2.2µF bottom end capacitor provided a 2000:1 ratio. The CVD output signal was sampled at 100kS/s with suitable anti-alias filters. This provided a DC-50kHz record of voltages up to 14kV_{rms} with 14-bit (2.44V) resolution and wide-band measurement system noise level below about 50mV_{rms}.
- High-frequency channel: a 110nF bottom-end capacitor with a 220Ω shunt resistor provided a ratio of 100:1 at high frequencies and a high-pass characteristic with a corner frequency of 10 kHz. The CVD output signal was processed by a Frequency Devices active 4-pole Butterworth filter with a 10 kHz corner frequency to further eliminate 50Hz signals and low-order harmonics. It was then sampled at 2MS/s with suitable anti-alias filters. This provided wide-band (10kHz-1MHz) records of high-frequency voltage components up to 1.4V_{rms} with 14-bit (0.24mV) resolution and wide-band measurement system noise below 20mV_{rms}. The narrow-band baseline noise levels in computed high-frequency voltage spectra were observed to be around 50µV.

The high-frequency voltage channel proved to be an excellent AM radio receiver and noise levels even with a shorting wire connected between the top and bottom terminals of the coupling capacitor were still 100mV_{rms}. When connected to the rig conductors (energised or un-energised), this rose to around 0.3-0.8V_{rms}. The narrow-band noise levels in computed high-frequency voltage spectra were observed to be around 50µV.

For Tests 822 to 1038, high-frequency phase-to-phase voltages were recorded. A second matched high-frequency voltage measurement channel was added and the outputs from the two high frequency CVDs were subtracted using a wide-band differential transformer. The active high-pass filter was replaced by a single stage passive RC filter in the input of each phase to the transformer. Tests confirmed the differential transformer reduced common mode high-frequency signals by 96%. However, it was found that the radio stations noise on the network was mainly not common mode.

Full details of the voltage measurement system are set out in *Appendix A: Voltage and current measurement*

10.7 Data management

The 1038 tests generated a large amount of data – test logs, visible and infrared video files, low and high frequency voltage and current records, laboratory analysis records, sample collection and storage records. Careful thought was given to effective information management and processes built on the following elements:

- Hard copy log sheet filled out as part of the test run procedure
- A formal detailed data management plan agreed by all team members
- The test number as the universal key to unite all data relating to a test
- An audited running sheet (as a worksheet in an MS Excel spreadsheet) to support all analysis
- Daily off-site back-up of all records.

Details of the data management plan are contained in *Appendix G: HRL Technology report*. The core test data (excluding data collected from Substation SV loggers) was around 15,000 files totalling about 250GB. All this data will be made freely available in the public domain.

10.8 Test ambient conditions

To simulate Code Red fire weather conditions, the ignition test area was maintained at 45°C and less than 25% relative humidity and a pedestal fan was used to replicate a 'swirling' hot wind. The temperature in the two containers was controlled by a Thermal Electric Elements 18kW fan heater in the sample conditioning container. It operated continuously throughout the test program.

The limited size of the ignition test space (5m x 2.3m x 2.3m) caused the wind velocity near the conductors to be uneven. The wind velocity at the height of the conductors was measured to be 12km/hr at the conductor nearest the fan and 11km/hr at the opposite end. As the fan was enclosed in the test space, backwards flow was observed at the roof and the floor with a wind speed of around 2.5km/hr.

The temperature in the test container was logged using a Lascar temperature and humidity probe. Spot check measurements were taken using a hand held thermocouple reader. A typical daily temperature and humidity profile is shown in Figure 94.

Figure 94: typical daily temperature and humidity profile in ignition test space (17 March 2015)

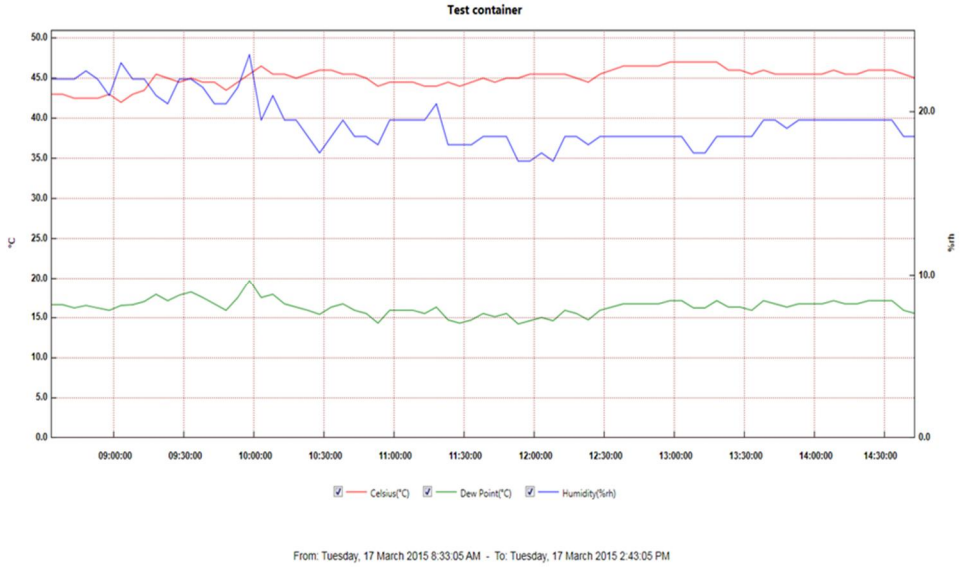

10.9 Laboratory analysis

Sub-samples were collected when the vegetation was loaded onto the test rig, i.e. immediately before each test. A short section was sawn from the thicker end of the branch or in the case of bush or grass tests, leaves and twigs or blades of grass were collected. Branch sub-samples generally consisted of a section of woody branch material around 10cm in length as shown in Figure 95.

Figure 95: sub-samples taken from vegetation samples immediately prior to tests

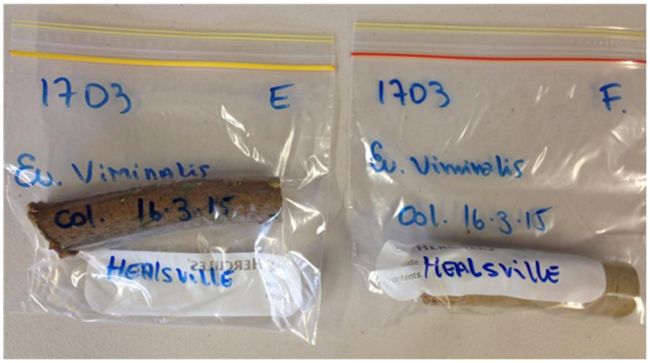

Each sub-sample was sealed in a plastic bag and kept in cold storage at around 2°C until the end of the day when they were taken to HRL Technology for laboratory analysis. At HRLT each sub-sample was assigned an HRLT sample code and all information on the sample bag was recorded. Every sub-sample was subject to moisture analysis and most (and in some stages of the test program, all) were subject to conductivity analysis.

10.9.1 Moisture analysis

The end sections of the sub-sample were removed and discarded, as is it was considered possible these sections had partially dried. A transverse section was then removed from the sub-sample, split into small slices, weighed in a pre-weighed aluminium moisture dish and dried at 110°C for 24 hours. After drying the sample material was re-weighed and a moisture loss percentage calculated. The distribution of measured sample moisture content is shown in Figure 96.

Figure 96: measured sample moisture content

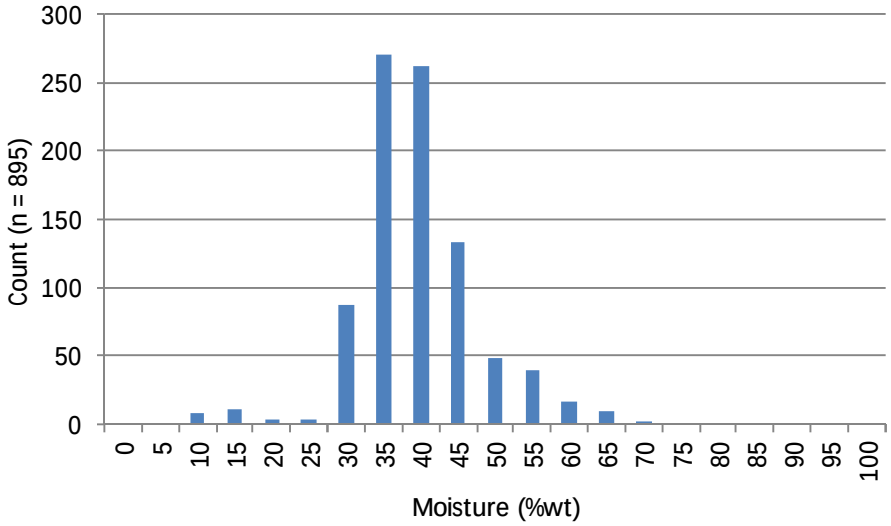

It was considered possible that the range of moisture content in tests was restricted by the mild and humid 2014-15 summer during which the samples were collected, though pre-test conditioning for 16-24 hours at 45°C was used in an attempt to offset this.

Figure 97 (Manna Gum moisture content analyses over the period of the whole test program) shows the effect of conditioning times, as well as some evidence of seasonal variation, i.e. some reduction in moisture levels late in the test program, though this may be an effect of the different sample harvesting locations used at different times.

Figure 97: variation of moisture content in Manna Gum samples throughout the test program

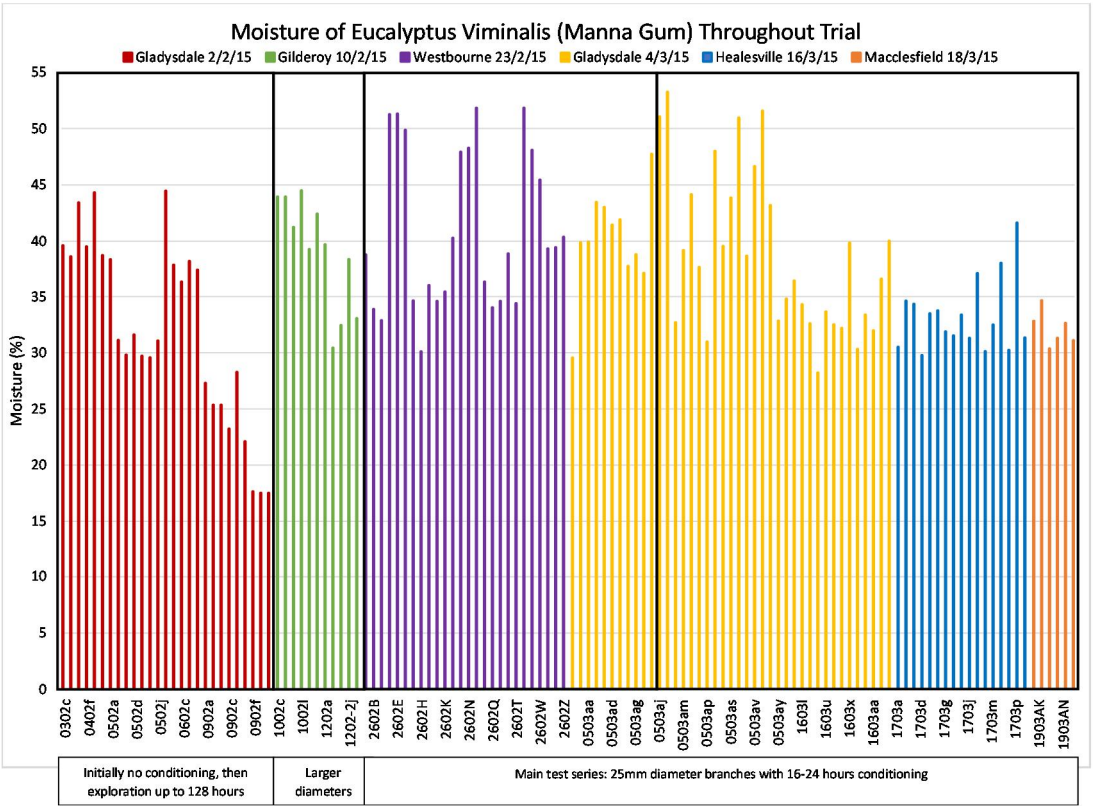

Some variation of moisture content by species was observed as shown in Figure 98. This did not appear to greatly influence comparative ignition outcomes for the different species. For example, the average measured sample moisture content of Native Daphne (38%) and Willow (39%) species were almost identical though tests showed they were at opposite ends of the fire risk spectrum.

Figure 98: variation of average moisture content by species

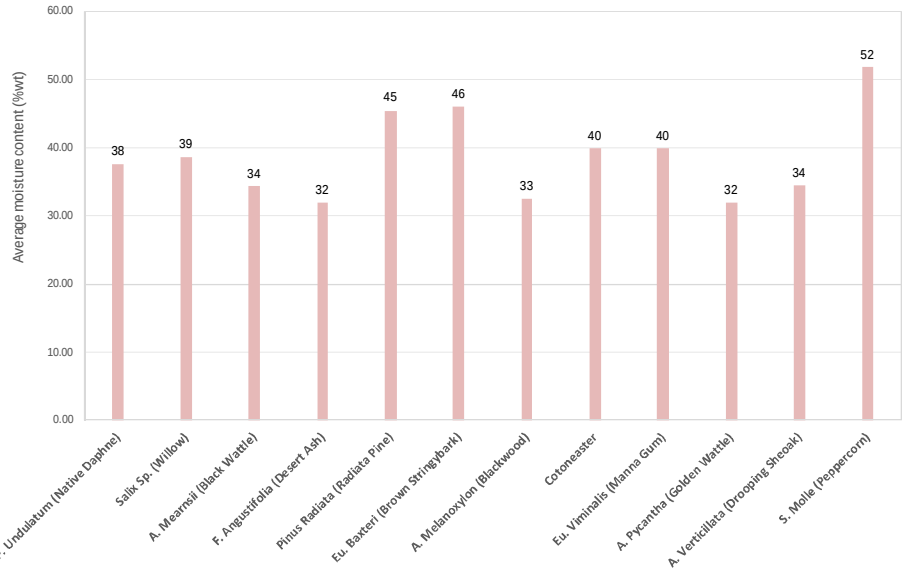

10.9.2 Conductivity analysis

A measurement was devised to indicate the content of ionic compounds in the vegetation. This measurement was performed on many samples – almost all in some later stages of the test program. The dried material from the moisture analysis was milled to a particle size less than 5mm and a two gram portion of this milled fraction was weighed into a beaker. 50mL of de-ionised water was added and the solution was boiled under reflux for 4 hours. The extract was then made up to 100ml and the electrical conductivity of the solution was measured using a TPS labCHEM-CP bench top conductivity meter and recorded. The distribution of measured sample conductivity values is shown in Figure 99.

Figure 99: measured conductivity of vegetation samples

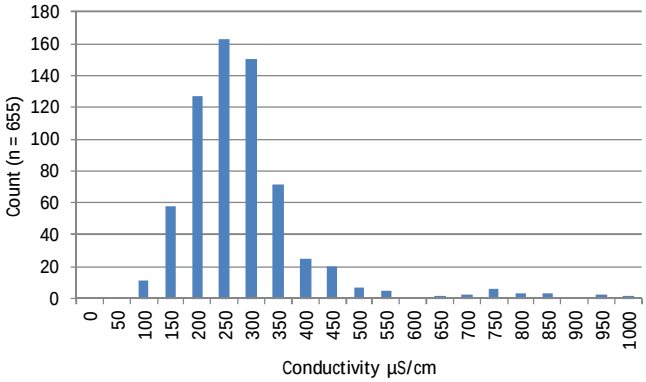

One outlier is not shown in Figure 96: conductivity tests of Date Palm fronds (an 'off-list' species) showed conductivity in the range 2000-4000 µS/cm which was about three times the maximum value measured for any other species.

The average measured conductivity of species on the test program selection list is shown in Figure 100. Schinus Molle (Peppercorn) stands out at about four times greater conductivity than the other species tested, which may indicate one reason for its low fire risk, consistent with the discussion set out in Section 6.4 above.

Figure 100: average measured conductivity by species

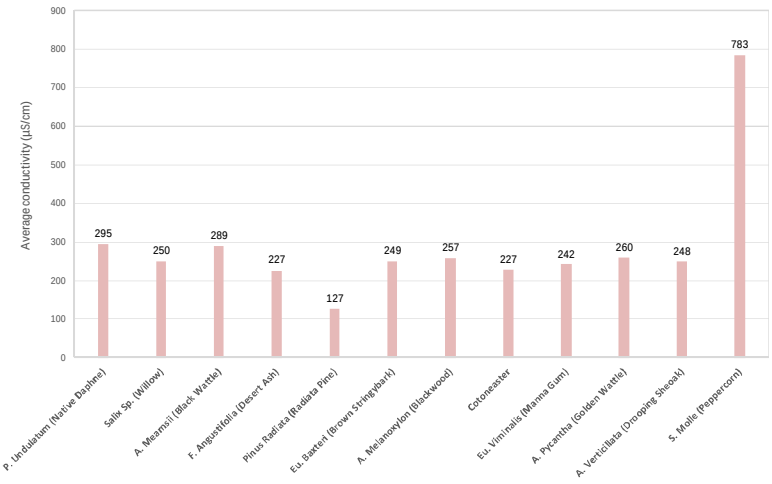

It is not known if the range of measured conductivity was constrained by the mild 2014-15 summer conditions or not.

10.9.3 Transverse profile measurements

A limited number of samples were subject to more comprehensive measurement to determine the transverse distribution of moisture and ionic (conductive) compounds. The above described methods determined the average across the sample. In the transverse profile assessments, material was taken from the centre of the sample, from the outer layer and from an intermediate layer. Each was analysed separately to reveal the distribution of moisture and conductivity across the sample. Some results of this type of analysis are set out in Section 4.4.2 above.

10.10 Vegetation sample procurement and management

At the experiment design stage a brief study was performed to assess options for management of moisture content of harvested samples – details of this study are set out in *Appendix G: HRL Technology report*. Vegetation samples were usually delivered to site on the day they were harvested. They were held in cold storage at 2°C until the day before they were tested. They were then stored overnight in the conditioning container for 16-24 hours prior to the test in an attempt to replicate vegetation condition from hot dry summer conditions.

Early proof-of-concept tests showed that large diameter samples took too much current for the test facility to safely test them, while small diameter samples were sometimes too flimsy to stay in place during a test. Sample suppliers were therefore requested to provide samples of 2.5m length with a stem diameter around 25mm as this combination was found to generally work well in tests. Variations in average measured diameter (thick end of branch) are shown in Figure 101.

Figure 101: variation of average diameter by species

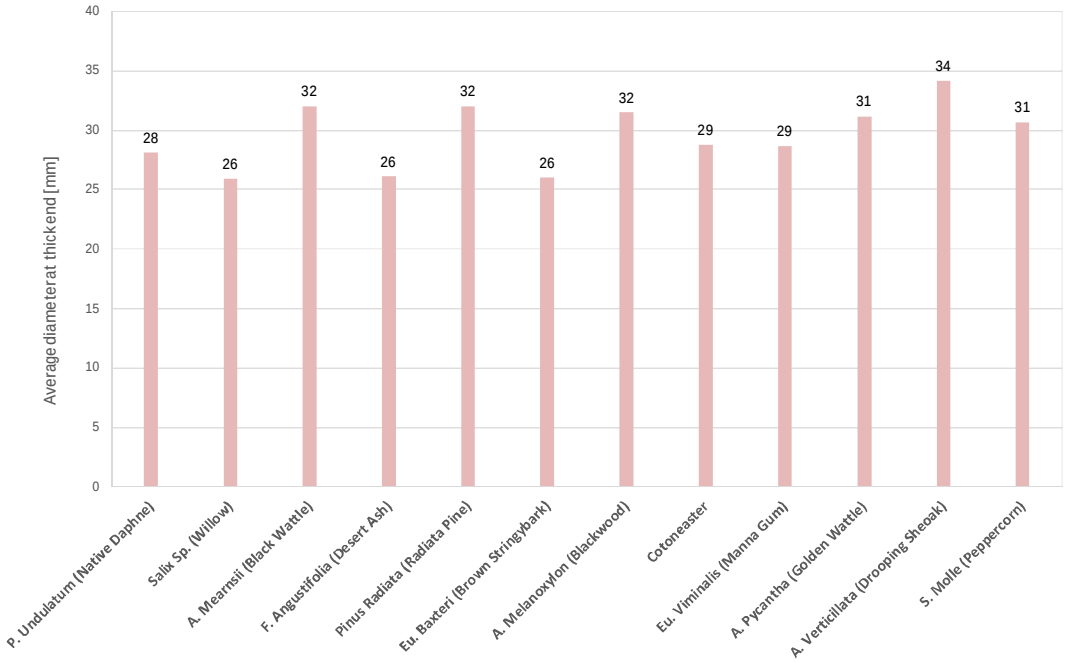

11 Appendices

The following appendices set out more detailed information on the material in the main report sections above:

Appendix A: Voltage and current measurement

Appendix B: Data processing

Appendix C: Vegetation fault signatures: experiment design

Appendix D: Test records

Appendix E: Associated research

Appendix F: Selection of candidate species

Appendix G: HRL Technology report

11.1 Appendix A: Voltage and current measurement

The target bandwidth for measurement of fault signatures was 1MHz. This was part of the specification of the project and is understood to be based on a review of protection systems development that indicated the optimum frequency for fault signature detection may be in the hundreds of kilohertz since this band may have lower attenuation on overhead powerline networks than higher frequencies. In addition, a measurement using partial discharge wireless sensors[26] at 200MS/s was also included.

The measurement systems were designed to achieve this bandwidth with low measurement noise. Two parallel overlapping measurement channels were used for each of voltage and current: low-frequency (bandwidth from DC to 50k Hz) and high-frequency (from 10 kHz to 1MHz). The measurement locations for most tests were in the test rig container, i.e. adjacent to the test rig.

11.1.1 Selection of measurement location

Two possible measurement locations were considered as indicated in Figure 102:

Figure 102: possible measurement locations for fault signature collection

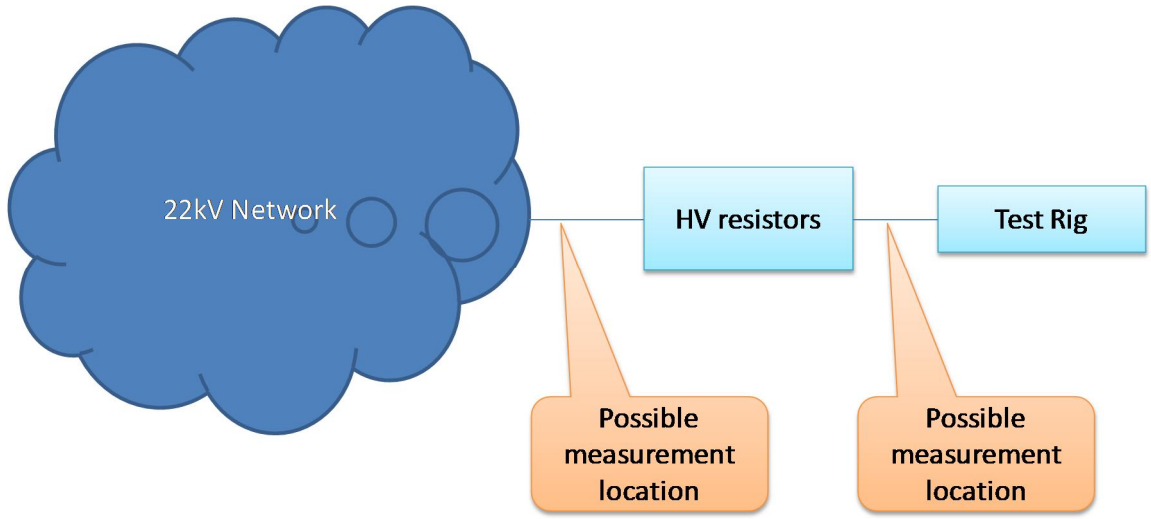

Some tests in the proof-of-concept series had voltage measurement upstream of the high voltage resistors. However, all ignition tests were done with voltage fault signature collected at the test rig. Fault current was measured at the test rig in all tests.

11.1.2 Wide-band measurement concept

A review of options led to the adoption of two-channel recording of each measured quantity to provide wide-band data across the full target bandwidth of DC to 1MHz:

[26] See IND Technology http://www.ind-technology.com.au/efd_system.php

Figure 103: concept for wide-band measurement (AA = anti-alias)

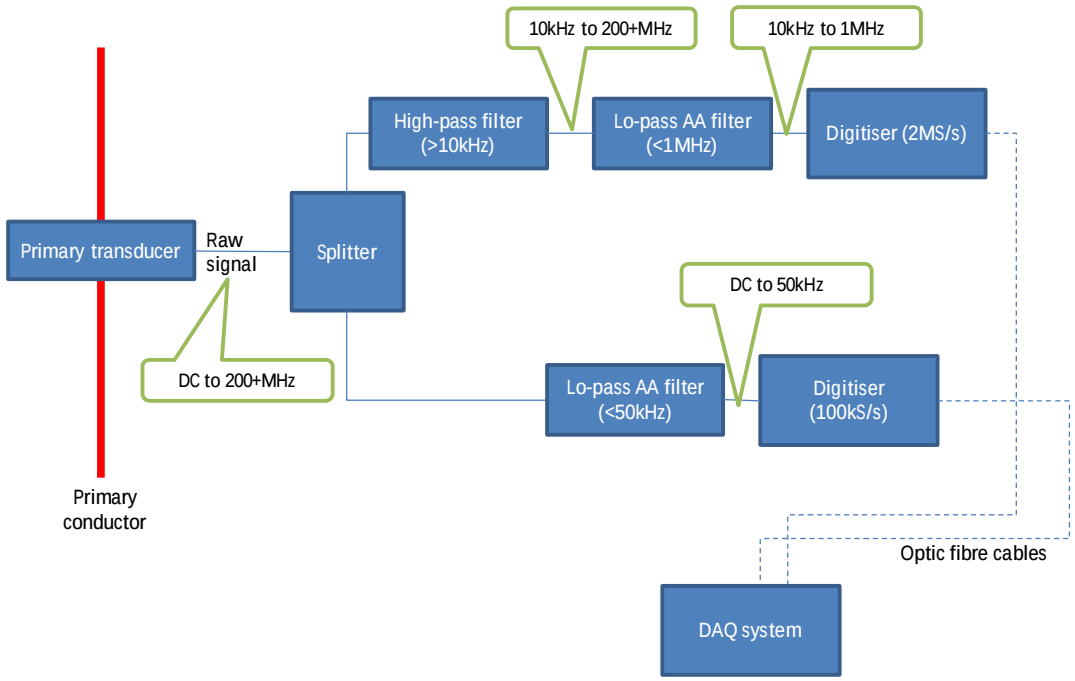

11.1.3 Measurement noise

The design maximised the signal-to-noise ratio (SNR) of the recorded voltage and current in the tests. There were multiple[27] potential sources of noise to be managed:

1. Induced noise: electrical signals induced in the measurement system wiring between the primary high voltage quantity and the digitiser input by stray capacitance and stray magnetic fields. This was managed by careful design of shielding and the use of coax cables for all interconnections. Single-point earthing was used throughout to avoid earth current loops and consequential voltage noise. The residual magnitude of induced noise is always very difficult to estimate and it is not included in the calculations outlined below. Induced noise proved to be material in the high-frequency voltage channel.

2. 'Quantisation noise' due to the finite granularity of the digitisation process. The HBM digitisers produced 14 bit values. If the one-bit 'gap' is taken as the peak-to-peak value of this noise, the rms value can be taken to be of the order of one half this 'gap' size, i.e. half of full scale (one quarter of the digitiser input span setting) divided by 8,192.

3. Aliassing noise due to the sampling rate being lower than the maximum frequency of the signal being sampled. In each configuration, the anti-alias filters in the digitisers were set to a corner frequency not higher than half the digitiser sampling rate, to eliminate this noise.

4. Johnson-Nyquist noise produced in any resistors in the measurement circuitry. The resulting noise voltage is proportional to the square root of each of bandwidth, temperature and resistance, as illustrated by[28]:

[27] These are added using a root-sum-of-squares method to estimate the total noise.

$$V_{rms}^2 / \Delta f = 4k_B TR$$

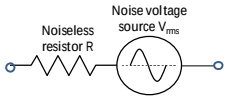

5. Thermal noise generated in the high pass filters.

    a. A Frequency Devices Model D64H4B 10 kHz active high-pass filter was used to remove low-frequency components from the voltage high-frequency channel. The data sheet specifies this module to have output noise of 400μV_{rms} (measured over the 5Hz to 2MHz band). Thermal noise generated in the Frequency Devices Model FMA01S filter mounting assembly (which contain multiple resistors and two op amps) is not specified in the product data sheets so was assumed to be of similar magnitude to that produced by the high-pass filters itself, i.e. 400μV_{rms}. Hence, the noise at the output of the filter when it was mounted in its assembly was assumed to be not more than 560μV_{rms}.

    b. A passive high-pass filter comprising a three-stage 'series C shunt R' circuit was used to remove low-frequency components from the high-frequency current channel. The final stage shunt resistor was 4.7kΩ, giving a wideband Johnson-Nyquist noise of 13μV_{rms}.

6. Digitiser noise: the HBM Model 610-2 digitiser data sheet specifies this to be '0.05% of full scale ±100μV' with a 50Ω termination. How the 50Ω termination relates to the proposed measurement configuration for the vegetation tests is not entirely clear, but the specified value has been used in the noise design calculations. The term 'full scale' was taken to be equal to half the span setting for the digitiser.

The above information was used to guide design choices for the voltage and current measurement systems. Actual noise and SNR results were measured in the proof-of-concept tests and again at intervals during the main test series.

11.1.4 Voltage measurement

Most high-frequency voltage measurement and all low-frequency voltage measurement was phase to ground, i.e. only one conductor voltage was measured and the nominal peak value of the measured 50Hz network voltage was 18kV. For Tests 822 to 1038, the high-frequency voltage measurement was phase-to-phase as described in 11.1.7 below.

The primary voltage transducer chain comprised:

- An Omicron Model MCC124 coupling capacitor of 1.1nF rated at 24kV working voltage and 50kV for one minute. These units are used for partial discharge measurements, so they are designed for very low noise generation. It was assumed they were noise-free. The coupling

[28] T is temperature in degrees Kelvin, k_B is the Boltzmann constant (1.4×10^{-23} joules/degree), Δf is the bandwidth over which the noise is measured, R is the resistance in which the noise is generated.

capacitor included inbuilt over-voltage protection which limited output voltage to 125 volts using a Multicomp TVS 1.5kE91CA transient voltage suppression diode rated at 1.5kW peak power in series with a 470Ω resistor – this would have no effect on noise generation.

- The coupling capacitor was connected by an RG58 (50Ω impedance) coaxial lead of 11 metres length to a Power Diagnostix Systems CTB2 termination box which provided a second stage of over-voltage protection in the form of a 350 volt spark-gap. Again, this over-voltage protection would have no effect on noise generation.
- The CTB2 termination box passed the signal to a custom built bottom-end capacitor box containing components designed to produce the frequency response required for that channel. The CVD output was connected to the digitiser input by a short coaxial cable.

The two voltage measurement channels (low-frequency and high-frequency) were each supplied by a dedicated coupling capacitor. The combined two-channel voltage measurement unit is shown in Figure 104:

Figure 104: Voltage measurement transducers

11.1.5 Voltage measurement system design

With a nominal CVD ratio at 50Hz of 2000:1, the 50Hz signal fed to the digitiser was $9V_{pk}$ so a digitiser span setting of 20 volts could avoid clipping and maximise the signal to noise ratio. To capture frequencies up to 10 kHz, the minimum required sampling rate would be 20kS/s. However, the minimum anti-alias filter bandwidth setting available from the HBM digitiser was 50 kHz and since the sampling rate had to be twice this to avoid aliasing noise, the chosen sampling rate was 100kS/s.

The various sources of noise were estimated to produce a total noise in the recorded signal equal to 10.27V_{rms} of primary recorded voltage as outlined here – there is no resistor in the CVD and no high pass filter so only quantisation and digitiser noise are present. It can be seen that digitiser noise is dominant:

Noise type	rms noise	Unit	Comment
Quantisation	1.22	volts	Half of a one-bit gap in the digitiser output levels
Johnson-Nyquist	-	-	No resistor
Filter+mounting	-	-	No filter
Digitiser	10.20	volts	0.05% of half the span plus 100µV_{rms}
Total noise	10.27	volts	Expressed in primary quantities

This arrangement was estimated to give a 50Hz SNR of 65dB which was considered more than adequate for recording of low frequency voltage components in the tests.

Assuming all signal components above 10kHz were accurately recorded in the HF channel, taking the two channels together, the only signals that might not be accurately recorded would be any high-order harmonics of the 50Hz waveform below 10kHz that are of magnitude less than about 10V_{rms}, i.e. less than 0.07% of the 50Hz fundamental. This was considered acceptable.

The design of the high-frequency voltage channel was more complex. The introduction of the active high-pass filter added an extra noise source. However countering this, the digitiser span could be set to a much lower value as the signal fed to the digitiser was much smaller after elimination of the low-frequency components, including the 50Hz fundamental. This greatly reduced digitiser and quantisation noise. The net result was a reduction in measurement system noise levels.

The 50Hz signal and its harmonics up to 1 kHz were treated as noise in the HF channel. The frequency response of the Frequency Devices Model D64H4B filter had a cut-off frequency of 10kHz and any harmonic of the 50Hz fundamental below 1kHz would be attenuated by at least 80dB (a factor of 10^4), i.e. the 50Hz fundamental would be of magnitude 1.3V_{rms} (equivalent primary volts) or 635µV_{rms} at the input to the digitiser. For a span setting of 80V (primary equivalent) the noise calculation was:

Noise type	rms noise	Unit	Comment
Quantisation	0.0024	volts	Half of a one-bit gap in the digitiser output levels
Johnson-Nyquist	0.0056	volts	At 320^{O}K (50^{O}C), measured over 2MHz.
Filter+mounting	1.1200	volts	560µV_{rms} at digitiser
Digitiser	0.2200	volts	0.05% of half the span plus 100µV_{rms}
<1kHz signals	1.2700	volts	635µV_{rms} at digitiser
Total noise	1.7076	volts	Expressed in primary quantities

Two noise sources dominated – the residual 50Hz harmonics and the 'filter plus assembly' thermal noise. The best way to address these was to reduce the 50Hz harmonics before they reach the active high-pass filter and use a lower CVD ratio so the 'filter plus assembly' noise is equivalent to a lower value of primary voltage.

To improve SNR in the HF channel, the CVD was modified to give it a high-pass character which achieved both these objectives:

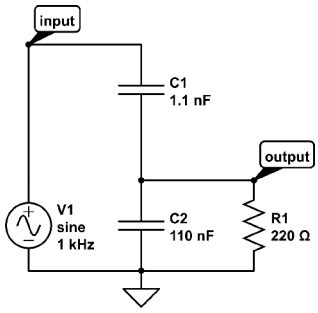

The calculated frequency response of the modified CVD was:

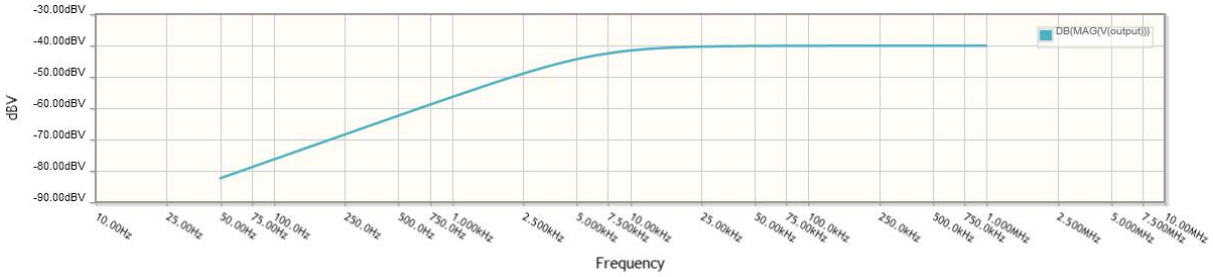

At frequencies above 10 kHz the effective voltage ratio of the CVD was now 100:1 (-40dB). At 50Hz, the ratio was 13,000:1, i.e. the 50Hz signal into the high pass filter would be just 1.0V_{rms} – which drops to 100 µV_{rms} at the digitiser input due to the filter. The added 220Ω resistor in the CVD produced a small amount of Johnson-Nyquist noise. For a digitiser span setting of 4 volts (primary equivalent, i.e. ±20mV at the digitiser), the noise calculation was:

Noise type	rms noise	Unit	Comment
Quantisation	0.000122	volts	Half of a one-bit gap in the digitiser output levels
Johnson-Nyquist	0.000281	volts	At 320^{O}K (50^{O}C), measured over 2MHz.
Filter+mounting	0.056000	volts	560µV_{rms} at digitiser
Digitiser	0.011000	volts	0.05% of half the span plus 100µV_{rms}
<1kHz signals	0.000400	volts	100µV_{rms} at digitiser
Total noise	0.057	volts	Expressed in primary quantities

With this arrangement, noise was about 4% of the largest sinusoidal waveform that could be recorded without clipping. A high frequency network voltage signal of 100mV_{rms} could be recorded with a 5dB SNR. Design options to reduce this noise level further were considered, but undesirable features of these solutions led to selection of the this arrangement as the final design.

11.1.6 Calibration tests – voltage channels

The voltage measurement system was calibrated and its frequency response measured between about 200Hz and 2MHz. This is shown in Figure 105.

Figure 105: voltage measurement system frequency response

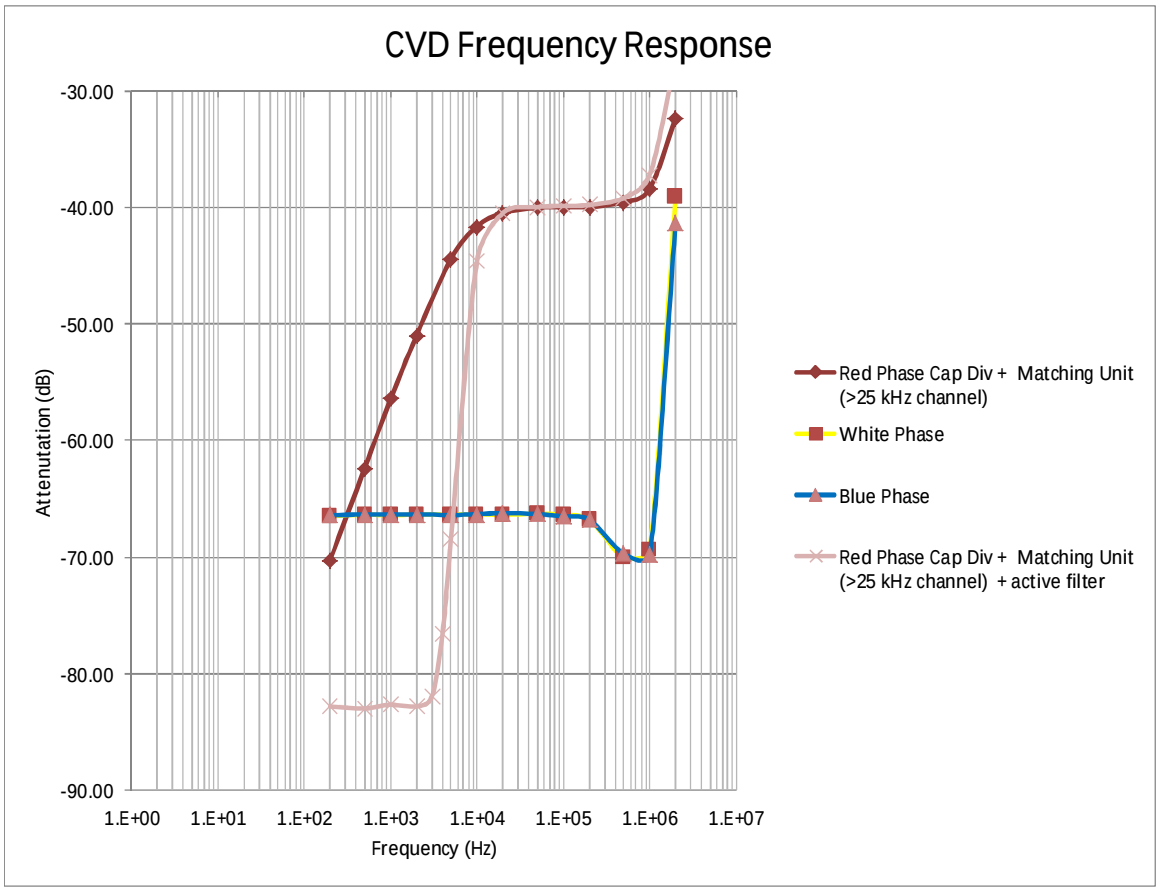

The high-frequency channel (labelled 'red phase') showed response to 1MHz as designed. The other two CVDs (white and blue phases) showed a 3dB ratio drop-off for frequencies between 500 kHz and 1 MHz. This performance was acceptable given that the theses were only used for the low-frequency channel which was using a 50 kHz low-pass anti-alias filter.

11.1.7 Phase-to-phase voltage measurement

In considering the challenge of fault signature detection in the presence in network voltages of significant background noise from AM radio stations, it was hypothesised that radio signal pick-up might be a common mode phenomenon, i.e. the radio signal picked up on one powerline phase may be similar to that picked up by another powerline phase. The easiest way to eliminate any common-mode noise source would be to measure phase-to-phase high frequency voltage fault signatures.

Simulation showed that the arrangement shown in Figure 106 could be used to do this.

Figure 106: modified CVD arrangement to record phase-to-phase fault signatures

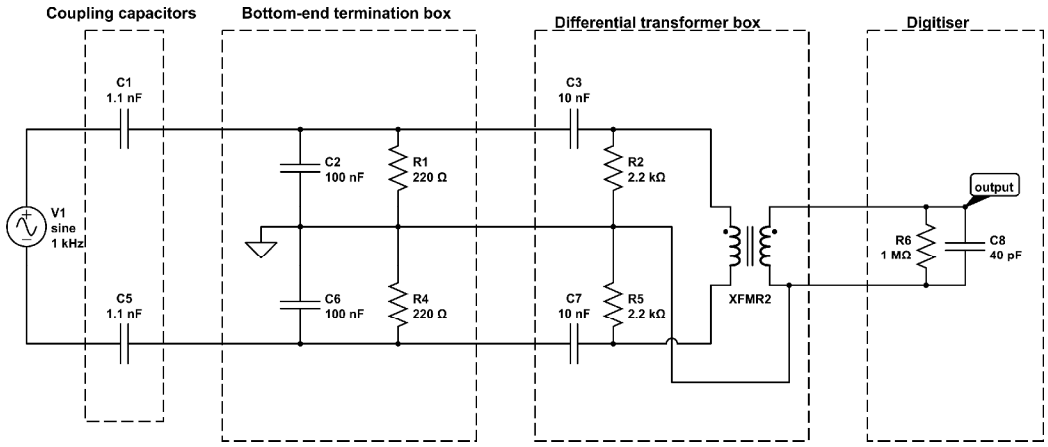

The design of the transformer used to subtract the phase voltages from each other was a challenge as it had to function accurately up to 1MHz. The design adopted used two lengths of coax cable wound bifilar (50+50 turns) on a ferrite toroid. The shield of the input coax was connected to the core at one end of the winding. This ensured any common mode currents due to capacitive coupling between windings did not flow in the core conductor. The shield of the output coax was connected to the core conductor of the output winding where that end of the winding connected to local earth. This further reduced capacitive coupling between windings. The whole transformer with its input high-pass filter was enclosed in a metal box as shown in Figure 107.

To ensure the 50Hz 'volts per turn' seen by the transformer was well below the ferrite's saturation level, an additional 'series C, shunt R' high-pass filter stage was inserted in each input connection.

Figure 107: differential transformer used to measure phase-to-phase high-frequency voltage signatures

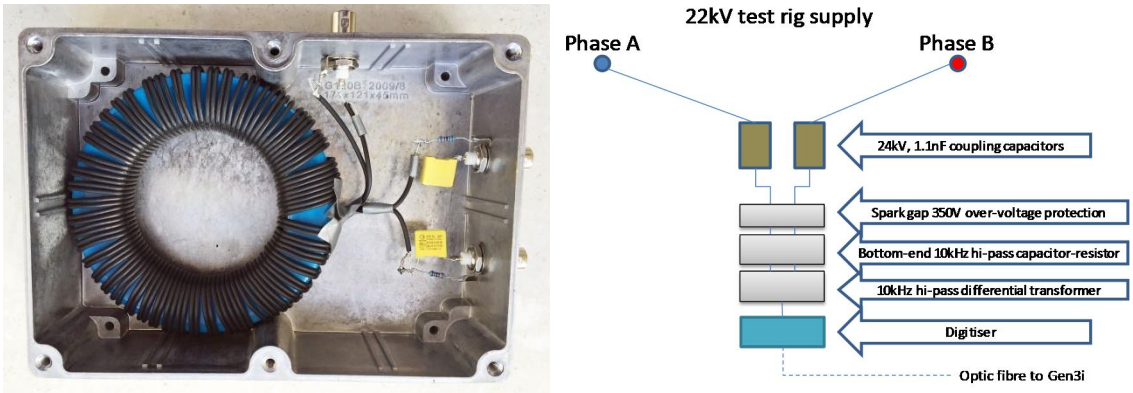

The simulated frequency response for phase-to-phase voltage signatures was as shown in Figure 108.

Figure 108: simulated frequency response of phase-to-phase fault signature measurement circuit

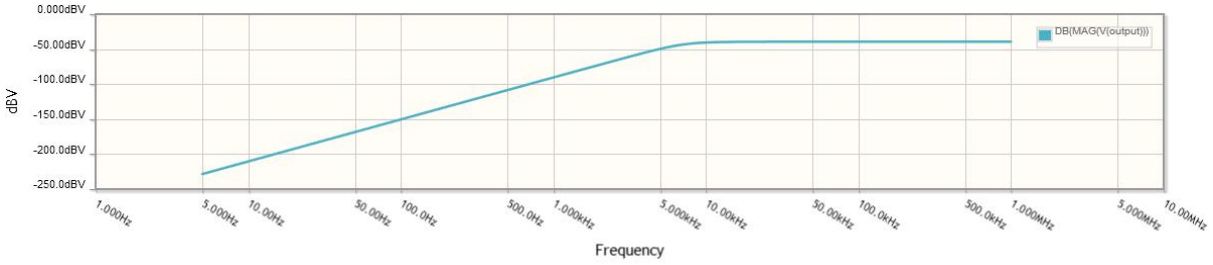

To test the accuracy of the transformer's differential function, an FFT was used to measure the amplitude of the carrier signals from two radio stations: ABC Radio National at 621 kHz and ABC Melbourne at 774 kHz. The test results are shown in Table 8.

Table 8: Tests on differential transformer in HF voltage measurement

Run	621 kHz (Volts)	774 kHz (Volts)	Configuration (active hi-pass filter in place for all runs)
89	0.014	0.023	Normal configuration for measurement of phase-to-earth voltage
90	0.0006	0.0008	Differential transformer in place, both coupling caps on same phase
91	0.021	0.033	Differential transformer in place, coupling caps on different phases
92	0.019	0.019	Differential transformer in place, coupling caps on different phases, one input to the differential transformer short-circuited by 50Ω
93	0.018	0.018	Normal configuration for measurement of phase-to-earth voltage

Tests showed the differential transformer was effective – when both inputs were connected to the same phase in Run 90, it cancelled 96% of the phase-to-earth voltage shown in Runs 89 and 93. Calibration Run 91 showed that the radio station signals were not pure common mode – the phase-to-phase amplitude was 1.3 to 1.6 times the phase-to-earth amplitude.

For the last week of tests (Test 822 to Test 1038) the HF voltage channel was connected phase-to-phase using the differential transformer. The arrangement of the primary voltage transducers is shown in Figure 109.

Figure 109: voltage measurement system for phase-to-phase voltage measurement

The active high-pass filter was omitted as the additional stage of hi-pass filtering in the differential transformer was sufficient to reduce the 50Hz signal to the target level. Elimination of the active filter reduced estimated wide-band measurement system noise to 11mV.

11.1.8 Current measurement

The primary current transducer was a HiLo Test Model 3P/200 coaxial shunt of 200mΩ resistance with ratings of 3kA peak, $8A_{rms}$ continuous, i^2t of $1300A^2s$ (for a temperature rise of 100°C) and flat frequency response from DC to 50MHz. The i^2t rating meant that maximum flashover current of 64 amps could be tolerated for 320ms without damage to the shunt. The current measurement transducer arrangement is shown in Figure 110.

Figure 110: current measurement transducers

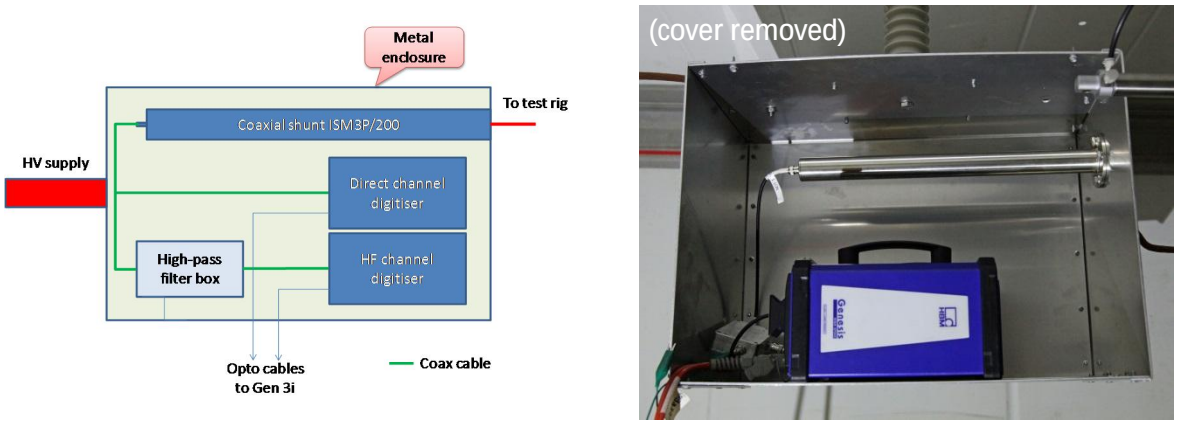

11.1.9 Current measurement system design

The shunt output signal went direct to the digitiser for the low-frequency channel and via a passive high-pass filter to the digitiser for the high-frequency channel. Johnson-Nyquist noise from the shunt was calculated to be in the nanovolt range at 50°C and was ignored.

If the maximum current in the tests was restricted to $6A_{rms}$, a $4V_{pk}$ ($\pm 2V_{pk}$) digitiser span (20A primary equivalent) could be used and the estimated noise in the low-frequency current channel was:

Noise type	rms noise	Unit	Comment
Quantisation	0.0006	amps	Half of a one-bit gap in the digitiser output levels
Filter+mounting	-	amps	No filter
Digitiser	0.0055	amps	0.05% of half the span plus $100\mu V_{rms}$
Total noise	0.0055	amps	Expressed in primary quantities

This would allow a current of $11mA_{rms}$ to be recorded with 6dB SNR.

11.1.10 High Frequency current channel

Initially, the use of an active high-pass filter similar to that used in the high-frequency voltage channel was considered. The high pass filter would reduce the 50Hz fundamental and its harmonics by 80dB (a factor of 10^4) providing flexibility to set the digitiser input span to a higher sensitivity. If the primary equivalent span was set to 200mA ($\pm 100mA_{pk}$ – the maximum sensitivity available with a 200mΩ shunt), total noise would be $3mA_{rms}$ (primary equivalent). The noise estimation was:

Noise type	rms noise	Unit	Comment
Quantisation	0.0000	amps	Half of a one-bit gap in the digitiser output levels
Filter+mounting	0.0028	amps	560µV$_{rms}$ at digitiser
Digitiser	0.0006	amps	0.05% of half the span plus 100µV$_{rms}$
<1kHz signals	0.0006	amps	assuming 6A$_{rms}$ of 50Hz primary current
Total noise	0.0029	amps	Expressed in primary quantities

This would allow a high frequency current of 6mA$_{rms}$ to be recorded with 6dB SNR. The 'filter plus assembly' noise dominates in this case and there is no easy way to improve this further without changing to a higher resistance shunt.

Given the large ratio between output impedance of the shunt (200mΩ) and input impedance of the digitiser (1MΩ), it was decided there was scope to use a passive filter and the following filter was considered:

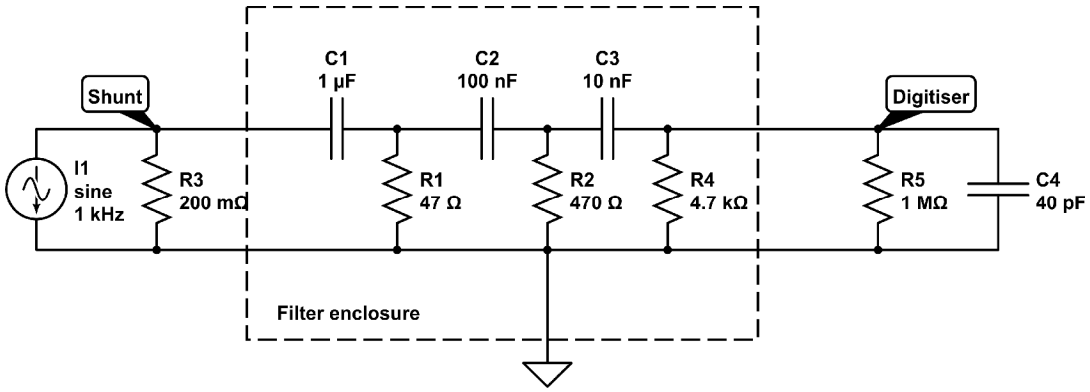

This had the calculated frequency response:

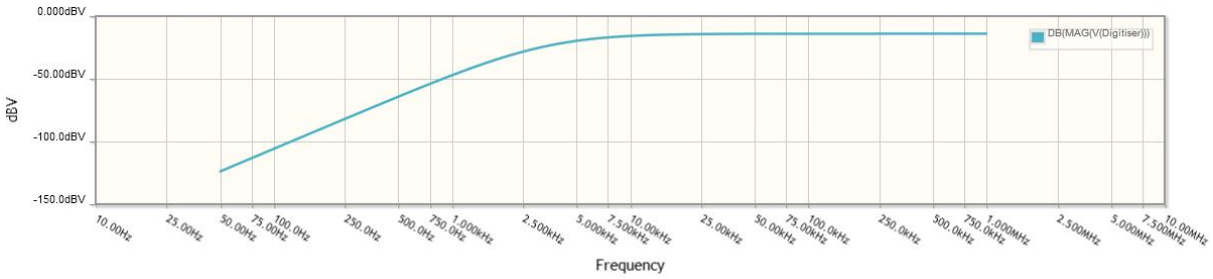

In terms of equivalent shunt resistance, this frequency response is:

Frequency	Response	Equivalent shunt value (V/A)
1MHz	-14.06dB	198mΩ
100kHz	-14.08dB	198mΩ
10kHz	-15.82dB	162mΩ
1kHz	-47.21dB	4.4mΩ
350Hz	-72.10dB	0.25mΩ

Frequency	Response	Equivalent shunt value (V/A)
250Hz	-81.96dB	0.08mΩ
150Hz	-95.10dB	0.02mΩ
50Hz	-123.90dB	0.0006mΩ

With this three-stage passive RC filter, the noise estimate was:

- Thermal noise: each of the resistors would generate thermal noise. However, noise in the 5kΩ output resistor will dominate as the resistor values in preceding filter stages are lower by at least a factor of ten. The noise in this resistor at 45°C was calculated to be 13μV_{rms} measured over the 2MHz band of interest. This is equivalent to 65μA_{rms} on the primary circuit, which was considered negligible. In reality, this noise would be further attenuated by the load presented by the preceding stages of the filter.
- Digitiser noise: The digitiser noise (as well as the maximum primary current that can be measured without clipping) depended on the input span. The Proof of Concept tests were used as a guide in the final choice of input span setting in the high frequency current channel. The options were:

Digitiser input setting	Primary equivalent span	Maximum primary current	Equivalent primary digitiser noise
±2V	20A	7.07A_{rms}	5.50mA_{rms}
±1V	10A	3.54 A_{rms}	3.00 mA_{rms}
±500mV	5A	1.77 A_{rms}	1.75 mA_{rms}
±200mV	2A	0.71 A_{rms}	1.00 mA_{rms}
±50mV	500mA	0.18 A_{rms}	0.63 mA_{rms}
±20mV	200mA	0.07 A_{rms}	0.55 mA_{rms}

- Quantisation noise: at ±50mV digitiser input span setting, the one-bit gap is 6µV so quantisation noise would be about 3μV_{rms} (15μA_{rms} input equivalent), which is negligible.
- Low frequency signals: the residual low-order harmonics below 1 kHz could still be present at the digitiser input. The lower frequencies would be more strongly attenuated, so the risk was considered higher at higher frequencies, e.g. from harmonics between 13th and 19th (650Hz to 950Hz). Before the tests there was no information on what range of frequency components to expect. A current of 4A_{rms} 50Hz fundamental with harmonic content typical of arc currents recorded in the 2014 REFCL Trial NER tests (e.g. Test 150 in which the soil

current was measured by a coaxial shunt) was considered as a possibly representative example. The REFCL Trial Test 150 fault current had the following waveform:

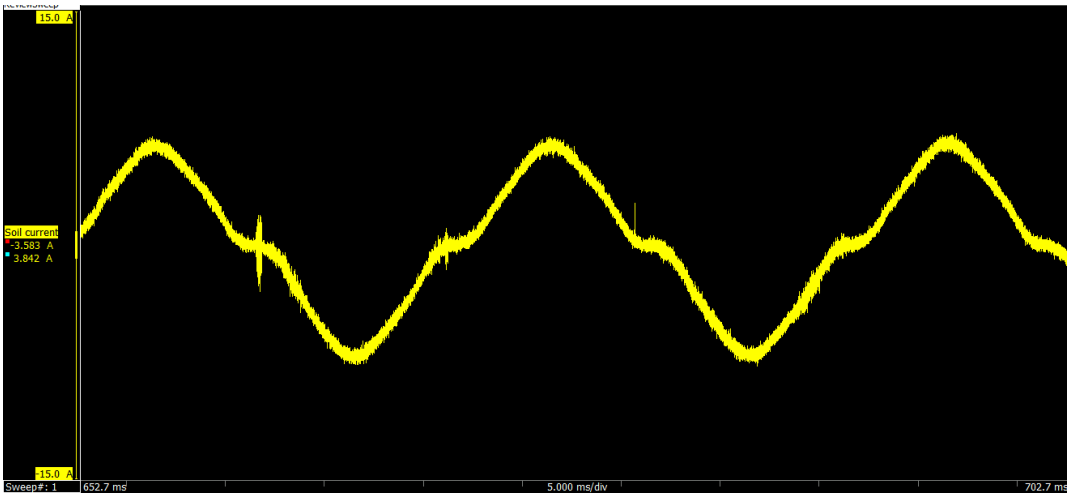

The current spectrum determined by FFT Analysis of this current (after down-sampling to get precisely 1024 data points over two 50Hz cycles), was multiplied by the three-stage RC high-pass filter response to find the magnitude of each harmonic at the filter output:

Harmonic number	Frequency (Hz)	Current (A_{rms})	Filter response (dB)	Filter output (μV_{rms})
1	50	4.071	-123.9dB	0.5
3	150	0.717	-95.1dB	2.6
5	250	0.118	-82.0dB	1.9
7	350	0.112	-73.2dB	4.9
9	450	0.025	-67.0dB	2.7
11	550	0.012	-61.8dB	1.6
13	650	0.010	-58.0dB	2.5
15	750	0.006	-54.0dB	2.4
17	850	0.009	-49.5dB	6.4
19	950	0.011	-48.3dB	8.8

Adding a root-sum-of-squares, the primary equivalent noise due to low frequency harmonic components was thus estimated at 66μA_{rms} which is negligible compared to digitiser noise.

It was concluded that the passive filter design offered superior overall SNR compared to an active filter in measurement of high frequency current components and this design was adopted for the test program.

11.1.11 Calibration tests – current channels

The current transducers were calibrated and their frequency response measured from DC to 1MHz. The coaxial shunt showed no deviation greater than 0.2dB (2.5%) from its nominal value of 200mΩ for frequencies between 20Hz and 2MHz. The measured frequency response of the passive high-pass filter is shown in Figure 111. The noise level in the frequency response measurement system degraded the accuracy at attenuations greater than 28-30dB. Recognising this limitation, it was considered the frequency response test confirmed performance was likely to be 'as designed'.

Figure 111: frequency response of passive high-pass filter used in current channel

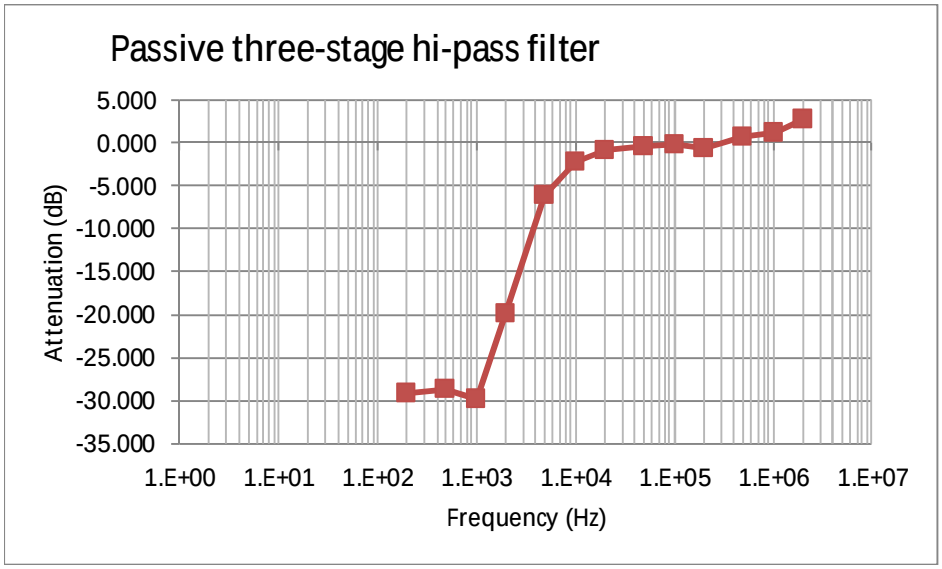

11.1.12 Measured voltage and current noise levels

Wide-band noise with current shunt open-circuit and coupling capacitors short-circuit was:

Quantity:	Voltage		Current	
Channel	Estimated	Measured	Estimated	Measured
Low-frequency	10.3 V_{rms}	5-7 V_{rms}	5.5 mA_{rms}	2.6 mA_{rms}
High-frequency	57 mV_{rms}	25 mV_{rms}*	0.6 mA_{rms}	0.25 mA_{rms}

* The measurement of high-frequency voltage noise was taken with the CVD input to the active high-pass filter short-circuited. If taken with the coupling capacitor short-circuited but not shielded, this measurement still contained some network background noise induced in the small physical loop formed by the measurement current path through the centre of the capacitor and the short circuit around its outside surface, which increased total noise to 115mV. With the input of the digitiser set to 'GND', HF voltage noise was 2 mV.

A typical measurement system noise record is shown in Figure 112 on page 122. This was recorded with the test rig conductors un-energised and with the HF voltage measured phase-to-phase but both coupling capacitors connected to the same phase.

11.1.13 Digitiser and DAQ settings

The HBM Model Gen3i mainframe was fitted with a HBM Model GN401 four channel optical input card fed by four HBM Model GN110-2 opto-isolated digitisers.

The digitisers operated at a constant 100MS/s sampling rate and incorporated anti-alias filters, analogue and digital, plus data decimation to reduce the effective sampling rate to match the chosen setting. All four channels were set to use the 10MHz corner-frequency 6-pole Bessel analogue low-pass anti-alias filter. A second low-pass anti-alias filter (a Bessel IIR digital filter) was set to 50 kHz on low-frequency channels and 1MHz on high-frequency channels.

All four channels were recorded continuously at 100kS/s and the two high-frequency channels were additionally sampled in 20ms sweeps each second during which the sampling rate increased to 2MS/s. The sweeps were triggered by an external 1Hz square wave signal which was not synchronised to the start of continuous recording or to the start of the test.

11.1.14 Off-site measurement systems

Three off-site measurement systems collected data during the tests. These were located outside the test area but still within the zone substation. They were:

1. IND Technology Pty Ltd: This was a two-phase remote sensing partial discharge detection system based on an Agilent Model DSO5034A Digital Storage Oscilloscope with two-channel 14 bit sampling at 500MS/s, i.e. one data point in each channel every 2ns. Sweeps of 2µs duration (1000 samples in each channel) were enabled every 100ms and triggered when a sensor output next exceeded a pre-set limit. Each sweep record included 0.5µs of pre-trigger data and 1.5µs of post-trigger data.

   Details of the IND Technology sensors (capacitive coupled dipole antennae with a bandwidth of 1MHz to 3GHz, located 0.5 metres below the high voltage phase conductor) are described in US Patent Application publication US 2014/0354293 A1.

   The IND data files were produced in National Instruments TDMS format. Test files comprise up to 500 sub-files each containing the data for one 2 µs sweep. If the record in the test file exceeded 50 seconds (500 sweeps), another test file was automatically generated. Test files can be opened in MS Excel with a suitable TDMS import plug-in.

2. Substation data logger: an Elspec power quality meter was connected to the secondary of the zone substation SV feeder metering current transformers and the secondary of the substation voltage transformer. This provided an indication of what can be detected at a zone substation using conventional equipment at low cost.

   Details of the Elspec PQM and its connections are:

Meter:	Elspec G4420
Memory:	4GB.
ADC:	16 bit.
Shortest transient detection:	39µs.
Voltage measurement:	
Sampling rate:	512 samples per 50Hz cycle
Effective bandwidth:	12.5kHz
Range:	0-900 V_{rms}
Resolution:	10 mV_{rms}
Voltage Transformer:	22,000V:110V

Current measurement:	
Sampling rate:	256 samples per 50Hz cycle
Effective bandwidth:	6.25 kHz
Range:	0-50A (5A nominal)
Resolution:	0.1 mA_{rms}
Effective CT ratio:	133.3:5
CT type:	Metering class 400/5
Test record data file:	
Format	Comma delimited values
Column A	Date and time (local)
Column B	Time (seconds)
Column C	Red to neutral volts
Column D	White to neutral volts
Column E	Blue to neutral volts
Column F	Neutral to earth volts
Column G	Red phase current
Column H	White phase current
Column I	Blue phase current
Column J	Neutral current

Part way through the test program, the white phase current input was moved to another feeder to capture low-frequency background current noise. From that test on, the neutral current value in the test record is longer correct.

3. GE Multilin F60 protection relay: this feeder protection product offers high-impedance fault detection and records waveforms of faults. The relay detected none of the 1,038 faults in the test program.

   Discussions and analysis of its non-response to faults in this test program confirmed that the term 'high impedance' in the operating context in which this relay is successfully applied (North America) refers to earth faults on four-wire high voltage networks that may draw tens or hundreds of amps. The relay would require major product development to offer value in fire risk reduction efforts in Victoria where fast detection and response to 0.5 amp faults is required.

Figure 112: Calibration run 73 – typical measurement system noise waveforms over one 20ms cycle – rig un-energised, HF voltage is phase-to-phase on same phase

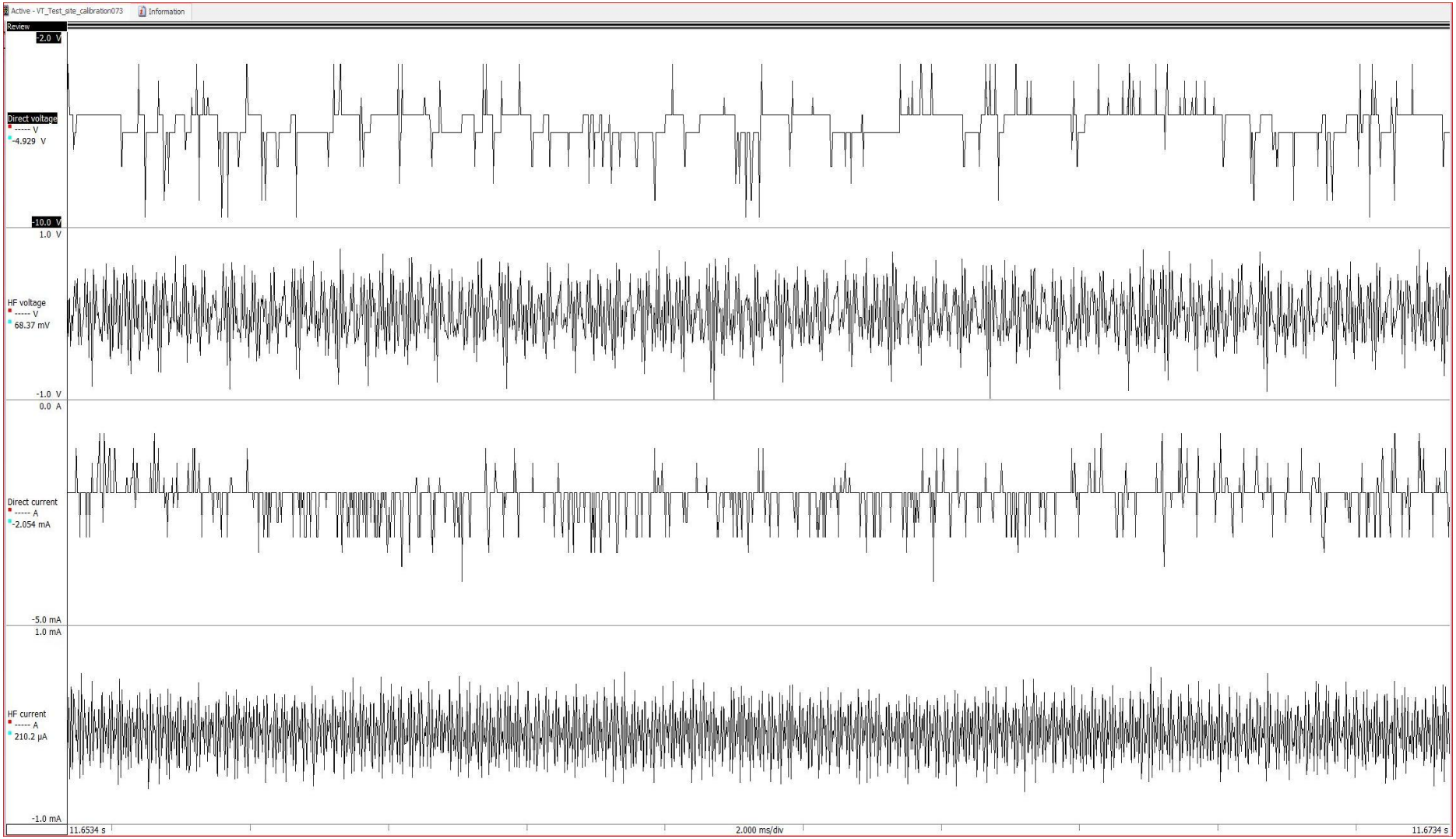

11.1.15 Summary of test site measurement system

The following measurement system configuration and settings were used in most tests:

Quantity	Channel	Transducer	Filter	Anti-alias	Conversion	Span	Clipping limit	Est. Noise
Voltage	Low-freq	CVD	None	Analog 10MHz + 50kHz digital	2100 V/V	42 kV	14.9 kV_{rms}	10.3 V_{rms}
	High freq	Modified CVD	One-stage RC + Active	Analog 10MHz + 1MHz digital	100 V/V	4 V	1.4 V_{rms}	57 mV_{rms}
Current	Low-freq	Coax shunt	None	Analog 10MHz + 50kHz digital	5A/V	20 A	7.1 A_{rms}	5.5 mA_{rms}
	High freq	Coax shunt	Three-stage RC	Analog 10MHz + 1MHz digital	5A/V	500mA	0.18 A_{rms}	0.6 mA_{rms}

The final voltage and current passive high-pass filters were:

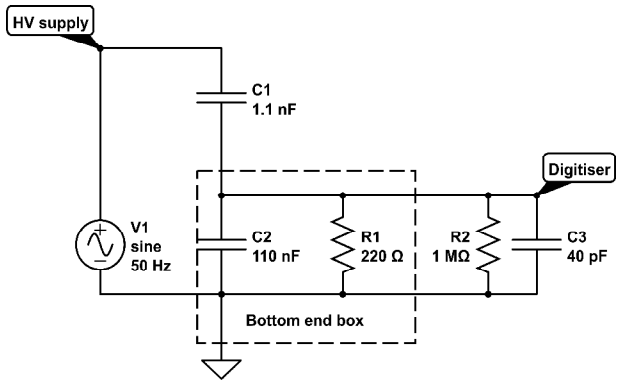

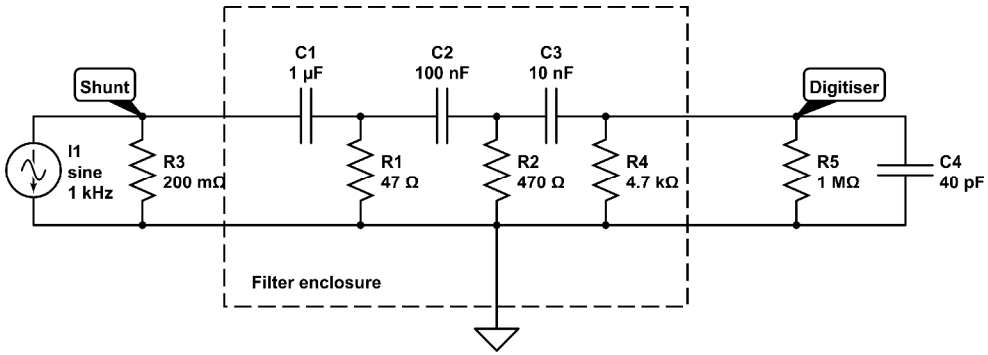

11.2 Appendix B: Data processing

The data capture and first-stage processing software was HBM Perception. The Perception data files were loaded into MatLab for further on-site processing immediately after each test. This produced a range of charts which revealed the detail of what had occurred in the test to guide decisions on future tests.

Following completion of the test program a more comprehensive range of charts was produced for each test to support analysis and reporting. The details of the MatLab processing script and settings are set out in *Appendix G: HRL Technology report*.

The range of charts available for each test is shown in Table 9.

Table 9: post-test analysis charts (example: Test 102 – Manna Gum phase-to-earth 2.0 amp limit with flashover)

	Current	Voltage
LF	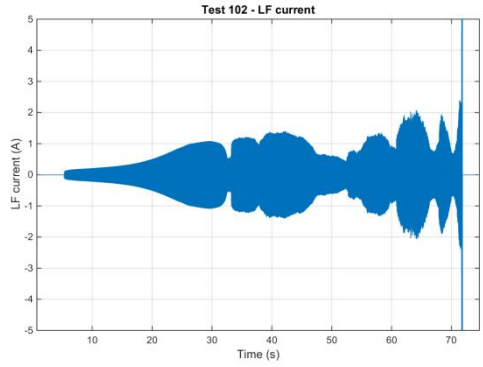	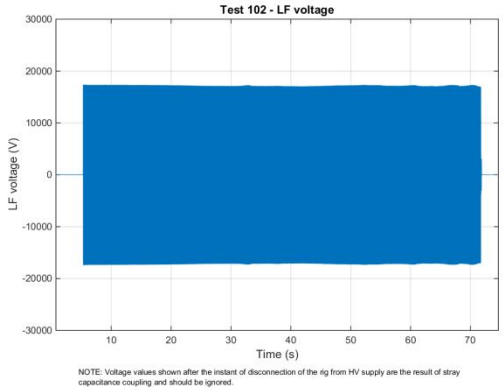
LF RMS	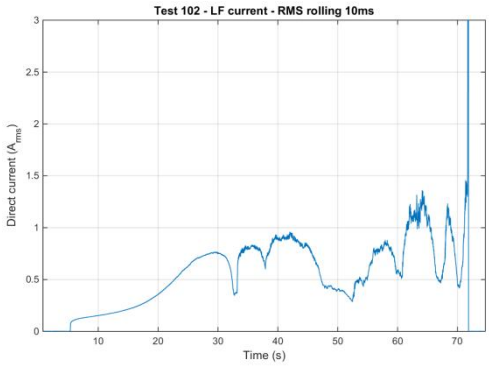	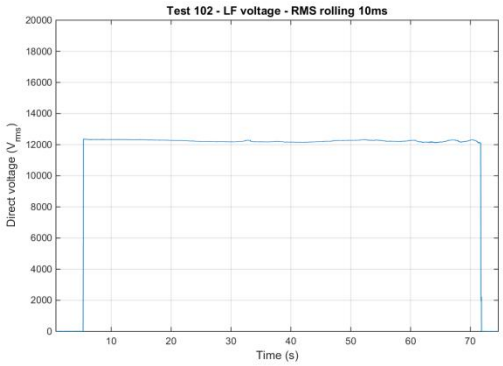

	Current	Voltage
LF detail – start point	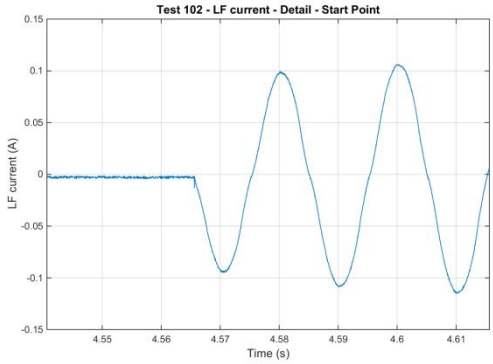	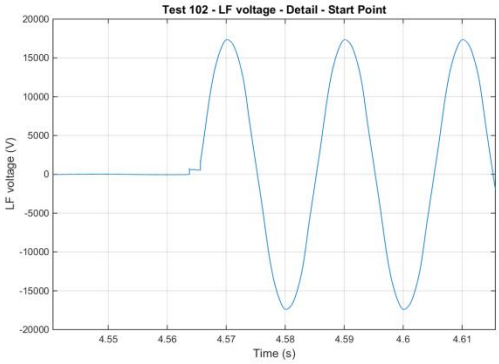
LF detail – mid point	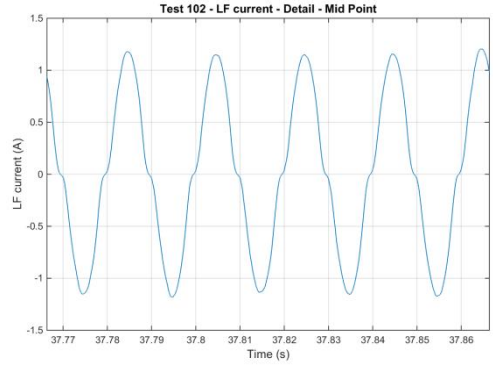	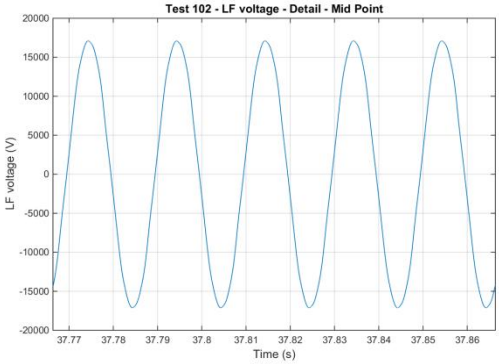
LF detail – end point	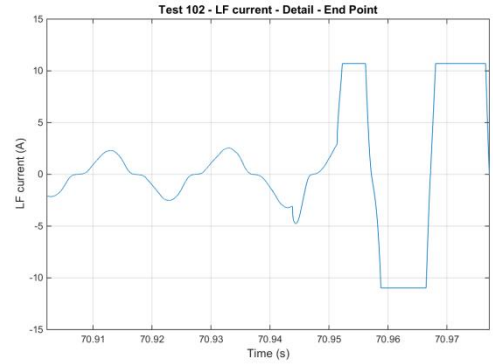	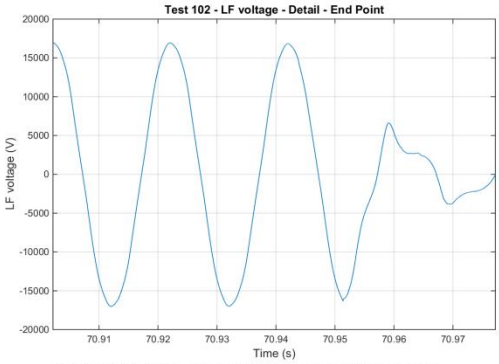

NOTE: Voltage values shown after the instant of disconnection of the rig from HV supply are the result of stray capacitance coupling and should be ignored.

	Current	Voltage
LF spectrogram	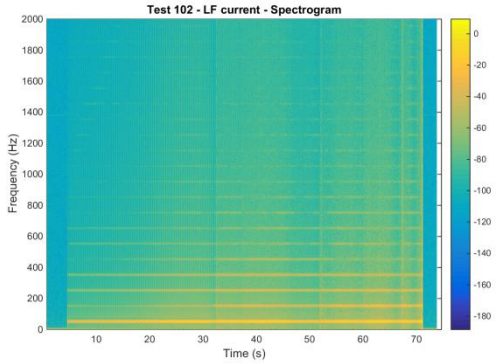	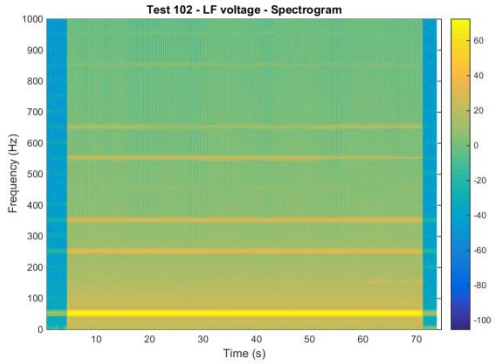
LF spectrum – mid-point – low range	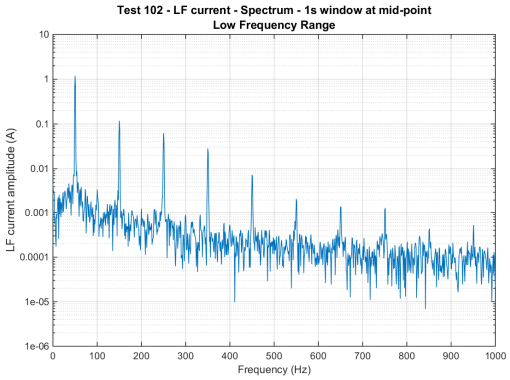	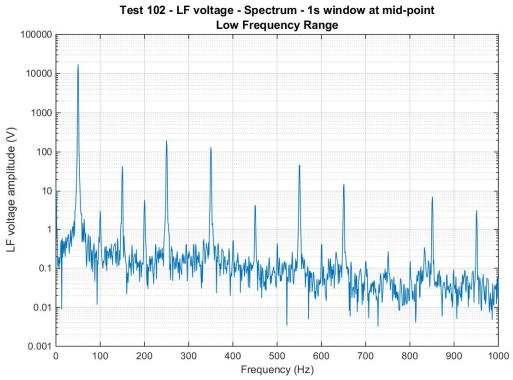
LF spectrum – mid point – mid range	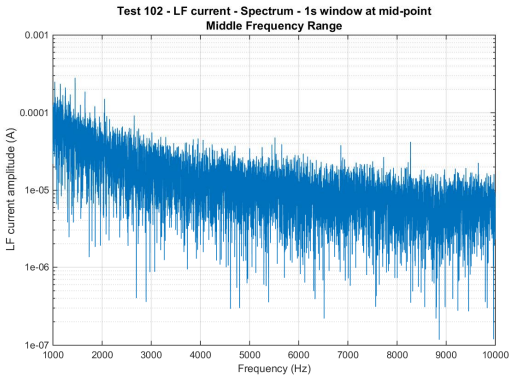	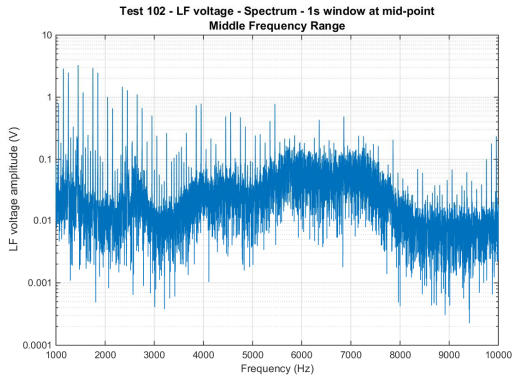

Current

Voltage

LF spectrum – mid point – high range

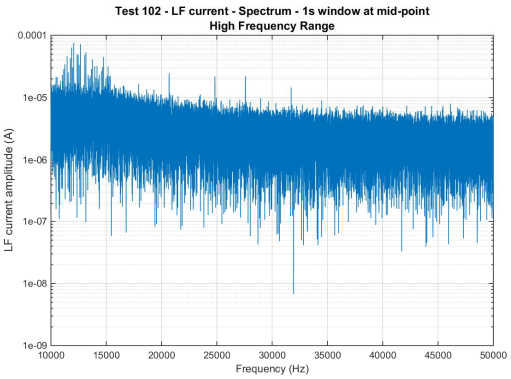

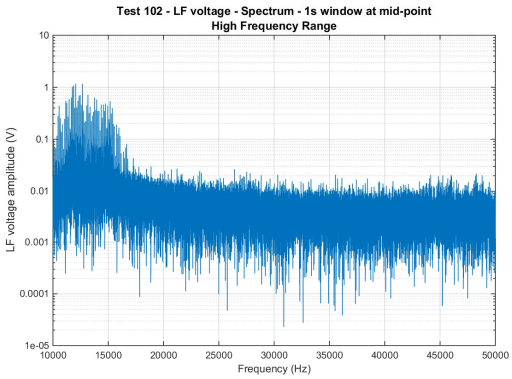

HF

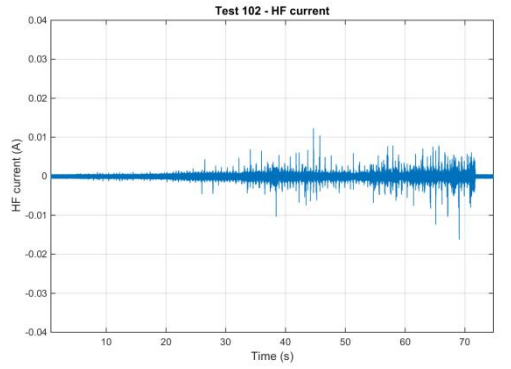

WARNING: Data shown is for 20ms sweeps recorded every second and placed end-to-end. Data between sweeps (98% of total duration) is not shown Time axis value shows position of sweep in test and does not indicate time scale within sweep data. Refer to project report for interpretation.

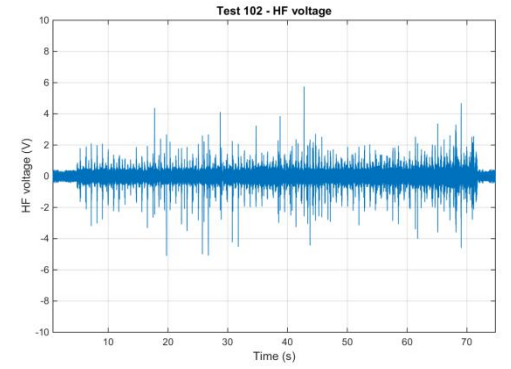

WARNING: Data shown is for 20ms sweeps recorded every second and placed end-to-end. Data between sweeps (98% of total duration) is not shown Time axis value shows position of sweep in test and does not indicate time scale within sweep data. Refer to project report for interpretation.

HF RMS

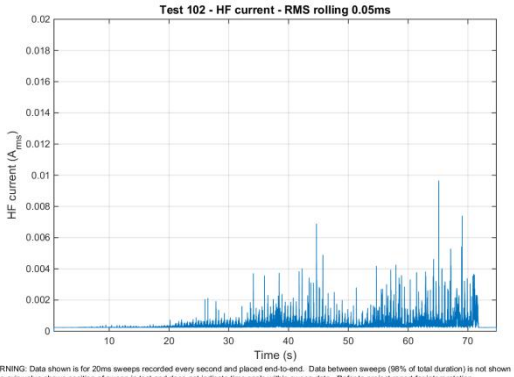

WARNING: Data shown is for 20ms sweeps recorded every second and placed end-to-end. Data between sweeps (98% of total duration) is not shown Time axis value shows position of sweep in test and does not indicate time scale within sweep data. Refer to project report for interpretation.

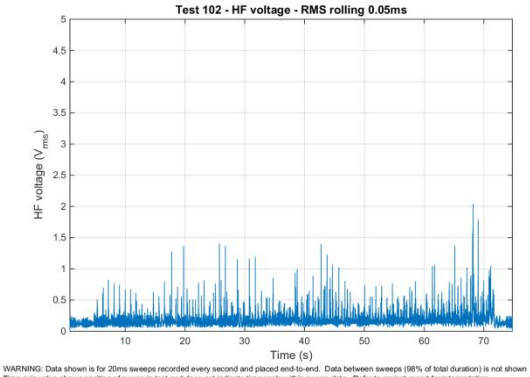

WARNING: Data shown is for 20ms sweeps recorded every second and placed end-to-end. Data between sweeps (98% of total duration) is not shown Time axis value shows position of sweep in test and does not indicate time scale within sweep data. Refer to project report for interpretation.

Current

Voltage

HF detail – start point

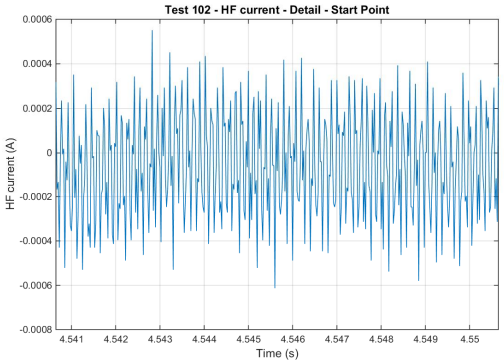

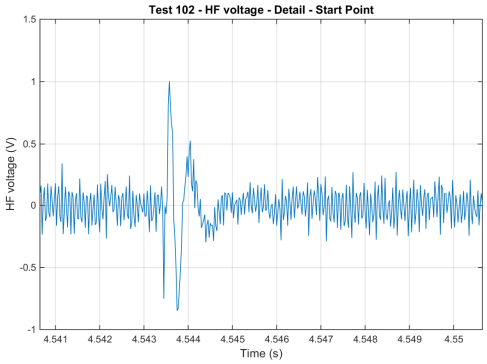

HF detail – mid point

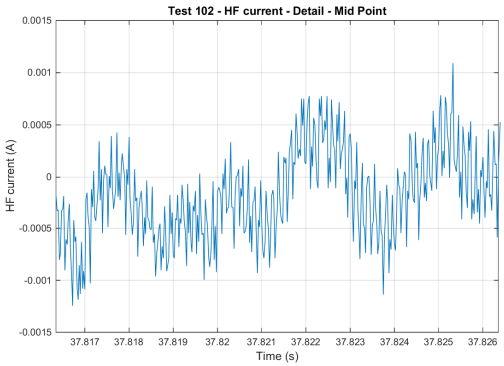

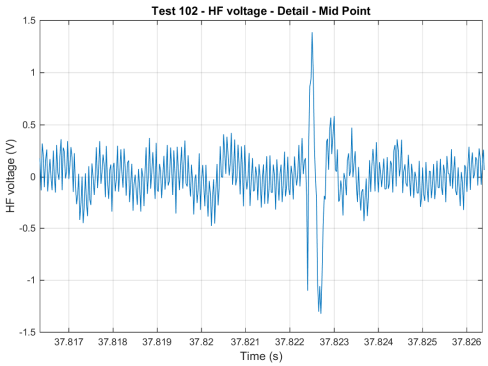

HF detail – end-point

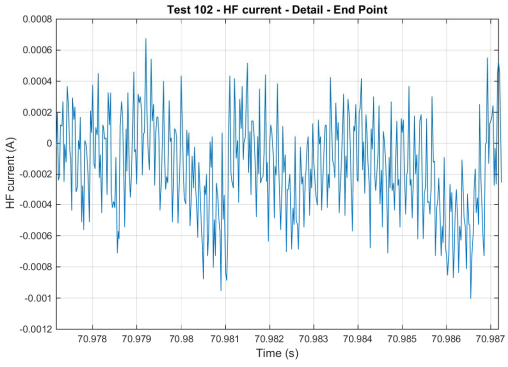

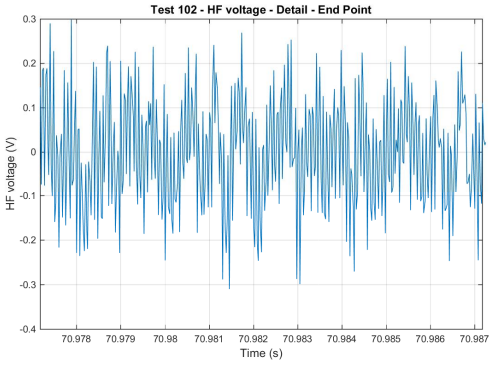

	Current	Voltage
HF spectrogram	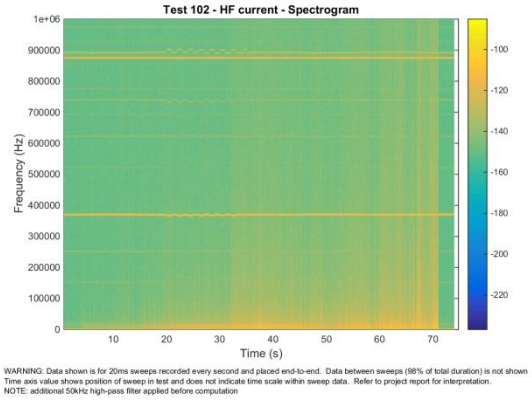 WARNING: Data shown is for 20ms sweeps recorded every second and placed end-to-end. Data between sweeps (98% of total duration) is not shown Time axis value shows position of sweep in test and does not indicate time scale within sweep data. Refer to project report for interpretation. NOTE: additional 50kHz high-pass filter applied before computation	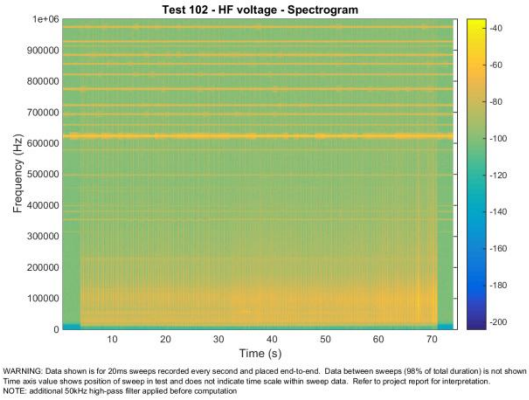 WARNING: Data shown is for 20ms sweeps recorded every second and placed end-to-end. Data between sweeps (98% of total duration) is not shown Time axis value shows position of sweep in test and does not indicate time scale within sweep data. Refer to project report for interpretation. NOTE: additional 50kHz high-pass filter applied before computation
HF spectrum – mid point – low range	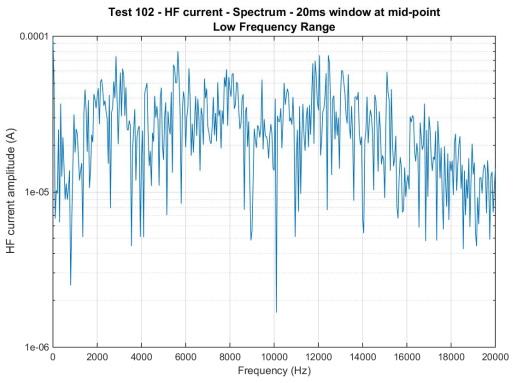	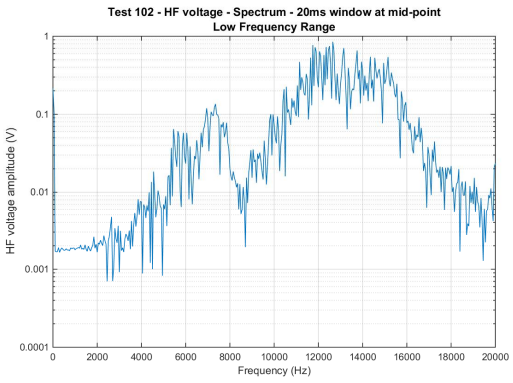
HF spectrum – mid point – mid range	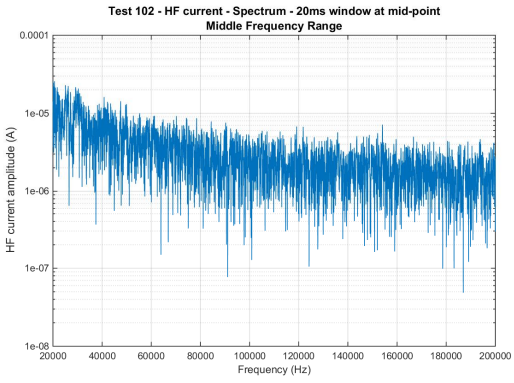	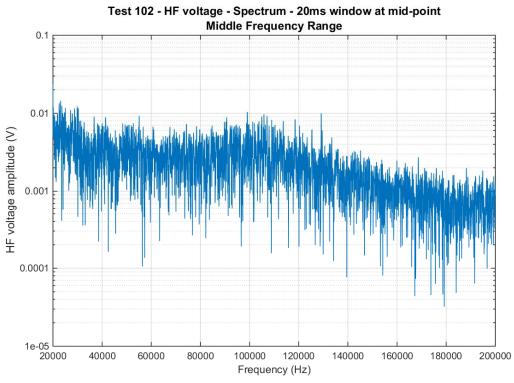

HF spectrum – mid point – high range

Current

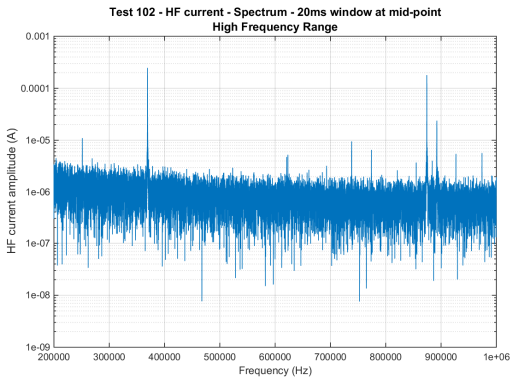

Voltage

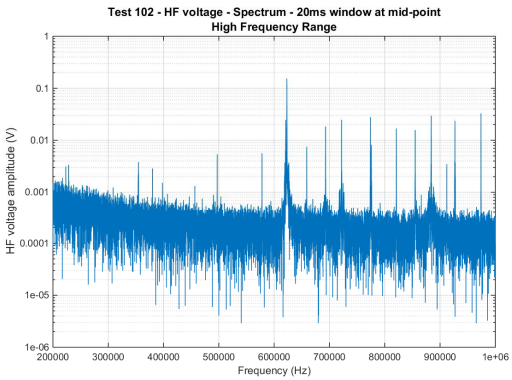

11.2.1 Interpretation of HF charts

The HF channels were sampled at 2MS/s for a short 20ms 'sweep' each second. Sweep triggering was not synchronised to the start of the test nor the master clock which generated the timestamps on the sampled data; it was triggered by an external 1Hz square wave signal feed to the Gen3i DAQ system by the test control PC.

Consideration was given how best to show this high-speed sweep data on a chart so it was meaningful to the viewer. It was decided the sweep records would be concatenated to provide a continuous file of high-speed data and this would be charted and processed as if it were a single continuous record of the test.

When viewing the HF charts or accessing the HF data, it must be recognised that it constitutes in fact a 'stitched together' series of short samples of a much longer record. In between these samples (for 98% of the test duration when a sweep of high speed sampling is not running) there is no high-frequency data. There is data in the 'inter-sweep' periods but it is unreliable as the sampling frequency is only 100kS/s and the anti-alias filter is set to 1MHz, i.e. anti-alias protection is missing. This data was discarded in generating the HF charts.

The horizontal axis on the HF charts has been expanded by a factor of 50 to show the position of the sweep in the test. However, it is not an indicator of the position of the data in the sweep. If the test duration was 20 seconds, 20 sweeps will have been recorded and placed end-to-end to form the chart, so one-twentieth of the chart is a single sweep: 20ms of high speed sampled data.

In the calculation of RMS values of HF data, a rolling 50µs window has been used to do the calculation. The window size was chosen to be equal to a half cycle of the lowest frequency component expected to be in the HF data. Given the 10 KHz corner frequency of the high-pass filters used in the measurement system, the lowest frequency is 10 kHz, one cycle of which is 100µs, so a half cycle is 50µs.

11.2.2 Interpretation of spectra

Frequency spectra were charted for both low-frequency and high-frequency channel data. Each spectrum was calculated over a finite window in time centred on the mid-point of the test. The values plotted on each spectrum chart are the amplitudes of the discrete Fourier transform of the signal at each particular frequency. To aid readability, log scales were used on the vertical axes and the spectra were split across three frequency ranges as listed in Table 10.

Table 10: parameters used in charting of frequency spectra

Channel:	LF	HF
Low range:	0-1kHz	0-20kHz
Middle range:	1kHz-10kHz	20kHz-200kHz
High range:	10kHz-50kHz	200kHz-1MHz
Window duration:	1s	20ms
Samples in window:	100,000	40,000

11.2.3 Interpretation of spectrograms

Spectrograms were used to provide an 'at a glance' view of what signals were recorded during the test. MatLab provides a spectrogram function where amplitude is represented by a logarithmic colour scale. The vertical axis is frequency. The horizontal axis is time. The spectrogram picture shows the presence and variation of every frequency component present in the recorded signal.

The following are relevant to interpretation of HF spectrograms:

- A constant frequency signal shows as a bright horizontal line.
- A burst of broad-band noise shows as a bright vertical band.
- The parameters set for the MatLab spectrogram function were designed to achieve a balance between horizontal (time) and vertical (frequency) resolution. The detailed settings are shown in the MatLab script below and explained in in *Appendix G: HRL Technology report*.
- In the HF voltage spectrogram a 50 kHz high-pass filter was sometimes applied before spectrogram processing to reduce industrial load noise in the signal to better reveal the smaller broad-band high frequency noise.
- The numeric scale shown on the colour bar up the right hand side of the spectrogram is equal to ten times the log (to the base ten) of the power spectral density of the signal at the particular frequency and time values that correspond to the location of the data point on the spectrogram. In turn, the power spectral density is the square of the discrete Fourier transform of the signal, divided by the sampling frequency. Further details on the calculation of the spectrograms can be found in published treatises on signal processing theory and analysis of time series data.

11.2.4 MatLab script used to produce charts

The MatLab script used to produce the charts contained in the test records data base (and in this report) is listed in *Appendix G: HRL Technology report*

11.3 Appendix C: Vegetation fault signatures: experiment design

One of the primary objectives of the vegetation conduction ignition test program was to compile a reference data base of fault signature records to support the development of more effective powerline protection system algorithms for early detection of vegetation faults.

Ideally, the recorded fault signatures should be the voltages and currents that would occur on a real network subjected to a vegetation fault. However, a number of factors work against achievement of this ideal:

1. Voltage and current signals caused by vegetation faults are known to include high frequency components – up to hundreds of megahertz. Accurate wide band measurement of small signals at such high frequencies can be a challenge in the presence of very much larger 50 Hertz quantities. The approach to this challenge is described in *Appendix A: Voltage and current measurement*.
2. There are no established models at the high frequencies involved, either for many of the network equipment items that shape network response or indeed for the vegetation fault processes themselves. Models generated by previous research projects (see *Appendix E: Associated research*) often call for data that is not readily available for real networks.
3. Fault signatures depend on many network properties. At frequencies above the audio range, electricity networks are essentially 'quiet' in that they have no internal sources of high frequency excitation. The high frequency currents and voltages produced by vegetation faults (including that special form of vegetation fault, leakage to cross-arms that causes pole fires) are thought to result from high frequency variations in the effective fault impedance. These impedance variations draw upon energy stored in the electric and magnetic fields created by the 50Hz power flow in the network, i.e. in the stray capacitances and leakage inductances that exist in all powerlines and network equipment items. Thus, the fault signature will depend as much on the network as on the fault.
4. There is no such thing as a single 'real network' in this context. Over the frequency range of interest, every network appears to be as individual as a fingerprint. Further, a network's response to a vegetation fault may vary markedly depending on relatively minor configuration changes, let alone such substantive changes as changes in capacitor bank switching and customer load variations, both of which constantly occur in normal network operation.
5. The safety of the test facility required that fault current be limited by the use of high voltage resistors or isolation transformers, both of which have complex high frequency responses of their own. Their presence, while essential, may affect the recorded fault signatures.

The basic configuration of the experiment is shown in Figure 113.

Figure 113: high level concept of vegetation tests on real network

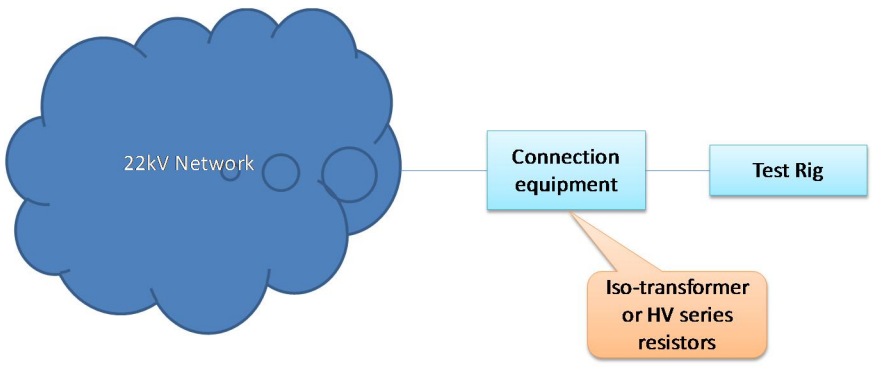

11.3.1 Availability of wide-band network models and data

Some past research projects have studied high frequency models for medium voltage (including 22kV) powerline networks, including some in Australia. At high frequencies, powerlines and network equipment items behave quite differently than they do at 50Hz:

- Eddy currents result in increased conductor resistance values through skin effect
- Magnetic hysteresis reduces effective transformer turns-ratios due to increased iron losses.
- Powerlines start to act like waveguides and antennae and radiation losses appear as a shunt resistance between phases and between each phase and earth.
- Parasitic effects such as stray turn-to-turn capacitance and leakage fluxes dominate over the normal 50Hz characterisation of transformer windings – they behave like transmission lines and at high frequencies act like capacitors between the winding terminals.
- The plastic materials used in underground cables exhibit complex molecular responses that are reflected in substantially increased dielectric losses.

The parameters required to characterise these changes are not found in manufacturers' data sheets and published design standards offer little or no guidance on high frequency response.

The few published research papers on wide-band modelling of distribution network equipment items have focussed on the simplest of them (usually small two winding transformers) and researchers have derived parameters empirically to match test measurements. Such models are typically very complex – see Figure 114 which shows a wide-band model for a simple 25kVA SWER transformer developed by the team at James Cook University in Townsville. The parameter value for each of the 19 elements was derived by matching the computed high frequency responses to the transformer responses measured in tests.

Figure 114: 50Hz and wideband models of a SWER transformer (source: Kikkert, James Cook University Townsville)

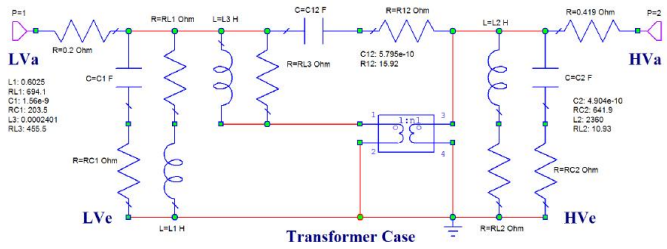

In summary, it is clearly not feasible to adequately model an entire real network with all its connected equipment to derive its high frequency response to vegetation conduction tests.

One conceptual option would be to record fault signatures using known source impedance so they can then be applied in broad-band network models. However if a network model is not really feasible, there may be less value in vegetation fault signatures recorded this way. Despite all its obvious challenges of repeatability, the recording of fault signatures using a real network as the power source may be the superior conceptual approach.

11.3.2 Signatures depend on network, connection and fault properties

Fault signatures depend as much on the network's high frequency characteristics as they do on the fault's characteristics. At the highest level of description, the equivalent circuit of a vegetation conduction test is shown in Figure 115 where each circuit element shown is a complex frequency-dependent impedance.

Figure 115: Vegetation conduction test schematic equivalent circuit (phase to phase fault)

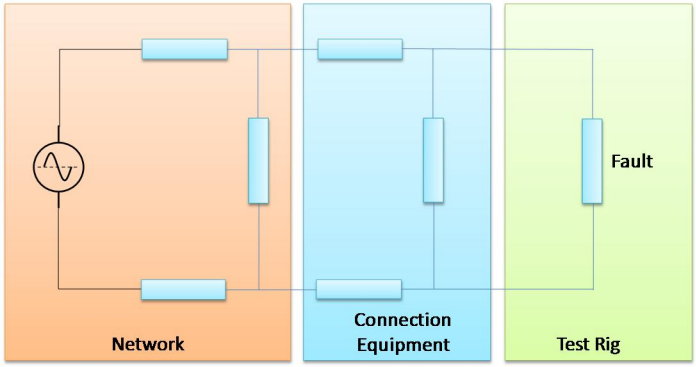

The equations for such a circuit show the fault current and the network voltage at the point of connection depend on all the elements shown in Figure 115. None of them can be assumed constant or ignored.

The fault itself is not an energy source[29]. It might be considered to act like a parallel combination of two impedances:

- One that is non-linear but reasonably symmetric and constantly connected. This impedance shapes the low frequency content of the fault current. It draws current from the networks 50Hz voltages – current that is a combination of 50Hz and harmonics of 50Hz.
- One that is highly non-linear, often asymmetric and usually intermittent, switching on and off randomly at high frequency. This draws current from local energy storages in the network (stray capacitances and inductances) in the form of very high frequency random noise in the megahertz range and higher. There appear to be two different mechanisms by which this impedance generates high frequency noise:
    - If local energy storages contain only low amounts of energy (e.g. when the 50Hz voltage is close to a zero-crossing), this impedance may draw little current. When they contain more energy (e.g. when the 50Hz voltage is close to a peak), this impedance may result in larger amounts of high-frequency noise. This type of effect can be seen in the burst of high-frequency noise near the peaks of the current waveform shown in Figure 116 below.
    - If the 50Hz current is high, it establishes durable current paths that short out the intermittent switching of this impedance. If it is low, i.e. near 50H zero crossings, it can be more easily interrupted so this impedance is free to generate high-frequency noise. In the extreme, this effect can generate large bursts of high-frequency noise at 50Hz zero-crossings associated with interruption and re-strike of arcs. This type of noise can also be seen in Figure 116 around the negative-going zero crossings.

The 2014 REFCL Trial illustrated the creation of high frequency noise in metal-soil/vegetation contact, illustrating asymmetry and random character. An example is shown in Figure 116. Similar effects may well be expected in vegetation tests.

[29] This makes direct application of published research studies of high frequency energy sources on powerline networks (e.g. for PLC communications) potentially problematic.

Figure 116: REFCL Trial test 192 – example of high frequency noise from soil/vegetation fault

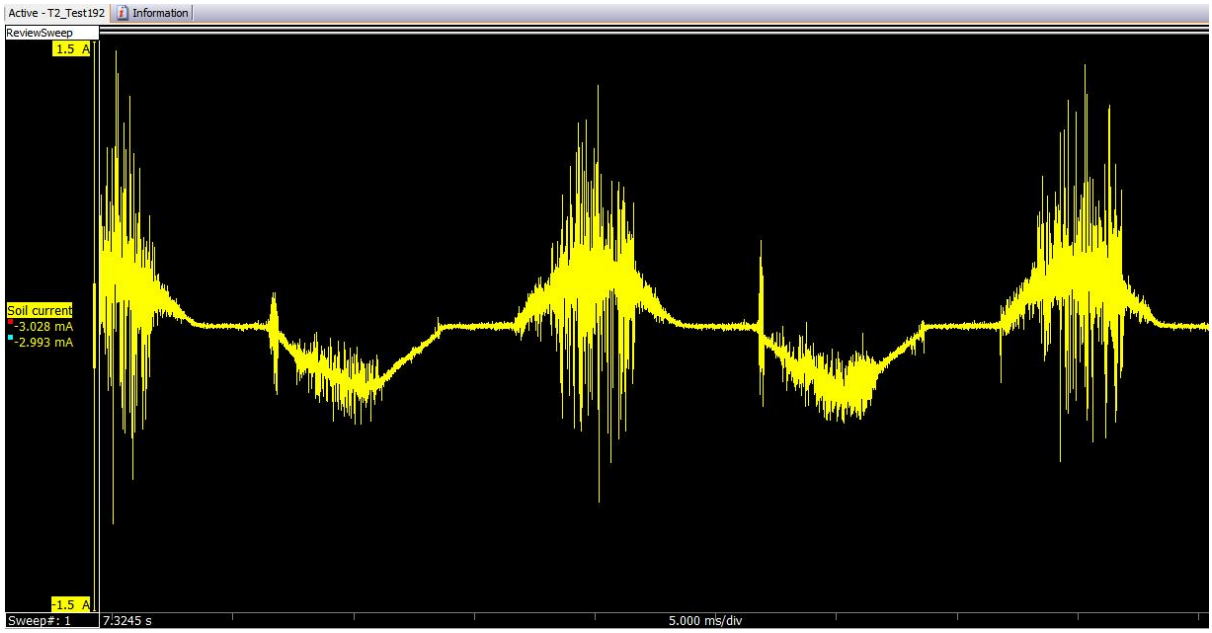

The fault signature will depend not only on the fault characteristics, i.e. the impedances and mechanisms described above, which are an electrical reflection of physical processes occurring at the point of vegetation contact with the conductor and along the current path within the vegetation; they will equally depend on the size and state of local energy storages presented by the network and the connection equipment between the network and the fault.

In summary, the fault signature can be expected to be influenced by just about everything.

11.3.3 Network high frequency responses

Very little research has been published containing actual measurements of high frequency responses of medium voltage distribution networks.

Modelling and simulations indicate many network components and networks as a whole, exhibit complex megahertz-range frequency responses in which narrow bands of frequencies may be attenuated whilst adjacent frequencies remain relatively unaffected. As frequencies increase further – to the tens and hundreds of megahertz – attenuation is thought to progressively increase due to energy losses from radio-frequency radiation.

Published measurements and simulations are generally for very small simple networks and for injection using a current or voltage source, not high-frequency excitation by time-variable non-linear fault impedance. A couple of examples are shown in Figure 117 and Figure 118.

Figure 117: simulated HF response of a small one-kilometre five-branch powerline network (Source: Amirshahi 2006)

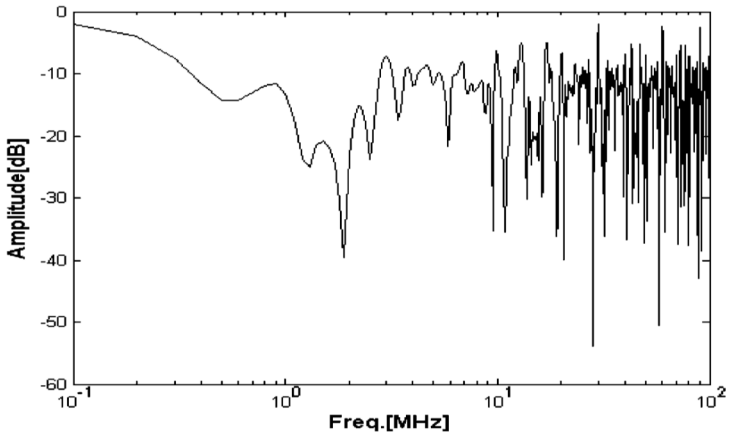

The measurements shown in Figure 118 do not show the multiple narrow-band resonances that appear in simulation results, but the actual injection and measurement technique is not fully clear from the published paper so it is possible this is an effect of transducer bandwidth limitations.

Figure 118: Measured high frequency responses of ERSE test network (Source: Tornelli & Capetta 2009)

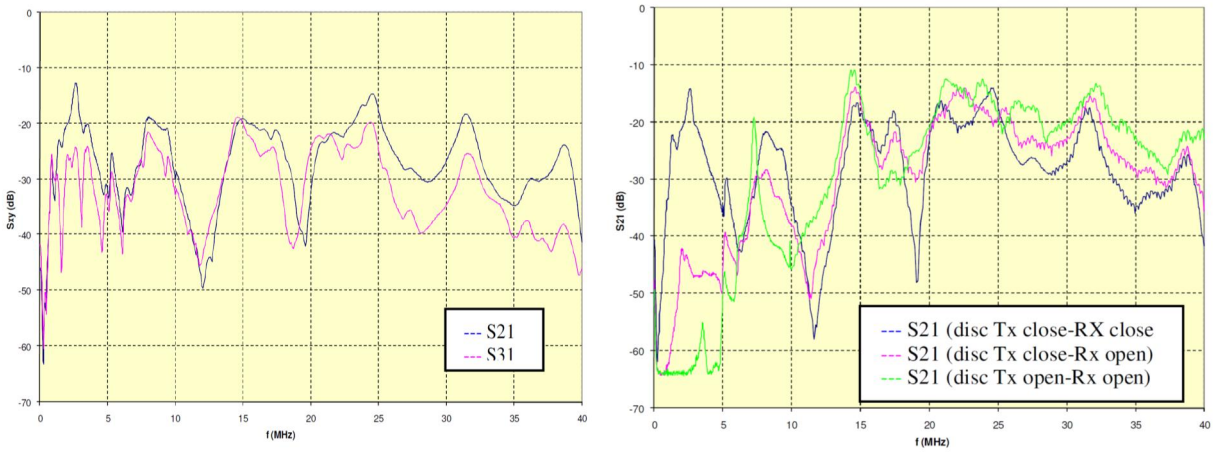

In summary, little or no data exists on the high-frequency response of real distribution networks like those in Victoria. The limited information available indicates this response is likely to be complex.

11.3.4 Safe network connection options

Two options were identified for reduction of risk to the 22kV network from the tests:

Current limiting resistors

In this option, the high voltage resistors procured for the 2014 REFCL Trial would be connected in series with the supply from the network to the test rig to limit current to safe levels should a flashover occur in the test rig. Up to 400 ohms could be inserted in each phase, giving a current limit of 28 amps for phase-to-phase tests and 32 amps for phase-to-earth tests.

The resistors are designed to deliver the nameplate value of resistance at 50Hz. Their high frequency response was not initially known but was considered likely to be complex. The resistor elements were coils of metal, either strip or wire, indicating multiple medium frequency resonances were possible before turn-to-turn capacitance would dominate their response at very high frequencies. The two high voltage resistors used in the REFCL Trial have quite different internal construction, so

their high frequency responses could be expected to differ (this was confirmed by test – see Table 12 on page 139).

Isolation transformers

In this option, two distribution transformers would be connected back-to-back between the network and the test rig.

Published research indicates that power transformers act as attenuators at medium to high frequencies. Published test results indicate that frequency components in the audio range can be reduced by a factor of 100 or more due to iron losses. At very high frequencies, the windings act like capacitors as the turn-to-turn stray capacitance dominates all other effects. Winding-to-winding capacitance provides a possible HV to LV transmission path with a similar attenuation factor of 50-100 times.

11.3.5 Comparison of options

The advantages and disadvantages of the two options when considered in the light of project objectives are set out in Table 11.

Table 11: comparison of network connection options

Option	Advantages	Disadvantages
Resistors	Fault is exposed (at least partially) to a real network so the recorded signature is likely to be as realistic as test constraints allow. At high frequency the resistor may look like a transmission line, i.e. like part of the network, so it may distort the signature less than other options.	Provides weaker isolation of tests from network – could be seen as having slightly higher risk to network. Less amenable to control of source impedance seen by the fault (if this were desired). Requires tests to be located next to a real high voltage network, i.e. not indoors.
Transformers	Reduced risk to network. May improve ability to control source impedance seen by the fault (if this were desired). Could allow tests to be located indoors.	Offers virtually no reflection of real network response back to the fault – recorded signature could be seen as unrealistic.

If the realism principle used in design of ignition test programs is regarded as the higher priority, then current limiting resistors appeared to be the superior option on balance. However, neither option offered completely compelling reasons for its adoption. If current limiting resistors were used, it was seen as prudent to measure their high frequency responses and publish them with the recorded signatures.

11.3.6 Controlled source impedance option

An alternative basis of experiment design would be to abandon the realism principle and strive instead to closely control the source impedance seen by the fault, i.e. focus on the fault as a

separate isolated process to be explored rather than the network-fault combination. For example, increasing the capacitance in the source supply path would reduce source impedance at high frequencies, thereby increasing the high frequency content of fault current and reducing the high frequency content of voltage disturbances produced by the fault.

There are two ways of increasing source capacitance:

1. Revert to underground cable supply to the test rig[30].
2. Fit high voltage capacitors on one of the poles carrying the overhead supply to the test rig.

Fault signatures recorded in such an arrangement could not be said to be representative of those that would normally occur in most real networks, recognising that fault signatures will always be open to criticism that they are unique to the network on which they have been recorded.

This option would have required a change to the objectives of the project. The goal of a reference data base of realistic fault signatures would be replaced by a goal of development of a model of a vegetation fault that could be used with any network simulation to generate signatures for the simulated network. However, research publications show that simulation of real networks continues to be severely constrained by data limitations and computational power constraints.

Whilst this alternative approach to experiment design was seen as potentially valid, it did not seem to offer sufficient additional benefits to warrant the change in project objectives that would be required for its adoption. Given the non-adoption of this option, the balance between the two network connection options outlined in Table 11 moved slightly more in favour of current limiting resistors rather than isolation transformers.

11.3.7 Conclusion: decisions on experiment design

Based on the above considerations, the test program used two 200Ω high voltage series resistors to connect the test rig to the 22kV network.

The two high voltage resistors were tested using a frequency response analyser. The results are shown in Table 12. The phase-to-earth tests were performed using resistor serial number 41754-02 as this was found to have the more ideal high-frequency characteristics. The phase-to-phase tests had both resistors in circuit, so there was a greater deviation from pure resistance and some internal resonances in the 600 kHz to 1MHz range.

[30] This arrangement was used in the 2014 REFCL Trial to bring the HV supply to the site under multiple HV lines. Whilst consideration of this option may prompt potential questions about the realism of the high frequency fault current components recorded in the 2014 REFCL Trial, they had no effect on REFCL ignition outcomes, i.e. on the validity of the REFCL Trial findings.

Table 12: frequency response of series 200Ω HV resistors

Resistor Serial No	R @ 1kHz	X @ 1kHz	High frequency response
41754-01	200 Ω	3.34mH	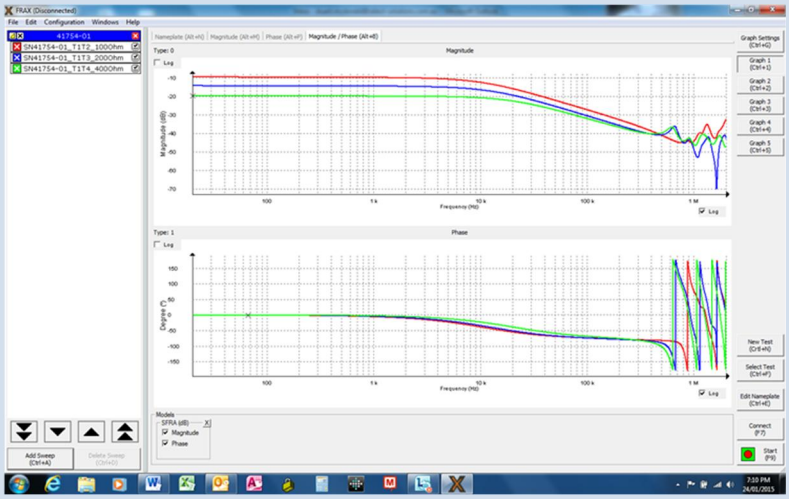
41754-02	200 Ω	0.45mH	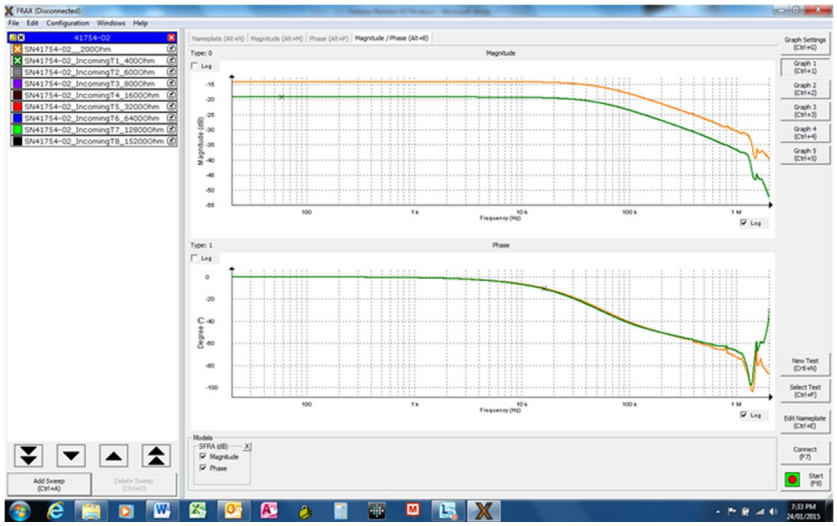

11.4 Appendix D: Test records

Full details of all tests are contained in the test program records data base which will be made available in the public domain. The records in the data base include:

1. Analysis spreadsheet, including the master copy of the run sheet summarising the key data for all tests and the master copy of the laboratory analysis records for all vegetation samples.
2. Scanned test log sheets which show for each test in addition to the data keyed into the analysis spreadsheet, the date, time, weather conditions and some visual observations.
3. The visible light and infrared videos of the test
4. The recorded electrical quantities (voltage and current, in low-frequency and high-frequency channels) in raw form. These can be accessed using the free HBM Perception viewer, which can also export data in various forms for further processing in Excel or MatLab.
5. The MatLab processed charts (32 per test) of the recorded electrical quantities which provide a quick reference view of the test.
6. The IND Technology records for the test: partial discharge detector outputs sampled at 500MHz.
7. The data recorded at Substation SV using metering CTs and VTs.

The following tables provide summary data for records of all tests and background noise checks in the test program.

11.4.1 Valid ignition tests

The following tests were confirmed by audit to be valid for calculation of fire probability. Tests on off-list species (highlighted rows) are shown for completeness but the results of such tests were not used in the derivation of findings presented in this report.

Date (2015)	Test	Type	I_{init} (amps)	Duration (ms)	I_{limit} (amps)	Flashover	Species	Conditioning time (hours)	Moisture (%wt.)	Conductivity (µS/cm)	Diameter (mm)	Fire result (1=fire)
12 Feb	75	ph-e	0.22	4000	0.5	N	Eu. Viminalis	16	39.7	249		0
	76	ph-e	0.24	2000	0.5	N	A. Pycnantha	16	28.7	142	45	0
	77	ph-e	0.13	6000	0.5	N	A. Pycnantha	16	27.9	212	30	0
	78	ph-e	0.19	5000	0.5	N	Eu. Baxteri	16	44.0	193	40	0
	79	ph-e	0.1	72000	0.5	N	Eu. Baxteri	16	35.5	210	30	1
	80	Bush	0.12	14000	0.5	N	K. Ericoides	16	33.7	153	35	0
	81	ph-e	0.04	31000	0.5	N	Eu. Viminalis	16	30.5	342	20	0
	82	ph-e	0.07	22000	0.5	N	Eu. Baxteri	16	38.6	140	35	0
	83	Bush	0.07	22000	0.5	N	K. Ericoides	16	33.6	178	20	1
	84	Bush	0.05	36000	0.5	N	K. Ericoides	16	30.4	276		1
	86	ph-e	0.13	60000	1	N	Eu. Viminalis	16	32.5	230	30	1
	87	ph-e	0.04	31000	1	N	A. Melanoxylon	178	32.1	373	30	1
	88	ph-e	0.07	58000	1	N	Eu. Baxteri	178	36.5	203	30	1
	89	Bush	0.14	18000	1	N	K. Ericoides	178	36.2	181	30	1
	90	ph-e	0.09	72000	1	Y	Eu. Baxteri	178	35.8	163	25	1
	91	ph-e	0.19	7000	1	N	A. Pycnantha	178				0
	92	ph-e	0.06	58000	1	N	Eu. Baxteri	178	34.7	189	30	1
	93	Bush	0.16	16000	1	N	K. Ericoides	178	33.7	160	35	0
	94	ph-e	0.08	23000	1	N	Eu. Baxteri	178				0
	95	ph-e	0.08	45000	1	N	Eu. Viminalis	178	38.4	195	30	0
	96	ph-e	0.04	84000	2	N	Eu. Baxteri	178	31.8	173	35	1
	97	ph-e	0.04	49000	2	Y	A. Pycnantha	178	29.8	275	30	1
	98	Bush	0.11	60000	2	Y	K. Ericoides	178	35.0	170	25	1
	99	ph-e	0.1	69000	2	Y	Eu. Baxteri	178				1
	100	ph-e	0.08	67000	2	Y	Eu. Baxteri	178	40.4	210	35	1
	101	Bush	0.16	37000	2	N	K. Ericoides	178	41.8	234	40	1
	102	ph-e	0.08	67000	2	Y	Eu. Viminalis	178	33.1	215	25	1
	103	ph-e	0.12	76000	2	N	Eu. Baxteri	178	41.7	185	45	1
13 Feb	106	ph-e	0.08	13000	0.5	N	C. Glaucophyllus	24	37.1	229		0
	107	ph-e	0.07	25000	0.5	N	C. Glaucophyllus	24	36.8	225		0
	108	ph-e	0.15	17000	1	N	C. Glaucophyllus	24	34.2	167		0

Date (2015)	Test	Type	I_{init} (amps)	Duration (ms)	I_{limit} (amps)	Flashover	Species	Conditioning time (hours)	Moisture (%wt.)	Conductivity (µS/cm)	Diameter (mm)	Fire result (1=fire)
	109	ph-e	0.08	18000	1	N	C. Glaucophyllus	24	39.6	232		0
	110	ph-e	0.17	26000	2	N	C. Glaucophyllus	24	36.6	159		0
	111	ph-e	0.17	20000	2	N	C. Glaucophyllus	24	35.5	139		0
	112	ph-e	0	170000	0.5	N	Eu. Regnans	24	12.8	177	20	0
	113	ph-e	0	180000	0.5	N	Eu. Regnans	24	11.5	175	25	0
	114	ph-e	0	184000	1	N	Eu. Regnans	24	10.8	188	25	0
	115	ph-e	0.03	18000	0.5	N	P. Undulatum	24	34.6	297	25	0
	116	ph-e	0.06	14000	0.5	N	P. Undulatum	24	32.5	226	30	0
	117	ph-e	0.05	29000	1	N	P. Undulatum	24	34.8	303	25	0
	118	ph-e	0.09	16000	1	N	P. Undulatum	24	33.4	263	20	0
	119	ph-e	0.08	54000	2	N	P. Undulatum	24	34.1	243	25	0
	120	ph-e	0.07	37000	2	N	P. Undulatum	24	34.1	250	30	0
	121	ph-e	0.06	9000	0.5	N	A. Melanoxylon	24	30.7	200		0
	122	ph-e	0.04	28000	0.5	N	A. Melanoxylon	24	36.0	287		0
	123	ph-e	0.09	11000	1	N	A. Melanoxylon	24	34.0	300		0
	124	ph-e	0.14	8000	1	N	A. Melanoxylon	24	36.9	315		0
	125	ph-e	0.05	67000	2	N	A. Melanoxylon	24	30.2	259		1
	126	ph-e	0.09	50000	2	N	A. Melanoxylon	24	35.2	261		1
13 Feb	127	ph-e	0.05	12000	0.5	N	A. Mearnsii	24	34.7	338		0
	128	ph-e	0.08	8000	0.5	N	A. Mearnsii	24	32.4	282		0
	129	ph-e	0.1	43000	1	N	A. Mearnsii	24	30.5	266		1
	130	ph-e	0.09	28000	1	N	A. Mearnsii	24	24.7	388		1
	131	ph-e	0.12	35000	2	N	A. Mearnsii	24	32.5	338		1
	132	ph-e	0.07	30000	2	N	A. Mearnsii	24	30.3	338		1
	133	Bush	0	26000	4	N	U. Europaeus	0	36.0	462		1
	134	Bush	0.04	13000	0.5	N	U. Europaeus	0	25.9	417		0
	135	Bush		12000	4	N	R. Fruticosus	0	49.3	443		1
	136	Bush		1000	0.5	N	R. Fruticosus	0				0
	137	Bush		200	0.5	N	R. Fruticosus	0				0
	138	Bush		7000	4	N	R. Fruticosus	0				1
	139	ph-e	0.12	6422	0.5	N	C. Glaucophyllus	0.25	42.3	212		0
	140	ph-e	0.08	14553	1	N	C. Glaucophyllus	0.25	42.8	328		0
	141	ph-e	0.09	65758	2	N	C. Glaucophyllus	0.25	42.7	353		1
	142	ph-e	0.17	34305	2	N	A. Mearnsii	0.5	37.3	269		1
	143	ph-e	0.33	44180	2	N	A. Mearnsii	0.5	35.3	218		0
	144	ph-e	0.07	9011	0.5	N	A. Mearnsii	0.5	38.8	332		0
	145	ph-e	0.11	3030	0.5	N	A. Mearnsii	0.5	41.0	434		0
	146	ph-e	0.07	40322	1	N	A. Mearnsii	0.5	35.5	276		1
	147	ph-e	0.19	4996	1	N	A. Mearnsii	0.5	38.2	323		0
	148	ph-e	0.093	8337	0.5	N	Salix sp.	0.25	42.2			0
16 Feb	149	ph-e	0.091	78353	0.5	Y	Salix sp.	0.25	40.5	203		1
	150	ph-e	0.094	49571	1	N	Salix sp.	0.25	45.2	393		1
	151	ph-e	0.149	71697	1	Y	Salix sp.	0.25	43.7	280		1
	152	ph-e	0.081	71021	2	Y	Salix sp.	0.25	40.0	234		1
	153	ph-e	0.139	85051	2	N	Salix sp.	0.25	41.1	216		1
	154	ph-e	0.237	38175	2	N	P. Undulatum	1	37.4	247	30	1
	155	ph-e	0.113	42925	2	N	P. Undulatum	1	39.0	224	30	1
	156	ph-e	0.348	714	0.5	N	P. Undulatum	1	38.5	212	35	0
	157	ph-e	0.102	7935	0.5	N	P. Undulatum	1	38.2	269	30	0
	158	ph-e	0.3	4078	1	N	P. Undulatum	1	39.0	304	30	0
	159	ph-e	0.115	12657	1	N	P. Undulatum	1	37.3	261	30	0
	161	ph-e	0.16	3595	0.5	N	A. Melanoxylon	24	33.0	279		0
	162	ph-e	0.1	14427	0.5	N	A. Melanoxylon	24	31.9	227		0
	163	ph-e	0.11	13101	1	N	A. Melanoxylon	24	30.4	200		0
	164	ph-e	0.303	3689	1	N	A. Melanoxylon	24	33.9	278		0
	165	ph-e	0.048	45484	2	N	A. Melanoxylon	24	28.0	236		0
	166	ph-e	0.223	1629	0.5	N	A. Melanoxylon	1	35.1	227		0
	167	ph-e	0.27	6122	1	N	A. Melanoxylon	1	37.0	232		0
	168	ph-e	0.309	9500	2	N	A. Melanoxylon	1	36.6	230		0
	169	ph-e	0.204	13211	2	N	A. Melanoxylon	1	34.2	213		0
	170	ph-e	0.146	2931	0.5	N	A. Mearnsii	0.25	37.7	325		0
	171	ph-e	0.151	4013	0.5	N	A. Mearnsii	0	35.4	257		0
17 Feb	172	ph-e	0.146	3020	0.5	N	A. Mearnsii	0	38.4	363		0
	173	ph-e	0.16	4977	0.5	N	A. Mearnsii	0	35.5	235		0
	174	ph-e	0.245	5686	1	N	A. Mearnsii	0	35.3	239		0
	175	ph-e	0.259	4898	1	N	A. Mearnsii	0	34.8	247		0
	176	ph-e	0.244	5257	1	N	A. Mearnsii	0	37.1	272		0
	177	ph-e	0.096	29439	1	N	A. Mearnsii	0	35.0	253		1
	178	ph-e	0.204	20576	2	N	A. Mearnsii	0	37.7	357		1
	179	ph-e	0.156	27135	2	N	A. Mearnsii	0	36.6	394		1
	180	ph-e	0.174	12730	2	N	A. Mearnsii	0	38.6	337		1
	181	ph-e	0.125	19721	2	N	A. Mearnsii	0	37.4	414		1
	182	Bush	0	8288	0.5	N	U. Europaeus	0.25	41.5	243		0
	183	Bush	0	16857	0.5	N	U. Europaeus	0.25	37.7	264		1
	184	Bush	0	11107	0.5	N	U. Europaeus	0.25	38.6	194		0

Date (2015)	Test	Type	I_{init} (amps)	Duration (ms)	I_{limit} (amps)	Flashover	Species	Conditioning time (hours)	Moisture (%wt.)	Conductivity (µS/cm)	Diameter (mm)	Fire result (1=fire)
	185	Bush	0	6715	1	N	U. Europaeus	0.25	35.7	189		0
	186	Bush	0	34433	1	N	U. Europaeus	0.25	40.7	277		1
	187	Bush	0.018	11700	1	N	U. Europaeus	2	38.3	236		0
	188	Bush	0	23016	1	N	U. Europaeus	2	34.3	213		1
	189	Bush	0	19866	2	N	U. Europaeus	2	37.2	263		1
	190	Bush	0	27316	2	N	U. Europaeus	2	38.3	246		0
	191	Bush	0.03	22802	2	N	U. Europaeus	2	36.1	221		1
	192	Bush	0.049	4331	0.5	N	R. Fruticosus	0.25	48.0	538		0
17 Feb	193	Bush	0.072	2690	1	N	R. Fruticosus	0.25	48.0	538		0
	194	Bush	0	5302	1	N	R. Fruticosus	0.25	39.7	377		0
	195	ph-e	0.181	5685	0.5	N	Eu. Baxteri	0.25	45.4	258		0
	196	ph-e	0.088	16332	0.5	N	Eu. Baxteri	0.25	49.8	297		0
	197	ph-e	0.046	29004	0.5	N	Eu. Baxteri	0.25	43.5	244		0
	198	ph-e	0.28	1592	0.5	N	Eu. Baxteri	0.25	47.4	240		0
	199	ph-e	0.113	70892	1	N	Eu. Baxteri	0.25	47.1	246		1
	200	ph-e	0.101	42665	1	N	Eu. Baxteri	0.25	45.1	229		0
	201	ph-e	0.095	48175	1	N	Eu. Baxteri	0.25	43.3	225		0
	202	ph-e	0.151	12305	1	N	Eu. Baxteri	0.25	52.0	263		0
	203	ph-e	0.303	11208	2	N	Eu. Baxteri	1	50.2	292		0
	204	ph-e	0.034	69575	2	Y	Eu. Baxteri	1	43.5	266		1
	205	ph-e	0.117	57353	2	Y	Eu. Baxteri	1	47.1	285		1
	206	ph-e	0	178927	2	N	Eu. Baxteri	1	50.5	257		0
	207	ph-e	0.128	89735	2	Y	Eu. Baxteri	0.25	50.6	265		1
	208	ph-e	0.179	52595	2	N	P. Undulatum	0.25	36.5	234	25	1
	209	ph-e	0.116	5928	0.5	N	P. Undulatum	0.25	36.3	279	25	0
	210	ph-e	0.065	8067	0.5	N	P. Undulatum	0.25	36.0	292	25	0
	211	ph-e	0.182	3129	0.5	N	P. Undulatum	0.25	39.4	275	30	0
	212	ph-e	0.081	12230	1	N	P. Undulatum	0.25	35.8	238	30	0
	213	ph-e	0.121	10658	1	N	P. Undulatum	0.25	36.4	274	25	0
	214	ph-e	0.141	11880	1	N	P. Undulatum	0.25	36.5	257	35	0
	215	ph-e	0.157	55531	2	N	P. Undulatum	0.25	35.2	261	30	1
	216	ph-e	0.034	24633	2	N	P. Undulatum	0.25	35.8	281	25	0
	217	ph-e	0.112	15559	0.5	N	F. Angustifolia	0.25	37.5	286		0
	218	ph-e	0.067	27185	0.5	N	F. Angustifolia	0.25	35.3	295		0
	219	ph-e	0.061	20471	0.5	N	F. Angustifolia	0.25	36.0	263		0
	220	ph-e	0.059	51519	0.5	N	F. Angustifolia	0.25	31.9	182		0
18 Feb	221	ph-e	0.079	54516	1	N	F. Angustifolia	0.25	33.0	193		0
	222	ph-e	0.058	93685	1	N	F. Angustifolia	0.25	36.2	251		1
	223	ph-e	0.058	97063	1	Y	F. Angustifolia	0.25	36.2	621		1
	224	ph-e	0.093	63156	1	N	F. Angustifolia	0.25	35.0	313		1
	225	ph-e	0.079	115306	2	Y	F. Angustifolia	0.25	35.1	256		0
	226	ph-e	0.063	117615	2	Y	F. Angustifolia	0.25	33.6	321		1
	227	ph-e	0.038	71071	2	N	F. Angustifolia	0.25	36.3	347		1
	228	ph-e	0.071	115119	2	N	F. Angustifolia	0.25	34.1	265		1
	229	ph-e	0.169	9296	0.5	N	Pinus Radiata	0.25	56.0	150		0
	230	ph-e	0.449	147211	2	N	Pinus Radiata	0.25	56.0	150		1
	231	ph-e	0.171	7947	0.5	N	Pinus Radiata	0.25	52.5	154		0
	232	ph-e	0.115	10106	0.5	N	Pinus Radiata	0.25	51.9	143		0
	233	ph-e	0.103	20158	1	N	Pinus Radiata	0.25	44.7	130		0
	234	ph-e	0.350	61951	1	N	Pinus Radiata	0.25	44.7	130		1
	235	ph-e	0.180	12739	1	N	Pinus Radiata	0.25	53.3	140		0
	236	ph-e	0.161	79735	2	N	Pinus Radiata	0.25	47.9	149		1
	237	ph-e	0.090	296891	2	Y	Pinus Radiata	0.25	44.4	117		1
	238	ph-e	0.081	188477	2	Y	Pinus Radiata	0.25	41.8	124		0
	239	ph-e	0.313	517	0.5	N	P. Undulatum	0.25	39.9	348		0
	240	ph-e	0.295	447	0.5	N	P. Undulatum	0.25	39.6	327		0
	241	ph-e	0.270	971	0.5	N	P. Undulatum	0.25	39.6	256		0
	242	ph-e	0.480	1792	1	N	P. Undulatum	0.25	39.3	349		0
	243	ph-e	0.445	2544	1	N	P. Undulatum	0.25	42.2	354		0
	244	ph-e	0.432	2076	1	N	P. Undulatum	0.25	39.4	360		0
	245	ph-e	0.262	12296	2	N	P. Undulatum	0.25	38.1	280		0
	246	ph-e	0.359	6042	2	N	P. Undulatum	0.25	39.4	306		0
	247	ph-e	0.156	47051	2	N	P. Undulatum	0.25	38.6	306		1
	248	ph-e	0.449	184	0.5	N	P. Undulatum	24	41.1	354		0
	249	ph-e	0.260	867	0.5	N	P. Undulatum	24	37.0	337		0
	250	ph-e	0.389	184	0.5	N	P. Undulatum	24	38.5	338		0
	251	ph-e	0.2	2503	0.5	N	P. Undulatum	24	35.9	239		0
	252	ph-e	0.339	18563	1	N	P. Undulatum	24	39.4	312		1
19 Feb	253	ph-e	0.227	6408	1	N	P. Undulatum	24	37.4	263		0
	254	ph-e	0.204	6276	1	N	P. Undulatum	24	36.3	256		0
	255	ph-e	0.515	698	1	N	P. Undulatum	24	38.8	317		0
	256	ph-e	0.509	3016	2	N	P. Undulatum	24	41.4	414		0
	257	ph-e	0.259	10896	2	N	P. Undulatum	24	37.1	337		0
	258	ph-e	0.346	3289	2	N	P. Undulatum	24	40.8	496		0
	259	ph-e	0.281	8657	2	N	P. Undulatum	24	37.4	257		0

Date (2015)	Test	Type	I_{init} (amps)	Duration (ms)	I_{limit} (amps)	Flashover	Species	Conditioning time (hours)	Moisture (%wt.)	Conductivity (µS/cm)	Diameter (mm)	Fire result (1=fire)
	260	ph-e	0.06	109311	2	Y	Pinus Radiata	24	33.0	123		1
	261	ph-e	0.041	226516	0.5	N	Pinus Radiata	24	39.3	108		0
	262	ph-e	0.065	18822	0.5	N	Pinus Radiata	24	34.0	149		0
	263	ph-e	0.092	20872	0.5	N	Pinus Radiata	24	45.7	151		0
	264	ph-e	0.091	32688	0.5	N	Pinus Radiata	24	38.7	134		0
	265	ph-e	0	443011	1	N	Pinus Radiata	24	47.1	127		1
	266	ph-e	0.173	38742	1	N	Pinus Radiata	24	53.9	151		0
	267	ph-e	0.08	49802	1	N	Pinus Radiata	24	41.4	140		0
	268	ph-e	0.053	185273	1	Y	Pinus Radiata	24	45.9	97		1
	269	ph-e	0.172	144704	2	N	Pinus Radiata	24	43.2	107		1
	270	ph-e	0.208	65706	2	N	Pinus Radiata	24	50.7	155		0
	271	ph-e	0.026	74547	0.5	N	Eu. Baxteri	24	32.8	232		1
	272	ph-e	0.075	16420	0.5	N	Eu. Baxteri	24	40.3	256		0
	273	ph-e	0.041	63413	1	N	Eu. Baxteri	24	41.7	267		1
	274	ph-e	0.065	70078	1	N	Eu. Baxteri	24	39.7	251		1
	275	ph-e	0.055	114373	2	N	Eu. Baxteri	24	33.1	203		1
	276	ph-e	0.058	51278	2	N	Eu. Baxteri	24	37.6	239		1
19 Feb	277	ph-e	0.048	27581	0.5	N	F. Angustifolia	24	31.6	258		0
	278	ph-e	0.088	16801	0.5	N	F. Angustifolia	24	41.1	271		0
	279	ph-e	0.032	61267	0.5	N	F. Angustifolia	24	30.7	238		0
	280	ph-e	0.034	46510	0.5	N	F. Angustifolia	24	31.1	257		0
	281	ph-e	0.018	84879	1	N	F. Angustifolia	24	31.4	339		0
	282	ph-e	0.042	91780	1	N	F. Angustifolia	24	31.0	274		1
	283	ph-e	0.056	51734	1	N	F. Angustifolia	24	32.3	258		0
	284	ph-e	0.018	203488	1	N	F. Angustifolia	24	28.6	215		0
	285	ph-e	0.032	100721	2	Y	F. Angustifolia	24	32.6	279		1
	286	ph-e	0.027	91567	2	N	F. Angustifolia	24	32.1	296		1
	287	ph-e	0.052	80439	2	N	F. Angustifolia	24	30.5	240		1
	288	ph-e	0.09	8237	0.5	N	Salix Sp.	16	40.8	390		0
	289	ph-e	0.067	10354	0.5	N	Salix Sp.	16	38.1	257		0
	290	ph-e	0.092	60103	2	N	Salix Sp.	16	37.4	271		1
	291	ph-e	0.091	36150	1	N	Salix Sp.	16	45.7	413		1
	292	ph-e	0.038	10856	0.5	N	Salix Sp.	16	41.5	315		1
	293	ph-e	0.083	50718	2	Y	Salix Sp.	16	38.3	394		1
	294	ph-e	0.05	70629	1	Y	Salix Sp.	16	39.8	223		1
	295	ph-e	0.17	4025	0.5	N	Salix Sp.	16	41.6	328		0
	296	ph-e	0.038	71262	2	Y	Salix Sp.	16	26.2	192		1
	297	ph-e	0.116	49853	1	N	Salix Sp.	16	41.1	278		1
	298	ph-e	0.126	8228	0.5	N	Salix Sp.	16	39.4	278		0
	299	ph-e	0.092	44740	2	Y	Salix Sp.	16	35.8	319		1
	300	ph-e	0.077	65108	1	N	Salix Sp.	16	40.5	294		1
	301	ph-e	0.05	38957	0.5	N	Salix Sp.	16	32.9	278		1
	302	ph-e	0.114	75001	2	Y	Salix Sp.	16	42.0	255		1
	303	ph-e	0.17	45724	1	Y	Salix Sp.	16	45.0	406		1
	304	ph-e	0.077	55424	2	Y	Salix Sp.	16	39.3	294		1
	305	ph-e	0.099	109167	1	N	Salix Sp.	16	40.8	271		1
	306	ph-e	0.188	44057	2	Y	Salix Sp.	16	43.1	342		1
	307	ph-e	0.131	65760	1	N	Salix Sp.	16	42.3	256		1
	308	ph-e	0.123	6857	0.5	N	Salix Sp.	16	43.4	247		0
	309	ph-e	0.087	63438	2	Y	Salix Sp.	16	37.1	242		1
	310	ph-e	0.125	57321	1	N	Salix Sp.	16	38.0	257		1
20 Feb	311	ph-e	0.08	70723	0.5	N	Salix Sp.	16	40.5	226		1
	312	ph-e	0.079	47049	2	Y	Salix Sp.	16	41.0	298		1
	313	ph-e	0.297	2080	1	N	P. Undulatum	16	39.6	426		0
	314	ph-e	0.323	526	0.5	N	P. Undulatum	16	38.7	251		0
	315	ph-e	0.225	1424	0.5	N	A. Mearnsii	16	34.3	350		0
	316	ph-e	0.073	30291	1	N	A. Mearnsii	16	33.4	308		1
	317	ph-e	0.06	30263	2	N	A. Mearnsii	16	31.0	402		1
	318	Bush	0.063	303214	0.5	N	K. Ericoides	16	30.8	164	30	0
	319	Bush	0.08	16882	0.5	N	K. Ericoides	16	32.7	127	35	1
	320	Bush	0.081	20067	1	N	K. Ericoides	16	36.3	169	30	1
	321	Bush	0.116	27000	1	N	K. Ericoides	16	33.0	128	30	0
	322	Bush	0.088	50546	2	N	K. Ericoides	16	32.3	140	20	1
	323	ph-e	0.235	2593	0.5	N	Eu. Baxteri	16	36.3	169	30	0
	324	ph-e	0.058	59199	1	N	Eu. Baxteri	16	37.5	203	35	1
	325	ph-e	0.056	83862	2	Y	Eu. Baxteri	16	40.5	188	35	1
	326	ph-e	0.121	16300	0.5	N	Eu. Baxteri	16	30.1	179	30	0
	327	ph-e	0.153	44388	1	N	Eu. Baxteri	16	35.7	195	0	1
	328	ph-e	0.002	283534	2	N	Eu. Baxteri	16	14.1	147	20	0
	329	Bush	0.036	4746	0.5	N	B. Marginata	0.25	57.5	924	0	0
	331	Bush	0.072	8685	0.5	N	B. Marginata	0.25	57.5	924	0	0
	332	Bush	0.075	25629	2	N	B. Marginata	0.5	61.3	715	30	0
	333	Bush	1.486	143	0.5	N	B. Marginata	0.5	61.3	715	30	0
	334	Bush	1.675	564	2	N	B. Marginata	0.75	61.3	715	30	0
	335	Bush	1.858	2823	4	N	B. Marginata	0.75	61.3	715	30	0.5

Date (2015)	Test	Type	I_{init} (amps)	Duration (ms)	I_{limit} (amps)	Flashover	Species	Conditioning time (hours)	Moisture (%wt.)	Conductivity (µS/cm)	Diameter (mm)	Fire result (1=fire)
23 Feb	336	ph-e	0.138	11535	0.5	N	A. Verticillata	0.5	44.9	240	30	0
	337	ph-e	0.195	5294	0.5	N	A. Verticillata	0.5	45.6	382	30	0
	338	ph-e	0.242	12989	2	N	A. Verticillata	0.5	41.5	224	40	0
	339	ph-e	0.258	8573	2	N	A. Verticillata	0.5	46.2	383	35	0
	340	ph-e	0.183	11057	1	N	A. Verticillata	0.5	39.1	267	35	0
	341	ph-e	0.238	7460	1	N	A. Verticillata	0.5	41.8	266	40	0
	342	ph-e	0.01	76280	2	N	Palm	0	16.0	1999	35	0
24 Feb	343	ph-e	0.076	23652	1	N	S. Molle	16	55.5	817	25	0
	344	ph-e	0.239	7326	1	N	S. Molle	16	51.3	692	50	0
	345	ph-e	0.246	3750	1	N	S. Molle	16	52.2	845	35	0
	346	ph-e	0.286	2847	1	N	S. Molle	16	50.3	744	20	0
	347	ph-e	0.075	11655	1	N	S. Molle	16	53.8	800	25	0
	348	ph-e	0.078	8822	1	N	S. Molle	16	48.4	746	15	0
	349	ph-e	0.263	5249	1	N	S. Molle	16	51.0	837	45	0
	350	ph-e	0.173	3917	0.5	N	A. Verticillata	16	35.6	283	50	0
	351	ph-e	0.146	21984	1	N	A. Verticillata	16	32.2	126	45	0
	352	ph-e	0.15	18134	1	N	A. Verticillata	16	37.9	271	25	0
	353	ph-e	0.119	21388	1	N	A. Verticillata	16	40.9	270	40	0
	354	ph-e	0.1	15342	1	N	A. Verticillata	16	36.6	186	40	0
	355	ph-e	0.111	13363	1	N	A. Verticillata	16	36.9	159	0	0
	356	ph-e	0.091	13376	1	N	A. Verticillata	16	33.0	193	0	0
	357	ph-e	0.151	9298	1	N	A. Verticillata	16	40.7	285	0	0
	358	ph-e	0.072	15535	1	N	A. Verticillata	16	44.1		0	0
	359	ph-e	0.183	12315	1	N	A. Verticillata	16	36.8	230	0	0
	360	ph-e	0.093	16537	1	N	A. Verticillata	16	37.1	208	0	0
	361	ph-e	0.126	13705	1	N	A. Verticillata	16	43.0	336	0	0
	362	ph-e	0.073	29959	1	N	A. Verticillata	16	31.9	142	0	0
	363	ph-e	0.128	18408	1	N	A. Verticillata	16	37.6	289	0	0
	364	ph-e	0.131	17487	1	N	A. Verticillata	16	37.6	289	0	0
	365	ph-e	0.047	46697	1	N	A. Verticillata	16	33.1	278	0	0
	366	ph-e	0.062	40570	1	N	A. Verticillata	16	32.0	188	0	1
	367	ph-e	0.112	13532	1	N	A. Verticillata	16	42.1	294	0	0
	368	ph-e	0.061	30965	1	N	A. Verticillata	16	38.7	266	0	0
	369	ph-e	0.341	6467	1	N	Paperbark	16	36.6	314	35	0
	370	ph-e	0.195	9316	1	N	Paperbark	16	37.6	434	25	0
	371	ph-e	0.268	7728	1	N	Paperbark	16	42.0	401	45	0
	372	ph-e	0.096	14635	1	N	Paperbark	16	37.8	362	35	0
	373	ph-e	0.232	10750	1	N	Paperbark	16	34.4	309	40	1
	374	ph-e	0.201	10952	1	N	Paperbark	16	38.0	335	35	0
	375	ph-e	0.061	103081	1	N	Maple tree	16	34.5	170	40	1
	376	ph-e	0.05	122379	1	Y	Maple tree	16	37.2	181	35	1
	377	ph-e	0.048	112816	1	Y	Maple tree	16	27.5	158	0	1
	378	ph-e	0.053	107412	1	N	Maple tree	16	35.0	192	0	1
	379	ph-e	0.051	80157	1	N	Maple tree	16	32.3	163	0	1
	380	ph-e	0.087	109510	1	Y	Maple tree	16	33.7	173	50	1
25 Feb	381	ph-e	0.41	326	0.5	N	Eu. Baxteri	16	52.4	406	25	0
	382	ph-e	0.193	4638	1	N	Eu. Baxteri	16	51.8	504	25	0
	383	ph-e	0.497	4690	2	N	Eu. Baxteri	16	55.4	327	30	0
	384	ph-e	0.146	7019	0.5	N	Eu. Baxteri	16	52.9	209	25	0
	385	ph-e	0.198	31717	1	N	Eu. Baxteri	16	47.1	351	20	1
	386	ph-e	0.44	53574	2	N	Eu. Baxteri	16	42.0	232	25	1
	387	ph-e	0.091	46027	0.5	N	Eu. Baxteri	16	44.0	271	25	0
	388	ph-e	0.183	6006	1	N	Eu. Baxteri	16	51.1	234	35	0
	389	ph-e	0.273	81916	2	N	Eu. Baxteri	16	49.0	236	0	1
	390	ph-e	0.416	257	0.5	N	Eu. Baxteri	16	54.1	318	0	0
	391	ph-e	0.176	9003	1	N	Eu. Baxteri	16	51.7	220	25	0
	392	ph-e	0.118	85332	2	Y	Eu. Baxteri	16	51.6	204	20	1
	393	ph-e	0.553	155	0.5	N	Eu. Baxteri	16	53.2	180	35	0
	394	ph-e	0.095	72106	1	N	Eu. Baxteri	16	51.0	193	15	0
	395	ph-e	0.222	98691	2	N	Eu. Baxteri	16	50.6	213	25	1
	396	ph-e	0.194	5104	0.5	N	Eu. Baxteri	16	52.3	195	25	0
	397	ph-e	0.341	5072	1	N	Eu. Baxteri	16	53.6	229	25	0
	398	ph-e	0.237	74584	2	Y	Eu. Baxteri	16	53.8	113	0	1
	399	ph-e	0.072	9560	0.5	N	A. Pycnantha	16	33.8	258	45	0
	400	ph-e	0.064	35415	1	N	A. Pycnantha	16	30.9	282	30	0
	401	ph-e	0.05	26566	2	N	A. Pycnantha	16	30.7	224	25	0
	402	ph-e	0.097	4912	0.5	N	A. Pycnantha	16	34.3	272	25	0
	403	ph-e	0.321	3221	1	N	A. Pycnantha	16	34.3	284	35	0
	404	ph-e	0.076	55403	2	N	A. Pycnantha	16	33.3	251	30	1
	405	ph-e	0.116	5074	0.5	N	A. Pycnantha	16	32.3	226	30	0
	406	ph-e	0.209	3768	1	N	A. Pycnantha	16	37.3	429	25	0
	407	ph-e	0.104	31645	2	N	A. Pycnantha	16	32.0	236	35	0
	408	ph-e	0.062	13130	0.5	N	A. Pycnantha	16	31.9	243	30	0
	409	ph-e	0.159	6634	1	N	A. Pycnantha	16	34.6	350	45	0
	410	ph-e	0.065	60538	2	Y	A. Pycnantha	16	31.2	242	25	1

Date (2015)	Test	Type	I_{init} (amps)	Duration (ms)	I_{limit} (amps)	Flashover	Species	Conditioning time (hours)	Moisture (%wt.)	Conductivity (µS/cm)	Diameter (mm)	Fire result (1=fire)
	411	ph-e	0.139	8777	0.5	N	A. Pycnantha	16	29.6	240	30	0
	412	ph-e	0.106	10498	1	N	A. Pycnantha	16	35.4	264	35	0
	413	ph-e	0.234	30175	2	N	A. Pycnantha	16	32.2	269	25	1
	414	ph-e	0.066	9924	0.5	N	A. Pycnantha	16	30.7	233	35	0
	415	ph-e	0.16	7422	1	N	A. Pycnantha	16	30.3	264	35	0
	416	ph-e	0.112	27789	2	N	A. Pycnantha	16	30.0	252	25	1
	417	ph-e	0.065	11010	0.5	N	A. Pycnantha	16	30.5	238	25	0
25 Feb	418	ph-e	0.353	1986	1	N	A. Pycnantha	16	37.2	305	40	0
	419	ph-e	0.132	37433	2	N	A. Pycnantha	16	31.9	272	25	1
	420	ph-e	0.103	5609	0.5	N	A. Pycnantha	16	31.8	274	25	0
	421	ph-e	0.045	48605	1	N	A. Pycnantha	16	30.3	285	25	0
	422	ph-e	0.117	42128	2	N	A. Pycnantha	16	29.9	185	0	0
	423	ph-e	0.09	60874	1	N	A. Pycnantha	16	30.7	280	0	1
26 Feb	424	ph-e	0.261	3656	0.5	Y	Eu. Viminalis	24	38.8	278	25	0
	425	ph-e	0.037	61281	1	Y	Eu. Viminalis	24	33.9	247	20	1
	426	ph-e	0.133	51976	2	Y	Eu. Viminalis	24	32.9	184	25	1
	427	ph-e	0.443	254	0.5	N	Eu. Viminalis	24	51.3	265	45	0
	428	ph-e	0.267	7567	1	N	Eu. Viminalis	24	51.3	265	40	0
	429	ph-e	0.324	10331	2	N	Eu. Viminalis	24	49.9	322	40	0
	430	ph-e	0.119	14114	0.5	N	Eu. Viminalis	24	34.7	174	25	0
	431	ph-e	0.111	56073	1	Y	Eu. Viminalis	24	30.1	182	25	1
	432	ph-e	0.133	62320	2	Y	Eu. Viminalis	24	36.0	250	25	1
	433	ph-e	0.13	9352	0.5	N	Eu. Viminalis	24	34.6	222	20	0
	434	ph-e	0.108	31381	1	N	Eu. Viminalis	24	35.4	165	25	1
	435	ph-e	0.166	72821	2	Y	Eu. Viminalis	24	40.3	214	25	1
	436	ph-e	0.162	7569	0.5	N	Eu. Viminalis	24	47.9	232	25	0
	437	ph-e	0.471	3024	1	N	Eu. Viminalis	24	48.3	378	35	0
	438	ph-e	0.31	10037	2	N	Eu. Viminalis	24	51.8	312	30	0
	439	ph-e	0.105	13058	0.5	N	Eu. Viminalis	24	36.3	275	20	0
	440	ph-e	0.134	33719	1	N	Eu. Viminalis	24	34.0	275	20	0
	441	ph-e	0.104	73567	2	Y	Eu. Viminalis	24	34.6	226	25	1
	442	ph-e	0.186	3590	0.5	N	Eu. Viminalis	24	38.9	212	45	0
	443	ph-e	0.081	19373	1	N	Eu. Viminalis	16	34.4	378	25	0
	444	ph-e	0.7	3768	2	N	Eu. Viminalis	16	51.8	333	40	0
	445	ph-e	0.312	732	0.5	N	Eu. Viminalis	16	48.1	238	35	0
	446	ph-e	0.123	73172	1	N	Eu. Viminalis	16	45.4	265	25	1
	447	ph-e	0.1	75924	2	Y	Eu. Viminalis	16	39.4	234	25	1
	448	ph-e	0.081	11719	0.5	N	Eu. Viminalis	16	39.5	210	20	0
	449	ph-e	0.196	8760	1	N	Eu. Viminalis	16	40.4	329	50	0
	450	ph-e	0.149	62909	1	Y	Teatree	16	32.6	196	25	1
	451	ph-e	0.191	9820	1	N	Teatree	16	35.5	182	30	0
	452	ph-e	0.111	58149	1	N	Teatree	16	34.5	177	25	1
	453	ph-e	0.123	64771	1	Y	Teatree	16	31.8	142	35	1
	454	ph-e	0.241	10496	1	N	Teatree	16	33.4	180	35	0
	455	ph-e	0.104	55902	1	N	Teatree	16	33.6	145	45	0
	456	ph-e	0.196	2996	1	N	Palm	16	66.4	3670	40	0
	457	ph-e	0.297	934	1	N	Palm	16	63.1	3480	40	0
	458	ph-e	0.229	3014	1	N	Palm	16	64.2	3240	40	0
	459	ph-e	0.37	841	1	N	Palm	16	60.1	3360	40	0
	460	ph-e	0.255	2417	1	N	Palm	16	60.6	2440	35	0
	461	ph-e	0.242	2895	1	N	Palm	16	58.8	3950	35	0
27 Feb	462	ph-e	0.21	3091	0.5	N	A. Mearnsii	16	34.5	295	30	0
	463	ph-e	0.057	47644	1	N	A. Mearnsii	16	33.9	185	35	1
	464	ph-e	0.195	36705	2	N	A. Mearnsii	16	34.2	225	35	1
	465	ph-e	0.121	6373	0.5	N	A. Mearnsii	16	36.8	289	30	0
	466	ph-e	0.205	5411	1	N	A. Mearnsii	16	32.5	307	35	0
	467	ph-e	0.132	33704	2	N	A. Mearnsii	16	32.7	306	35	1
	468	ph-e	0.082	17143	0.5	N	A. Mearnsii	16	32.0	149	35	0
	469	ph-e	0.194	7024	1	N	A. Mearnsii	16	27.8	255	25	0
	470	ph-e	0.205	33743	2	N	A. Mearnsii	16	31.8	252	35	1
	471	ph-e	0.148	6053	0.5	N	A. Mearnsii	16	33.2	248	30	0
	472	ph-e	0.146	26234	1	N	A. Mearnsii	16	34.9	329	25	1
	473	ph-e	0.098	59379	2	Y	A. Mearnsii	16	31.2	167	35	1
	474	ph-e	0.174	6239	0.5	N	A. Mearnsii	16	36.4	241	35	0
	475	ph-e	0.036	103313	1	N	A. Mearnsii	16	30.5	157	25	1
	476	ph-e	0.186	44487	2	N	A. Mearnsii	16	32.0	197	35	1
	477	ph-ph	0.239	1175	0.5	N	A. Mearnsii	16	34.3	207	30	0
	478	ph-ph	0.265	3051	1	N	A. Mearnsii	16	30.5	161	25	0
	479	ph-ph	0.189	24257	2	N	A. Mearnsii	16	28.1	134	30	1
	480	ph-ph	0.125	1588	0.5	N	A. Mearnsii	16	32.6	215	15	0
	481	ph-ph	0.431	1167	1	N	A. Mearnsii	16	34.0	242	35	0
	482	ph-ph	0.146	14165	2	N	A. Mearnsii	16	32.8	196	40	1
	483	ph-ph	0.326	637	0.5	N	P. Undulatum	16	32.9	234	15	0
	484	ph-ph	0.554	795	1	N	P. Undulatum	16	36.6	299	30	0
	485	ph-ph	0.55	2176	2	N	P. Undulatum	16	37.8	300	40	0

Date (2015)	Test	Type	I_{init} (amps)	Duration (ms)	I_{limit} (amps)	Flashover	Species	Conditioning time (hours)	Moisture (%wt.)	Conductivity (µS/cm)	Diameter (mm)	Fire result (1=fire)
	486	ph-ph	0.81	152	0.5	N	P. Undulatum	16	36.6	268	35	0
	487	ph-ph	0.199	4133	1	N	P. Undulatum	16	33.9	258	20	0
	488	ph-ph	0.413	3165	2	N	P. Undulatum	16	33.4	225	30	0
	489	ph-ph	0.219	984	0.5	N	P. Undulatum	16	34.1	250	25	0
	490	ph-ph	0.272	2113	1	N	P. Undulatum	16	34.6	253	20	0
	491	ph-ph	0.463	2602	2	N	P. Undulatum	16	38.6	354	25	0
	492	ph-ph	0.293	520	0.5	N	P. Undulatum	16	36.0	244	30	0
	493	ph-ph	0.215	2447	1	N	P. Undulatum	16	34.9	265	30	0
	494	ph-ph	0.127	17712	2	N	P. Undulatum	16	31.2	186	25	1
	495	ph-ph	0.254	822	0.5	N	P. Undulatum	16	34.7	249	25	0
	496	ph-ph	0.49	1308	1	N	P. Undulatum	16	35.0	243	25	0
	497	ph-ph	0.267	10378	2	N	P. Undulatum	16	34.4	288	20	1
27 Feb	498	ph-ph	0.404	203	0.5	N	P. Undulatum	16	35.4	342	20	0
	499	ph-ph	0.226	2608	1	N	P. Undulatum	16	35.0	267	25	0
	500	ph-ph	0.267	12530	2	N	P. Undulatum	16	31.7	275	20	1
	501	ph-ph	0.147	2045	0.5	N	P. Undulatum	16	32.0	237	25	0
	502	ph-ph	0.421	1359	1	N	P. Undulatum	16	34.5	318	25	0
	503	ph-ph	0.464	2915	2	N	P. Undulatum	16	35.4	263	25	0
	504	Bush	0.023	7925	1	N	R. Fruticosus	16	31.8		15	1
	505	Bush	0.05	2944	2	N	R. Fruticosus	4	43.7		0	1
	506	Bush	1.232	937	4	N	R. Fruticosus	4	43.7		0	1
	507	Bush	0	8283	2????	N	R. Fruticosus	4	31.4		0	1
	508	Bush	0	1028	0.5	N	R. Fruticosus	4	39.3		0	0
	509	Bush	0	5083	2	N	R. Fruticosus	4	46.9		0	1
	510	Bush	0.081	1776	1	N	R. Fruticosus	4	43.7		0	0
3 Mar	511	Bush	0.047	3429	0.5	N	R. Fruticosus	4	36.1		0	0
	512	Bush	0.072	7960	2	N	R. Fruticosus	4	57.5		0	0
	513	Bush	0.068	1214	1	N	R. Fruticosus	4	14.6		0	0
	514	Bush	0.14	2146	0.5	N	R. Fruticosus	4	39.2		0	0
	515	Bush	0.281	4245	2	N	R. Fruticosus	4	50.0		0	1
	516	Bush	0	7411	0.5	N	R. Fruticosus	4	25.3		0	0
	517	Bush	0	4570	1	Y	R. Fruticosus	4	41.9		0	1
	522	grass	0	118350	0.5	N	L. Longifolia	48	7.4		0	0
	523	grass	0	166534	1	N	L. Longifolia	48	6.2		0	0
	524	grass	0	1682	2	Y	L. Longifolia	48	9.6		0	1
	525	grass	0	100957	2	N	L. Longifolia	48	5.4		0	0
	526	grass	0	1751	1	Y	L. Longifolia	48	5.8		0	1
	527	grass	0.005	106654	0.5	N	L. Longifolia	48	5.6		0	0
	528	grass	0.023	1770	2	Y	L. Longifolia	48	6.2		0	1
	529	grass	0.011	82401	1	N	L. Longifolia	48	7.5	141	0	0
	530	ph-e	0.02	105195	2	Y	Salix Sp.	24	30.3	182	25	1
	531	ph-e	0.048	109129	1	N	Salix Sp.	24	34.9	129	40	1
	532	ph-e	0.038	73429	2	Y	Eu. Viminalis	24	29.6	76	25	0
	533	ph-e	0.037	96404	0.5	N	Salix Sp.	24	34.0	168	20	0
	534	ph-e	0.036	96660	2	Y	Salix Sp.	24	35.8	64	25	1
	535	ph-e	0.021	111182	1	Y	Salix Sp.	24	33.0	166	15	0
	536	ph-e	0.026	88794	0.5	Y	Salix Sp.	24	34.3	151	25	0
	537	ph-e	0.037	94219	2	N	Salix Sp.	24	35.2	196	35	1
	538	ph-e	0.041	73110	1	Y	Salix Sp.	24	37.6	158	25	0
	539	ph-e	0.048	81477	0.5	N	Salix Sp.	30	31.2	127	30	1
	540	ph-e	0.034	90438	1	Y	Salix Sp.	30	35.7	160	25	0
	541	ph-e	0.025	82613	0.5	Y	Salix Sp.	30	37.5	144	20	1
	542	ph-ph	0.046	30423	0.5	N	Salix Sp.	30	33.9	156	25	1
5 Mar	543	ph-ph	0.058	32679	1	Y	Salix Sp.	30	35.2	96	25	1
	544	ph-ph	0.055	26532	2	Y	Salix Sp.	30	36.1	76	15	0
	545	ph-ph	0.033	21927	0.5	N	Salix Sp.	30	34.6	105	25	1
	546	ph-ph	0.048	29485	1	N	Salix Sp.	30	33.6	236	25	1
	547	ph-e	0.145	7067	0.5	N	Eu. Viminalis	30	39.9	170	30	0
	548	ph-e	0.048	64359	1	N	Eu. Viminalis	30	40.0	425	25	1
	549	ph-e	0.147	31498	2	Y	Eu. Viminalis	30	43.5	200	25	1
	550	ph-e	0.074	29292	0.5	N	Eu. Viminalis	30	43.0	146	35	1
	551	ph-e	0.2	46273	1	N	Eu. Viminalis	30	41.5	209	20	1
	552	ph-e	0.128	53249	2	Y	Eu. Viminalis	30	41.9	165	25	1
	553	ph-e	0.088	10716	0.5	N	Eu. Viminalis	30	37.8	151	30	0
	554	ph-e	0.029	58306	1	N	Eu. Viminalis	30	38.8	192	15	1
	555	ph-e	0.129	70914	2	N	Eu. Viminalis	30	37.1		40	1
	556	ph-e	0.361	41628	2	N	Eu. Viminalis	30	47.7	317	40	1
	557	ph-ph	0.96	155	0.5	N	Eu. Viminalis	30	51.1	440	50	0
	558	ph-ph	0.649	379	1	N	Eu. Viminalis	30	53.3	296	45	0
	559	ph-ph	0.143	20341	2	Y	Eu. Viminalis	30	32.7	321	15	1
	560	ph-ph	0.555	166	0.5	N	Eu. Viminalis	30	39.2	324	40	0
	561	ph-ph	0.628	521	1	N	Eu. Viminalis	30	44.2	478	35	0
	562	ph-ph	0.423	7156	2	N	Eu. Viminalis	30	37.7	364	25	1
	563	ph-ph	0.1	2571	0.5	N	Eu. Viminalis	30	31.0	291	15	0
	564	ph-ph	0.336	1618	1	N	Eu. Viminalis	30	48.0	266	25	0

Date (2015)	Test	Type	I_{init} (amps)	Duration (ms)	I_{limit} (amps)	Flashover	Species	Conditioning time (hours)	Moisture (%wt.)	Conductivity (µS/cm)	Diameter (mm)	Fire result (1=fire)
	565	ph-ph	0.252	18156	2	N	Eu. Viminalis	30	39.6	260	45	1
	566	ph-ph	0.296	391	0.5	N	Eu. Viminalis	30	43.9	414	35	0
	567	ph-ph	0.987	153	1	N	Eu. Viminalis	30	51.0	232	45	0
	568	ph-ph	0.29	10818	2	N	Eu. Viminalis	30	38.7	337	40	0
	569	ph-ph	0.506	172	0.5	N	Eu. Viminalis	30	46.7	322	35	0
	570	ph-ph	0.536	661	1	N	Eu. Viminalis	30	51.6	331	40	0
	571	ph-ph	0.34	2896	2	N	Eu. Viminalis	30	43.2	208	40	0
5 Mar	572	ph-ph	0.073	4735	0.5	N	Eu. Viminalis	30	32.8	195	25	0
	573	ph-ph	0.246	2580	1	N	Eu. Viminalis	30	34.8	194	30	0
	576	ph-e	0.059	66205	0.5	N	Eu. Baxteri	16	35.8	243	20	1
	577	ph-e	0.081	58609	1	N	Eu. Baxteri	16	32.2	109	25	1
	578	ph-e	0.064	54767	2	Y	Eu. Baxteri	16	30.0	222	25	1
	579	ph-e	0.116	6686	0.5	N	Eu. Baxteri	16	36.1	224	40	0
	580	ph-e	0.16	53109	1	N	Eu. Baxteri	16	40.9	275	30	1
	581	ph-ph	0.338	504	0.5	N	Eu. Baxteri	16	42.7	219	30	0
	582	ph-ph	0.17	3554	1	N	Eu. Baxteri	16	40.2	232	30	0
	583	ph-ph	0.236	12714	2	N	Eu. Baxteri	16	42.9	355	30	1
	584	ph-ph	0.429	204	0.5	N	Eu. Baxteri	16	50.1	207	35	0
	585	ph-ph	0.298	1893	1	N	Eu. Baxteri	16	39.9	214	30	0
	586	ph-ph	0.219	20728	2	N	Eu. Baxteri	16	36.8	230	25	1
	587	ph-ph	0.171	8197	2	N	Eu. Baxteri	16	39.5	255	25	0
	588	ph-ph	0.158	2006	0.5	N	Eu. Baxteri	16	41.2	272	20	0
	589	ph-ph	0.094	17089	1	N	Eu. Baxteri	16	36.8	329	25	0
	590	ph-ph	0.444	188	0.5	N	Eu. Baxteri	16	37.6	166	30	0
	591	ph-ph	0.252	2237	1	N	Eu. Baxteri	16	41.5	196	35	0
	592	ph-ph	0.055	15916	2	Y	Eu. Baxteri	16	36.5	187	20	1
	593	ph-ph	0.198	1160	0.5	N	Eu. Baxteri	16	42.9	187	25	0
	594	ph-ph	0.448	12409	4	N	Eu. Baxteri	16	42.9	149	25	1
6 Mar	595	ph-e	0.015	190305	0.5	N	F. Angustifolia	16	28.8	120	0	0
	596	ph-e	0.022	217413	1	Y	F. Angustifolia	16	28.9	269	30	1
	597	ph-e	0.018	138583	2	Y	F. Angustifolia	16	32.5	173	30	1
	598	ph-e	0.02	117142	0.5	N	F. Angustifolia	16	31.6	160	25	1
	599	ph-e	0.009	174373	1		F. Angustifolia	16	29.7	234	35	1
	600	ph-e	0.022	113460	2	Y	F. Angustifolia	16	32.6	137	25	0
	601	ph-e	0.01	136083	0.5	Y	F. Angustifolia	16	29.5	145	25	1
	602	ph-e	0.011	142162	1	Y	F. Angustifolia	16	29.4	152	15	1
	603	ph-e	0.012	124992	2		F. Angustifolia	16	29.8	181	25	0
	604	ph-e	0.034	144049	1		F. Angustifolia	16	31.7	134	30	1
	605	ph-e	0.03	72322	0.5	N	F. Angustifolia	16	32.7	116	40	1
	606	ph-e	0.013	224715	2	Y	F. Angustifolia	16	27.9	108	25	0
	607	ph-e	0.011	163309	0.5	N	F. Angustifolia	16	28.0	134	20	0
	608	ph-e	0.013	194093	1	N	F. Angustifolia	16	30.0	156	25	1
	609	ph-e	0.063	64810	2	N	F. Angustifolia	16	32.3	141	30	1
	610	ph-e	0.011	158819	0.5	Y	F. Angustifolia	16	29.4	143	30	0
	611	ph-e	0.006	441182	1	N	F. Angustifolia	16	27.4	119	20	1
	612	ph-e	0.009	173464	2	Y	F. Angustifolia	16	27.3	179	15	0
	613	ph-ph	0.015	39367	1		F. Angustifolia	16	30.1	137	15	1
	614	ph-ph	0.006	48167	1		F. Angustifolia	16	27.8	337	20	1
	615	ph-ph	0.137	7770	1	N	A. Mearnsii	16	32.9	308	10	1
	616	ph-ph	0.101	9815	2	N	A. Mearnsii	16	30.4	491	45	1
	617	ph-ph	0.278	2197	1	N	A. Mearnsii	16	38.5	437	25	1
	618	ph-ph	1.511	160	1	N	A. Mearnsii	16	42.6	274	30	0
	619	ph-ph	0.286	1677	1	N	A. Mearnsii	16	34.3	509	45	0
	620	ph-ph	0.044	1950	1	N	A. Mearnsii	16	38.9	407	30	0
	621	ph-ph	0.118	2926	1	N	A. Mearnsii	16	39.2	260	30	1
	622	ph-ph	0.163	13409	2	Y	A. Mearnsii	16	39.3	315	50	0
	623	ph-ph	1.438	428	2	N	A. Mearnsii	16	44.7	535	20	0
	624	ph-ph	3.106	162	2	N	A. Mearnsii	16	45.7	453	25	0
	625	ph-ph	0.192	4463	2	N	A. Mearnsii	16	35.5	355	40	1
	626	ph-ph	0.013	9891	2	N	A. Mearnsii	16	31.9	467	45	1
	627	ph-ph	0.513	156	0.5	N	A. Mearnsii	16	35.5	242	30	0
13 Mar	628	ph-ph	0.421	237	0.5	N	A. Mearnsii	16	25.6	248	35	0
	629	ph-ph	0.222	1398	0.5	N	A. Mearnsii	16	44.5	248	20	0
	633	ph-ph	0.421	261	0.5	N	A. Mearnsii	16	42.2	243	25	0
	635	ph-ph	0.038	2524	0.5	N	A. Mearnsii	16	37.9	433	35	0
	637	ph-ph	0.574	164	0.5	N	A. Mearnsii	16	38.6	198	30	0
	639	ph-ph	0.204	1584	0.5	N	A. Mearnsii	16	45.7	235	50	0
	641	ph-e	0.134	25174	0.5	N	Pinus Radiata	16	44.2	120	40	1
	642	ph-e	0.091	104096	1	Y	Pinus Radiata	16	43.1	116	25	1
	643	ph-e	0.185	130610	2	N	Pinus Radiata	16	45.7	85	40	0
	644	ph-e	0.18	14029	0.5	N	Pinus Radiata	16	28.4	128	35	0
	645	ph-e	0.067	105198	1	N	Pinus Radiata	16	47.7	120	35	1
	646	ph-e	0.289	64563	2	N	Pinus Radiata	16	53.0	96	25	0
	647	ph-e	0.087	34907	0.5	N	Pinus Radiata	16	45.6	100	25	0
	648	ph-e	0.142	102154	1	N	Pinus Radiata	16	40.7	93	35	1

Date (2015)	Test	Type	I_{init} (amps)	Duration (ms)	I_{limit} (amps)	Flashover	Species	Conditioning time (hours)	Moisture (%wt.)	Conductivity (µS/cm)	Diameter (mm)	Fire result (1=fire)
	649	ph-e	0.105	139331	2	N	Pinus Radiata	16	42.4	241	30	1
16 Mar	650	ph-ph	0.246	13696	2	N	P. Undulatum	16	33.0	312	25	1
	651	ph-ph	0.296	12597	4	N	P. Undulatum	16	34.8	204	25	1
	652	ph-ph	0.181	2703	1	N	P. Undulatum	16	31.1	226	35	0
	653	ph-ph	0.268	11364	2	N	Eu. Viminalis	16	36.4	290	30	1
	654	ph-ph	0.099	6939	1	N	P. Undulatum	16	30.0	256	30	0
	655	ph-ph	0.215	10022	2	N	P. Undulatum	16	32.8	305	30	1
16 Mar	656	ph-ph	0.22	12983	4	Y	P. Undulatum	16	32.4	303	30	1
	657	ph-ph	0.262	2094	1	N	P. Undulatum	16	33.6	307	35	0
	658	ph-ph	0.13	7521	2	N	P. Undulatum	16	33.9	222	30	0
	659	ph-ph	0.201	16781	4	N	P. Undulatum	16	32.6	290	30	1
	660	ph-ph	0.173	2787	1	N	P. Undulatum	16	34.2	220	20	0
	661	ph-ph	0.197	4015	1	N	Eu. Viminalis	16	34.3	167	25	0
	662	ph-ph	0.179	17470	4	Y	Eu. Viminalis	16	32.6	257	30	1
	663	ph-ph	0.097	14279	2	N	P. Undulatum	16	31.6	247	20	1
	664	ph-ph	0.222	13938	4	N	P. Undulatum	16	33.5	281	35	1
	665	ph-ph	0.186	2953	1	N	P. Undulatum	16	34.3	303	30	0
	666	ph-ph	0.237	6601	2	N	P. Undulatum	16	33.7	270	30	1
16 Mar	667	ph-ph	0.223	14352	4	N	P. Undulatum	16	33.9	269	35	1
	668	ph-ph	0.38	265	0.5	N	P. Undulatum	16	34.5	135	35	0
	669	ph-ph	0.105	18105	1	N	Eu. Viminalis	16	28.2	225	25	0
	670	ph-ph	0.166	13202	2	Y	Eu. Viminalis	16	33.7	184	25	1
	671	ph-ph	0.09	15835	4	Y	Eu. Viminalis	16	32.5	186	25	1
	672	ph-ph	0.172	6223	1	N	Eu. Viminalis	16	32.2	92	20	0
	673	ph-ph	0.269	4296	2	N	Eu. Viminalis	16	39.9	122	35	1
	674	ph-ph	0.133	18858	4	N	Eu. Viminalis	16	30.3	143	40	0
	675	ph-ph	0.193	4662	1	N	Eu. Viminalis	16	33.4	144	30	0
	676	ph-ph	0.176	15956	2	N	Eu. Viminalis	16	32.0	175	25	1
	677	ph-ph	0.191	20914	4	Y	Eu. Viminalis	16	36.6	190	30	1
	678	ph-ph	0.131	5307	1	N	Eu. Viminalis	16	40.0	200	25	0
17 Mar	679	ph-ph	0.058	16040	1	N	Eu. Viminalis	16	30.5	270	25	1
	680	ph-ph	0.099	11989	2	N	Eu. Viminalis	16	34.6	265	30	1
	681	ph-ph	0.17	13413	4	N	Eu. Viminalis	16	34.4	309	35	1
	682	ph-ph	0.086	11594	1	N	Eu. Viminalis	16	29.8	290	15	0
	683	ph-ph	0.209	11150	2	N	Eu. Viminalis	16	33.5	241	25	1
	684	ph-ph	0.148	14494	4	Y	Eu. Viminalis	16	33.8	249	25	1
	685	ph-ph	0.109	3735	1	N	Eu. Viminalis	16	31.9	280	25	0
	686	ph-ph	0.044	24646	2	Y	Eu. Viminalis	16	31.5	285	15	1
	687	ph-ph	0.185	15462	4	Y	Eu. Viminalis	16	33.4	240	30	1
	688	ph-ph	0.093	15230	0.5	N	Eu. Viminalis	16	31.3	330	25	0
	689	ph-ph	0.158	10071	2	N	Eu. Viminalis	16	37.1	276	20	1
	690	ph-ph	0.065	4867	0.5	N	Eu. Viminalis	16	30.1	279	20	0
	691	ph-ph	0.225	12164	2	N	Eu. Viminalis	16	32.5	355	30	1
	692	ph-ph	0.275	11848	4	Y	Eu. Viminalis	17	38.1	244	25	0
	693	ph-ph	0.045	7172	0.5	N	Eu. Viminalis	18	30.2	396	20	0
	694	ph-ph	0.15	10123	4	Y	Eu. Viminalis	19	41.6	268	20	0
	695	ph-ph	0.127	3762	0.5	N	Eu. Viminalis	20	31.4	272	25	0
	696	ph-e	0.03	34299	2	N	A. Verticillata	20	30.6	307	30	0
	697	ph-e	0.051	21750	0.5	N	A. Verticillata	20	30.4	237	35	0
	698	ph-e	0.051	42466	2	N	A. Verticillata	20	29.1	202	30	0
	699	ph-e	0.03	44013	0.5	N	A. Verticillata	20	27.7	264	25	0
	700	ph-e	0.029	45245	2	N	A. Verticillata	20	29.3	265	25	0
	701	ph-e	0.038	34872	0.5	N	A. Verticillata	20	26.5	260	25	0
	702	ph-e	0.036	46730	2	N	A. Verticillata	20	30.0	247	35	1
	703	ph-e	0.037	18191	0.5	N	A. Verticillata	20	28.9	165	30	0
	704	ph-e	0.01	86462	2	Y	A. Verticillata	20	24.0	215	30	0
	705	ph-e	0.031	36290	0.5	N	A. Verticillata	20	30.2	242	35	0
	706	ph-e	0.048	40319	2	N	A. Verticillata	20	31.0	213	40	0
	707	ph-e	0.052	17318	0.5	N	A. Verticillata	20	29.8		40	0
18 Mar	708	ph-e	0.015	143777	2	Y	F. Angustifolia	16	29.0		25	1
	709	ph-ph	0.045	39204	1	N	F. Angustifolia	16	28.1		25	1
	710	ph-ph	0.12	8783	1	N	F. Angustifolia	16	35.8		25	0
	711	ph-ph	0.107	10433	1	N	F. Angustifolia	16	35.4		35	0
	712	ph-ph	0.053	11979	1	N	F. Angustifolia	16	27.1		25	0
	713	ph-ph	0.035	33458	1	N	F. Angustifolia	16	29.4		25	0
	714	ph-ph	0.126	15917	1	N	F. Angustifolia	16	32.1		35	0
	715	ph-ph	0.07	24900	2	N	F. Angustifolia	16	35.6		35	1
	716	ph-ph	0.067	31755	2	Y	F. Angustifolia	16	32.4		30	0
	717	ph-ph	0.034	45270	2	Y	F. Angustifolia	16	28.7		30	0
	718	ph-ph	0.085	34721	2	Y	F. Angustifolia	16	34.1		30	1
	719	ph-ph	0.063	33412	2	Y	F. Angustifolia	16	31.0		30	0
	720	ph-ph	0.092	30252	2	Y	F. Angustifolia	16	34.3		30	1
	721	ph-e	0.088	39690	2	Y	A. Melanoxylon	20	30.9		30	1
	722	ph-ph	0.048	17803	0.5	N	F. Angustifolia	20	27.5		25	0
	723	ph-ph	0.058	17043	0.5	N	F. Angustifolia	20	28.5		30	0

Date (2015)	Test	Type	I_{init} (amps)	Duration (ms)	I_{limit} (amps)	Flashover	Species	Conditioning time (hours)	Moisture (%wt.)	Conductivity (µS/cm)	Diameter (mm)	Fire result (1=fire)
	724	ph-ph	0.057	17377	0.5	N	F. Angustifolia	20	27.8		30	0
	725	ph-ph	0.071	10070	0.5	N	F. Angustifolia	20	35.7		25	0
	726	ph-ph	0.113	8799	0.5	N	F. Angustifolia	20	34.6		30	0
	727	ph-ph	0.037	22285	0.5	N	F. Angustifolia	20	31.4		25	0
	728	ph-e	0.077	13591	0.5	N	A. Melanoxylon	20	35.5		30	0
	729	ph-e	0.048	21093	0.5	N	A. Melanoxylon	20	34.7		30	0
	730	ph-e	0.059	19169	1	N	A. Melanoxylon	20	35.9		30	0
	731	ph-e	0.063	48981	2	Y	A. Melanoxylon	20	32.0		30	1
	732	ph-e	0.056	22393	0.5		A. Melanoxylon	20	27.7		40	1
	733	ph-e	0.072	32302	1	Y	A. Melanoxylon	20	30.5		35	1
	734	ph-e	0.042	52410	2	N	A. Melanoxylon	20	29.4		25	1
	735	ph-e	0.061	20694	0.5	N	A. Melanoxylon	20	30.2		25	0
	736	ph-e	0.043	57394	1	N	A. Melanoxylon	20	35.4		35	0
	737	ph-e	0.052	46178	2	N	A. Melanoxylon	20	31.2		30	0
18 Mar	738	ph-e	0.093	7716	0.5	N	A. Melanoxylon	20	32.1		25	0
	739	ph-e	0.123	7464	1	N	A. Melanoxylon	20	32.2		30	1
	740	ph-e	0.04	23645	2	N	A. Melanoxylon	20	29.7		35	1
	741	ph-e	0.036	28398	0.5	N	A. Melanoxylon	20	33.7		40	0
	742	ph-e	0.056	37417	1	N	A. Melanoxylon	20	32.3		35	1
	743	ph-e	0.077	62470	2	Y	A. Melanoxylon	20	29.9		30	1
	744	ph-e	0.115	9203	0.5	N	A. Melanoxylon	20	33.6		35	0
	745	ph-e	0.07	41664	1	N	A. Melanoxylon	20	28.0		30	0
	746	ph-e	0.096	23909	0.5	N	C. Glaucophyllus	16	37.6		35	0
	747	ph-e	0.102	107453	1	N	C. Glaucophyllus	16	37.2		35	1
	748	ph-e	0.079	69321	2	Y	C. Glaucophyllus	16	38.4		15	1
	749	ph-e	0.094	16859	0.5	N	C. Glaucophyllus	16	40.4		25	0
	750	ph-e	0.365	7293	1	N	C. Glaucophyllus	16	41.6		35	0
	751	ph-e	0.173	36930	2	N	C. Glaucophyllus	16	43.3		25	0
	752	ph-e	0.179	7135	0.5	N	C. Glaucophyllus	16	40.0		25	0
	753	ph-e	0.166	11215	1	N	C. Glaucophyllus	16	40.6		30	1
	754	ph-e	0.184	78028	2	Y	C. Glaucophyllus	16	41.5		25	1
	755	ph-e	0.146	4950	0.5	N	C. Glaucophyllus	16	45.2		15	0
	756	ph-e	0.262	8291	1	N	C. Glaucophyllus	16	40.4		35	0
	757	ph-e	0.21	56988	2	Y	C. Glaucophyllus	16	39.4		30	1
	758	ph-e	0.364	1079	0.5	N	C. Glaucophyllus	16	41.5		30	0
	759	ph-e	0.115	23498	1	N	C. Glaucophyllus	16	39.2		30	0
	760	ph-e	0.075	100537	2	Y	C. Glaucophyllus	16	40.5		15	1
	761	ph-e	0.249	3093	0.5	N	C. Glaucophyllus	16	39.3		30	0
	762	ph-e	0.215	9887	1	N	C. Glaucophyllus	16	40.5		30	0
	763	ph-e	0.409	10783	2	N	C. Glaucophyllus	16	41.4		35	0
	764	ph-e	0.254	3009	0.5	N	C. Glaucophyllus	16	41.0		35	0
	765	ph-e	0.381	6123	1	N	C. Glaucophyllus	16	40.7		40	0
19 Mar	766	ph-e	0.136	39240	0.5	N	Pinus Radiata	16	47.1		35	0
	767	ph-e	0.25	78677	1	N	Pinus Radiata	16	42.4		30	1
	768	ph-e	0.115	162474	2	Y	Pinus Radiata	16	48.1		35	1
	769	ph-e	0.071	30609	0.5	N	Pinus Radiata	16	44.5		25	0
	770	ph-e	0.045	187137	1	Y	Pinus Radiata	16	44.8		35	1
	771	ph-e	0.051	261440	2	Y	Pinus Radiata	16	51.3		35	1
	772	ph-e	0.167	8117	0.5	N	Pinus Radiata	16	47.2		35	0
	773	ph-e	0.193	100173	1	N	Pinus Radiata	16	58.1		30	0
	774	ph-e	0.02	290068	2	Y	Pinus Radiata	16	37.8		20	0
	775	ph-e	0.073	124253	0.5	N	Pinus Radiata	16	41.2		35	1
	776	ph-e	0.093	94743	1	N	Pinus Radiata	16	45.9		35	1
	777	ph-e	0.102	87472	2	Y	Pinus Radiata	16	44.5		30	1
	778	ph-ph	0.232	38412	1	N	Pinus Radiata	16	52.9		25	1
	779	ph-ph	0.066	48515	1	N	Pinus Radiata	16	39.3		30	0
	780	ph-ph	0.074	52196	1	N	Pinus Radiata	16	40.1		30	1
	781	ph-ph	0.151	2623	0.5	N	Eu. Viminalis	16	32.8		20	0
	782	ph-ph	0.171	2806	0.5	N	Eu. Viminalis	16	34.7		20	0
	783	ph-ph	0.099	3886	0.5	N	Eu. Viminalis	16	30.4		25	0
	784	ph-ph	0.11	4121	0.5	N	Eu. Viminalis	16	31.3		20	0
	785	ph-ph	0.301	10631	4	Y	Eu. Viminalis	16	32.6		25	1
	786	ph-ph	0.372	16379	4	Y	Eu. Viminalis	16	31.1		30	1
	787	ph-e	0.038	33107	0.5	N	A. Verticillata	16	29.6		25	0
	788	ph-e	0.108	26684	2	N	A. Verticillata	16	30.1		40	0
	789	ph-e	0.072	17135	0.5	N	A. Verticillata	16	27.5		40	0
	790	ph-e	0.053	47900	2	Y	A. Verticillata	16	27.8		30	1
	791	ph-e	0.107	12263	0.5	N	A. Verticillata	16	31.6		30	0
20 Mar	794	ph-ph	0.245	20261	2	N	Eu. Baxteri	16	43.0		30	1
	795	ph-e	0.038	64538	2	N	A. Verticillata	16	27.7		30	0
	796	ph-e	0.031	93690	2	Y	A. Verticillata	16	28.7		40	0
	797	ph-ph	0.076	12212	1	N	A. Verticillata	16	26.6		40	1
	798	ph-ph	0.135	6969	1	N	A. Verticillata	16	28.5		25	0
	799	ph-ph	0.072	22063	1	N	A. Verticillata	16	26.9		25	0
	800	ph-ph	0.123	7824	1	N	A. Verticillata	16	28.7		40	0

Date (2015)	Test	Type	I_{init} (amps)	Duration (ms)	I_{limit} (amps)	Flashover	Species	Conditioning time (hours)	Moisture (%wt.)	Conductivity (µS/cm)	Diameter (mm)	Fire result (1=fire)
	801	ph-ph	0.086	7637	1	N	A. Verticillata	16	29.5		40	0
	802	ph-ph	0.266	2965	1	Y	Eu. Baxteri	16	39.2		30	0
	803	ph-ph	0.162	22720	2	Y	Eu. Baxteri	16	33.9		25	1
	804	ph-ph	0.337	1583	1	N	Eu. Baxteri	16	36.2		30	0
	805	ph-ph	0.177	7975	2	N	Eu. Baxteri	16	38.6		35	0
	806	ph-ph	0.274	1834	1	N	Eu. Baxteri	16	35.2		45	0
	807	ph-ph	0.404	10959	2	N	Eu. Baxteri	16	39.6		25	1
20 Mar	808	ph-ph	0.107	4802	1	N	Eu. Baxteri	16	39.2		30	0
	809	ph-ph	0.214	14544	2	N	Eu. Baxteri	16	34.6		30	1
	810	ph-ph	0.514	695	1	N	Eu. Baxteri	16	41.0		30	0
	811	ph-ph	0.213	19282	2	N	Eu. Baxteri	16	38.7		30	1
	812	ph-ph	0.19	10153	1	N	Eu. Baxteri	16	30.5		20	1
	813	ph-ph	0.316	1744	2	N	Eu. Baxteri	16	38.1		30	0
	814	ph-ph	0.29	1806	1	N	Eu. Baxteri	16	32.7		20	0
	815	ph-ph	0.135	21128	4	Y	Eu. Baxteri	16	33.3		25	1
	816	ph-ph	0.152	13922	4	Y	Eu. Baxteri	16	36.8		25	1
	817	ph-ph	0.333	14698	4	N	Eu. Baxteri	16	39.3		40	1
	818	ph-ph	0.151	21036	4	Y	Eu. Baxteri	16	38.4		25	0
	819	ph-ph	0.375	9637	4	Y	Eu. Baxteri	16	39.6		30	1
	820	ph-ph	0.273	15523	4	Y	Eu. Baxteri	16	31.2		25	0
	821	ph-ph	0.116	20557	4	Y	Eu. Baxteri	16	37.5		20	1
	822	ph-ph	0.106	6316	0.5	N	Salix Sp.	2	34.5		30	0
	823	ph-ph	0.112	11402	1	N	Salix Sp.	2	40.5		30	0
	824	ph-ph	0.09	28779	2	N	Salix Sp.	2	35.0		30	0
	825	ph-ph	0.078	29298	2	N	Salix Sp.	2	34.9		35	0
	826	ph-ph	0.182	2338	0.5	N	Salix Sp.	2	41.3		35	0
	827	ph-ph	0.112	18131	1	N	Salix Sp.	2	36.2		30	1
	828	ph-ph	0.12	26706	2	Y	Salix Sp.	2	34.6		30	0
	829	ph-ph	0.144	3397	0.5	N	Salix Sp.	2	39.3		30	0
	830	ph-ph	0.082	22737	1	Y	Salix Sp.	2	37.0		0	0
	831	ph-ph	0.152	18922	2	N	Salix Sp.	2	39.1		0	0
	832	Grass	5	1	0.5	Y	P. Labillardieri	4	12.1		0	1
	833	Grass	5	0	0.5	Y	P. Labillardieri	4	-		0	1
	834	Grass	5	0	0.5	Y	P. Labillardieri	4	-		0	1
	835	Grass	0	0	0.5		P. Labillardieri	4	-		0	0
	836	Grass	0	0	0.5		P. Labillardieri	4	-		0	0
	837	ph-ph	0.124	3457	0.5	N	Salix Sp.	6	36.2		30	0
	838	ph-ph	0.152	5030	1	N	Salix Sp.	6	34.8		30	0
	839	ph-ph	0.108	35690	2	Y	Salix Sp.	6	34.2		30	0
	840	ph-ph	0.049	5381	0.5	N	Salix Sp.	6	36.4		25	0
	841	ph-ph	0.076	25198	1	Y	Salix Sp.	6	34.7		20	0
23 Mar	842	ph-ph	0.05	25648	2	Y	Salix Sp.	6	34.8		25	0
	843	ph-ph	0.081	5855	0.5	N	Salix Sp.	6	35.9		30	0
	844	ph-ph	0.062	18878	1	N	Salix Sp.	6	34.9		25	0
	846	ph-ph	0.317	546	0.5	N	P. Undulatum	7	34.8		30	0
	847	ph-ph	0.418	7756	4	N	P. Undulatum	7	35.5		30	1
	848	ph-ph	0.224	1442	0.5	N	P. Undulatum	7	34.2		25	0
	849	ph-ph	0.31	11019	4	N	P. Undulatum	7	35.5		25	1
	850	ph-ph	0.265	931	0.5	N	P. Undulatum	7	35.0		25	0
	851	ph-ph	0.35	19200	4	Y	P. Undulatum	7	33.7		30	1
	852	ph-ph	0.508	164	0.5	N	P. Undulatum	7	36.3		40	0
	853	ph-ph	0.319	16417	4	Y	P. Undulatum	7	35.7		20	1
	854	ph-ph	0.491	16794	4	N	P. Undulatum	7	34.5		35	1
	855	ph-ph	0.216	16040	4	Y	P. Undulatum	7	33.8		35	1
	856	ph-ph	0.553	4957	4	N	P. Undulatum	7	34.1		30	0
	857	ph-ph	0.5	173	0.5	N	P. Undulatum	7	37.3		35	0
	858	ph-ph	0.118	7786	1	N	P. Undulatum	7	34.3		15	0
	859	ph-ph	0.212	16635	2	Y	P. Undulatum	16	35.5		15	1
	860	ph-ph	0.444	6335	4	N	P. Undulatum	16	35.4		40	1
	861	ph-ph	0.694	145	0.5	N	P. Undulatum	16	39.7		35	0
	865	ph-ph	0.282	1940	1	N	P. Undulatum	16	35.3		25	0
	866	ph-ph	0.994	1056	2	N	P. Undulatum	16	38.7		35	0
	867	ph-ph	0.576	8274	4	N	P. Undulatum	16	38.2		25	1
	868	ph-ph	0.071	14360	0.5	N	F. Angustifolia	16	27.8		40	0
	869	ph-ph	0.02	47255	2	Y	F. Angustifolia	16	26.9		25	0
	870	ph-ph	0.04	21466	0.5	N	F. Angustifolia	16	27.0		30	0
	871	ph-ph	0.031	45273	2	Y	F. Angustifolia	16	28.8		20	1
	872	ph-ph	0.065	15001	0.5	N	F. Angustifolia	16	29.6		30	0
24 Mar	873	ph-ph	0.104	30666	2	Y	F. Angustifolia	16	30.5		35	0
	874	ph-ph	0.104	6950	0.5	N	F. Angustifolia	16	35.7		25	0
	875	ph-ph	0.012	56340	2	Y	F. Angustifolia	16	26.7		15	0
	876	ph-ph	0.033	36525	0.5	N	F. Angustifolia	16	27.0		25	0
	877	ph-ph	0.023	27876	2	Y	F. Angustifolia	16	29.2		25	1
	878	ph-ph	0.019	70821	0.5	N	F. Angustifolia	16	26.0		25	1
	879	ph-ph	0.024	20188	1	Y	F. Angustifolia	16	32.0		10	0

Date (2015)	Test	Type	I_{init} (amps)	Duration (ms)	I_{limit} (amps)	Flashover	Species	Conditioning time (hours)	Moisture (%wt.)	Conductivity (µS/cm)	Diameter (mm)	Fire result (1=fire)
	880	ph-ph	0.01	53039	2	Y	F. Angustifolia	16	25.4		25	1
	881	ph-ph	0.024	23825	0.5	N	F. Angustifolia	16	28.1		30	0
	882	ph-ph	0.074	17269	1	Y	F. Angustifolia	16	37.1		20	0
	883	ph-ph	0.152	4134	1	N	A. Mearnsii	16	35.0		25	1
	884	ph-ph	0.43	2825	2	N	A. Mearnsii	16	35.6		35	0
	885	ph-ph	0.078	3290	0.5	N	A. Mearnsii	16	34.6		15	0
	886	ph-ph	0.181	2161	1	N	A. Mearnsii	16	31.5		20	0
	887	ph-ph	0.127	10490	2	Y	A. Mearnsii	16	32.3		20	1
	888	ph-ph	0.576	161	0.5	N	A. Mearnsii	16	34.1		35	0
	889	ph-ph	0.382	1240	1	N	A. Mearnsii	16	34.4		30	0
	890	ph-ph	0.518	1363	2	N	A. Mearnsii	16	46.2		25	0
	891	ph-ph	0.135	2484	0.5	N	A. Mearnsii	16	27.9		20	0
	893	ph-ph	0.12	9845	1	N	A. Mearnsii	16	30.7		20	1
	894	ph-ph	0.156	15870	2	Y	A. Mearnsii	16	33.9		35	1
	895	ph-ph	0.241	857	0.5	N	A. Mearnsii	16	34.6		20	0
	896	ph-ph	0.226	1841	1	N	A. Mearnsii	16	31.6		25	0
	897	ph-ph	0.345	2321	2	N	A. Mearnsii	16	31.0		35	0
	898	ph-ph	0.278	762	0.5	N	A. Mearnsii	16	35.8		35	0
24 Mar	899	ph-ph	0.34	1049	1	N	A. Mearnsii	16	31.7		35	0
	900	ph-ph	0.125	12218	2	Y	A. Mearnsii	16	31.0		20	0
	903	ph-ph	0.091	43984	1	Y	Pinus Radiata	16	41.5		40	0
	904	ph-ph	0.102	31049	1	N	Pinus Radiata	16	42.8		40	0
	905	ph-ph	0.067	42682	1	Y	Pinus Radiata	16	39.0		30	1
	906	ph-ph	0.41	2123	1	N	Pinus Radiata	16	50.9		40	0
	907	ph-ph	0.119	31370	1	N	Pinus Radiata	16	41.5		40	1
	908	ph-ph	0.075	28385	1	N	Pinus Radiata	16	41.4		35	0
	909	ph-ph	0.153	21247	1	N	Pinus Radiata	16	39.1		45	0
	910	ph-ph	0.124	52700	2	Y	Pinus Radiata	16	43.2		25	0
	911	ph-ph	0.139	29588	2	N	Pinus Radiata	16	43.9		40	1
	912	ph-ph	0.039	19711	2	Y	F. Angustifolia	16	33.6		30	0
	913	ph-ph	0.261	5279	2	N	A. Verticillata	16	34.5		30	1
	914	ph-ph	0.461	2694	2	N	A. Verticillata	16	38.9		30	0
	915	ph-ph	0.275	7238	2	N	A. Verticillata	16	37.5		30	0
	916	ph-ph	0.302	6530	2	N	A. Verticillata	16	39.5		30	1
	917	ph-ph	0.324	4809	2	N	A. Verticillata	16	35.1		30	1
	918	ph-ph	0.233	4869	2	N	A. Verticillata	16	38.0		30	0
	919	ph-ph	0.511	2762	2	N	A. Verticillata	16	38.5		30	0
	920	ph-ph	0.391	3378	2	N	A. Verticillata	16	38.1		25	0
	921	ph-ph	0.417	3842	2	N	A. Verticillata	16	39.8		35	0
	922	ph-ph	0.295	8793	2	N	A. Verticillata	16	38.3		30	1
	923	ph-ph	0.339	7435	2	N	A. Verticillata	16	34.7		25	1
	924	ph-ph	0.543	3184	2	N	A. Verticillata	16	38.3		30	0
	925	ph-ph	0.355	2457	1	N	A. Verticillata	16	39.8		30	0
	926	ph-ph	0.261	3023	1	N	A. Verticillata	16	37.6		30	0
	927	ph-ph	0.517	1647	1	N	A. Verticillata	16	54.2		30	0
	928	ph-ph	0.358	2315	1	N	A. Verticillata	16	37.9		35	0
	929	ph-ph	1.093	175	1	N	A. Verticillata	16	40.2		40	0
	931	ph-ph	0.049	15498	0.5	N	F. Angustifolia	16	27.7		30	0
	932	ph-ph	0.144	9360	1	N	F. Angustifolia	16	29.1		35	0
25 Mar	933	ph-ph	0.043	22822	1	N	F. Angustifolia	16	27.7		25	0
	934	ph-ph	0.056	21610	1	N	F. Angustifolia	16	27.2		30	0
	935	ph-ph	0.062	22805	1	N	F. Angustifolia	16	27.5		30	0
	936	ph-ph	0.014	48971	2	Y	F. Angustifolia	16	26.2		25	0
	937	ph-e	0.022	153501	1	N	F. Angustifolia	16	27.1		30	0
	938	ph-e	0.024	133627	2	Y	F. Angustifolia	16	29.0		30	0
	939	ph-e	0.026	169080	1	N	F. Angustifolia	16	27.1		30	1
	940	ph-e	0.035	135471	2	Y	F. Angustifolia	16	27.6		30	1
	941	ph-e	0.017	130476	0.5	Y	F. Angustifolia	16	26.9		25	1
	942	ph-e	0.012	133360	1	N	F. Angustifolia	16	28.4		20	1
	943	ph-e	0.024	179295	2	N	F. Angustifolia	16	27.2		30	1
	944	ph-e	0.007	201877	0.5	Y	F. Angustifolia	16	26.1		20	1
	945	ph-e	0.011	124912	0.5	N	F. Angustifolia	16	27.6		10	0
	946	grass	0	49594	0.5	N	P. Labillardieri	170	8.3		0	0
	947	grass	0	31302	0.5	N	P. Labillardieri	170	8.3		0	0
	948	grass	0	33046	0.5	N	P. Labillardieri	170	4.4		0	0
	949	grass	0	52099	0.5	N	P. Labillardieri	170	-		0	0
	950	grass	0	33400	0.5	N	L. Longifolia	170	-		0	0
	951	grass	0	29981	1	N	L. Longifolia	170	-		0	0
	952	grass	0	29330	1	N	L. Longifolia	170	-		0	0
	953	ph-e	0.078	90722	2	N	C. Glaucophyllus	16	39.5		0	1
	954	ph-e	0.083	116792	2	Y	C. Glaucophyllus	16	38.3		0	1
26 Mar	955	ph-e	0.071	112143	1	N	C. Glaucophyllus	16	40.6		25	1
	956	ph-e	0.136	13341	0.5	N	C. Glaucophyllus	16	40.7		25	0
	957	ph-e	0.123	90247	2	Y	C. Glaucophyllus	16	40.3	186	25	1
	958	ph-e	0.212	13673	1	N	C. Glaucophyllus	16	39.9	204	25	0

Date (2015)	Test	Type	I_{init} (amps)	Duration (ms)	I_{limit} (amps)	Flashover	Species	Conditioning time (hours)	Moisture (%wt.)	Conductivity (µS/cm)	Diameter (mm)	Fire result (1=fire)
	959	ph-e	0.089	12123	0.5	N	C. Glaucophyllus	16	39.0	206	25	0
	960	ph-e	0.159	98701	2	Y	C. Glaucophyllus	16	39.0	252	25	1
	961	ph-e	0.143	12240	1	N	C. Glaucophyllus	16	41.2	235	20	0
	962	ph-e	0.104	10757	0.5	N	C. Glaucophyllus	16	41.2	207	20	0
	963	ph-e	0.118	74690	2	N	C. Glaucophyllus	16	39.0		25	1
	964	ph-e	0.125	45059	1	N	C. Glaucophyllus	16	41.2		35	0
	965	ph-e	0.099	12374	0.5	N	C. Glaucophyllus	16	41.3		25	0
	966	ph-e	0.122	115402	2	N	C. Glaucophyllus	16	38.8		50	1
	967	ph-e	0.201	5067	1	N	Schinus Molle	16	50.3		30	0
	968	ph-e	0.291	2116	1	N	Schinus Molle	16	54.0		30	0
	969	ph-e	0.446	1366	1	N	Schinus Molle	16	57.1	917	30	0
	970	ph-e	0.373	2731	1	N	Schinus Molle	16	55.6	764	35	0
	971	ph-e	0.358	3426	1	N	Schinus Molle	16	53.7	717	35	0
	972	ph-e	0.246	1632	0.5	N	Schinus Molle	16	54.0	823	35	0
	973	ph-e	0.22	5399	2	N	Schinus Molle	16	53.3	825	30	0
	974	ph-e	0.29	963	0.5	N	Schinus Molle	16	52.5	857	35	0
	975	ph-e	0.379	4486	2	N	Schinus Molle	16	60.3		40	0
26 Mar	976	ph-e	0.262	1144	0.5	N	Schinus Molle	16	53.2		30	0
	977	ph-e	0.223	5788	2	N	Schinus Molle	16	54.3		35	0
	978	ph-e	0.296	883	0.5	N	Schinus Molle	16	53.0		40	0
	979	ph-e	0.257	5093	2	N	Schinus Molle	16	50.9		25	0
	980	ph-e	0.426	179	0.5	N	Schinus Molle	16	48.7		40	0
	981	ph-e	0.198	7692	2	N	Schinus Molle	16	52.9		35	0
	982	ph-e	0.468	160	0.5	N	Schinus Molle	16	54.6		35	0
	983	ph-e	0.277	5316	2	N	Schinus Molle	16	51.2		25	0
	984	ph-e	0.274	898	0.5	N	Schinus Molle	16	51.5		40	0
	985	ph-e	0.315	6191	2	N	Schinus Molle	16	53.5		30	0
	986	ph-ph	1.064	2017	8	N	Schinus Molle	16	50.7		30	0
	987	ph-ph	0.747	7325	10	N	Schinus Molle	16	51.5		40	0
	988	ph-e	0.151	11159	2	N	A. Melanoxylon	16	37.3		25	1
	989	ph-e	0.189	4394	0.5	N	A. Melanoxylon	16	34.9		35	0
	990	ph-e	0.224	4629	1	N	A. Melanoxylon	16	36.3		35	0
	991	ph-e	0.178	8864	2	N	A. Melanoxylon	16	36.2		40	0
	992	ph-e	0.392	431	0.5	N	A. Melanoxylon	16	37.2		35	0
	993	ph-e	0.168	6277	1	N	A. Melanoxylon	16	38.0		35	0
	994	ph-e	0.147	10366	2	N	A. Melanoxylon	16	36.1		25	1
	995	ph-ph	0.595	549	1	N	A. Melanoxylon	16	36.5		30	0
	996	ph-ph	0.158	2667	1	N	A. Melanoxylon	16	35.9		40	0
	997	ph-ph	0.223	2105	1	N	A. Melanoxylon	16	31.1		35	0
	998	ph-ph	0.248	1202	1	N	A. Melanoxylon	16	37.1		20	0
	999	ph-ph	0.215	1767	1	N	A. Melanoxylon	16	32.3		25	0
	1000	ph-ph	0.331	1104	1	N	A. Melanoxylon	16	36.2		35	0
	1001	ph-ph	0.709	326	1	N	A. Melanoxylon	16	37.9		40	0
	1002	ph-ph	0.329	856	1	N	A. Melanoxylon	16	51.3		40	0
	1003	ph-ph	0.55	606	1	N	A. Melanoxylon	16	38.9		35	0
	1004	ph-ph	0.169	3694	2	N	A. Melanoxylon	16	36.0		30	0
	1005	ph-ph	0.179	15370	2	N	Salix Sp.	16	36.1		25	1
	1006	ph-ph	0.187	1402	0.5	N	Salix Sp.	16	38.3		25	0
	1007	ph-ph	0.238	2304	1	N	Salix Sp.	16	37.8		35	0
	1008	ph-ph	0.242	10626	2	N	Salix Sp.	16	36.7		30	0
	1009	ph-ph	0.176	1350	0.5	N	Salix Sp.	16	39.9		25	0
27 Mar	1010	ph-ph	0.221	2833	1	N	Salix Sp.	16	36.1		35	0
	1011	ph-ph	0.154	18679	2	N	Salix Sp.	16	34.5		30	1
	1012	ph-ph	0.171	2729	0.5	N	Salix Sp.	16	35.5		30	0
	1013	ph-ph	0.143	8397	1	N	Salix Sp.	16	37.6		25	0
	1014	ph-ph	0.259	3317	2	N	Salix Sp.	16	39.0		35	0
	1015	ph-ph	0.168	1624	0.5	N	Salix Sp.	16	40.4		25	0
	1016	ph-ph	0.188	5207	1	N	Salix Sp.	16	35.1		35	0
	1017	ph-ph	0.19	15817	2	Y	Salix Sp.	16	40.2		25	1
	1018	ph-ph	0.214	1235	0.5	N	Salix Sp.	16	40.9		25	0
	1019	ph-ph	0.235	2784	1	N	Salix Sp.	16	35.7		30	0
	1020	ph-ph	0.213	19155	2	N	Salix Sp.	16	35.9		35	0
	1021	ph-ph	0.277	1007	0.5	N	Salix Sp.	16	36.7		40	0
	1022	ph-ph	0.212	2680	1	N	Salix Sp.	16	38.8		35	0
	1023	ph-ph	0.31	3457	2	N	Salix Sp.	16	38.7		30	0
	1024	ph-ph	0.159	17328	4	Y	Salix Sp.	16	35.9		25	1
	1025	ph-ph	0.153	16429	4	Y	Salix Sp.	16	36.2		35	0
	1026	ph-ph	0.199	18351	4	Y	Salix Sp.	16	37.7		25	1
	1027	ph-ph	0.082	14543	0.5	N	F. Angustifolia	16	27.8		25	0
	1028	ph-ph	0.026	43493	1	Y	F. Angustifolia	16	27.1		20	0
	1029	ph-ph	0.009	104905	2	Y	F. Angustifolia	16	22.4		15	1
	1030	ph-ph	0.02	34030	0.5	N	F. Angustifolia	16	26.6		20	0
	1031	ph-ph	0.163	23628	1	N	F. Angustifolia	16	35.2		25	0
	1032	ph-ph	0.05	45659	2	Y	F. Angustifolia	16	26.9		30	1
	1033	ph-ph	0.086	7409	0.5	N	F. Angustifolia	16	28.4		35	0

Date (2015)	Test	Type	I_{init} (amps)	Duration (ms)	I_{limit} (amps)	Flashover	Species	Conditioning time (hours)	Moisture (%wt.)	Conductivity (µS/cm)	Diameter (mm)	Fire result (1=fire)
	1034	ph-ph	0.035	49262	1	N	F. Angustifolia	16	26.2		35	0
	1035	ph-ph	0.043	37597	2	Y	F. Angustifolia	16	27.3		25	0
	1036	ph-ph	0.069	19519	1	N	F. Angustifolia	16	26.7		35	0
	1037	ph-ph	0.026	39836	1	N	F. Angustifolia	16	25.9		35	1
	1038	ph-ph	0.115	7726	1	N	F. Angustifolia	16	30.3		40	0

11.4.1 Invalid ignition tests

The following tests were performed for the purposes of rig commissioning and calibration, exploration of vegetation ignition processes and influencing factors, reclose studies, ad hoc issue investigations and demonstrations for visitors.

These tests were not included in the calculation of fire probabilities presented in this report.

Date (2015)	Test	Type	I_{init} (amps)	Duration (ms)	I_{limit} (amps)	Flashover	Species	Conditioning time (hours)	Moisture (%wt.)	Conductivity (µS/cm)	Diameter (mm)
	1										
	2	ph-ph							41.0	200	33
	3	ph-ph							41.8	210	34
3 Feb	4	ph-ph	0.27	22000			Eu. Viminalis	0	39.6	244	30
	5	ph-ph	0.25	14000		Y	A. Melanoxylon	0	36.2	229	30
	6	ph-ph	0.13	20000			A. Melanoxylon	0	39.7	264	35
	7	ph-ph	0.26	18000		Y	A. Melanoxylon	0	40.8	265	35
	8	ph-ph	0.29	19000		Y	Eu. Viminalis	0	38.7	174	30
	9	ph-ph		31000			Eu. Viminalis	0	43.5	193	25
	10	ph-ph		21000			Eu. Viminalis	0	39.6	185	30
	11	ph-ph		28000			Eu. Viminalis	0.75	44.3	207	35
	12	ph-ph	0.35	16000			A. Melanoxylon	0.75	37.1	218	30
4 Feb	13	ph-ph	0.33	11000		Y	A. Melanoxylon	0.75	42.4	313	30
	14	ph-ph	0.33	15000		Y	A. Melanoxylon	0.75	39.5	319	30
	15	ph-ph	0.21	16000		Y	A. Melanoxylon	0.75	39.8	301	35
	16	ph-ph	0.31	12000		Y	A. Melanoxylon	0.75	41.8	330	35
	17	ph-ph	0.29	6000			A. Melanoxylon	0.75	38.0	217	30
	18	ph-ph	0.23	29000		Y	Eu. Viminalis	0.75	38.8	191	30
	20	ph-ph	0.28	30000		Y	Eu. Viminalis	16	38.4	179	30
	21	ph-ph		28000		Y	Eu. Viminalis	16	31.1	239	25
5 Feb	22	ph-ph		31000		Y	Eu. Viminalis	16	29.8	183	30
	23	ph-ph		26000		Y	Eu. Viminalis	16	31.6	168	35
	24	ph-ph		35000		Y	Eu. Viminalis	16	29.7	177	30
	25	ph-ph		23000		Y	Eu. Viminalis	16	29.6	162	
	26	ph-ph		29000		Y	Eu. Viminalis	16	31.1	165	
	27	ph-ph		9000		N	A. Melanoxylon	16	29.6	293	25
	28	ph-ph		5000		N	A. Melanoxylon	16	29.7	212	30
5 Feb	29	ph-ph		8000		N	A. Melanoxylon	16	29.7	212	30
	30	ph-ph		10000		Y	A. Melanoxylon	16	29.1	225	30
	31	ph-ph		2000		N	Eu. Viminalis	0	44.5	139	90
	32	Bush		2000		N	A. Melanoxylon	0			
	33	Bush		34000		Y	Eu. Viminalis	0	37.9	194	25
	34	Bush	0	14000		N					
	35	Bush	0.02	14000		Y					
6 Feb	36	ph-e	0.05	114000		Y	Eu. Viminalis	24	36.3	248	25
	37	ph-e	0.15	75000		N	Eu. Viminalis	24	38.3	246	25
	38	ph-e		91000		Y	Eu. Viminalis	24	37.5	231	35
	39	ph-ph		23000			Eu. Viminalis	24			
	40	ph-ph	0	48000		Y	Eu. Viminalis	64	27.3	211	30
	41	ph-ph	0	609000		N	Eu. Viminalis	64	25.4	241	25
	42	ph-ph	0	57000		Y	Eu. Viminalis	64	25.4	241	25
	43	ph-ph	0	49000		Y	Eu. Viminalis	64	23.2	235	30
9 Feb	44	ph-ph	0.09	30000		Y	Eu. Viminalis	64	28.3	176	30
	45	ph-ph	0.01	71000		Y	Eu. Viminalis	64	22.1	172	30
	46	ph-ph	1.2	6000		N	Eu. Viminalis	128	17.7	172	
	47	ph-ph	0	26000		N	B. Marginata	0	58.4	967	
	48	ph-ph	0	24000		N	B. Marginata	0	55.3	661	
	49	ph-ph		2000		N	Eu. Viminalis	128	17.5	193	
	50	ph-ph		1000		N	Eu. Viminalis	128	17.5	193	
	51	ph-ph	1.1	3000		N	Eu. Viminalis	0	44.0	188	45
	52	ph-ph	3.4	12000		N	Eu. Viminalis	0	44.0	188	45
10 Feb	53	ph-ph	0.63	17000		N	Eu. Viminalis	0	41.3	219	45
	54	ph-ph	0.06	22000		Y	Eu. Baxteri		36.7	234	25
	55	ph-ph	0.22	23000		N	Eu. Baxteri		47.2	167	35
	56	ph-ph	0.08	25000		Y	Eu. Baxteri		43.4	190	30
	57	ph-ph	0.17	28000		Y	Eu. Baxteri		43.9	166	45
	58	ph-e	0.02	101000		Y	Eu. Baxteri		40.9	190	25

Date (2015)	Test	Type	I_{init} (amps)	Duration (ms)	I_{limit} (amps)	Flashover	Species	Conditioning time (hours)	Moisture (%wt.)	Conductivity (µS/cm)	Diameter (mm)
	59	ph-e	0.47	102000		Y	Eu. Baxteri		45.8	181	30
	60	ph-e	0.09	91000		Y	Eu. Baxteri		45.7	153	30
	61	ph-e	0.15	90000		N	Eu. Viminalis	0	44.5	226	35
	62	ph-e	0.05	88000		Y	Eu. Viminalis	0	39.3	197	30
	63	ph-e	0.17	104000		Y	Eu. Viminalis	0	42.4	224	30
	64	ph-e	0.18	2000		Y	Eu. Baxteri	0.7	46.6	216	25
	65	ph-e	0.33	19000		Y	Eu. Baxteri	16	35.5	153	30
	66	ph-e	0.07	81000		Y	Eu. Baxteri	0.7	43.7	203	30
	67	ph-e	0.2	76000		Y	Eu. Baxteri	16	30.1	214	30
	68	ph-ph	2.2	9000		N	Eu. Baxteri	160	14.1	259	
11 Feb	69	ph-e	0	7000		N	B. Marginata	60	56.2	771	
	70	ph-e	1.5	4000		N	B. Marginata	60	56.2	771	
	71	ph-ph	0.24	29000		Y	Eu. Baxteri	16	39.3	180	30
	72	ph-e	0.13	117000		Y	Eu. Baxteri	16	35.5	171	35
	73	ph-ph	0.22	22000		Y	Eu. Baxteri	16			
	74	ph-ph	0.6	17000		Y	Eu. Baxteri	16	39.1	178	40
12 Feb	104	ph-e	0.17	50000	4	N	Eu. Baxteri	178	48.0	198	60
20 Feb	330	Bush	0.233	17.136	2	Y	B. Marginata	0.25	57.5	924	0
	518	grass	0	605	2	N	L. Longifolia	0	55.7		0
3 Mar	519	grass	0	28	2	Y	L. Longifolia	0	55.7		0
	520	grass	0	2751	0.5	N	L. Longifolia	0	56.6		0
	521	grass	0.011	1996	1	N	L. Longifolia	0	63.1		0
6 Mar	574	ph-e	0.166	6831	0.5	N	Eu. Baxteri	16	35.7	148	35
6 Mar	575	ph-e	0.02	74571	1	Y	Eu. Baxteri	16	29.6	208	25
	630	ph-ph	0.308	17711	4	Y	A. Mearnsii	16	44.5	242	20
	631	ph-ph	0.445	13734	4	Y	A. Mearnsii	16	25.6	467	35
	632	ph-ph	0.839	5527	4	N	A. Mearnsii	16	35.5	243	30
13 Mar	634	ph-ph	0.572	10572	4	N	A. Mearnsii	16	42.2	433	25
	636	ph-ph	0.128	7575	4	N	A. Mearnsii	16	37.9	198	35
	638	ph-ph	0.812	10810	4	N	A. Mearnsii	16	38.6	235	30
	640	ph-ph	0.296	17033	4	N	A. Mearnsii	16	45.7	111	50
20 Mar	792	ph-e	0.607	4584	1	N	Allocasuarina Verticillata	16	31.6		30
	793	ph-e	0.931	30360	2	N	Allocasuarina Verticillata	16	31.6		30
	845	ph-ph	0.048	10454	2		Salix Sp.	6	38.5		20
23 Mar	862	ph-ph	0.732	390	1	N	P. Undulatum	16	39.7		35
	863	ph-ph	1.126	1010	2	N	P. Undulatum	16	39.7		35
	864	ph-ph	1.981	1616	4	N	P. Undulatum	16	39.7		35
	892	ph-ph			1	N	A. Mearnsii	16	35.4		30
24 Mar	901	ph-ph	0.15	35954	1	N	Pinus Radiata	16	40.5		35
	902	ph-ph	0.084	11853	1		Pinus Radiata	16	43.6		35
25 Mar	930	ph-ph	0.188	8701	1	N	Allocasuarina Verticillata	16	34.2		25

11.4.2 Background network voltage noise records

The following network background noise checks were performed. NB: LF volts in all records are 7.2% low (compared to Substation SV metering) due to a calibration factor in the DAQ system. This was discovered early in the program and it was decided to leave it in place to avoid the potential issues of having two slightly different scales in the test records data base. Logged data includes:

Type	Run	Date	Time	LF Volts (kV_{rms})	HF Volts (mV_{rms})	LF Amps (mA_{rms})	HF Amps (mA_{rms})
Phase-earth	36	23-Feb-15	1412				
	37	23-Feb-15	1508				
	38	23-Feb-15	1518				
	39	23-Feb-15	1525				
	40	24-Feb-15	0821	12.30	290	2.8	0.235
	41	24-Feb-15	1215	12.46	820	2.1	0.240
	42	24-Feb-15	1625	12.50	770	3.1	0.247
	43	25-Feb-15	0810	12.41	770	2.1	0.243
	44	25-Feb-15	1150	12.28	880	2.1	0.245
	47	25-Feb-15	1503	12.18	780	2.7	0.249
	48	26-Feb-15	0818	12.18	780	3.1	0.234
	49	26-Feb-15	1201	12.20	730	2.3	0.246
	50	26-Feb-15	1422	12.30	750	2.4	0.247
	51	27-Feb-15	0801	12.30	720	1.5	0.237
	52	27-Feb-15	1234	12.30	780	2.7	0.249
	53	27-Feb-15	1357	12.20	760	2.1	0.249
	54	3-Mar-15	1054	12.35	224	3.3	0.235
	55	3-Mar-15	1409	12.26	790	2.4	0.240
	56	3-Mar-15	1524	12.29	870	2.7	0.240
	57	5-Mar-15	0758	12.52	740	2.0	0.250

Type	Run	Date	Time	LF Volts (kV_{rms})	HF Volts (mV_{rms})	LF Amps (mA_{rms})	HF Amps (mA_{rms})
	58	5-Mar-15	0829				
	59	5-Mar-15	0907				
	60	5-Mar-15	1223	12.73	850	2.6	0.242
	61	5-Mar-15	1636	12.58	1250	2.5	0.240
	62	6-Mar-15	0813	12.36	1100	0.6	0.240
	63	6-Mar-15	1156	12.53	1100	2.5	0.245
	64	6-Mar-15	1425	12.65	1100	1.8	0.240
	65	13-Mar-15	0812	12.72	730	2.5	0.250
	66	13-Mar-15	1220	12.59	750	2.1	0.250
	77	17-Mar-15	1214	12.41	860	2.5	0.250
	78	17-Mar-15	1436	12.33	930	2.3	0.250
	79	18-Mar-15	0837	12.40	800	0.8	0.244
	80	18-Mar-15	1325	12.30	700	2.5	0.250
	81	18-Mar-15	1601	12.37	1100	2.1	0.250
	82	19-Mar-15	0816	12.54	750	2.8	0.240
	83	19-Mar-15	1202	12.46	760	2.3	0.250
	87	19-Mar-15	1524	12.36	990	2.2	0.250
	88	20-Mar-15	0830	12.36	800	0.8	0.235
	89	20-Mar-15	0830	12.36	800	0.8	0.235
	93	20-Mar-15	0929	12.58	1250	2.7	0.245
	94	20-Mar-15	1532	12.54	800	2.3	0.250
	95	23-Mar-15	0852	12.88	700	4.5	0.270
Phase to phase	91	20-Mar-15	0903	12.57	635	2.5	0.245
	100	24-Mar-15	0814	12.50	65	0.8	0.260
	101	24-Mar-15	1145	12.67	608	2.5	0.250
	102	24-Mar-15	1428	12.80	600	2.6	0.160
	103	25-Mar-15	0821	12.36	930	2.9	0.255
	104	25-Mar-15	1244	12.35	350	2.4	0.258
	105	25-Mar-15	1556	12.42	830	2.6	0.260
	106	26-Mar-15	0802	12.42	740	2.1	0.250
	107	26-Mar-15	1227	12.52	740	2.4	0.256
	108	26-Mar-15	1612	12.56	590	2.6	0.253
	109	27-Mar-15	0817	12.50	514	2.8	0.250
	110	27-Mar-15	1143	12.50	390	2.1	0.255
	111	27-Mar-15	1145	12.50	430	2.6	0.254
	112	27-Mar-15	1512	12.60	620	2.7	0.256

Substation SV had 22kV capacitor banks which were switched to support network voltages during the afternoons of six days during the test program as follows:

Date	Time	SV capacitor bank CB status changed to
9/02/2015	1320	Closed
	1820	Open
10/02/2015	1130	Closed
	1840	Open
11/02/2015	0950	Closed
	1810	Open
12/02/2015	1310	Closed
	1820	Open
13/02/2015	1040	Closed
	1820	Open
19/03/2015	1130	Closed
	1750	Open

11.4.3 Calibration tests

A number of calibration tests are included in test program records. They were performed to test changes to measurement systems and to check measurement system noise levels. Details logged include:

Run	Date	Time	LF Volts (kV_{rms})	HF Volts (mV_{rms})	LF Amps (mA_{rms})	HF Amps (mA_{rms})	Notes on configuration
30	13-Feb-15	1455	12.2 kV_{rms}				
31	13-Feb-15	1530	5.3 V_{rms}	305	2.3	0.250	All DC coupled
32	13-Feb-15	1531	4.5 V_{rms}	1.9	2.2	0.067	All GND
33	13-Feb-15	1532	4.7 V_{rms}	275	2.5	0.364	All AC coupled
45	25-Feb-15	1202	4.8 V_{rms}	127	2.9	0.190	Digitiser inputs shorted
46	25-Feb-15	1204	5.0 V_{rms}	1.95	2.2	0.064	GND
67	16-Mar-15	0851	n/a	30	0.5		Input to HF volts hi-pass filter shorted Diff tfr#1, no LF volts
68	16-Mar-15	0940	n/a	21	3.0	0.244	Input to HF volts hi-pass filter shorted Diff tfr#1, no LF volts
69	16-Mar-15	0958	n/a	5.4	3.0	0.247	No hi-pass filter, blue phase shorted at entry to diff tfr, no LF volts
70	16-Mar-15	1006	n/a	302	2.8	0.247	No hi-pass filter, red phase shorted at entry to diff tfr, no LF volts

71	16-Mar-15	1009	n/a				Diff tfr#1, no LF volts
72	16-Mar-15	1056	n/a	1.5	2.9	0.247	Diff tfr#1, no LF volts
73	16-Mar-15	1231	n/a	150	2.4	0.248	Both inputs connected to red phase of diff tfr#1, no LF volts
74	16-Mar-15	1236	n/a	159	2.2	0.249	Same with conductors energised
75	16-Mar-15	1640	12.25 kV_{rms}	21.9	2.4	0.255	
76	17-Mar-15	0845	12.41 kV_{rms}	22.5	3.0	0.240	
84	19-Mar-15	1333	12.41 kV_{rms}	700	2.6	0.250	Diff Tfr #2 in service
85	19-Mar-15	1345	12.42 kV_{rms}	750	2.2	0.250	Diff Tfr #2 and hi-pass filter in service
86	19-Mar-15	1414	12.42 kV_{rms}	840	2.2	0.250	Back to normal
90	20-Mar-15	0849	12.70 kV_{rms}	29	2.7	0.245	Diff tfr #2 with both inputs on same phase
92	20-Mar-15	0917	12.50 kV_{rms}	590	2.9	0.243	
96	23-Mar-15	0855	6.7 V_{rms}	2.6	2.7	0.063	GND normal
97	23-Mar-15	1547	5.4 V_{rms}	2.4	1.9	0.070	GND - all power off in containers
98	23-Mar-15	1555	5.1 V_{rms}	1.9	2.1	0.066	GND - heaters unplugged and power off at SVW switchboard
99	23-Mar-15	1607	5.5 V_{rms}	1.9	2.1	0.065	GND - back to normal

11.5 Appendix E: Associated research

Development of the concept for this research project drew upon a variety of previous research investigations listed below. These lists do not constitute a comprehensive survey of available literature. They record those sources that were most influential in shaping this research project.

11.5.1 Ignition studies

1. *Fire Ignition by Contact between Green Vegetation and High Voltage Conductors*, A D Stokes, Sydney University Electrical Engineering.
2. *A review of the incidence of medium and high voltage overhead electric power lines in causing forest fires*, J F Martinez-Canales, C. Alvanez and J V Valero, CIRED 97.
3. *Flammability of some fuel beds common in the South-European ecosystem*, M Guijarro et al, 2002.
4. *Touch Potential Voltage at Ground Level and Aloft in Trees Contacting Energized Distribution Conductors*, EPRI Report 1018463, 2008.
5. *Bushfire Ignition from Electric Faults - A Review of Technical Literature*, HRL Technology Report No: HLC/2010/440, March 2011

11.5.2 Fault signatures

1. *Modelling Power Transformers at Power Line Carrier Frequencies*, Cornelis J Kikkert, School of Engineering and Physical Sciences, James Cook University, Townsville
2. *Modelling Power transformers to Support the Interpretation of Frequency Response Analysis*, Stephen J Mitchell and James S Welsh, School of Electrical and Computer Engineering, University of Newcastle, 2001.
3. *Models for Capacitive Effects in Iron Core Transformers*, Daniel Ioan and Irina Munteanu, Electrical Engineering Department, University of Bucharest, 1999.
4. *Wide Band Modelling of Power Transformers*, Bjorn Gustavsen, SINTEF Research, Trondheim, 2002.
5. *Transformer model for calculation of high frequency transmitted over-voltages*, Bruno Jurisic, Electricité de France R&D.
6. *High-frequency characteristics of overhead multi-conductor power lines for broadband communications*, Pouyan Amirshahi and Mohsen Kavehrad, CICTR, Pennsylvania State University, 2006.
7. *Effect of MV/LV transformer substations on MV power line signals propagation*, Carlo Tornelli and Luciano Capetta, Third Workshop on Power Line Communications, Udine Italy 2009.
8. *Distribution high impedance fault detection utilising high frequency current components*, B Mike Aucoin and B Don Russell, IEEE PAS Vol 101, No 6 June 1982.
9. *Characterisation of electrical incipient fault signature resulting from tree contact with electric distribution feeders*, K L Butler et al, Department of Electrical Engineering, Texas A&M University, 1999.
10. *Characteristics of a simulated high impedance fault, T R Blackburn and Lee Thian Pau, School of Electrical Engineering and Computer Science, University of NSW, 1985.*

11.6 Appendix F: Selection of candidate species

Powerline Bushfire Safety Program – Vegetation Specifications for Electricity Conduction Testing

Revision History

Version	Date	Change	Author	Reviewer	Approver
1.0	15.09.2014	First issue	G. Wright	R. Skene	
2.0	18.09.2014	Second issue	G. Wright	M.Tshaikiwsky	R. Skene
3.0	25.09.2014	Third issue	G. Wright	M.Tshaikiwsky	R. Skene

Summary

The Powerline Bushfire Safety Program (PBSP) was established in December 2011 for the purpose of implementing recommendations 27 and 32 of the Victorian Bushfire Royal Commission (VBRC). This is further defined by recommendations 1 to 6 of the Powerline Bushfire Safety Taskforce.

The primary outcome anticipated through implementation of the PBSP is a reduction in harm to people and property. A key component in delivering this expectation will be achieved by exploring and implementing innovative measures to reduce the likelihood of electricity assets causing bushfires.

Adverse interaction between vegetation and electricity assets maintains the potential to cause significant fire events. It is therefore essential to better understand the relationship between vegetation and electric lines. Of specific importance fires starts generated through electricity conduction.

The Department of State Development and Business Innovation (DSDBI) requested Energy Safe Victoria (ESV) undertake desktop research and analysis of vegetation likely to exist within the vicinity of electric lines. This process is to take into consideration factors that may influence associated fire risks as a result of electricity conduction.

The outcomes of the research and analysis project are detailed within this report.

Contents

Approval

Author

Signature_____ Date_____

Author name: GARY WRIGHT

Reviewer

Signature_____ Date_____

Reviewer name: MIKE TSHAIKIWSKY

Approver

Signature_____ Date_____

Approver name: ROBERT SKENE

1. Introduction

Many thousand native and exotic plant species exist within close proximity to electricity assets throughout Victoria. Many of these maintain the potential to adversely impact on this infrastructure, with vegetation contact with powerlines being a significant cause of fire starts.

Since inception the PBSP has sought to reduce the risk of bushfire starts. The State is seeking to increase the understanding of the fire risk, due to conduction of electricity in vegetation, by undertaking electrical tests of a representative sample of vegetation in appropriate environmental conditions.

The results of this testing will be used to define the range of current electrical signatures and length of time the conduction occurs that pose the highest fire risk at times of high bushfire risk.

DSDBI requested ESV assistance in the development of a data base of common vegetation species that may occur near electric lines.

1.1. Purpose

The purpose of this project is to develop a listing of common types of vegetation that exist in the PSBP's current highest fire consequence areas. Such a vegetation listing will be used as a basis for the testing to determine the electrical conduction of common species within those areas of the state.

1.2. Background

DSDBI initially issued a Request for Quotation (RFQ) for the production a listing of the vegetation prevalent around powerlines.

This request to the market did not result in a suitable organisation to undertake this work and DSDBI requested ESV assist in the development of a list.

1.3. Methodology

The extent of vegetation species throughout Victoria is vast and as such a defined project methodology was required to ensure appropriate, logical and accountable outcomes were facilitated. In addition a project plan was devised to identify key stages and appropriate delivery dates.

The initial phase involving review of the RFQ to identify primary project objectives and to further establish research parameters. Considerations included:

- Identifying project coverage (consequence areas, geography, vegetation density)
- Vegetation types (upper storey, middle storey, ground storey)
- Vegetation characteristics (moisture content, bark composition, failure habits)
- Review of test scenarios

Consultation between DSDBI and ESV confirmed the key points of interest were aligned with anticipated outcomes.

1.4. Scope of investigation

Investigation was conducted to take into consideration 4 primary research parameters. This included:

- Region of project coverage
- Vegetation types
- Vegetation characteristics
- Test scenarios

A summary of these parameters is detailed as follows.

1.4.1. Region of project coverage

The area of focus for this project was defined as the PSBP's current highest fire consequence areas.

The area of research was to then determine the specific municipal organisations and other stakeholders existing within these areas. Such organisations were to be utilised as fundamental points of reference in the endeavour to identify endemic vegetation species.

1.4.2. Vegetation types

The type of vegetation that exists within Victoria varies considerably. This may occur in many ways. Such variations include:

- General growth habits
- Growth rates
- Geographical distribution
- Origin

The purpose of this area of review was to categorise vegetation types to assist with species grouping. The main outcome anticipated to be assisting with a reduction of species sample size to a practical and manageable extent.

1.4.3. Vegetation characteristics

Consideration of general vegetation characteristics was necessary in determining an appropriate test selection. Physical similarities exist within and across vegetation species. They were therefore considered likely to produce similar results with respect to proposed testing regimes.

By taking into account such features and categorising accordingly it was considered testing would facilitate more effective and efficient use of resource. It would also allow for development of a more appropriate cross section of test situations.

1.4.4. Review of test scenarios

Adverse interaction between electricity conductors and vegetation may occur in various ways and result in differing outcomes. The purpose of this category of investigation was to consider scenarios proposed by DSDBI in which electricity conduction testing may occur.

Consideration was to be placed in identifying test sample characteristics relevant to each scenario.

1.5. Method of analysis

When determining the requirements and best means to obtain information and data relevant to research parameters various considerations were taken into account. The associated rationale in supporting the method of analysis is detailed as follows.

1.5.1 Region of project coverage

Comparison of PBSP highest fire risk areas and municipal boundary mapping was recognised as the most effective means of determining organisations key to the project. Implementing this process would therefore provide for an efficient means for consultation to obtain the required vegetation species data.

1.5.2 Vegetation types

Vegetation types are extensive and can vary considerably on both a micro or macro environmental basis. Electricity conduction testing of a large cross section of species to account for this variation would be cost preventative.

By identifying factors typical to various vegetation species and types it was anticipated a more effective and efficient test sample could be compiled. This was a significant factor taken into consideration when sourcing and collating vegetation species data.

Areas of consideration included:

- Species prevalence and distribution
- Classification (i.e. indigenous, native, exotic, weed, environmental weed)
- Growth habit (i.e. tree, shrub, ground cover)
- Flammability

1.5.3 Vegetation characteristics

The nature and general features of vegetation can vary significantly across species. This may also be the case within a species type. For the purpose of conduction testing preparation of effective test samples needed to take this into consideration. Effective grouping of vegetation maintaining similar characteristics was required. This enabled development of a more concise and relevant sample size.

The parameters of consideration included:

- General moisture or sap content
- Bark composition (i.e. thick / thin bark, fibrous / smooth, etc.)
- Canopy density
- Vegetation growth rates and habits

1.5.4 Test scenarios

Determining likely scenarios whereby opportunity would exist to facilitate fire ignition were viewed as essential in the development and programming of appropriate test models.

For this purpose 5 test scenarios were proposed by DSDBI for consideration in the paper titled “Very High Impedance Fault Testing- Vegetation Sample Selection”. These scenarios included:

- **Scenario 1:** Bare conductor contacting a tree branch
- **Scenario 2:** Tree branch in contact with two bare phase conductors
- **Scenario 3:** Bare conductor down and resting on small bushes or grasses.
- **Scenario 4:** Bare conductor down on dry ground and in close proximity to or in contact with vegetation.
- **Scenario 5:** Conductor down and in contact with a mixture of bushes, grasses and ground.

These scenarios were to be utilised as a basis for proposing vegetation test samples.

2. Results and discussion

Extensive research and data collection occurred to encompass the requirements of the RFQ. Collation of sourced information was performed to take into consideration issues relevant to the scope of investigation and methods of analysis. Results of this process are as detailed.

2.1. Project coverage

The areas within Victoria most recently identified as being the highest priority with respect to bush fire risk are documented within the report titled “Areas of Highest Priority to Reduce the Chance of Bushfires Starting near Powerlines in Victoria for the Summer of 2013-2014”.

The report prepared in 2013 by Dr. Kelvin Tolhurst, Department of Forest and Ecosystem Science, University of Melbourne, Creswick, Victoria.

The sections particularly relevant to this project being fire consequence mapping. An extract from the Tolhurst report of particular relevance to this project is depicted in Figure 1:

Utilising this information facilitated identification of municipal organisations that occurred within the highest consequence bushfire risk areas. The relevant organisations are detailed in Figure 2 and Figure 3.

Figure 1: Ignition risk mitigation priority areas as indicated when using “ash Wednesday” weather and current fire history

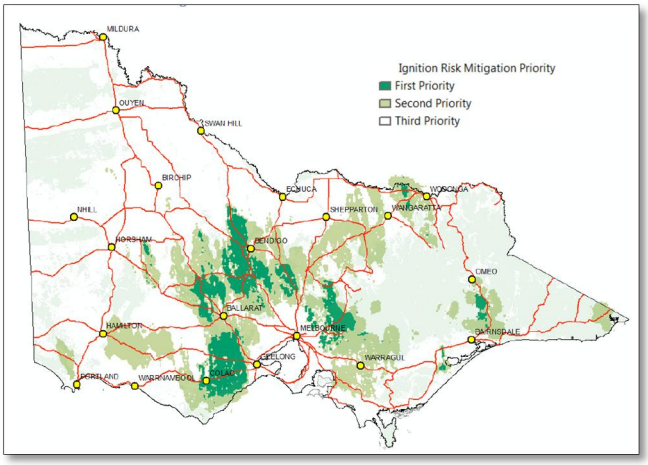

Figure 2: Municipal organisation map

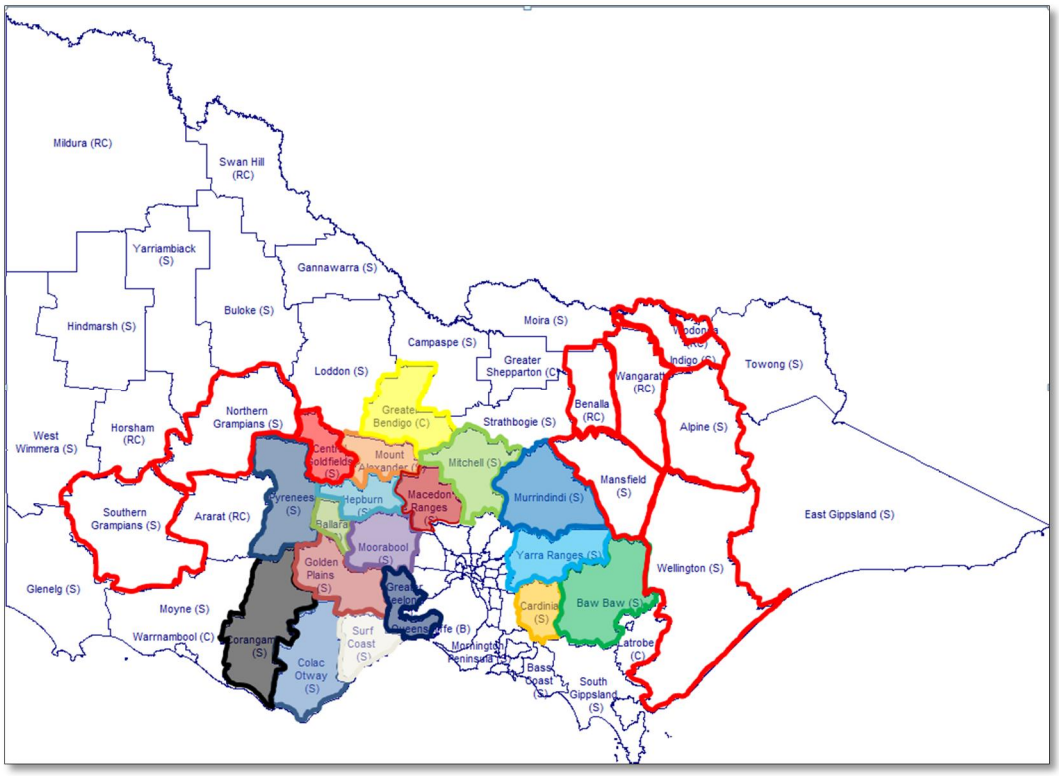

Figure 3: Municipal organisation list

- Ballarat City Council
- Baw Baw Shire Council
- Cardinia Shire Council
- Central Goldfields Shire Council
- Colac Otway Shire Council
- Corangamite Shire Council
- Golden Plains Shire Council
- Greater Bendigo City Council
- Greater Geelong City Council
- Hepburn Shire Council
- Macedon Ranges Shire Council
- Mitchell Shire Council
- Moorabool Shire Council
- Mount Alexander Shire Council
- Murrindindi Shire Council
- Pyrenees Shire Council
- Surf Coast Shire Council
- Yarra Ranges Shire Council

Typically municipal organisations hold comprehensive information relating to vegetation species common to the area. A review of this information was completed and a comprehensive data base of plant species established. The data base has not been included within the context of this report. Notwithstanding correlation of this information enabled determination of the most common species occurring within the regions of focus.

2.2. Vegetation types and characteristics

The common species database developed through the investigation process was condensed to establish a test priority list consisting of 24 priority species. The test priority list is detailed in Figure 4 and has been compiled taking into consideration the various influencing factors identified within the context of the research project.

Vegetation growth habits are approximated by the following mature height dimensions:

- Ground Storey – 0 to 1.5m
- Middle Storey – 1.5 to 8.0m
- Upper Storey – greater than 8.0m

The list can be considered a concise representation of vegetation likely to occur within the vicinity if electric lines throughout the high bushfire risk areas within the state.

They are therefore proposed for the purpose of sample collection and electricity conduction testing. This recommendation is consistent with the requirements of the RFQ.

Figure 4: Test priority list

BOTANICAL NAME	COMMON NAME	GROWTH HABIT	FLAMMABILITY*	VOLATILE VAPOUR*	SAP COMPOSITION*	BARK TYPE	CANOPY DENSITY
Acacia mearnsii	Black Wattle	upper storey	high	likely	low moisture, high resin	smooth	dense
Acacia melanoxylon	Blackwood	upper storey	high	likely	low moisture, high resin	rough	dense
Allocasuarina verticillata	Drooping Sheoke	upper storey	moderate	unlikely	low moisture, low resin	intermediate	intermediate
Cotoneaster glaucophyllus	Cotoneaster	upper storey	low	unlikely	high moisture, low resin	smooth	dense
Eucalyptus baxteri	Brown Stringybark	upper storey	high	likely	low moisture, high resin	rough	dense
Eucalyptus goniocalyx	Long-leaf Box	upper storey	high	likely	low moisture, high resin	intermediate	dense
Eucalyptus viminalis	Manna Gum	upper storey	high	likely	low moisture, high resin	smooth	sparse
Fraxinus angustifolia	Desert Ash	upper storey	low	unlikely	high moisture, low resin	smooth	dense
Pinus Radiata	Radiata Pine	upper storey	high	likely	high moisture, high resin	rough	dense
Pittosporum undulatum	Sweet Pittosporum	upper storey	low	likely	high moisture, high resin	smooth	dense
Salix sp.	Willow	upper storey	low	unlikely	high moisture, low resin	smooth	dense
Schinus Molle	Peppercorn Tree	upper storey	moderate	not classified	not classified	intermediate	dense
Acacia pycnantha	Golden Wattle	middle storey	high	likely	low moisture, high resin	smooth	dense
Banksia marginata	Silver Banksia	middle storey	high	unlikely	low moisture, low resin	intermediate	dense
Bursaria spinosa	Sweet Bursaria	middle storey	high	unlikely	low moisture, low resin	intermediate	dense
Cytisus Scoparius	English Broom	middle storey	high	likely	low moisture, high resin	intermediate	dense
Kunzea ericoides	Burgan	middle storey	high	likely	low moisture, low resin	intermediate	dense
Lycium ferocissium	African Boxthorn	middle storey	moderate	not classified	not classified	smooth	sparse
Lomandra longifolia	Spiny-headed Mat-rush	ground storey	low	unlikely	high moisture, low resin	not applicable	not applicable
Nasella neesiana	Chilean Needlegrass	ground storey	high	unlikely	low moisture, low resin	not applicable	not applicable
Poa labillardierei	Common Tussock-grass	ground storey	high	unlikely	low moisture, low resin	not applicable	not applicable
Rubus fruiticosus	Blackberry	ground storey	low	not classified	not classified	not applicable	not applicable
Themeda triandra	Kangaroo Grass	ground storey	moderate	unlikely	low moisture, low resin	not applicable	not applicable
Ulex europaeus	Gorse	ground storey	high	not classified	not classified	not applicable	not applicable

Native Species | Exotic Species | * Classifications only applicable November to March. Classification may vary during other times of year.

Priority species selection criteria included:

- Prevalence and distribution
- Categorisation (i.e. upper, middle or ground storey)
- Growth rates and habit
- Moisture, oil, sap content
- Bark composition
- Origin status (i.e. indigenous, native, weed)

It should be noted that particular species may not be suited to all test scenarios. Further discussion with respect to this matter is detailed more thoroughly within this report.

2.3. Test scenarios

The test scenarios proposed by DSDBI were considered with respect to how they may be applicable in an actual electricity conduction event. The types and characteristics of vegetation likely to be affected were also contemplated.

Implementation of scenario 1, 2, & 3 were considered being the most likely test regimes to provide beneficial data. Descriptions of how vegetation and electric lines may interact were formed. This included branch diameter estimations that should this information be utilised when obtaining test samples.

Scenario 1: Bare conductor contacting a tree branch

- Contact relevant to this scenario maybe as a result of:
  - Conductor sag or sway
  - Vegetation growing into conductor
  - Vegetation failure

  - Electrical infrastructure failure

- Vegetation characteristic potentially affected in this scenario may include:
  - Small incidental foliage (diameter < 10mm)
  - Canopy branches (diameter < 150mm)
  - Large structural branches (diameter > 150mm)

Scenario 2: Tree branch in contact with two bare phase conductors

- Contact relevant to this scenario maybe as a result of:
  - Vegetation growing into conductor
  - Vegetation failure onto conductor
  - Electrical infrastructure failure onto conductor

- Vegetation characteristic potentially affected in this scenario may include
  - small incidental foliage (diameter < 10mm)
  - canopy branches (diameter < 150mm)
  - large structural branches (diameter > 150mm)

Scenario 3: Bare conductor down and resting on small bushes or grasses.

- Contact relevant to this scenario maybe as a result of:
  - Vegetation failure onto conductor resulting in conductor failure
  - Electrical infrastructure failure

- Vegetation characteristic potentially affected in this scenario may include
  - small incidental foliage (diameter < 10mm)
  - canopy branches (diameter < 150mm)

The priority species list has been correlated to more precisely identify proposed test samples applicable to specific scenarios. This is detailed in Figure 5.

Figure 5: Test scenario recommendations

BOTANICAL NAME	COMMON NAME	TEST SCENARIO 1	TEST SCENARIO 2	TEST SCENARIO 3
Acacia mearnsii	Black Wattle	yes	yes	unlikely
Acacia melanoxylon	Blackwood	yes	yes	unlikely
Allocasuarina verticillata	Drooping Sheoke	yes	yes	unlikely
Cotoneaster glaucophyllus	Cotoneaster	yes	yes	unlikely
Eucalyptus baxteri	Brown Stringybark	yes	yes	unlikely
Eucalyptus goniocalyx	Long-leaf Box	yes	yes	unlikely
Eucalyptus viminalis	Manna Gum	yes	yes	unlikely
Fraxinus angustifolia	Desert Ash	yes	yes	unlikely
Pinus Radiata	Radiata Pine	yes	yes	unlikely
Pittosporum undulatum	Sweet Pittosporum	yes	yes	unlikely
Salix sp.	Willow	yes	yes	unlikely
Schinus Molle	Peppercorn Tree	yes	yes	unlikely
Acacia pycnantha	Golden Wattle	possibble	possible	yes
Banksia marginata	Silver Banksia	possibble	possible	yes
Bursaria spinosa	Sweet Bursaria	possibble	possible	yes
Cytisus Scoparius	Englllish Broom	no	no	yes
Kunzea ericoides	Burgan	no	no	yes
Lycium ferocissium	African Boxthorn	no	no	yes
Lomandra longifolia	Spiny-headed Mat-rush	no	no	yes
Nasella neesiana	Chilean Needlegrass	no	no	yes
Poa labillardierei	Common Tussock-grass	no	no	yes
Rubus fruiticosus	Blackberry	no	no	yes
Themeda triandra	Kangaroo Grass	no	no	yes
Ulex europaeus	Gorse	no	no	yes
Upper storey		Middle Storey		Ground Storey

Whilst not represented as a specific test scenario a common feature of many Eucalyptus species represented throughout Victoria is that of a deciduous cambium or bark layer. This typically is a seasonal process and involves long strips of bark material measuring many metres in length being shed throughout the year.

When positioned in close proximity to bare electric lines this maintains high potential for making contact with electricity conductors. It is suggested electricity conduction testing of this type of debris would be a worthy inclusion in the test regime.

Scenario 2 would be the most appropriate model for this issue to be tested. Bark material being best sourced from *Eucalyptus viminalis* (Manna Gum).

3. Conclusions

The effects of electricity conductors and vegetation coming into contact can result in significant fire starts that in turn can lead to extensive property damage and in worst case loss of life. This has been evidenced through Victoria's past and recent history.

The PBSP has been established to develop innovative programs to mitigate the likelihood of the occurrence of bushfire events. This has included the development of a research program into characterising powerline fault signatures and the need to characterise vegetation in proximately to powerlines in certain highest fire consequence areas developed by DSDBI.

This report and the underpinning research have endeavoured to encompass the requirements of the RFQ for Vegetation Specifications for Electricity Conduction Testing. The outcomes of the project have included the development of the priority species list and relevant test scenarios.

4. Recommendations

It is considered the vegetation identified within the priority species list provides a representative cross section of vegetation types that are likely to occur within high bushfire risk and consequence areas throughout the state.

It is therefore suggested this be utilised as a reference for sourcing vegetation samples for the purpose of performing electricity conduction testing.

5. References

- CFA, 2011, "Landscaping for Bushfire, Garden Design and Plant Selection", Victoria.
- DSDBI, 2014, "*Powerline Bushfire Safety Program. Part A: Specifications, Request for Quotation (RFQ), Vegetation Specifications for Electricity Conduction Testing",* Melbourne Victoria.
- Dr. Kelvin Tolhurst, 2013, *"Areas of Highest Priority to Reduce the Chance of Bushfires Starting near Powerlines in Victoria for the Summer of 2013-2014"*, University of Melbourne, Creswick, Victoria.
- *"Very High Impedance Fault Testing – Vegetation Sample Selection DRAFT"*
- http://www.ballarat.vic.gov.au
- http://www.ballarat.vic.gov.au/media/61126/landscape%20guidelines%20for%20development%20in%20the%20city%20of%20ballarat.pdf
- http://www.bawbawshire.vic.gov.au
- http://www.bendigo.vic.gov.au/Environment/Biodiversity/Indigenous_Plants_of_Bendigo
- http://www.bendigo.vic.gov.au/Environment/Biodiversity</body><style type="text/css" > .no-js { display:block !important; } .js { display:none !important; } </style>
- http://www.cardinia.vic.gov.au
- http://www.centralgoldfields.com.au
- http://www.colacotway.vic.gov.au/Files/Page1_weeds.pdf
- http://www.colacotway.vic.gov.au/Page/Download.asp?name=Page2_weeds.pdf&size=1641295&link=../Files/Page2_weeds.pdf
- http://www.colacotway.vic.gov.au/Page/page.asp?Page_Id=568&h=0
- http://www.corangamite.vic.gov.au/index.php/about-corangamite-shire
- http://www.corangamite.vic.gov.au/index.php/wfmenucpanel/council-services/environmental-management/i-want-to-know/weeds
- http://www.gbcma.vic.gov.au/downloads/WeedsOfTheGB/GBWeedBook3rdEdLR.pdf
- http://www.geelongaustralia.com.au/community/environment/article/item/8ce5b0193c1659e.aspx
- http://www.goldenplains.vic.gov.au
- http://www.goldenplains.vic.gov.au/page.aspx?u=349
- http://www.hepburn.vic.gov.au
- http://www.mitchellshire.vic.gov.au/downloads/Services/Environment_and_Waste/Environment/NativeGardenBrouchuresml.pdf
- http://www.moorabool.vic.gov.au
- http://www.mountalexander.vic.gov.au/Files/Environment/Top_Ten_Bushland_Bullies_of_Mt_Alex_Shire.pdf
- http://www.mountalexander.vic.gov.au/Page/Download.asp?name=Environment/Weeds_Identification_Guide_North_Central_Victoria.pdf&size=6337168&link=../Files/Environment/Weeds_Identification_Guide_North_Central_Victoria.pdf
- http://www.murrindindi.vic.gov.au
- http://www.pyrenees.vic.gov.au/Your_Council/Publications
- http://www.surfcoast.vic.gov.au/My_Environment/Environment_Publications/Indigenous_Plants_-_Botanical_Name
- http://www.surfcoast.vic.gov.au/My_Environment/Weeds_of_the_Surf_Coast_Shire
- http://www.weeds.org.au/cgi-bin/weedident.cgi?tpl=region.tpl&state=vic&region=ncv
- http://www.yarraranges.vic.gov.au
- https://sites.google.com/site/macedonflora/plant-lists/alphabetical/por-xer

11.7 Appendix G: HRL Technology report

Prepared for
Department of Economic Development,
Jobs, Transport and Resources

IGNITION OF VEGETATION BY ELECTRICAL CONDUCTION AT HIGH VOLTAGE TEST EQUIPMENT AND PROCEDURES

Report No: HLC/2015/074

July 2015

by

Blake Stewart, Marc Listmangof and Sam Creek

HRL Technology Pty Ltd
ABN 95 062 076 199

The energy experts

Part of the HRL group of companies

www.hrlt.com.au
info@hrl.com.au

*ISO 9001 Quality Management certified
by BSI under certificate number FS605116

Mulgrave (Head Office)*, VIC
Level 1, Unit 9
677 Springvale Rd
Mulgrave 3170
Australia
Tel +61 3 9565 9888
Fax +61 3 9565 9879

Coopers Plains*, QLD
Unit 2
33 - 37 Rosedale St
Coopers Plains 4108
Australia
Tel +61 7 3423 4300
Fax +61 7 3345 5937

Perth, WA
Level 1
100 Havelock St
West Perth 6005
Australia
Tel +61 8 6160 6003

Morwell*, VIC
Tramway Rd
Private Bag No. 1
Morwell 3840
Australia
Tel +61 3 5132 1500
Fax +61 3 5132 1580

Prepared for:

Department of Economic Development,

Ashley Hunt

HRL Report Archive
File: 50145308

Revision Details

Revision	Date	Reviewed by	Approved by	Comments
1	30.04.2015	A. Czerwinski		
2	11.5.2015	D. Coldham		

Table of Contents

1. Introduction

HRL Technology (HRLT), with assistance from Marxsen Consulting, Energy Safe Victoria (ESV), United Energy (UE) and ZNX, designed and constructed a test space for the Powerline Bushfire Safety Program (PBSP) Vegetation Conduction Testing Study. The test space was designed to allow the study to be performed safely and efficiently at United Energy's Springvale West (SVW) sub-station. The test space was used to perform tests under simulated Code Red fire risk conditions, prepare vegetation samples prior to testing and to house equipment for capturing video and fault signature data.

This report provides details of the safety infrastructure, test rig setup, experimental conditions in the test space, sample preparation and laboratory analysis of samples. The report also details the MATLAB processing component of the data acquisition system. Specifics relating to the feeder, HV supply space, control and data acquisition systems, voltage and current measurement devices and video recording and test configurations are outlined in Section 9 of the main Marxsen Consulting Vegetation Conduction Study report to which this document forms an Appendix.

2. Test Space Overview

The test space consisted of a sample conditioning cell and test cell housed within two modified 40 foot shipping containers. The test cell was segregated into a camera space, test space and HV space by removable, transparent polycarbonate barriers. The test conductors were supported on an adjustable frame located in the test space. The whole test rig was mounted on rails and could be moved into the conditioning cell during maintenance. A schematic diagram showing the layout of the two cells is provided in Figure 1. Features of the test space are described throughout the report.

3. Safety Infrastructure

3.1 Door Interlocks and HV Warning Beacons

The protection systems incorporated into the test space served to support the higher order of protection provided through controlled site access, galvanic isolation of the control hut from the test space, operational procedures and by the interlocks programmed into the SEL351S protection system used to control the HV supply circuit switching.

In addition, electromagnetic locks installed on the right hand door of both cells were interlocked through the SEL351S protection system, which also controlled visual LED warning beacons installed at the entrance to the test cell. The beacons were clearly visible from the control hut in full daylight. Access to the containers was only permitted when a green 'safe' LED status was displayed. The design of the containers meant it was not possible to open the left hand doors without opening the right sides first and the possibility of leaving a left hand door open with the right side locked was addressed by physically isolating the left hand doors by padlock during all test days. The status of the door locks was incorporated into the protection logic such that a green LED status could only be displayed once the HV supply to the cell was opened and earthed and the test controller manually unlocked both doors at the SEL351S control. Equally, the cell supply could not be energised unless the test controller locked both cell doors and the locked status confirmation was subsequently received.

3.2 Zones and Access within Test Space

Physical barriers were installed between the HV space, test space and the video space inside the test cell. The barriers were constructed from transparent polycarbonate sheets and housed in a Unistrut frame which allowed the barrier to be opened and closed.

An electrical access permit (EAP) was required to open the barriers and access the HV space. The test space could be isolated from the HV space by two pneumatically actuated voltage supply probes (Figure 2) operated from the control hut. Access to the test space did not require an EAP when the HV probes were withdrawn and an earthed slot cover was closed and locked in place to prevent the probes from accidentally being connected while under permit. The test space could be isolated from the conditioning cell by a lockable sliding hatch. A sliding pin between the test and conditioning cells performed the function of an interlock between the hatch and slot cover, ensuring that the sliding hatch could only be opened once the slot cover was closed. Additionally, access to the test space once the sliding hatch was opened required the HV operator to check that the test rig was not energised using a Modiewark, place a physical earth on the test rig and then remove the flexible leads between the test rig and the bus bars using the earthing stick. After this procedure was complete, the HV operator and Test Rig Operator were able to access the test rig and camera space.

An EAP was not required to access the fuel conditioning cell provided that either the sliding hatch or the slot cover remained closed. The camera space did not require an EAP to be accessed.

3.3 Atmosphere and Fire

The risk of fire spreading from the test area to equipment and fittings, or of excessive smoke and harmful gas build up, was identified during the design stage and addressed by incorporating a carbon dioxide extinguisher and fire blankets in the conditioning area. The extinguisher was operated by hand and throughout the project the extinguisher was only used on a small number of occasions where a significant fire had occurred. The extinguisher was regularly used to cool the floor of the test rig after a fire event to improve the clarity of the IR video for the succeeding run.

Two wind powered exhaust fans were used to purge any smoke or potentially harmful gases from the test space prior to entering either cell. The fans expelled gases to the atmosphere via a 300 mm diameter opening in the roof of the test container. One fan was mounted in the test area and the other was mounted in the HV area. Because the pedestal fan was directed towards the HV area, this area filled with smoke during some tests. No extraction fan was required in the video camera area as the pedestal fan prevented smoke entering this area.

When entering the containers, the Test Rig Operator wore an oxygen sensor and a full face mask with a Class P3 particulate filter.

3.4 Electrical Earthing

The earth grid at SVW was extended to cover all areas within the test perimeter. The test area was covered by crushed rock and copper cables protruding directly from the grid served as earthing points.

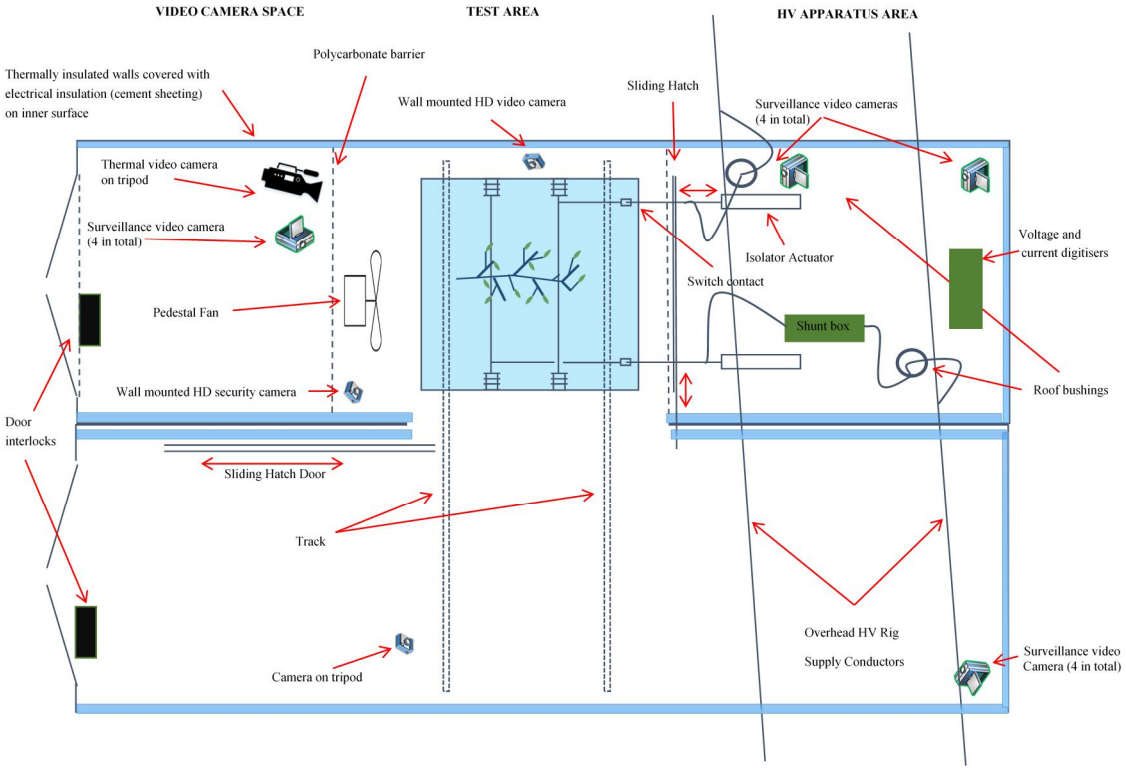

Figure 1 Schematic of Vegetation Study test space

Figure 2 Test area showing slot cover with probes withdrawn (A.), test rig (B.) and sliding hatch (C.)

The SVW control room provided 415 V three phase and 240 V single phase power to both cells. Both containers, all metal fittings within the cells, the HV fault circuit and HV shunt circuit were earthed via copper earth bars running along the fixed walls inside each cell. Electrical devices within the containers were connected to the earth bars and the earth bars in each cell were connected using insulated cables passed through ducts between the cells. The containers were earthed at two locations to the local earth grid.

3.5 Surveillance Cameras

In addition to the IR and HD video cameras used to record the vegetation tests, five radio transmitted surveillance cameras provided a live feed of the test space, HV probes and fuel conditioning cell to the control hut. An HD surveillance camera in the test area provided a live feed of the test rig and a surveillance camera aimed at the slot cover was used to ensure the area was safe to enter. The remaining cameras were used to monitor personnel within the cells.

4. Test Area

4.1 Test Rig

The vegetation samples were tested in a specially designed test facility constructed by HRLT. The test rig and conditioning space were enclosed in two insulated shipping containers to facilitate accurate temperature control, construction, earthing, for ease of transport and to allow the test space to be securely locked during testing. The test area was heated using an 18 kW electric fan heater (manufactured by Thermal Electric Elements Pty ltd) to maintain a temperature of 45°C during testing. The heater was equipped with a thermostat and the heater was run continuously throughout the study. The heater was located in the conditioning chamber. All surfaces in the container were earthed and the floor was lined with cement sheeting because of its high electrical and flame resistivity and to minimise trip hazards. Vegetation samples were stored in the conditioning container prior to testing to reduce the moisture content of the fresh samples to replicate vegetation from dry summer conditions. The conditioning container was accessed via the front door which was fitted with a remote control interlock which locked the doors during testing. The test container was accessed by an interlocked sliding hatch which connected the two adjacent containers.

The test area contained the test rig (shown in Figure 2) which supported the test sample on two conductor cables. The conductors were connected to the bus bars by flexible drop down cables which could be earthed for the different operating configurations. By earthing one conductor, the test rig operated in the phase-to-earth (branch touching wire) configuration. With both conductors alive, the test rig operated in the phase-to-phase (branch across wires) configuration. An earthed trolley was also used to support vegetation samples for grass and bush tests (Figure 3). The test rig was mounted on tracks to allow the rig to be slid out of the test area and into the conditioning container to allow for maintenance and modification work.

The test rig was constructed using Unistrut hollow steel channels which allowed the conductor spacing to be changed. Because the duration of each test was very short, the conductor spacing was kept at the maximum distance of 1.4 m. The test rig was fitted with a pneumatic piston which was used to pull two pins supporting each end of one of the conductors. This allowed the conductor to be ‘dropped’ onto a sample to replicate a powerline falling into vegetation. The conductor fell 300 mm after the pin was removed and achieved a velocity of approximately 2 m/s.

4.1.1 Phase to Earth (Branch Touching Wire) Test

The test rig was designed to operate with one conductor earthed. The objective was to simulate a tree branch touching a powerline.

For these tests, the conductor nearest to the video space area was earthed and disconnected from the energised bus bar. The resistor banks replicated the resistance of the tree trunk to simulate a branch touching the conductor. The conductor at the HV end of the test area was energised and the current flowed through the branch sample. This conductor was supported on adjustable arms of the test rig which could be 'dropped' remotely using a pneumatic piston as described above. This allowed tests to be performed where the conductor was energised before contact was made with the sample. However, for all but a few of the phase to earth tests the conductor was energised with the branch sample already resting on the test rig.

Tests could be performed with a pedestal fan operating to replicate wind. For the majority of the tests, the wind direction was from the video camera end of the test space (trunk end of the branch sample) to the HV area (leaf end of the branch sample).

4.1.2 Phase to Phase (Branch across Wires) Tests

The test rig was also operated with both conductors energised on separate phases through the overhead bus bars. The objective was to replicate a tree branch resting across two powerline conductors.

The test rig was operated with the same configuration discussed in section 4.1.1.

4.1.3 Phase to Earth (Wire into Vegetation) Tests

While in the phase to earth configuration, the test rig could also operate with the energised conductor dropping into a bush or grass sample as shown in Figure 3. The objective was to replicate a powerline falling into low lying vegetation.

The test rig was operated with the same configuration discussed in section 4.1.1 however the vegetation sample was supported by an earthed trolley to allow the sample height to be adjusted.

Figure 3 Test rig in 'Bush/Grass Test' configuration

4.2 Wind Speed

The test area conditions were set to simulate those of a Code Red bushfire risk day. A pedestal fan was used to replicate wind at a height of 10m. The fan was capable of producing wind at 25-27 km/h when tested in an open area, however inside the test facility the achievable wind speed was much lower and much more turbulent due to the polycarbonate baffles and the many obstructions including branches and the test rig. The wind velocity across the branch samples was measured using a handheld Testo anemometer. The velocity at branch height and half way between the conductors varied between 4 km/h and 15 km/h depending on the amount of foliage on the sample. Because the test space was enclosed, backdraft was observed along the roof, walls and floor around the sample. The wind speed was measured a few centimetres from surfaces and was approximately 2 km/h in the opposite direction to the prevailing wind, i.e. back towards the fan. This can be observed in numerous test videos as small particles are blown back towards the fan at ground level.

4.3 Temperature and Humidity

To simulate a Code Red day the test area was heated to 45°C using an electric heater. The humidity in the test area was not adjusted but did reduce to around 25% because of the elevated air temperature. The temperature and humidity were measured using a Lascar temperature probe. The location of the probe was altered throughout the study until a reliable reading was obtained. Initially the probe was located behind the glass wool sheeting to protect the probe from fire damage, however the probe was exposed to a draft which gave lower temperature readings than were measured using a thermocouple on the wall adjacent to the test rig. On the 18th February 2015 the probe was relocated to below the HD video camera in the test area and reliable readings were taken throughout the remainder of the testing. The electric heater was run continuously throughout the tests and the settings were only adjusted when the ambient temperature began to decrease towards the end of the study. The temperature and humidity readings are shown in Table 1 and a typical daily temperature and humidity profile is shown in Figure 4**Error! Reference source not found.**.

Table 1 Daily Temperature and Humidity Readings in the Conduction Test Space

Date	Duration [hr:min]	Average Temperature [°C]	Average Relative Humidity [%]	Ambient Temperature (3pm) [°C][1]
Thursday, 5 February 2015	7:05	42.0	17.3	26
Friday, 6 February 2015	3:15	38.9	30.0	34.3
Monday, 9 February 2015	8:00	32.7	35.1	27.3
Tuesday, 10 February 2015	7:25	43.0	25.9	27
Wednesday, 11 February 2015	8:00	33.4	33.5	22.7
Thursday, 12 February 2015	9:20	42.7	25.9	21.9
Friday, 13 February 2015	1:55	27.3	17.8	31.4
Monday, 16 February 2015	8:20	38.8	20.6	22
Tuesday, 17 February 2015	8:00	39.9	28.2	19.6
Wednesday, 18 February 2015	9:40	44.6	25.7	19.9
Thursday, 19 February 2015	7:45	44.1	29.4	26.1
Friday, 20 February 2015	7:50	43.3	29.5	24.3
Monday, 23 February 2015	3:00	39.9	38.7	19.7
Tuesday, 24 February 2015	7:50	40.3	23.7	20
Wednesday, 25 February 2015	6:40	44.8	26.2	25.7
Thursday, 26 February 2015	5:45	44.9	26.6	22.4
Friday, 27 February 2015	5:35	44.5	24.7	23.1
Tuesday, 3 March 2015	5:00	43.1	25.8	21
Thursday, 5 March 2015	8:05	40.9	20.6	17.6
Friday, 6 March 2015	5:50	43.8	23.7	29.2
Friday, 13 March 2015	3:55	43.4	21.6	20.1
Monday, 16 March 2015	8:05	44.1	22.8	24
Tuesday, 17 March 2015	6:10	45.1	19.5	25.9
Wednesday, 18 March 2015	7:30	47.2	23.5	22.8
Thursday, 19 March 2015	6:55	45.5	23.0	31.9
Friday, 20 March 2015	7:00	43.0	21.3	19.7
Monday, 23 March 2015	7:20	43.7	28.3	24.6
Tuesday, 24 March 2015	5:55	41.2	20.7	12.6
Wednesday, 25 March 2015	7:25	46.2	17.7	17.4
Thursday, 26 March 2015	7:35	45.3	16.4	17
Friday, 27 March 2015	6:40	42.7	20.7	17

Temperature probe location

5 February Temperature probe located on test cell floor. Probe not used during test days 2/2, 3/2 and 4/2

11 February Probe re-located to the join between containers, reading affected by outside temperature

13 February Battery failure. Temperature probe stopped working.

18 February Probe relocated to sample height, good temperature and humidity results

[1] Bureau of Meteorology, Moorrabbin, Victoria February 2015 Daily Weather Observations. Available from http://www.bom.gov.au/climate/dwo/201502/html/IDCJDW3052.201502.shtml.[4 April 2015]

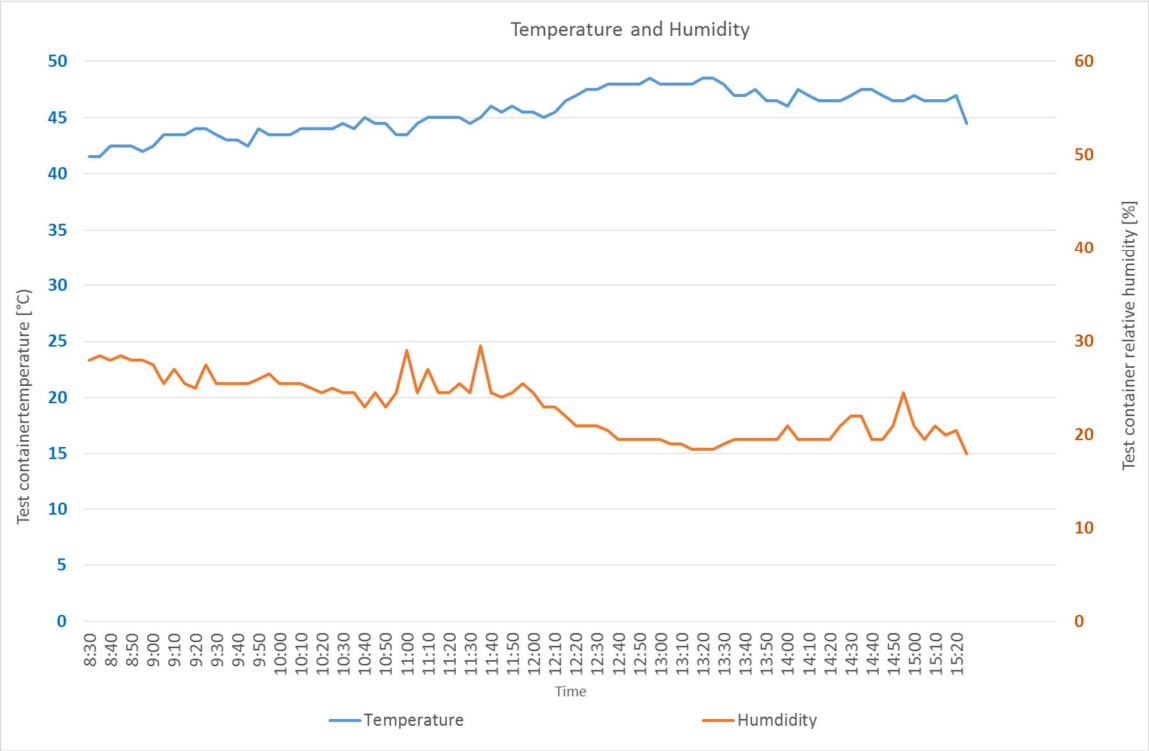

Figure 4 Typical temperature and humidity profile in test area (19th March 2015)

5. Sample Management

5.1 Sample Collection

Branch samples were collected by vegetation management companies that were sub-contracted by HRLT. During the proof of concept testing the branch samples were provided by Ace Tree and during the test program all branch samples were supplied by Asplundh. The required tree, bush and grass species were stipulated in the PBSP Tender Detail document[2] and a list was supplied to the vegetation collectors.

Fresh samples were delivered to the test facility on the day of collection. Once on-site, the branch samples were cut to length and any unwanted limbs were removed to ensure that no branches could cause a premature flashover by touching the test rig once energised. The prepared branches were generally straight and did not have any limbs hanging close to the test rig when resting on the conductors. The prepared branches were stored in refrigerated trailers to reduce moisture loss.

The vegetation collectors were not able to provide any of the grass samples and could only provide some of the bush samples, therefore live samples were purchased from a local nursery for these tests.

[2] Powerline Bushfire Safety Program (PBSP) – Research and Development Program, Provision of Resources to Undertake Vegetation Conduction Testing, Version 1, 5th January 2015, page 40-41

5.2 Sample Specifications

The specifications for the tree branches were provided in the proposed Test Program in the Tender Detail document. The specifications included species, branch diameter and branch length. The date and location where the samples were collected was recorded. The specific branch requirements are listed in Table 2.

Table 2 Sample requirements

Description	Value/Requirement	Comments
Branch length	Minimum of 2.5 m	Branches shorter than 2.5 m often fell off the test rig during testing
Branch diameter	Nominally 25 mm at 'cut' end Some tests required diameters up to 100 mm	For the majority of tests the smallest branches which met the length requirement were used. These were labelled as "nominal 25 mm" in the run sheets but varied between 10 mm and 50 mm depending on the species. Most samples were between 25 mm and 35 mm.
Date and location	The date and location of collection were recorded for all samples	To account for natural variation in samples grown in different locations, the number of each species collected at any one time was restricted to 30. Therefore branches from several locations were required to complete the testing of each species.

5.3 Sample Management and Quality Control

A sample number was assigned to each branch, bush or grass sample that was tested during the study. The samples were given a sample number which was the date of testing and an alphabetical identifier i.e. the first sample on the 3rd February was labelled 0302a. The sample number, species and the collection date and location were recorded on the run sheet for each test. The laboratory analysis results for each sample were copied into the Run Sheet Excel file[3]. The analysis methods are described in section 5.6.

5.4 Sample Conditioning: Pre-Trial Study into Moisture Loss

HRL conducted a rudimentary trial into the effect of sample storage on moisture content using limbs of approximately 10-15 mm diameter cut from a live cotoneaster tree on the 7th of January 2015. Branch and leaf samples from the limbs were analysed for moisture following preparation and storage under the following six conditions:

[3] PBSP_Runsheet and analysis_10-4-15_Master.xlsx

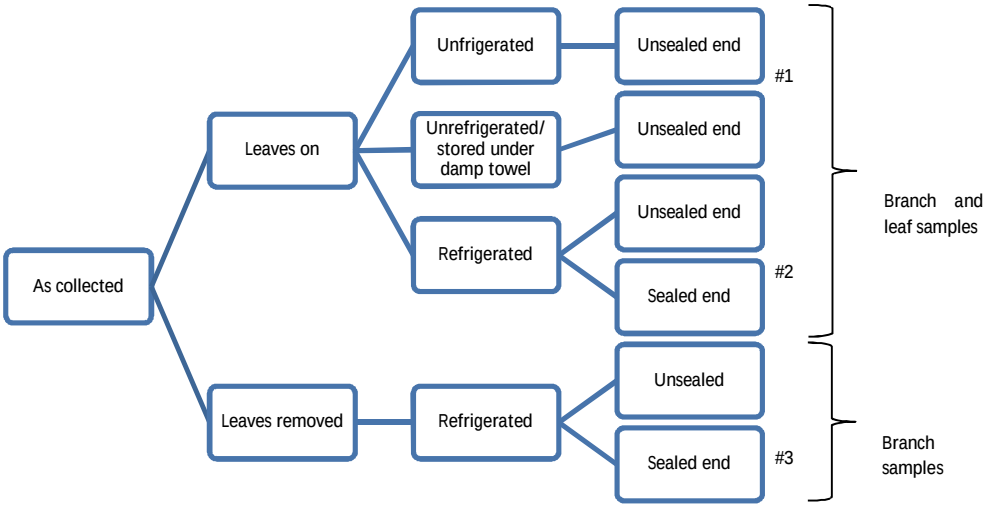

The moisture content of the samples was determined in the as received condition and after one and six days' storage for each storage option. The study was designed to provide an indication of the effect of removing leaves from branches, refrigerating samples and sealing the ends of samples on moisture loss.

Results of moisture analysis performed over a six day period are presented relative to each sample's starting moisture in Figures 5 for samples of branches and in Figure 6 for the leaves. The initial moisture content of the branch samples was around 40% and in the worst case (unrefrigerated and no treatments) this decreased to 29% after 6 days. The initial moisture content for the leaf samples was around 55% and this decreased to approximately 21% after 6 days with o treatment.

The various storage options significantly reduced moisture loss and the findings provide evidence that moisture loss in vegetation samples can be minimised by:

- Refrigerating samples: 2 positive results observed in 2 comparisons
- Removing leaves from branch samples: 2 positive results observed in 2 comparisons
- Sealing the ends of samples: 2 positive and 1 negligible result in three comparison
- Covering samples with moist towels - not refrigerated: 2 positive results in 2 comparisons

5.5 Sample Conditioning – Proof of Concept and Throughout Study

The effect of drying was assessed during the proof of concept testing. Samples were tested as-received and after varying periods of conditioning at 45°C. Because the weather during the test program was cool and wet, the conditioning regime used for the majority of tests involved 16 to 24 hours conditioning at 45°C prior to testing. This slightly reduced the moisture content of the branch samples, however the actual impact of a dry summer on the moisture content of fresh samples was not measured and can only be confirmed by a separate study.

Some bush and grass samples were tested using live plants. These were conditioned at 45°C for around 1 week without watering.

Prior to being tested or conditioned, the samples were stored in a cool room at around 2°C. Despite the observations in the Pre-trial study into moisture loss, measures such as sealing the ends were not taken due to the large number of samples required for the study.

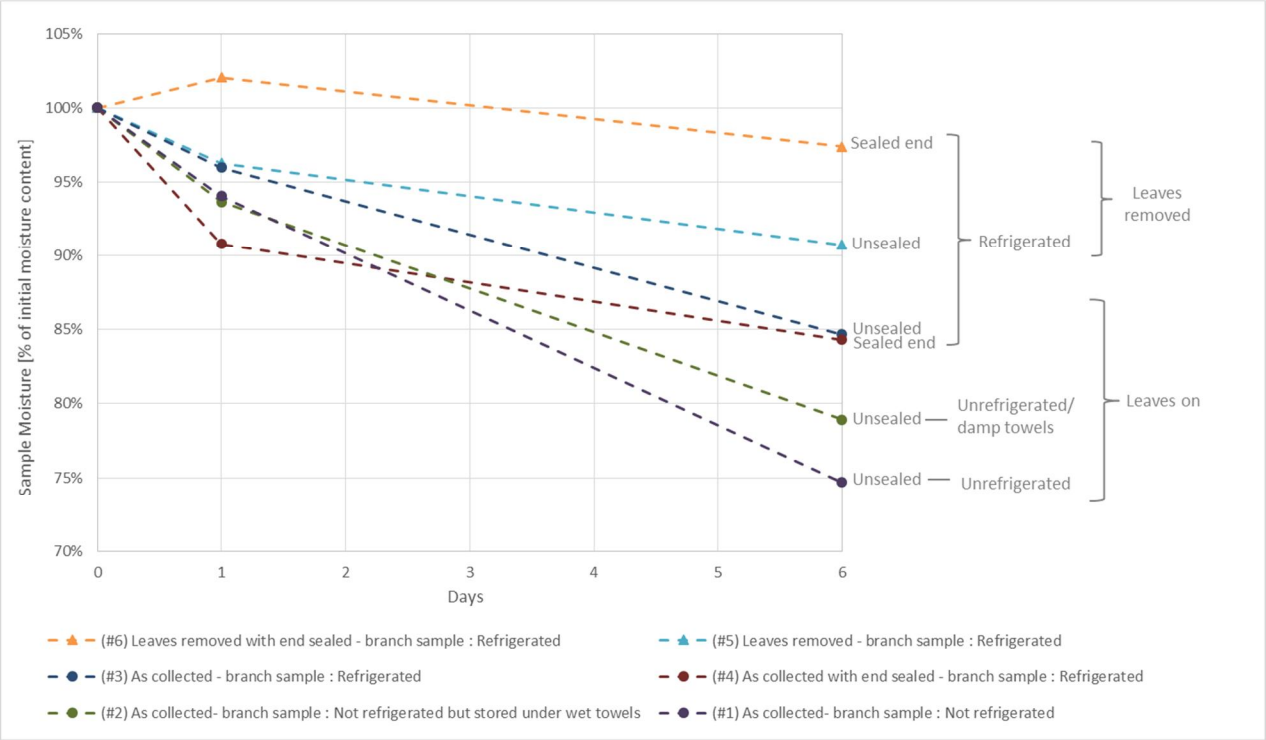

Figure 5. Branch sample moisture results – relative to initial moisture content

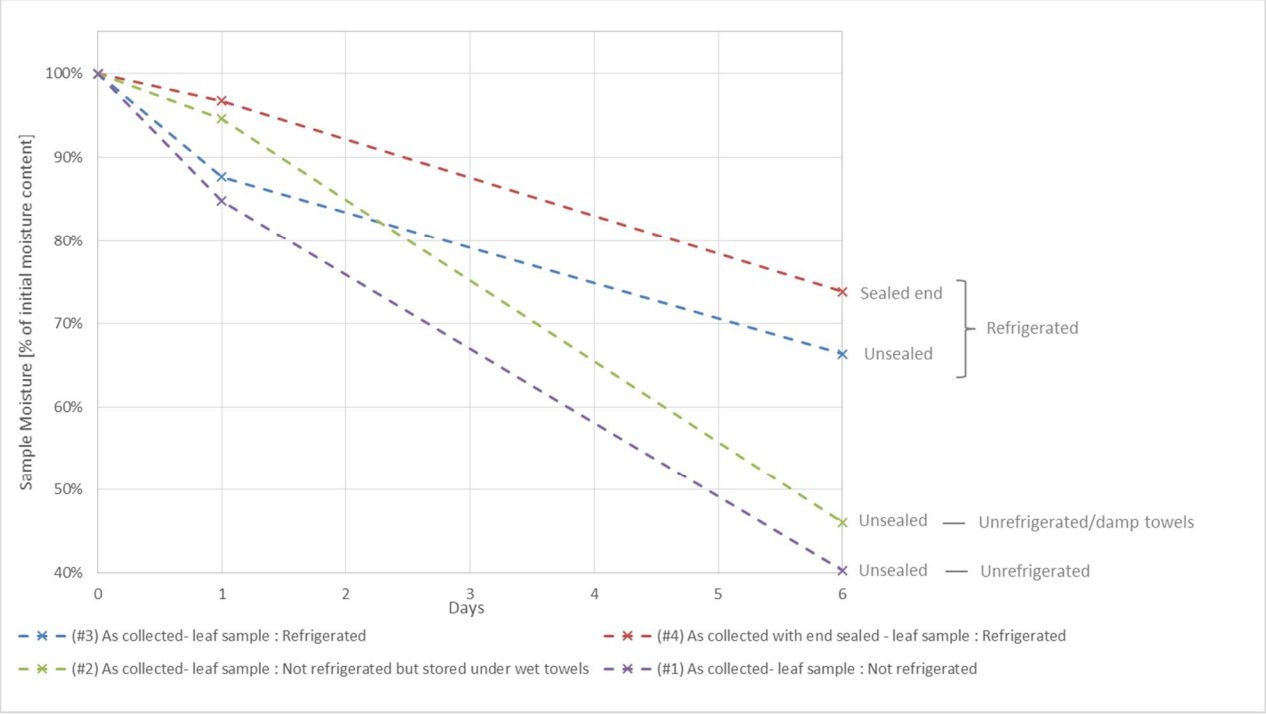

Figure 6. Leaf sample moisture results – relative to initial moisture content

5.6 Sample Analysis

The moisture content of almost every samples was measured and for a number of samples the electrical conductivity was also measured. The laboratory procedures for the moisture and conductivity measurement are described below. The results for each species are shown in Figure 7 and Figure 8.

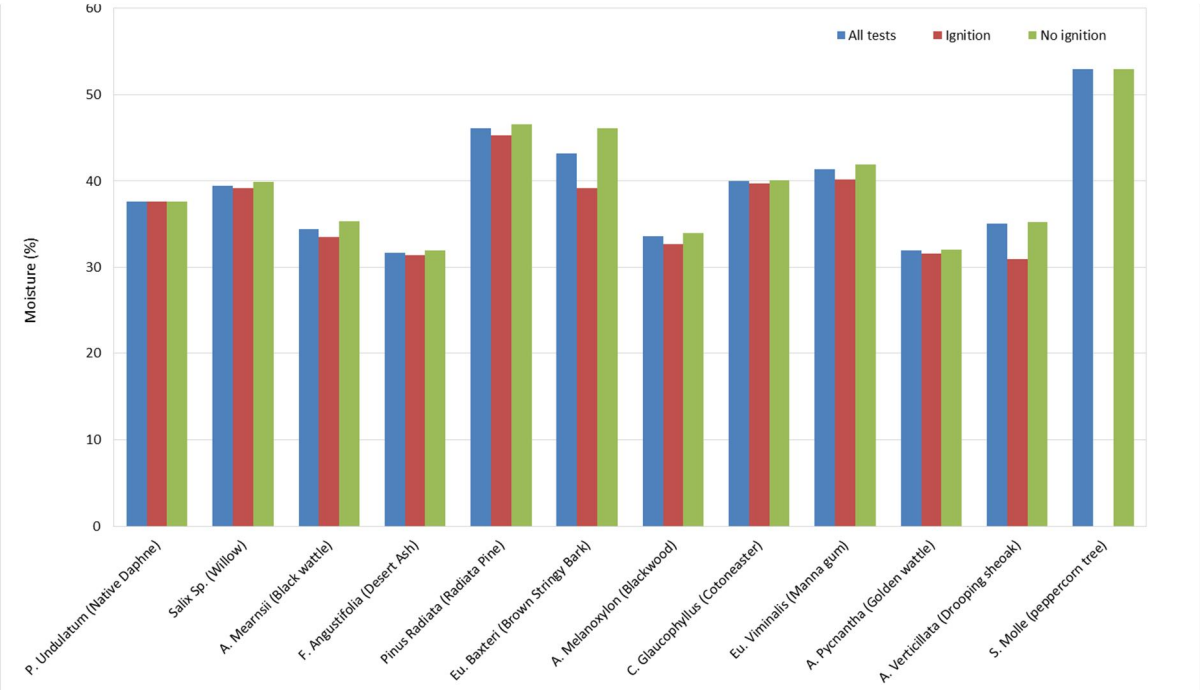

Figure 7 Average moisture by species (phase - earth tests)

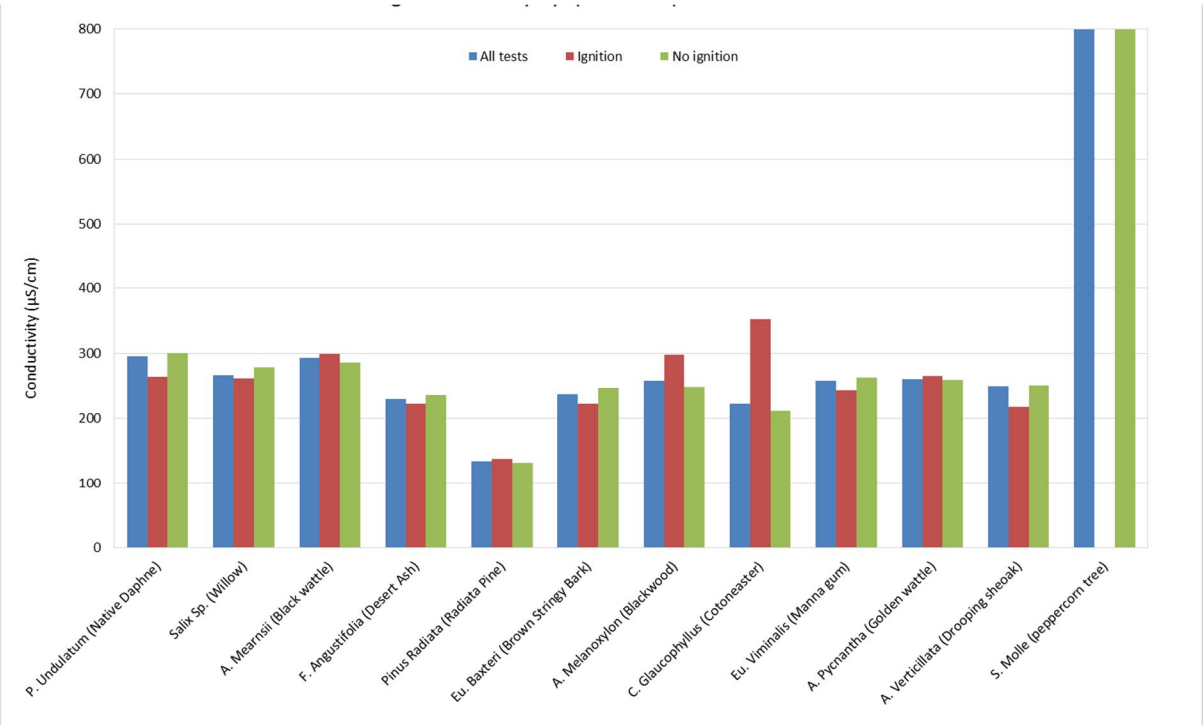

Figure 8 Average conductivity by species (phase - earth tests)

It can be seen that the average moisture content was consistently between 30% and 45% across all species with the exception of peppercorn tree. The average conductivity was between 200 µS/cm and around 300 µS/cm for most species except for the radiata pine and the peppercorn tree.

5.6.1 Moisture Analysis

Moisture content was determined on 1014 test samples. The method used for moisture analysis is summarised below:

1. Sub-samples were collected shortly before conduction testing by removing a section from the end of the branch sample.
2. The sub-samples were sealed in a plastic bags and kept in a cool room at around 2°C
3. At the end of each day the sub-samples were taken to the HRLT laboratory
4. At HRLT the samples were assigned a HRL sample code and all information on the sample bags was recorded. Samples generally consisted of a section of woody branch material 10-20 cm in length (see Figure 9).
5. A 5 mm to 25 mm long piece was removed from the end of the sub-sample and discarded, as is it possible that this section had partially dried. A second section typically 25 to 50 mm long was then removed from the sub-sample, split into small slices. This sample was weighed then dried at 110°C for 24 h.
6. After 24h the sample was re-weighed and a moisture loss percentage was calculated.

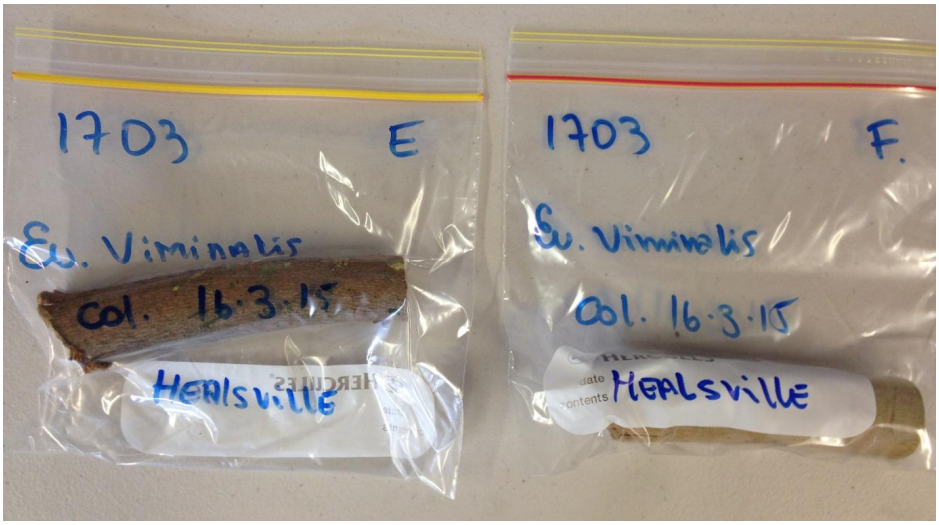

Figure 9 Sub-samples in sealed bags

5.6.2 Electrical Conductivity

Electrical conductivity was measured on 674 test samples using the method summarised below:

1. The dried sub-sample (from the moisture analysis) was milled to less than 5 mm and a 2 g sub-sample of this milled fraction was taken.
2. 50mL of deionised water was added to the sample and the solution was boiled under reflux for 4 hours
3. The extract was collected and made up to 100 ml and the electrical conductivity of this solution was then measured using a TPS labCHEM-CP bench top conductivity, pH and temperature meter.

6. HRLT MATLAB Data Processing

6.1 Functionality of MATLAB 'VT_data_processing.m' script

6.1.1 Data importing and reduction

The MATLAB script was set up to import PNRF data files from HBM Perception software.

HBM offer a 'PNRF Reader Toolkit' through their website. This toolkit features a 'MATLAB example' file which provides basic functionality for importing PNRF files directly into MATLAB. The functionality of HBMs script was incorporated into the 'VT_data_processing.m' script.

The data recording in the testing program was standardised to 4 channels with 2 channels sampling continuously at 100,000 samples per second and another 2 channels with 20 ms duration high speed sweeps occurring every second, sampling at $2x10^6$ samples per second. This sampling regime was used to reduce the file size while allowing periods of each test to be viewed at a higher resolution. Channels 1 and 3 were imported in continuous mode and Channels 2 and 4 were imported in sweep mode (Table 3).

Table 3 DAQ channel numbers and specifications

Channel Number	Measurement	Anti-aliasing filter
1	Direct Voltage	50kHz
2	HF Voltage	1MHz
3	Direct Current	50khz
4	HF Current	1MHz

If test durations exceeded one minute, MATLAB began to have issues in importing the data (Slowing down, hanging etc.) as found during testing on a high end PC. After the data has been imported, there are two options for data reduction that exist within the script:

- Downsample the data
- For the HF sweeps, skip every nth sweep

This 'skip sweeps' feature was set to aggressively cut more data when processing was done during site testing days to speed up data processing. It was not used during post-test batch processing.

6.1.2 Raw data charts

Since the GEN3i records data in engineering units, there is no manipulation performed to the recorded data. It is simply charted against time. The time array is created manually in the script based on the sample frequency, starting at zero.

6.1.3 Detailed data charts

Similar to the raw data charts, the detailed charts simply show the detail of the start, middle and end of the recorded signal. The locations of the start and middle of the signal were determined based on a threshold, whereby the recorded current or voltage data should value rise above what was considered the noise level it was assumed to be the signal.

6.1.4 RMS time history charts

The RMS calculation is determined from:

$$RMS = \sqrt{\frac{1}{(t_2 - t_1)} \int_{t_1}^{t_2} v^2 . dt}$$

as presented in the document 'Calculation of RMS value', Marxsen Consulting, 4/5/2014. The rolling window length (which is t_2-t_1 in the above formula) used for the direct current and the direct voltage channels was 10ms. This ensured that all 50Hz cycles, and multiples of 50Hz cycles were calculated accurately.

The rolling window length for the HF current and the HF voltage channels was 0.05 ms (50 µs). This ensured that all cycles with a frequency of 10kHz or greater had the RMS calculation run at least a half cycle over them.

6.1.5 Frequency spectrum charts

DFT bins were spaced at intervals of Fs/N where Fs is the sample rate and N is the length of the input time series.

6.1.6 Testing LF voltage spectrograms with different window sizes.

The waveform was constant with no zeroes on either side and Fs = 100kHz. Other specifications are detailed in Table 4.

Power of 2 window size was not used. This is typically used to speed up the algorithm, but in practice makes little difference.

Table 4 Frequency Spectrum Specifications

Input	LF voltage & LF current channels	HF voltage & HF current channels
Array length	100,000	40,000
Window length	100,000	40,000
Window type	Hann	Hann
Bin size (Hz)	1.0	50

6.1.7 Spectrogram charts

A spectrogram is a visual representation of the frequency content of data as it varies with time. The spectrogram charts were produced using the spectrogram function in MATLAB. The key inputs used for this function are shown in Table 5.

Table 5 Key inputs for spectrogram charts

Input	LF voltage & LF current channels	HF voltage & HF current channels
Window type	Hamming (default)	Hamming (default)
Window length	16,384	1,024
Window overlap	8,192	512
FFT window size	16,384	1,024

Spectrograms will always have a trade-off in time resolution and frequency resolution. A larger window size and FFT window size will increase frequency resolution but decrease time resolution. Window overlap controls how ‘smeared’ the signal appears on the chart. A standard overlap of half the window size has been used.

LF current and LF voltage channels were sampled at 100,000 samples per second. At this sampling speed, the largest duration wave of 50Hz corresponds to 2,000 elements. Therefore a 16,384 element window will capture over 8 full cycles and perform averaging.

LF current and LF voltage channels were sampled at 100kS/s. At this sampling speed, the largest duration wave of 50Hz corresponded to 2,000 data elements. Therefore a 16,384 element window captured over 8 full cycles and performed averaging.

HF current and HF voltage channels are sampled at 2MS/s. At this sampling speed, the largest duration wave of 10kHz corresponded to 200 data elements so a 1,024 element window captured over 5 full cycles and performed averaging.

General notes about spectrogram graphs:

> Most spectrograms have regular faint vertical lines. This is called 'spectral leakage' and is due to the windowing of the data. When the data at the edges of the window are at different values and different gradients and the window is wrapped around for the FFT calculation, there is no longer a smooth transition, often there is a discontinuity. This discontinuity creates a high frequency wave. Using a Hamming window eliminates some spectral leakage, as compared to a standard rectangular window. MATLAB uses a Hamming window for the spectrogram function by default.

6.2 Testing

6.2.1 Dummy waveforms

Some dummy waveforms were created to test the program as listed in Table 6.

Table 6 Specifications of 'dummy' waveforms

	Benchmark 1	**Benchmark 2**	**Benchmark 3**	**Benchmark 4**
Simulated channel	LF Voltage	HF Voltage	LF Current	HF Current
Sampling frequency (S/s)	100k	2M	100k	2M
Time duration (s)	20	0.1	20	0.1
Y1	1800*sin(2π*50t)	1*sin(2π*100,000t)	0.1*t*sin(2π*50t)	0.01*sin(2π*100,000t)
Y2	100*sin(2π*150t)	0.1*sin(2π*500,000t)	0.01* t*sin(2π*150t)	0.001*sin(2π*500,000t)
Y3	100*sin(2π*10,000t)	0.01*sin(2π*800,000t)	0.01* t*sin(2π*10,000t)	0.001*sin(2π*800,000t)
Function Y	Y1+Y2+Y3	Y1+Y2+Y3	Y1+Y2+Y3	Y1+Y2+Y3

The benchmark 1 and 3 waveforms are of 20 second length with 1 second of flat zero line on either size to test the transitions from no voltage to active voltage. Benchmark 3 has an additional multiplication by 't' to simulate a linear rise in current.

The various dummy waveforms are illustrated in the following figures.

6.2.2 Test 1 – Direct Voltage

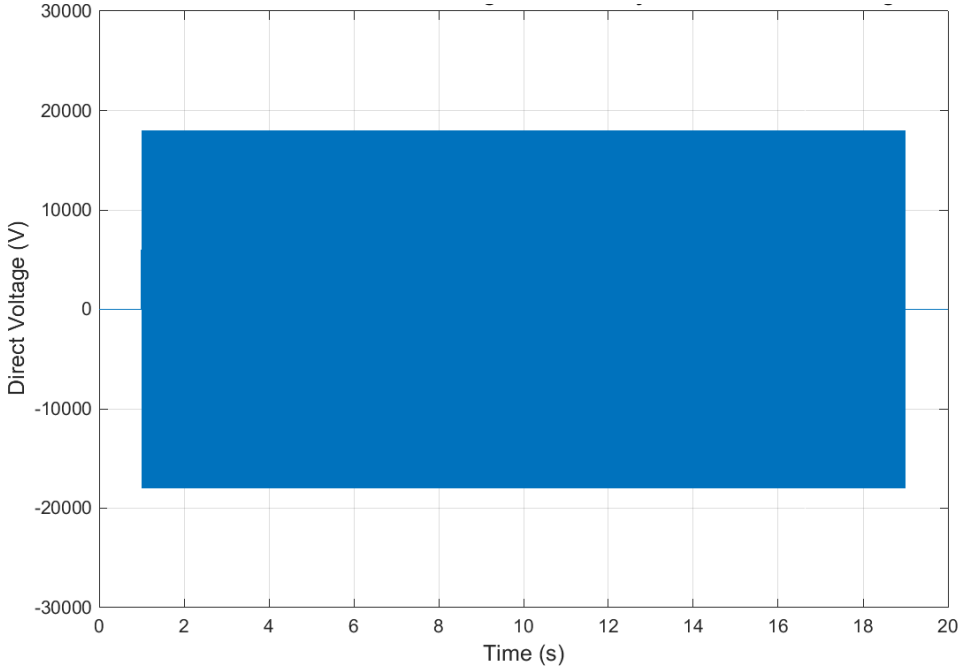

Figure 10 Test benchmark 1 –direct voltage time history – continuous recording

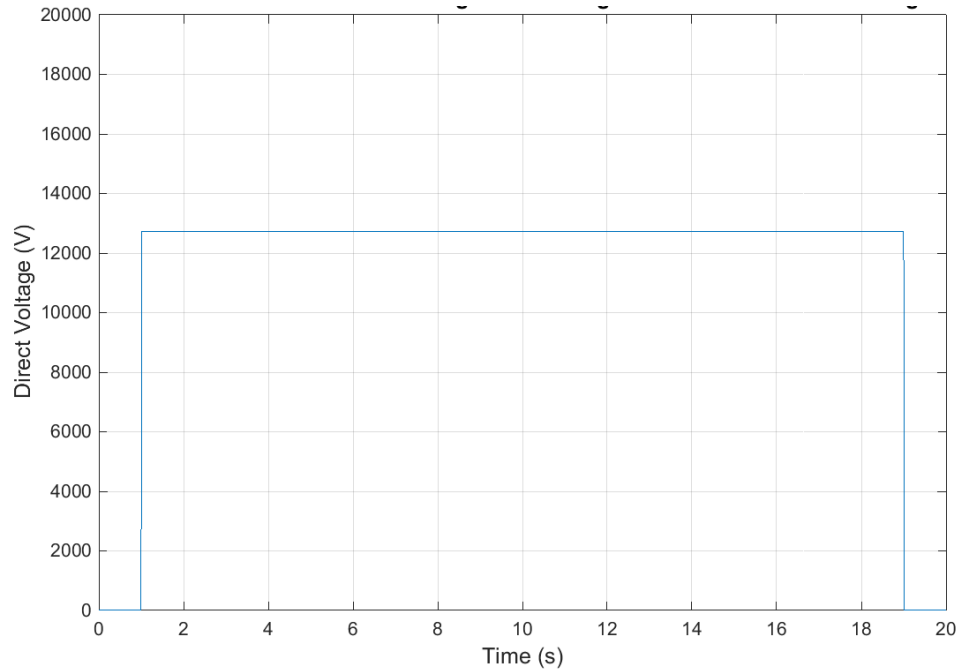

Figure 11 Test benchmark 1 - direct voltage RMS rolling 10ms - continuous recording

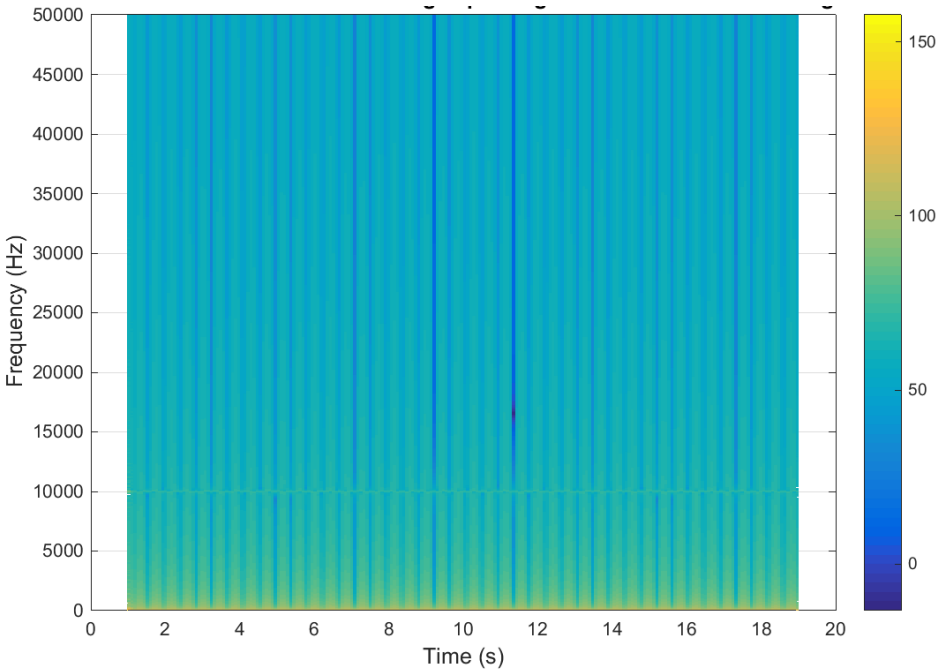

Figure 12 Test benchmark 1 - direct voltage spectrogram - continuous recording

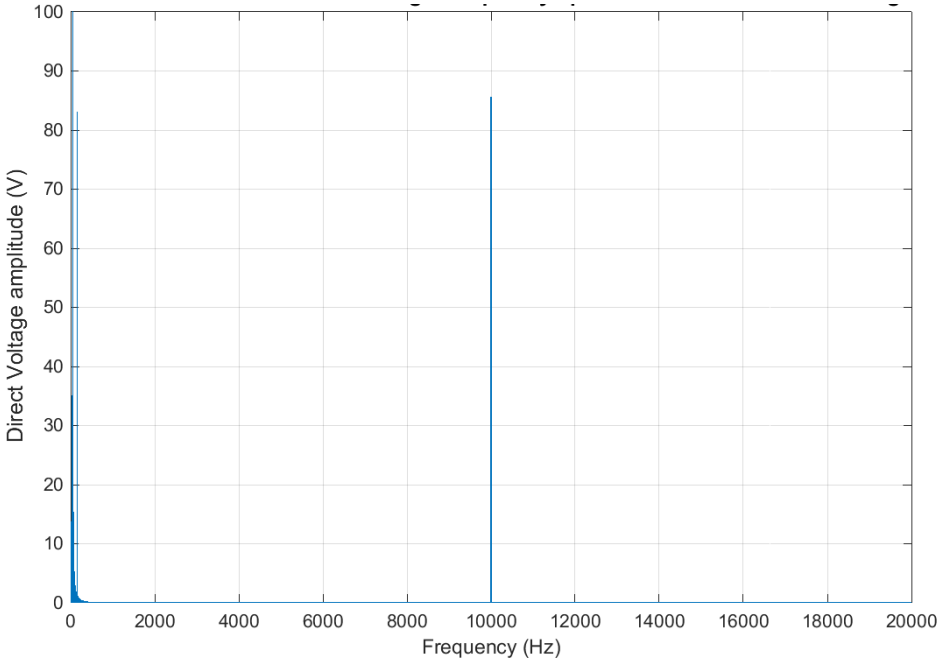

Figure 13 Test benchmark 1 - direct voltage frequency spectrum - continuous recording

6.2.3 Test 2 – High frequency voltage

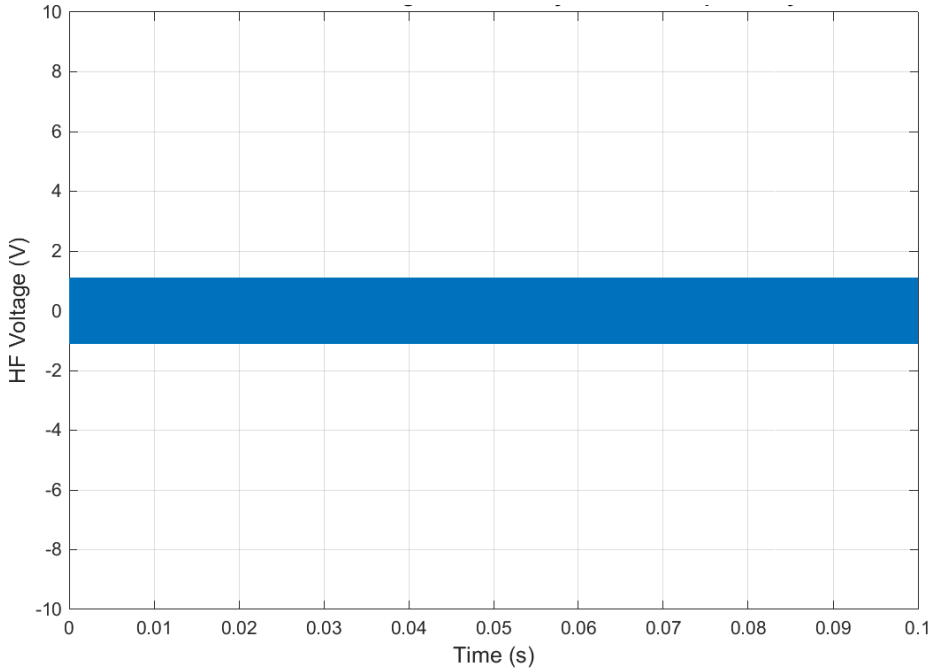

Figure 14 test benchmark 2 - HF time history - 20ms sweeps, every second

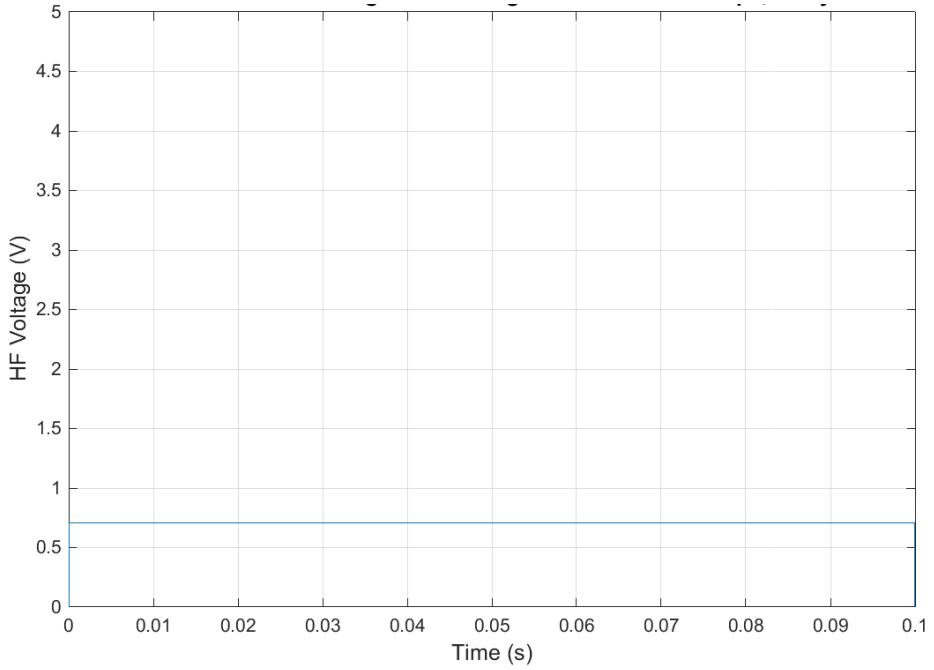

Figure 15 Test benchmark 2 - HF voltage RMS rolling 0.05ms - 20ms sweeps, every second

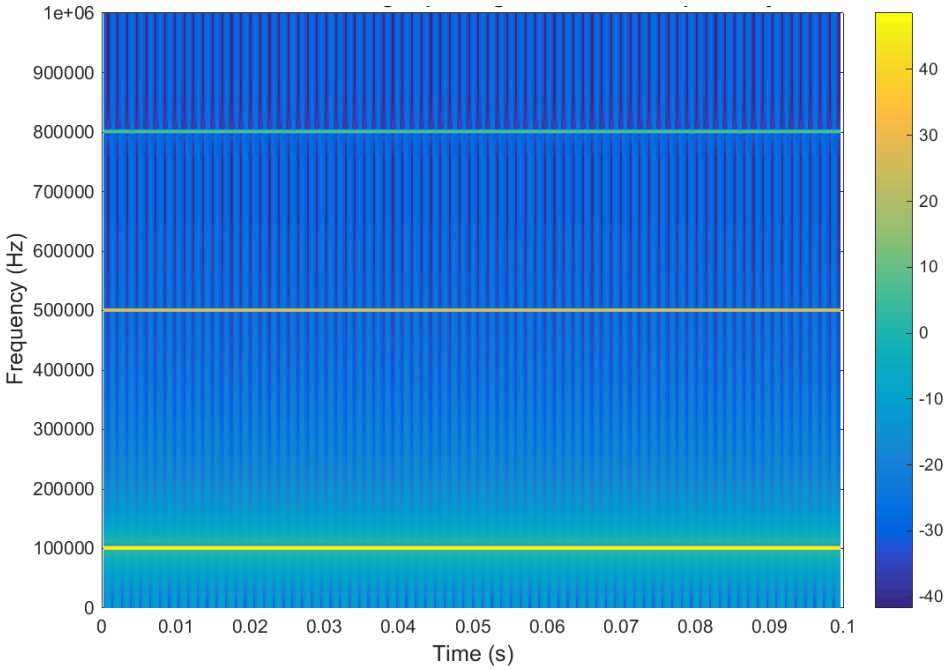

Figure 16 Test benchmark 2 - HF voltage spectrogram - 20ms sweeps, every second

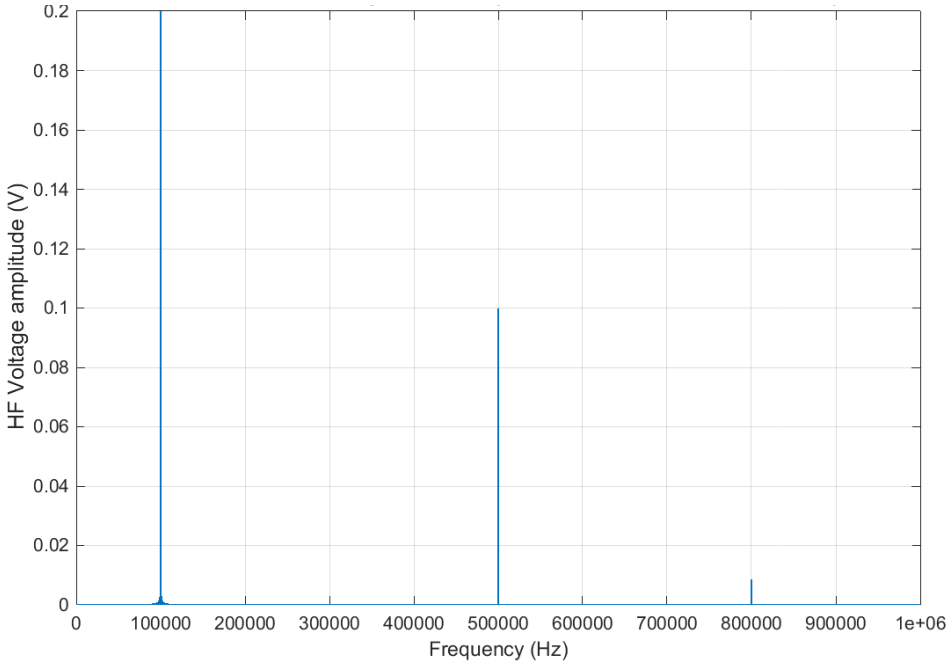

Figure 17 Test benchmark 2 - HF voltage frequency spectrum - 20ms sweeps, every second

6.2.4 Test 3 – Direct current

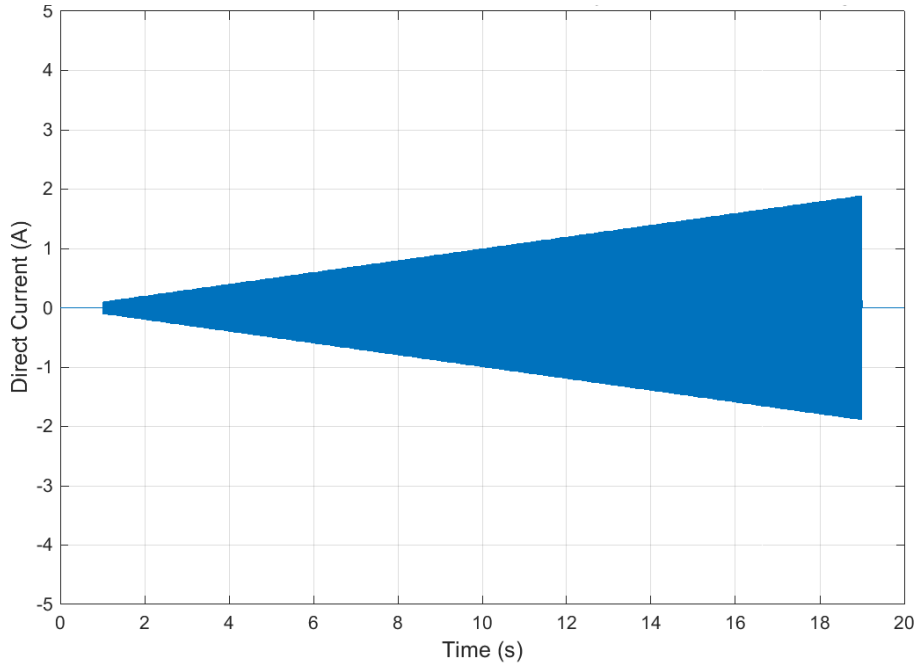

Figure 18 Test benchmark 3 - direct current time history - continuous recording

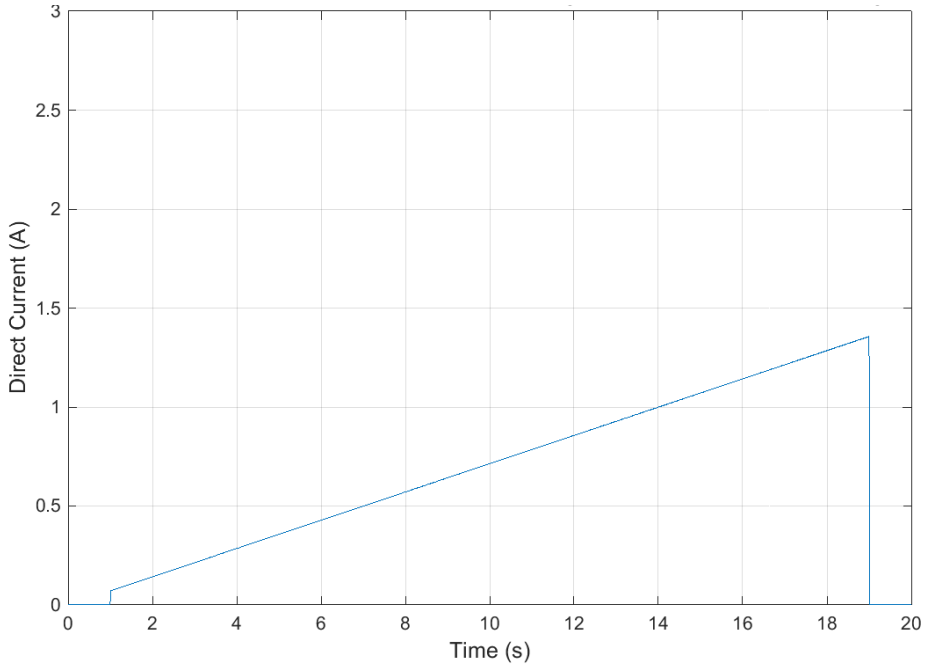

Figure 19 Test benchmark 3 direct current RMS rolling 10ms - continuous recording

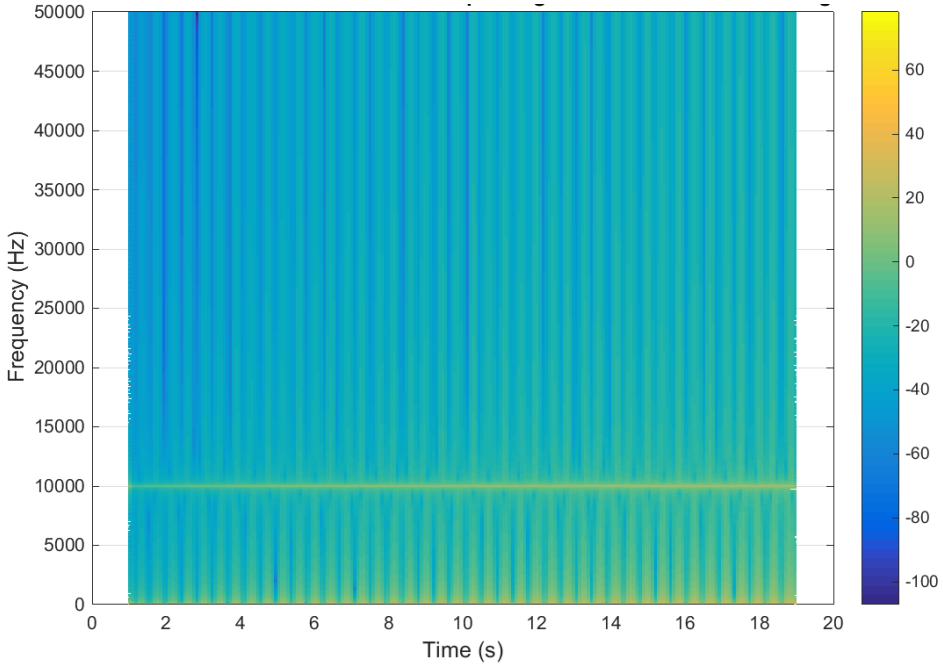

Figure 20 Test benchmark 3 - direct current spectrogram - continuous recording

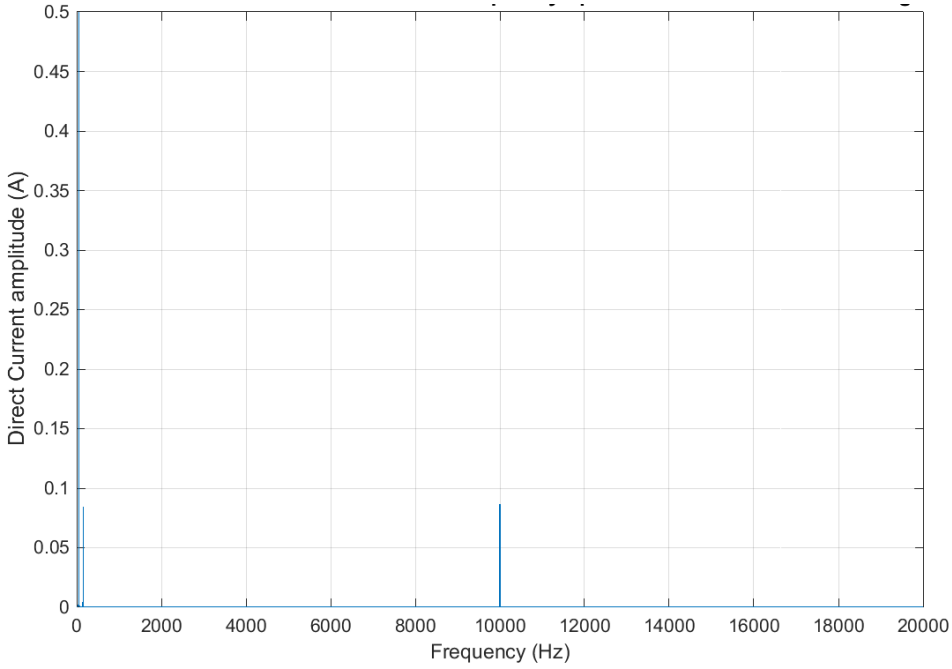

Figure 21 Test benchmark 3 - direct current frequency spectrum - continuous recording

6.2.5 Test 4 – High frequency current

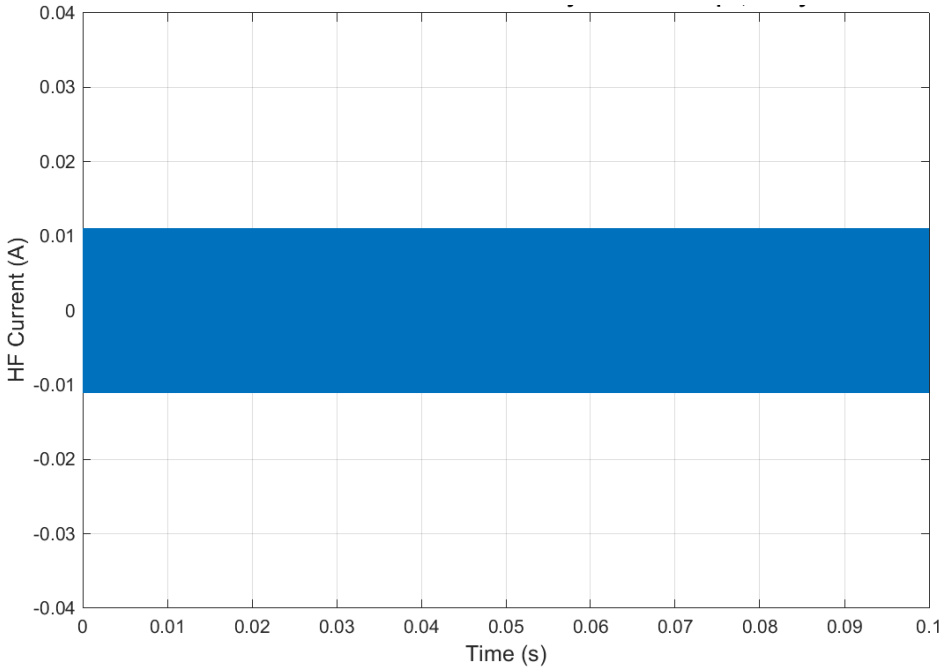

Figure 22 Test benchmark 4 - HF current history - 20ms sweeps, every second

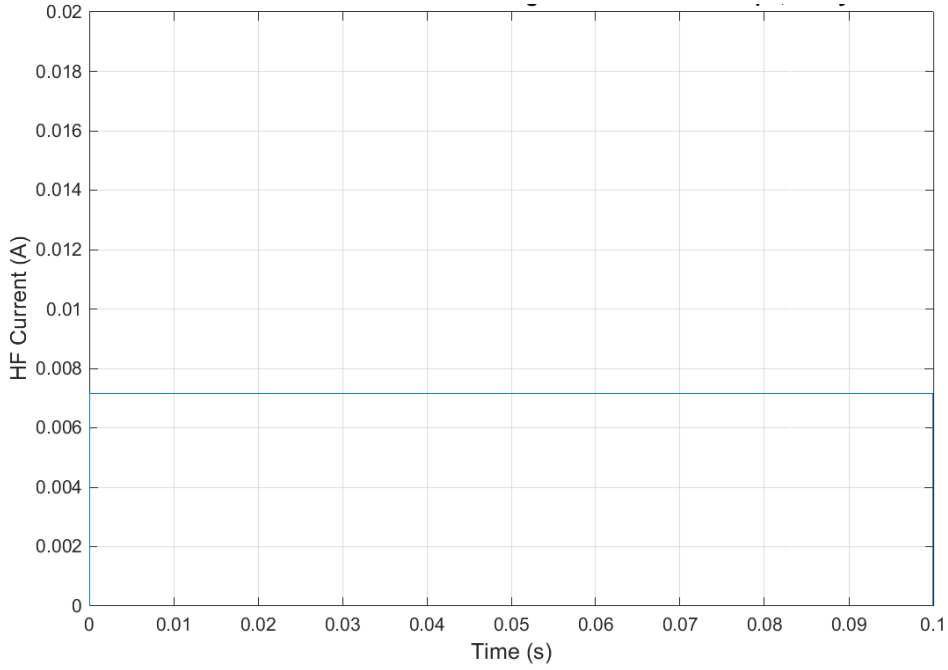

Figure 23 Test benchmark 4 - HF current RMS rolling 0.05ms - 20ms sweeps, every second

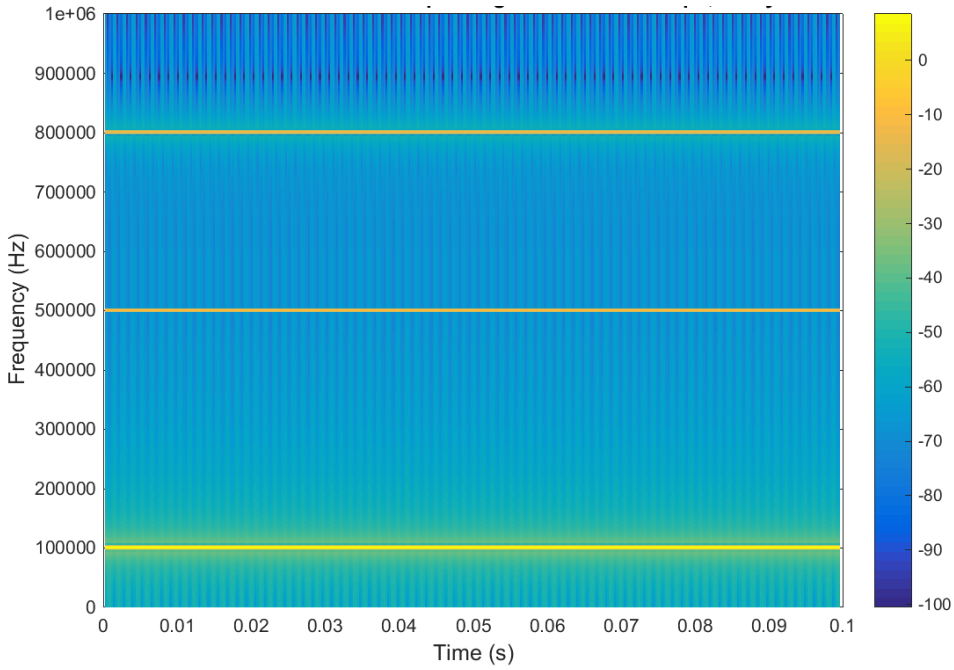

Figure 24 Test benchmark 4 - HF current spectrogram - 20ms sweeps, every second

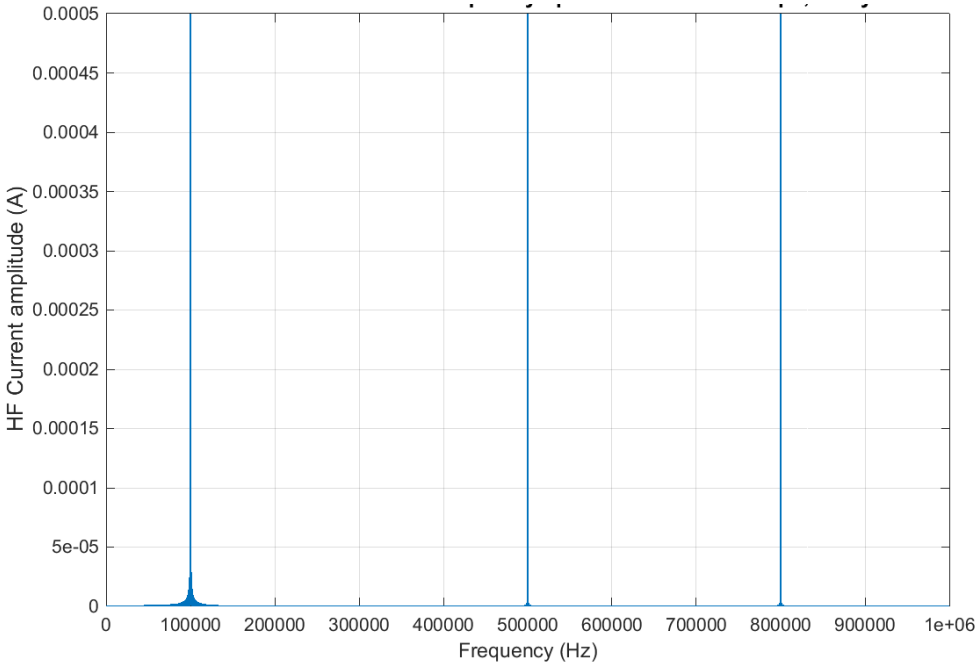

Figure 25 Test benchmark 4 - HF current frequency spectrum - 20ms sweeps, every second

6.3 Matlab Code

This section contains the Matlab script used to collect and analyse data and to produce graphs from the testing data. It should be noted that some formatting may not have carried across from the Matlab file and so the relevant Matlab file should be sought for clarification.

```
%% VT_data_processing_v12_SC
%This code was produced by HRL Technology for the Vegetation Testing
%Program run at Springvale substation in the summer of 2015.  It's
```

```
%purpose was to quickly and efficiently produce a vast amount of plots
%to help in the interpretation of the data from the testing.
%Authors of this code are Marc Listmangof and Samuel Creek.


% Version 12 - Mid time code altered so as to properly find the
% appropriate mid time for the HF data.
% Various graph comments added.
% Spectrogram code amended.
% FFT's plotted as log scales and in 3 different viewing ranges.
% Other minor changes.
% RMS plots altered to plot 3 detailed plots alongside the Time History
% details.
% Butterworth filter removed.

% Version 11 - HF and LF times aligned.  Multiple scaled FFT plots added.
% Multiple minor notes added. Spectrogram code adjustments made as per
%Mathworks' suggestions. Output folder changed to 'Version 5'.

% Version 10 - HF charts fixed. Note added about filter box not being
% earthed between test 1 to 47, for all the HF current charts (time
% history, RMS, FFT, spectrogram). FFT charts updated with new length
% windows (40,000 and 100,000) of the Hamming type. Added note about
% stitching of data (Note2). Enable 50kHz high pass filter for HF voltage
% for time histories, RMS and spectrogram (not FFT). Now outputs to folder
% 'Version 4'

%Version 9 - Changes made to graphs at Tony's request.  Batch processing to
%create zoomed mid, start and end time of lf complete.  (hf time histories
%and fft's still need to be completed)
%
% Version 8 - Changes the HF spectrogram settings to 16384,8192,16384 and
reruns all graphs
% into version 3 folder. This one runs a batch on the FEA machine.
% VERSION 7 - Adds a high pass filter to the HF voltage channel to
eliminate
% the 600Hz and 12kHz background noise in the network. Adds skip_sweep
% factor which automatically skips every nth sweep depending on the data
duration.
% This eliminates the need to ever down sample the data. Fixed time axis
for the
% stitched HF charts. Adds different windows size inputs into the
spectrogram depending on
% whether it's continuous data or sweeps data. Added option to skip the
% downsampling code entirely to save processing time.
% Version 6 - Adds a line to copy across the new .pnrf file from shared
folder
% into the DSDBI Data folder to save the user from doing this manually each
time.
% Version 5 - Adds a high pass filter for the high frequency current
channel
% 13-2-15 - At end of day, line 'sf = surf(T,F,10*log10(abs(S)));' changed
% to 'sf = surf(T,F,20*log10(abs(S)));'

%% INITIALISE
clear all;
close all;
clc;
```

```
Files_to_process = [711, 713, 722:726, 747, 750, 765, 778, 849, 925, 930,
1036];%[503:521, 523:541, 543:545, 547:554, 556:559, 561, 563:564,
567,568,571,574:581, 586:587, 589:610, 612:614, 616:617, 621:622, 628,
630:631, 635,636,641:645,647:649, 656,657, 662,668:671, 674:702, 704:708,
712, 714:721, 727:746, 748:749, 751:764, 766:777, 779:848, 850:891,
893:929, 931:1035];%[14:28, 30:50, 52:84, 86:104, 106:164, 166:251,
253:329, 331:341, 343:352, 354:373, 375:422, 424:477, 479, 481, 486];
%Files that don't exist/errors occurred = 85,105,330 - Perception file
internal error/format problems,

Output_folder = 'Version 7';

% Chose which charts to process. Y for yes and N for no.
Time_history_chart = 'N';
RMS_chart = 'Y';
FFT_chart = 'N';
Spectrogram_chart = 'Y';

% Choose whether to downsample the data. This is not necessary anymore,
% since 'skip_sweeps' was implemented.
Downsample_data = 'N';

time_array_start = 0; % Units: seconds

%Select Y to align the LF charts with the HF charts, otherwise select N for
%them to plot as they are.
aligned_details = 'Y';

% continuous recording parameters
f_sample_continuous = 100000;   % 100 kS/S
f_downsampled_continuous = 100000; % 100 kS/s
downsampling_ratio_continuous =
f_sample_continuous/f_downsampled_continuous;

% Sweep recording parameters
f_sample_sweep = 2000000; % 2 MS/s
f_downsampled_sweep = 2000000; % 2 MS/s. Change to 200kS/s if Matlab is
struggling.
downsampling_ratio_sweep = f_sample_sweep/f_downsampled_sweep;

sweep_skips = 1; % This factor determines how much of the sweep data to
use. 1 will not skip any sweeps, 2 will skip every 2nd sweep, 3 will skip
every 3rd sweep, and so on...

Recorder = 1; % Recorder number.1=R_A, 2=R_B

%     Import Type
%     1 = DataSourceSelect_Continuous
%     2 = DataSourceSelect_Sweeps
%     3 = DataSourceSelect_Mixed

Import_type_string = {'continuous recording', '20ms sweeps, every second'};
Import_type_select = [2];   % Import continuous data, then sweeps in next
loop. Use [1,2] for both.

% The sweeps parameters were changed during testing:
% Test 1 to 7 had 10ms sweeps every 2 seconds.
% Test 8 to 13 had 10ms sweeps every 1 second.
```

```
% Test 14 onwards had 20ms sweeps every 1 second.

% Channel #     Channel Name
% 1             Direct/LF Voltage
% 2             HF Voltage
% 3             Direct/LF Current
% 4             HF Current

Channel_select_continuous = [1,3];  % For both continuous channels use
[1,3].
Channel_select_sweep = [2,4];   % For both HF sweep channels use [2,4].

RMS_rolling_window_time = [10,0.05,10,0.05];   % In milliseconds. Four
elements corresponding to channel numbers

%Batch run graph limits for appropriate channels
y_limits_raw = {[-30000 30000], [-10 10], [-5 5], [-0.04 0.04]};
y_limits_RMS = {[0 20000], [0 5], [0 3], [0 0.02]};
y_limits_spectrogram = {[0 1000], [0 1000000], [0 2000], [0 1000000]};
y_limits_fft = {[0 250], [0 1.0], [0 1.0], [0 0.001]};
x_limits_fft = {[0 1000],[0 20000],[0 1000],[0 20000];[1000 10000],[20000
200000],[1000 10000],[20000 200000]; [10000 50000],[200000 1000000],[10000
50000],[200000 1000000]};
frequency_range = {'Low Frequency Range'; 'Middle Frequency Range'; 'High
Frequency Range'}; %for fft plot headings
RMS_range = {'Start Point'; 'Mid Point'; 'End Point'};

lf_zoom_window = 10000;     %LF zoom window, 10000 samples, equivalent to
0.1s
hf_zoom_window = 40000;     %HF zoom window, 40000 samples, 1 sweep/20ms

scrsz = get(0,'ScreenSize');    %Get the screen size for plotting later

% Initialise variables
data_downsampled_combined = [];

% Add note on charts between test 1 and 47 to say that the hi-pass filter
% box in the shunt enclosure wasn't earthed
Note1 = 'NOTE: High pass filter enclosure not earthed. Data may be
contaminated';
Note2 = ['WARNING: Data shown is for 20ms sweeps recorded every second and
placed end-to-end.  Data between sweeps (98% of total duration) is not
shown', char(10), 'Time axis value shows position of sweep in test and does
not indicate time scale within sweep data.  Refer to project report for
interpretation.'];
Note3 = 'NOTE: Data filtered with a 50kHz high pass filter';


%% IMPORT PNRF DATA FILE
%Access .pNRF file format reader
FromDisk = actxserver('Perception.Loaders.pNRF');
FromDisk.get;
FromDisk.invoke;

for File = Files_to_process

    Filename = strcat('C:\Jobs\DSDBI Vegetation Testing program\Data\VT',
num2str(File,'%03i'), '.pnrf');
```

```
    %Access all relevant data for file
    MyData = FromDisk.LoadRecording(Filename);
    MyData.get;
    MyData.invoke;
    MyData.Recorders.get;
    MyData.Recorders.invoke;

    MyData.Recorders.Item(Recorder).get;
    MyData.Recorders.Item(Recorder).invoke;
    MyData.Recorders.Item(Recorder).Channels.get;
    MyData.Recorders.Item(Recorder).Channels.invoke;

    %Create output folder for graphs
    if exist(strcat(['C:\Jobs\DSDBI Vegetation Testing program\Data
Processing\', Output_folder, '\Test ', num2str(File,'%03i')]), 'dir') == 0
        mkdir(strcat(['C:\Jobs\DSDBI Vegetation Testing program\Data
Processing\', Output_folder, '\Test ', num2str(File,'%03i')]));
    end

    %% DETERMINING MID-TIME CURRENT SIGNAL

        %% IMPORT LF CURRENT & HF CURRENT CHANNELS OF DATA
        for Channel = [3:4]

            % Set parameters depending on the import type
            if Channel == 3 % LF Current data (continous)
                Import_type = 1;
                Channel_select = Channel_select_continuous;
                downsampling_ratio = downsampling_ratio_continuous;
                f_downsampled = f_downsampled_continuous;
            elseif Channel == 4 % HF Current data (sweeps)
                Import_type = 2;
                Channel_select = Channel_select_sweep;
                downsampling_ratio = downsampling_ratio_sweep;
                f_downsampled = f_downsampled_sweep;

            else fprintf('Selected import type not supported\n')
            end

            %Accessing .pNRF data for particular channel
            MyData.Recorders.Item(Recorder).Channels.Item(Channel).get;
            MyData.Recorders.Item(Recorder).Channels.Item(Channel).invoke;

            ItfData =
MyData.Recorders.Item(Recorder).Channels.Item(Channel).DataSource(Import_ty
pe);
            ItfData.get;
            ItfData.invoke;

            sweep_times = ItfData.Sweeps.get;

            StartTime = sweep_times.StartTime;
            EndTime = sweep_times.EndTime;
            SegmentsOfData = ItfData.Data(StartTime, EndTime);
            SegmentsOfData.get;
            SegmentsOfData.invoke;
```

```
            SegmentsOfData.Item(1).get;
            SegmentsOfData.Item(1).invoke;

            DataSourceResultType = 4;   % The data can be retrieved as
floating point data (4), integer data (2) and original data (-1).
            FirstSample = 1;    % the first sample to retrieve
            ResultCount = 10000000;    % the number of samples to retrieve.
10 million points.
            Reduction = 1; % reduction factor
            n=1; %Keep track of data points to import

            % Segments of data to skip for the sweeps imports - none for
this
            % case
            sweep_skips = 1;
            reduction_factor_text = '';


            %% Import all data segments for current channel
            for Segment = 1:sweep_skips:SegmentsOfData.Count

                % Import the first 10M lines of data segment
                fprintf('Importing channel %d, data segment %d\n', Channel,
Segment);
                WaveformData{Segment} =
SegmentsOfData.Item(Segment).Waveform(DataSourceResultType, FirstSample,
ResultCount, Reduction);
                data = WaveformData{1, Segment};

                % While the current data segment is a full 10M points. This
                % part of the code should run for the continious type
import
                while length(data) == ResultCount

                    % Choose whether to downsample the data
                    if strcmp(Downsample_data,'Y') == 1
                        fprintf('Downsampling channel %d, data segment
%d\n', Channel, Segment);
                        Data_downsampled =
zeros(floor(length(data)/downsampling_ratio), 1);   % Initliase the array
                        y=1;
                        for x = 1:downsampling_ratio:length(data)
                            Data_downsampled(y) =
mean(data(x:x+downsampling_ratio-1));
                            y=y+1;
                        end
                    else % If data is not downsampled,
                        Data_downsampled = data;
                    end

                    % Insert the latest part of the latest data segment
into the combined array
                    data_downsampled_combined = [data_downsampled_combined
Data_downsampled];

                    % Import the next 10M data points of the current data
                    % segment
                    n = n + ResultCount;    % Increment the data index
```

```
                    WaveformData{Segment} =
SegmentsOfData.Item(Segment).Waveform(DataSourceResultType, FirstSample+n,
ResultCount, Reduction);
                    data = WaveformData{1, Segment};
                end

                % If the current chunk of the segment of data is less than
10
                % million points. This part of the code should run for the
                % sweeps imports
                if length(data) < ResultCount

                    % Choose whether to downsample the data
                    if strcmp(Downsample_data,'Y') == 1
                        fprintf('Downsampling channel %d, data segment
%d\n', Channel, Segment);

                        %First remove small bit of data at end of array
that is after the
                        %largest factor of the downsampled_ratio_sweep
                        remove = mod(length(data), downsampling_ratio);

                        Data_downsampled =
zeros(floor(length(data)/downsampling_ratio), 1);   % Initliase the array
                        y=1;
                        for x = 1:downsampling_ratio:length(data)-remove
                            Data_downsampled(y) =
mean(data(x:x+downsampling_ratio-1));
                            y=y+1;
                        end

                    else % If data is not downsampled,
                        Data_downsampled = data;
                    end

                    % Insert the latest chunk of the latest data segment
into the combined array
                    data_downsampled_combined = [data_downsampled_combined
Data_downsampled];

                else fprintf('No data!\n');
                end

            end



            %%  Creating Detailed Window Boundaries

            data = data_downsampled_combined;
            T = 1/f_downsampled;                    % Sample time
            L = length(data);                     % Length of signal


            if Channel == 3
                % Find the start and end time of the current signal and
write to
```

```
                % excel file
                start_current_index = find(abs(data)>0.02, 20);
                end_current_index = find(abs(data)>0.02, 20, 'last');
                start_current_index =
start_current_index(1,length(start_current_index));
                end_current_index = end_current_index(1,1);
                current_start_time =
start_current_index/f_downsampled+time_array_start;
                current_end_time =
end_current_index/f_downsampled+time_array_start;
                current_duration = current_end_time - current_start_time;
                current_duration_index = end_current_index -
start_current_index;
                flashover_start_index = find(abs(data)>10, 1);
                flashover_start_time = flashover_start_index/f_downsampled
+time_array_start;

                % Write start and end of the current signal times to an
excel
                % spreadsheet
                xlfilename = 'Current start times2.xlsx';

                %Writing of headings
                if File == 1
                    xlswrite(xlfilename, 'Test File Number', 1, 'A1');
                    xlswrite(xlfilename, 'Current Start Time (s)', 1,
'B1');
                    xlswrite(xlfilename, 'Current End Time (s)', 1, 'C1');
                    xlswrite(xlfilename, 'Current Duration (s)', 1, 'D1');
                    xlswrite(xlfilename, 'Flashover Start Time (s)', 1,
'E1');
                end

                xlrow = File + 1;
                %Writing of data
                xlswrite(xlfilename, File, 1, strcat(['A',
num2str(xlrow)]));
                xlswrite(xlfilename, current_start_time, 1, strcat(['B',
num2str(xlrow)]));
                xlswrite(xlfilename, current_end_time, 1, strcat(['C',
num2str(xlrow)]));
                xlswrite(xlfilename, current_duration, 1, strcat(['D',
num2str(xlrow)]));
                if(isempty(flashover_start_index) == 1)
                else
                    xlswrite(xlfilename, flashover_start_time, 1,
strcat(['E', num2str(xlrow)]));
                end

                %% LF Zoom Window

                %Mid Current - LF detail window
                lf_current_mid_time_index =
round((current_duration_index/2)) + start_current_index;
                lf_current_mid_time =
lf_current_mid_time_index/f_downsampled;

                lf_mid_window_end_index = lf_current_mid_time_index +
(lf_zoom_window/2);
```

```
                lf_mid_window_start_index = lf_current_mid_time_index -
(lf_zoom_window/2);

                lf_mid_window_end_time =
lf_mid_window_end_index/f_downsampled;
                lf_mid_window_start_time =
lf_mid_window_start_index/f_downsampled;

                lf_mid_data_end_index = lf_mid_window_end_index;
                lf_mid_data_start_index = lf_mid_window_start_index;

                %Initial Current - LF detail window
                lf_start_window_start_index = start_current_index -
(lf_zoom_window/4);
                lf_start_window_end_index = lf_start_window_start_index +
(lf_zoom_window*(3/4));

                lf_start_window_start_time =
lf_start_window_start_index/f_downsampled;
                lf_start_window_end_time =
lf_start_window_end_index/f_downsampled;

                %Final Current - LF detail window (accounting for
flashover)
                if (isempty(flashover_start_index) == 1) %if flashover has
not occurred
                    lf_end_window_end_index = end_current_index +
(lf_zoom_window/4);
                    lf_end_window_start_index = lf_end_window_end_index -
(lf_zoom_window*(3/4));

                    lf_end_window_end_time =
lf_end_window_end_index/f_downsampled;
                    lf_end_window_start_time =
lf_end_window_start_index/f_downsampled;
                else %if flashover has occurred
                    lf_end_window_end_index = flashover_start_index +
(lf_zoom_window/4);
                    lf_end_window_start_index = lf_end_window_end_index -
(lf_zoom_window*(3/4));

                    lf_end_window_end_time =
lf_end_window_end_index/f_downsampled;
                    lf_end_window_start_time =
lf_end_window_start_index/f_downsampled;
                end
            end


            %% HF Zoom Window
            if Channel == 4

                f_downsampled = f_downsampled_sweep;

                %Mid current zoom window - time history chart
                hf_mid_window_start_index = ((round(lf_current_mid_time)-1)
* (f_downsampled/(sweep_skips*50)))+1;
```

```
                hf_mid_window_end_index = hf_mid_window_start_index +
hf_zoom_window-1;

                hf_mid_window_start_time = StartTime +
hf_mid_window_start_index/(f_downsampled/(sweep_skips*50));
                hf_mid_window_end_time = StartTime +
hf_mid_window_end_index/(f_downsampled/(sweep_skips*50));

                %Start current zoom window - time history chart
                hf_start_window_start_index =
((ceil(lf_start_window_start_time)-1) *(f_downsampled/(sweep_skips*50)))+1;
                hf_start_window_end_index = hf_start_window_start_index +
hf_zoom_window-1;

                hf_start_window_start_time = StartTime +
hf_start_window_start_index/(f_downsampled/(sweep_skips*50));
                hf_start_window_end_time = StartTime +
hf_start_window_end_index/(f_downsampled/(sweep_skips*50));

                %End current zoom window - time history chart
                hf_end_window_start_index =
(floor(lf_end_window_end_time)*(f_downsampled/(sweep_skips*50)))+1;
                hf_end_window_end_index = hf_end_window_start_index +
hf_zoom_window-1;

                hf_end_window_start_time = StartTime +
hf_end_window_start_index/(f_downsampled/(sweep_skips*50));
                hf_end_window_end_time = StartTime +
hf_end_window_end_index/(f_downsampled/(sweep_skips*50));

            %%  LF DETAILS ALIGNED
            %   For the alignment of the LF details to the HF details

            %Mid Current - LF detail window
                alf_mid_window_start_index =
round(hf_mid_window_start_time*f_downsampled_continuous);
                alf_mid_window_start_time =
alf_mid_window_start_index/f_downsampled_continuous;
                alf_mid_window_end_index = alf_mid_window_start_index +
lf_zoom_window;
                alf_mid_window_end_time =
alf_mid_window_end_index/f_downsampled_continuous;

                %Initial Current - LF detail window
                alf_start_window_start_index =
round(hf_start_window_start_time*f_downsampled_continuous);
                alf_start_window_start_time =
alf_start_window_start_index/f_downsampled_continuous;
                alf_start_window_end_index = alf_start_window_start_index +
lf_zoom_window;
                alf_start_window_end_time =
alf_start_window_end_index/f_downsampled_continuous;

                %Final Current - LF detail window (accounting for
flashover)
                alf_end_window_start_index =
round(hf_end_window_start_time*f_downsampled_continuous);
```

```
                alf_end_window_start_time =
alf_end_window_start_index/f_downsampled_continuous;
                alf_end_window_end_index = alf_end_window_start_index +
lf_zoom_window;
                alf_end_window_end_time =
alf_end_window_end_index/f_downsampled_continuous;

            end

            % Clear variables for next run
            clear data;
            clear data_downsampled_combined;
            clear data_length;
            clear time_array;
            clear WaveformData;
            data_downsampled_combined = [];

        end


    %% IMPORT INDIVIDUAL CHANNELS OF DATA

for Import_type = Import_type_select

    % Set parameters depending on the import type
    if Import_type == 1 % Continious data
        Channel_select = Channel_select_continuous;
        downsampling_ratio = downsampling_ratio_continuous;
        f_downsampled = f_downsampled_continuous;
    elseif Import_type == 2 % Sweeps data
        Channel_select = Channel_select_sweep;
        downsampling_ratio = downsampling_ratio_sweep;
        f_downsampled = f_downsampled_sweep;
        %spectrogram_f_downsampled = f_downsampled/50;   % For the
spectrogram X axis.
    else fprintf('Selected import type not supported\n')
    end

for Channel = Channel_select

        MyData.Recorders.Item(Recorder).Channels.Item(Channel).get;
        MyData.Recorders.Item(Recorder).Channels.Item(Channel).invoke;

        ItfData =
MyData.Recorders.Item(Recorder).Channels.Item(Channel).DataSource(Import_ty
pe);
        ItfData.get;
        ItfData.invoke;

        sweep_times = ItfData.Sweeps.get;

        StartTime = sweep_times.StartTime;
        EndTime = sweep_times.EndTime;
        SegmentsOfData = ItfData.Data(StartTime, EndTime);
        SegmentsOfData.get;
        SegmentsOfData.invoke;

        SegmentsOfData.Item(1).get;
```

```
        SegmentsOfData.Item(1).invoke;

        DataSourceResultType = 4;   % The data can be retrieved as floating
point data (4), integer data (2) and original data (-1).
        FirstSample = 1;    % the first sample to retrieve
        ResultCount = 10000000;    % the number of samples to retrieve. 10
million points.
        Reduction = 1; % reduction factor
        n=1; %Keep track of data points to import

        % The following factors determine how many segments of data to skip
for the sweeps imports
            sweep_skips = 1;
            reduction_factor_text = '';


        %% Import all data segments for current channel
        for Segment = 1:sweep_skips:SegmentsOfData.Count

            % Import the first 10M lines of data segment
            fprintf('Importing channel %d, data segment %d\n', Channel,
Segment);
            WaveformData{Segment} =
SegmentsOfData.Item(Segment).Waveform(DataSourceResultType, FirstSample,
ResultCount, Reduction);
            data = WaveformData{1, Segment};

            % While the current data segment is a full 10M points. This
            % part of the code should run for the continious type import
            while length(data) == ResultCount

                % Chose whether to downsample the data
                if strcmp(Downsample_data,'Y') == 1
                    fprintf('Downsampling channel %d, data segment %d\n',
Channel, Segment);
                    Data_downsampled =
zeros(floor(length(data)/downsampling_ratio), 1);   % Initliase the array
                    y=1;
                    for x = 1:downsampling_ratio:length(data)
                        Data_downsampled(y) =
mean(data(x:x+downsampling_ratio-1));
                        y=y+1;
                    end
                else % If data is not downsampled,
                    Data_downsampled = data;
                end

                % Insert the latest part of the latest data segment into
the combined array
                data_downsampled_combined = [data_downsampled_combined
Data_downsampled];

                % Import the next 10M data points of the current data
                % segment
                n = n + ResultCount;    % Increment the data index
                WaveformData{Segment} =
SegmentsOfData.Item(Segment).Waveform(DataSourceResultType, FirstSample+n,
ResultCount, Reduction);
```

```
                data = WaveformData{1, Segment};
            end

            % If the current chunk of the segment of data is less than 10
            % million points. This part of the code should run for the
            % sweeps imports
            if length(data) < ResultCount

                % Choose whether to downsample the data
                if strcmp(Downsample_data,'Y') == 1
                    fprintf('Downsampling channel %d, data segment %d\n',
Channel, Segment);

                    %First remove small bit of data at end of array that is
after the
                    %largest factor of the downsampled_ratio_sweep
                    remove = mod(length(data), downsampling_ratio);

                    Data_downsampled =
zeros(floor(length(data)/downsampling_ratio), 1);   % Initliase the array
                    y=1;
                    for x = 1:downsampling_ratio:length(data)-remove
                        Data_downsampled(y) =
mean(data(x:x+downsampling_ratio-1));
                        y=y+1;
                    end

                else % If data is not downsampled,
                    Data_downsampled = data;
                end

                % Insert the latest chunk of the latest data segment into
the combined array
                data_downsampled_combined = [data_downsampled_combined
Data_downsampled];

            else fprintf('No data!\n');
            end

        end

        %%  DATA PROCESSING AND CHARTING

        data = data_downsampled_combined;
        T = 1/f_downsampled;                    % Sample time
        L = length(data);                     % Length of signal

        % Create the time array
        if Import_type == 1     % For continious data, create the time
array
            time_array_end = (L-1)/f_downsampled+time_array_start;
            time_array = time_array_start:1/f_downsampled:time_array_end;
        elseif Import_type == 2     % For sweeps data, the effective
frequency is f_downsampled/(50*sweep_skips) for 20ms sweeps
            time_array_start = StartTime;
            time_array_end = (L-
1)/(f_downsampled/(sweep_skips*50))+time_array_start;
```

```
            time_array =
time_array_start:1/(f_downsampled/(sweep_skips*50)):time_array_end;
        end


        %Change data title to LF instead of direct, if neccessary
        titlecheck = ItfData.Name(1:2);
        if strcmp(titlecheck,'HF') == 1;
            Graphtitle = ItfData.Name;
        else
            finalchar = length(ItfData.Name);
            Graphtitle = strcat('LF', ItfData.Name(7:finalchar));
        end

        Test_number_str = MyData.title;
        Test_no = Test_number_str(isstrprop(Test_number_str,'digit'));


        %% Define zoomed windows to use for charting

        if Import_type == 1;    %LF channel detail windows

            if aligned_details == 'Y'
                mid_window_start_index = alf_mid_window_start_index;
                mid_window_end_index = alf_mid_window_end_index;
                end_window_start_index = alf_end_window_start_index;
                end_window_end_index = alf_end_window_end_index;
                start_window_start_index = alf_start_window_start_index;
                start_window_end_index = alf_start_window_end_index;
                mid_window_start_time = alf_mid_window_start_time;
                mid_window_end_time = alf_mid_window_end_time;
                end_window_start_time = alf_end_window_start_time;
                end_window_end_time = alf_end_window_end_time;
                start_window_start_time = alf_start_window_start_time;
                start_window_end_time = alf_start_window_end_time;
            else
                mid_window_start_index = lf_mid_window_start_index;
                mid_window_end_index = lf_mid_window_end_index;
                end_window_start_index = lf_end_window_start_index;
                end_window_end_index = lf_end_window_end_index;
                start_window_start_index = lf_start_window_start_index;
                start_window_end_index = lf_start_window_end_index;
                mid_window_start_time = lf_mid_window_start_time;
                mid_window_end_time = lf_mid_window_end_time;
                end_window_start_time = lf_end_window_start_time;
                end_window_end_time = lf_end_window_end_time;
                start_window_start_time = lf_start_window_start_time;
                start_window_end_time = lf_start_window_end_time;
            end

        elseif Import_type == 2;    %HF channel detail windows
            mid_window_start_index = hf_mid_window_start_index;
            mid_window_end_index = hf_mid_window_end_index;
            end_window_start_index = hf_end_window_start_index;
            end_window_end_index = hf_end_window_end_index;
            start_window_start_index = hf_start_window_start_index;
            start_window_end_index = hf_start_window_end_index;
            mid_window_start_time = hf_mid_window_start_time;
            mid_window_end_time = hf_mid_window_end_time;
```

```
            end_window_start_time = hf_end_window_start_time;
            end_window_end_time = hf_end_window_end_time;
            start_window_start_time = hf_start_window_start_time;
            start_window_end_time = hf_start_window_end_time;
        end

        if File == 1:13
            Test1to13_Note = [char(10), 'NOTE: Time scale may be incorrect.
Refer to test logs for sweep settings and adjust accordingly.'];
        else
            Test1to13_Note = '';
        end


        %% PLOT TIME HISTORY CHARTS
        if strcmp(Time_history_chart, 'Y')==1;

            %Plot zoomed time history of mid time history
            if or(Channel == 1, Channel == 3);
                time_array_zoomed =
mid_window_start_time:1/f_downsampled:mid_window_end_time;
            elseif or(Channel == 2, Channel == 4);
                time_array_zoomed =
mid_window_start_time:1/(f_downsampled/(sweep_skips*50)):mid_window_end_tim
e;
            end
            data_current_zoomed =
data(mid_window_start_index:mid_window_end_index);

            % Plotting
            figure('Position',[1 1 scrsz(3) scrsz(4)]);
            axes1 = axes('Parent',gcf, 'Position',[0.15 0.17 0.8 0.75]);
            plot(time_array_zoomed, data_current_zoomed)
            title(strcat(['Test ', num2str(Test_no), ' - ', Graphtitle, ' -
', 'Detail', ' - ', 'Mid Point']), 'interpreter', 'none', 'Fontsize', 12);
            ylabel(strcat(Graphtitle, ' (', ItfData.YUnit, ')' ),
'Fontsize', 12);
            set(gca,'xlim', [mid_window_start_time mid_window_end_time]);
            Y_ticks = get(gca,'YTick');
            set(gca,'YTickLabel',sprintf('%g\n',Y_ticks));
            set(gca, 'Xgrid','on', 'Ygrid','on');
            box on;
            if (Channel == 4) && (File <=47)
                text(time_array_zoomed(1), Y_ticks(1)-(Y_ticks(end)-
Y_ticks(1))*0.15, [Test1to13_Note, char(10), Note1], 'Fontsize', 8);
            elseif (Import_type == 2)
                text(time_array_zoomed(1), Y_ticks(1)-(Y_ticks(end)-
Y_ticks(1))*0.15, Test1to13_Note, 'Fontsize', 8);
            end

            if Import_type == 2
                xlabel('Time', 'Fontsize', 12);
                set(gca, 'xticklabel', {[]});
                text(time_array_zoomed(1), Y_ticks(1)-(Y_ticks(end)-
Y_ticks(1))*0.15, strcat('Note: Data shown is of one 20 ms sweep, sampled
at 2 MS/s, starting at: ', num2str(round(mid_window_start_time, 3)),
's'),'Fontsize', 8);
            else
                xlabel('Time (s)', 'Fontsize', 12);
```

```
            end

            saveas(gca,strcat(['Data Processing\', Output_folder, '\',
'Test ', num2str(Test_no),'\','Test ', num2str(Test_no), ' - ', Graphtitle,
' - Detail - Mid Point.png']));
            %close;

            % Plot zoomed time history of end signal
            if or(Channel == 1, Channel == 3);
                time_array_zoomed =
end_window_start_time:1/f_downsampled:end_window_end_time;
            elseif or(Channel == 2, Channel == 4);
                time_array_zoomed =
end_window_start_time:1/(f_downsampled/(sweep_skips*50)):end_window_end_tim
e;
            end
            data_current_zoomed =
data(end_window_start_index:end_window_end_index);

            %Plotting
            figure('Position',[1 1 scrsz(3) scrsz(4)]);
            axes1 = axes('Parent',gcf, 'Position',[0.15 0.17 0.8 0.75]);
            plot(time_array_zoomed, data_current_zoomed)
            title(strcat(['Test ', num2str(Test_no), ' - ', Graphtitle, ' -
Detail - End Point']), 'interpreter', 'none', 'Fontsize', 12);
            ylabel(strcat(Graphtitle, ' (', ItfData.YUnit, ')' ),
'Fontsize', 12);
            set(gca,'xlim', [end_window_start_time end_window_end_time]);
            Y_ticks = get(gca,'YTick');
            set(gca,'YTickLabel',sprintf('%g\n',Y_ticks));
            set(gca, 'Xgrid','on', 'Ygrid','on');
            box on;
            if (Channel == 4) && (File <=47)
                text(time_array_zoomed(1), Y_ticks(1)-(Y_ticks(end)-
Y_ticks(1))*0.15, [Test1to13_Note, char(10), Note1], 'Fontsize', 8);
            elseif (Import_type == 2)
                text(time_array_zoomed(1), Y_ticks(1)-(Y_ticks(end)-
Y_ticks(1))*0.15, Test1to13_Note, 'Fontsize', 8);
            end

            if Channel == 1
                text(time_array_zoomed(1), Y_ticks(1)-(Y_ticks(end)-
Y_ticks(1))*0.15, ['NOTE: Voltage values shown after the instant of
disconnection of the rig from HV supply are the result of stray' ,
char(10),'capacitance coupling and should be ignored.'], 'Fontsize', 8);
            end

            if Import_type == 2
                xlabel('Time', 'Fontsize', 12);
                set(gca, 'xticklabel', {[]});
                text(time_array_zoomed(1), Y_ticks(1)-(Y_ticks(end)-
Y_ticks(1))*0.15, strcat('Note: Data shown is of one 20 ms sweep, sampled
at 2 MS/s, starting at: ', num2str(round(end_window_start_time, 3)), 's'),
'Fontsize',8);
            else
                xlabel('Time (s)', 'Fontsize', 12);
            end
```

```
            saveas(gca,strcat(['Data Processing\', Output_folder, '\',
'Test ', num2str(Test_no),'\','Test ', num2str(Test_no), ' - ', Graphtitle,
' - ', 'Detail - End Point.png']));
            %close;

            % Plot zoomed time history of start signal
            if or(Channel == 1, Channel == 3);
                time_array_zoomed =
start_window_start_time:1/f_downsampled:start_window_end_time;
            elseif or(Channel == 2, Channel == 4);
                time_array_zoomed =
start_window_start_time:1/(f_downsampled/(sweep_skips*50)):start_window_end
_time;
            end
            data_current_zoomed =
data(start_window_start_index:start_window_end_index);

            %Plotting
            figure('Position',[1 1 scrsz(3) scrsz(4)]);
            axes1 = axes('Parent',gcf, 'Position',[0.15 0.17 0.8 0.75]);
            plot(time_array_zoomed, data_current_zoomed)
            title(strcat(['Test ', num2str(Test_no), ' - ', Graphtitle, ' -
Detail - Start Point']), 'interpreter', 'none', 'Fontsize', 12);
            ylabel(strcat(Graphtitle, ' (', ItfData.YUnit, ')' ),
'Fontsize', 12);
            set(gca,'xlim', [start_window_start_time
start_window_end_time]);
            Y_ticks = get(gca,'YTick');
            set(gca,'YTickLabel',sprintf('%g\n',Y_ticks));
            set(gca, 'Xgrid','on', 'Ygrid','on');
            box on;
            if (Channel == 4) && (File <=47)
                text(time_array_zoomed(1), Y_ticks(1)-(Y_ticks(end)-
Y_ticks(1))*0.15, [Test1to13_Note, char(10), Note1], 'Fontsize', 8);
            elseif (Import_type == 2)
                text(time_array_zoomed(1), Y_ticks(1)-(Y_ticks(end)-
Y_ticks(1))*0.15, Test1to13_Note, 'Fontsize', 8);
            end

            if Import_type == 2
                xlabel('Time', 'Fontsize', 12);
                set(gca, 'xticklabel', {[]});
                text(time_array_zoomed(1), Y_ticks(1)-(Y_ticks(end)-
Y_ticks(1))*0.15, strcat('Note: Data shown is of one 20 ms sweep, sampled
at 2 MS/s, starting at: ', num2str(round(start_window_start_time, 3)),
's'), 'Fontsize',8);
            else
                xlabel('Time (s)', 'Fontsize', 12);
            end

            saveas(gca,strcat(['Data Processing\', Output_folder, '\',
'Test ', num2str(Test_no),'\','Test ', num2str(Test_no) ' - ', Graphtitle,
' - Detail - Start Point.png']));
            %close;


            % Plot full time history of data
            figure('Position',[1 1 scrsz(3) scrsz(4)]);
            axes1 = axes('Parent',gcf, 'Position',[0.15 0.17 0.8 0.75]);
```

```
            plot(time_array, data)
            title(strcat([ 'Test ', num2str(Test_no), ' - ', Graphtitle]),
'interpreter', 'none', 'Fontsize', 12)
            xlabel('Time (s)', 'Fontsize', 12);
            ylabel(strcat(Graphtitle, ' (', ItfData.YUnit, ')' ),
'Fontsize', 12);
            if Import_type == 2 %use auto scaling for HF channels
            else
                set(gca,'ylim', y_limits_raw{Channel});
            end
            set(gca,'xlim', [time_array_start time_array_end]);
            Y_ticks = get(gca,'YTick');
            set(gca,'YTickLabel',sprintf('%g\n',Y_ticks));
            set(gca, 'Xgrid','on', 'Ygrid','on');
            box on;

            if (Channel == 4) && (File <=47)
                FTH_note1 = [char(10), Note1];
            else
                FTH_note1 = '';
            end
            if Import_type == 2     % If it's sweep data, provide warning
about stitching.
                FTH_note2 = [char(10), Note2];
                text(time_array_start-time_array_end*0.15, Y_ticks(1)-
(Y_ticks(end)-Y_ticks(1))*0.12, strcat(reduction_factor_text, FTH_note1,
FTH_note2, Test1to13_Note), 'Fontsize', 8);
            else
                FTH_note2 = '';
                text(time_array_start-time_array_end*0.152, Y_ticks(1)-
(Y_ticks(end)-Y_ticks(1))*0.12, reduction_factor_text, 'Fontsize', 8);
            end

            if Channel == 1
                text(time_array_start-time_array_end*0.152, Y_ticks(1)-
(Y_ticks(end)-Y_ticks(1))*0.12, ['NOTE: Voltage values shown after the
instant of disconnection of the rig from HV supply are the result of stray'
, char(10),'capacitance coupling and should be ignored.'], 'Fontsize', 8);
            end
            saveas(gca,strcat(['Data Processing\', Output_folder, '\',
'Test ', num2str(Test_no),'\', 'Test ', num2str(Test_no), ' - ',
Graphtitle, '.png']));
            %close;
        end


        %% CALCULATE RMS
        % Calculate the rolling 10ms RMS for each signal
        if strcmp(RMS_chart, 'Y')==1

            % 1. square values
            % 2. take 10ms rolling average
            % 3. square root values

            data_length = length(data);

            data_rolling_RMS = zeros(data_length,1);

            data_squared = (data(1:data_length)).^2;
```

```
            RMS_rolling_window_length =
(RMS_rolling_window_time(Channel)/1000)*f_downsampled;

            x=RMS_rolling_window_length;
            for t = (RMS_rolling_window_length/2+1):data_length-
RMS_rolling_window_length/2     % (first index+1) to last index -
rollig_window_length
                data_rolling_RMS(x) = sqrt(mean(data_squared(t-
RMS_rolling_window_length/2:t+(RMS_rolling_window_length/2-1))));  %
rolling RMS of data squared
                x=x+1;
            end

            % Plot rolling RMS of data for the full time history
            figure('Position',[1 1 scrsz(3) scrsz(4)]);
            axes1 = axes('Parent',gcf, 'Position',[0.15 0.17 0.8 0.75]);
            plot(time_array, data_rolling_RMS)
            title(strcat([ 'Test ', num2str(Test_no), ' - ', Graphtitle, '
- RMS rolling ', num2str(RMS_rolling_window_time(Channel)), 'ms']),
'interpreter', 'none', 'Fontsize', 12)
            xlabel('Time (s)', 'Fontsize', 12);
            ylabel(strcat(ItfData.Name, ' (', ItfData.YUnit, '_{rms})' ),
'Fontsize', 12);
            if Import_type == 1
                set(gca,'ylim', y_limits_RMS{Channel});
            end
            set(gca,'xlim', [time_array_start time_array_end]);
            set(gca, 'Xgrid','on', 'Ygrid','on');
            Y_ticks = get(gca,'YTick');
            set(gca,'YTickLabel',sprintf('%g\n',Y_ticks));
            box on;

            if (Channel == 4) && (File <= 47)
                RMS_note1 = [char(10), Note1];
            else
                RMS_note1 = '';
            end
            if Import_type == 2     % If it's sweep data, provide warning
about stitching.
                RMS_note2 = [char(10), Note2];
                text(time_array_start-time_array_end*0.15, Y_ticks(1)-
(Y_ticks(end)-Y_ticks(1))*0.12, strcat(reduction_factor_text, RMS_note1,
RMS_note2, Test1to13_Note), 'Fontsize', 8);
            else
                RMS_note2 = '';
                text(time_array_start-time_array_end*0.15, Y_ticks(1)-
(Y_ticks(end)-Y_ticks(1))*0.12, reduction_factor_text, 'Fontsize', 8);
            end

            saveas(gca,strcat(['Data Processing\', Output_folder, '\',
'Test ', num2str(Test_no),'\', 'Test ', num2str(Test_no), ' - ',
Graphtitle, ' - RMS rolling ', num2str(RMS_rolling_window_time(Channel)),
'ms.png']));

            if Import_type == 2

                %Creating an array for the limits of the following graphs
```

```
                detail_window_array = [start_window_start_time,
start_window_end_time; mid_window_start_time, mid_window_end_time;
end_window_start_time, end_window_end_time];

                for i = 1:3
                  title(strcat([ 'Test ', num2str(Test_no), ' - ',
Graphtitle, ' - RMS rolling ', num2str(RMS_rolling_window_time(Channel)),
'ms', char(10) ,RMS_range{i}]), 'interpreter', 'none', 'Fontsize', 12)

                  xlabel('Time', 'Fontsize', 12);
                  ylabel(strcat(ItfData.Name, ' (', ItfData.YUnit,
'_{rms})' ), 'Fontsize', 12);
                  %set(gca,'ylim', y_limits_RMS{Channel});
                  ylim auto;
                  set(gca,'xlim', [detail_window_array(i,1)
detail_window_array(i,2)]);
                  set(gca, 'Xgrid','on', 'Ygrid','on');
                  set(gca, 'xticklabel', {[]});
                  Y_ticks = get(gca,'YTick');
                  set(gca,'YTickLabel',sprintf('%g\n',Y_ticks));
                  box on;

                  if (Channel == 4) && (File <= 47)
                      RMS_note1 = [char(10), Note1];
                  else
                      RMS_note1 = '';
                  end

                  % If it's sweep data, provide warning about stitching.
                  text(detail_window_array(i,1)-(detail_window_array(i,2)-
detail_window_array(i,1))*0.15, Y_ticks(1)-(Y_ticks(end)-Y_ticks(1))*0.12,
strcat(RMS_note1, char(10), 'Note: Data shown is of one 20 ms sweep,
sampled at 2 MS/s, starting at: ', num2str(round(detail_window_array(i,1),
3)), 's'), 'Fontsize', 8);

                  saveas(gca,strcat(['Data Processing\', Output_folder,
'\',  'Test ', num2str(Test_no),'\', 'Test ', num2str(Test_no), ' - ',
Graphtitle, ' - RMS rolling ', num2str(RMS_rolling_window_time(Channel)),
'ms - ', RMS_range{i}, '.png']));

                end
            end

            close all;
        end

        %% Create spectrogram
        if strcmp(Spectrogram_chart, 'Y')==1

            figure('Position',[1 1 scrsz(3) scrsz(4)]);
            axes1 = axes('Parent',gcf, 'Position',[0.15 0.17 0.8 0.75]);
            if Import_type == 1
                [S,F,T,P] =
spectrogram(data,16384,8192,16384,f_downsampled,'yaxis');
            elseif Import_type == 2 % Scale back the HF data based on 20ms
sweeps & sweep_skip factor (multiply by 50*sweep_skips)
                [S,F,T,P] =
spectrogram(data,1024,512,1024,f_downsampled,'yaxis');
```

```
                T = T*50*sweep_skips;
            end
            sf = surf(T,F,10*log10(abs(P)));
            sf.EdgeColor = 'none';
            axis tight
            view(0,90)
            colorbar;
            title(strcat([ 'Test ', num2str(Test_no), ' - ', Graphtitle, '
- Spectrogram']), 'interpreter', 'none', 'Fontsize', 12)
            xlabel('Time (s)', 'Fontsize', 12);
            ylabel('Frequency (Hz)', 'Fontsize', 12);
            set(gca,'ylim', y_limits_spectrogram{Channel});
            set(gca,'xlim', [time_array_start time_array_end]);
            set(gca, 'Xgrid','on', 'Ygrid','on');
            Y_ticks = get(gca,'YTick');
            set(gca,'YTickLabel',sprintf('%g\n',Y_ticks));
            box on;

            if (Channel == 4) && (File <=47)
                Spectro_note1 = [char(10), Note1];
            else
                Spectro_note1 = '';
            end
            if Import_type == 2     % If it's sweep data, provide warning
about stitching.
                Spectro_note2 = [char(10), Note2];
                Spectro_note3 = [char(10), ''];%'NOTE: additional 50kHz
high-pass filter applied before computation'];
                text(time_array_start-time_array_end*0.15, Y_ticks(1)-
(Y_ticks(end)-Y_ticks(1))*0.15, strcat(reduction_factor_text,
Spectro_note1, Spectro_note2, Spectro_note3, Test1to13_Note), 'Fontsize',
8)
            else
                text(time_array_start-time_array_end*0.15, Y_ticks(1)-
(Y_ticks(end)-Y_ticks(1))*0.15, reduction_factor_text, 'Fontsize', 8)
            end
            saveas(gca,strcat(['Data processing\', Output_folder, '\',
'Test ', num2str(Test_no),'\', 'Test ', num2str(Test_no), ' - ',
Graphtitle, ' - Spectrogram.png']));
            close all;
        end

        %% FFT ANALYSIS - This chart deliberately needs to be plotted last
        % because the data to be charted gets reverted back to the
        % non-filtered version only for the HF voltage channel.
        if strcmp(FFT_chart, 'Y')==1

            % Take a single window from the mid point of the current
            if Import_type == 1; % Continuous data (LF channesls)
                % Check to see if there is a full second of data where the
                % LF current is flowing
                if (end_window_end_index-start_window_start_index >=
100000) % If a full second exists.
                    FFT_Note2 = '';
                else % Use a shortened window
                    FFT_Note2 = [char(10), 'NOTE: Part of the data analysed
has no current flowing.']; % Replace the Note2 variable at the start of the
script. They cannot occur together.
                end
                NFFT = 100000;  % 1 second window
```

```
                fft_window_title = '1s window at mid-point';
                data =
data(mid_window_start_index:(mid_window_start_index+NFFT-1));
                % Hanning window
                data_HannWnd = 2*data.*hanning(NFFT)';      % factor of 2
correction for hanning window
                Y = fft(data_HannWnd,NFFT)/NFFT;
                f = f_downsampled/2*linspace(0,1,NFFT/2+1);
                FFT_Note3 = '';
                FFT_Note4 = '';

            elseif Import_type == 2
                % Check to see if there is a full 20ms of data where the
                % HF current is flowing
                if (end_window_end_index-start_window_start_index >= 40000)
% If a full 20ms exists.
                    FFT_Note2 = '';
                else % Use a shortened window
                    FFT_Note2 = [char(10),'NOTE: Part of the data analysed
has no current flowing.'];
                end
                NFFT = 40000;   % 20ms window
                fft_window_title = '20ms window at mid-point';
                data =
data(mid_window_start_index:(mid_window_start_index+NFFT-1));
                % Hanning window
                data_HannWnd = 2*data.*hanning(NFFT)';      % factor of 2
correction for hanning window
                Y = fft(data_HannWnd,NFFT)/NFFT;
                f = f_downsampled/2*linspace(0,1,NFFT/2+1);
                FFT_Note3 = [char(10), 'NOTE: No additional 50kHz high-pass
filter applied before computation'];
                FFT_Note4 = Test1to13_Note;
            end

            for i = 1:3
            figure('Position',[1 1 scrsz(3) scrsz(4)]);
            axes1 = axes('Parent',gcf, 'Position',[0.15 0.17 0.8 0.75]);
            semilogy(f,2*abs(Y(1:NFFT/2+1)))
            title(strcat([ 'Test ', num2str(Test_no), ' - ', Graphtitle, '
- Spectrum - ', fft_window_title, char(10) ,frequency_range{i}]),
'interpreter', 'none', 'Fontsize', 12)
            xlabel('Frequency (Hz)')
            ylabel(strcat(Graphtitle, ' amplitude (', ItfData.YUnit, ')' ),
'Fontsize', 12);
            set(gca, 'Xgrid','on', 'Ygrid','on');
            set(gca,'xlim', x_limits_fft{i,Channel});
            Y_ticks = get(gca,'YTick');
            set(gca,'YTickLabel',sprintf('%g\n',Y_ticks));
            X_ticks = get(gca,'XTick');
            set(gca,'XTickLabel',sprintf('%g\n',X_ticks));
            box on;
            if (Channel == 4) && (File <=47)
                FFT_Note1 = [char(10), Note1];
            else
                FFT_Note1 = '';
            end
            text(X_ticks(1), Y_ticks(1)-(Y_ticks(end)-Y_ticks(1))*0.12,
strcat(FFT_Note1, FFT_Note2, FFT_Note3, FFT_Note4), 'Fontsize', 8);
```

```
            saveas(gca,strcat(['Data processing\', Output_folder, '\',
'Test ', num2str(Test_no),'\', 'Test ', num2str(Test_no), ' - ',
Graphtitle, ' - Frequency Spectrum', ' - ',frequency_range{i}, '.png']));
            close;
            end
        end



        % Clear variables for next run
        clear data;
        clear data_downsampled_combined;
        clear data_length;
        clear data_rolling_RMS;
        clear data_squared;
        clear F;
        clear L;
        clear P;
        clear S;
        clear T;
        clear time_array;
        clear WaveformData;
        data_downsampled_combined = [];

end



end

if length(Files_to_process)>1
    close all;
end

end
```